

STATE OF OREGON
DEPARTMENT OF GEOLOGY AND MINERAL INDUSTRIES
1005 State Office Building
Portland, Oregon 97201

OPEN-FILE REPORT O-82-7

GEOLOGY AND GEOTHERMAL RESOURCES
OF THE CASCADES, OREGON

George R. Priest and Beverly F. Vogt, Editors
Oregon Department of Geology and Mineral Industries
1982

The work was supported by the U.S. Department of
Energy (Cooperative Agreement No. DE-FC07-79ID12044).

NOTICE

The Oregon Department of Geology and Mineral Industries is publishing this paper because the subject matter is consistent with the mission of the department.

To facilitate timely distribution of information, this paper has not been edited to our usual standards.

TABLE OF CONTENTS

	Page
CHAPTER 1. INTRODUCTION, by George R. Priest	1
CHAPTER 2. OVERVIEW OF THE GEOLOGY AND GEOTHERMAL RESOURCES OF THE CENTRAL OREGON CASCADES, by George R. Priest, Neil M. Woller, Gerald L. Black and Stanley H. Evans	5
ABSTRACT	5
INTRODUCTION	6
PREVIOUS WORK	7
GENERAL GEOLOGY OF THE CASCADES	9
VOLCANIC STRATIGRAPHY	11
Introduction	11
General discussion	16
Volcanic rocks of the early Western Cascades (40-18 m.y. B.P.)	20
Volcanic rocks of the late Western Cascades (18-9 m.y. B.P.)	22
Volcanic rocks of the early High Cascades (9-4 m.y. B.P.)	24
Volcanic rocks of the late High Cascades (4-0 m.y. B.P.)	27
STRUCTURAL GEOLOGY	29
Introduction	29
North-south and north-northwest-trending normal faults	29
Age of north-south and north-northwest-trending faults	34
Northwest-trending faults with lateral movement	35
Age of northwest-trending faults with lateral movement	36
N. 20 ⁰ -40 ⁰ W. normal faults and intrusives	38
Age of N. 20 ⁰ -40 ⁰ W. normal faults and intrusives	38
Northeast-trending faults	39
Age of northeast-trending faults	39
Folds	40
Age of folds	41
Structural interpretations and speculations	41
PETROCHEMISTRY	45
Introduction	45
Analytical methods	45

Recalculation of data	46
Nomenclature	46
Methods of comparison	48
Comparisons	51
SPECULATIONS ON THE TECTONIC SETTING OF VOLCANIC EPISODES FROM COMPOSITIONAL EVIDENCE	57
Introduction	57
Early Western Cascade episode	58
Late Western Cascade episode	59
High Cascade episode	59
Conclusions	61
KNOWN AND PROBABLE HYDROTHERMAL SYSTEMS	61
POTENTIAL RESERVOIR ROCKS FOR HYDROTHERMAL CIRCULATION	65
RECOMMENDED GEOTHERMAL EXPLORATION TARGETS	67
CONCLUSIONS	69
ACKNOWLEDGMENTS	70
CHAPTER 3. PRELIMINARY GEOLOGY OF THE OUTERSON MOUNTAIN-DEVILS CREEK AREA, MARION COUNTY, OREGON, by George R. Priest and Neil M. Woller	71
ABSTRACT	71
INTRODUCTION	71
PREVIOUS WORK	73
STRATIGRAPHY	75
Introduction	75
Volcanic rocks of the late Western Cascades	77
Lavas of Outerson Mountain (Tmo)	77
Tuffs of Outerson Mountain (Tmt)	79
Volcanic rocks of the early High Cascades	82
Upper Miocene-Pliocene lavas (Tmp)	82
Subvolcanic intrusive rocks (Tmi)	83
Volcanic rocks of the late High Cascades	84
STRUCTURAL GEOLOGY	84
Folds and regional tilting	84
Faults	85
Conclusions	87
GEOTHERMAL RESOURCES	88

CHAPTER 4. GEOLOGY OF THE COUGAR RESERVOIR AREA, LANE COUNTY, OREGON, by George R. Priest and Neil M. Woller	92
ABSTRACT	92
INTRODUCTION	92
PREVIOUS WORK	94
GEOLOGIC HISTORY	95
STRATIGRAPHY	96
Introduction	96
Volcanic rocks of the early Western Cascades	99
Tuffs of Cougar Reservoir (Totc)	99
Volcanic rocks of the late Western Cascades	100
Introduction	100
Dacite intrusive of Cougar Dam (Tmvic)	101
Tuffs of Rush Creek (Tmrt)	102
Basaltic lavas of the East Fork (Tme)	104
Andesites of Walker Creek (Tmw)	104
Andesites of Castle Rock (Tmcr)	106
Tuffs of Tipsoo Butte (Tmtt)	106
Volcanic rocks of the early High Cascades	107
Lavas of Tipsoo Butte (Tml)	107
Pliocene-Pleistocene mudflow deposits (QTpm)	110
Glacial and fluvial deposits (Qgf)	110
Pleistocene gravels (Qpg)	110
Unconsolidated Recent colluvium (Qc), alluvium (Qal), and landslide deposits (Qls)	111
STRUCTURAL GEOLOGY	111
Introduction	111
Cougar fault	111
Local tilting and folding	113
GEOOTHERMAL RESOURCES	115
CONCLUSIONS	117
 CHAPTER 5. GEOLOGY OF THE LOOKOUT POINT AREA, LANE COUNTY, OREGON, by Neil M. Woller and George R. Priest	 119
ABSTRACT	119

INTRODUCTION	119
VOLCANIC STRATIGRAPHY	121
Introduction	121
Volcanic rocks of the early Western Cascades	123
Oligocene and lower Miocene tuffs and lavas (undifferentiated)	
(Totl)	123
Lavas of Lookout Point (Tolp)	124
Lavas of Hardesty Mountain (Toh)	125
Lavas of Black Canyon (Tml/Tmli)	125
Volcanic rocks of the late Western Cascades	128
Miocene andesitic lavas (Tma/Tmi)	128
Volcanic rocks of the early High Cascades	129
Upper Miocene lavas (Tmu)	129
Volcanic rocks of the late High Cascades	129
Pliocene-Pleistocene(?) basaltic lavas (QTb)	129
STRUCTURE	130
DISCUSSION AND CONCLUSIONS	133
CHAPTER 6. GEOLOGY OF THE SWIFT CREEK AREA, LANE COUNTY, OREGON, by	
Neil M. Woller	135
ABSTRACT	135
LOCATION AND PHYSIOGRAPHY	135
EUGENE-DENIO FAULT/FRACTURE ZONE--PREVIOUS WORK	137
HIGH CASCADE MARGIN	138
VOLCANIC STRATIGRAPHY	138
Introduction	138
Volcanic rocks of the late Western Cascades	140
Older volcanoclastic sediments and lavas (Tmo)	140
Basaltic rocks of Tumblebug Creek (Tmb/Tmbi)	141
Andesitic rocks of Moss Mountain (Tma)	142
Volcanic rocks of the early High Cascades	144
Miocene-Pliocene basaltic lavas (Tpb)	144
Volcanic rocks of the late High Cascades	145
Pleistocene basaltic rocks (Qb)	145
Mazama pumice-fall deposit	146

STRUCTURE	146
DISCUSSION AND CONCLUSIONS	149
GEOHERMAL POTENTIAL	150
CHAPTER 7. HEAT FLOW OF THE OREGON CASCADES, by Gerald L. Black, David D. Blackwell, and John L. Steele	152
ABSTRACT	152
INTRODUCTION	152
DATA COLLECTION	157
CASCADE HEAT FLOW	158
WESTERN CASCADE-WILLAMETTE VALLEY HEAT FLOW	158
HIGH CASCADE HEAT FLOW	160
WESTERN CASCADE-HIGH CASCADE BOUNDARY REGION	161
INTERPRETATION OF THE HEAT-FLOW TRANSITION ZONE	162
ORIGIN OF HOT SPRINGS	166
GEOHERMAL POTENTIAL OF THE CASCADES	168
REFERENCES CITED	173
APPENDICES	185
APPENDIX A. NEW K-Ar DATA	185
APPENDIX B. CHEMICAL ANALYSES OF ROCK SAMPLES	186
APPENDIX C. EXPLANATION OF TOWNSHIP-RANGE LOCATION SYSTEM	197
APPENDIX D. TEMPERATURE AND HEAT-FLOW DATA FOR THE OREGON CASCADES .	198

ILLUSTRATIONS

	Page
FIGURES	
1.1. Map showing locations of drill holes and areas studied during central Cascade geothermal project	2
2.1. Regional stratigraphic units used by various workers in the Cascades compared with time categories of distinctive volcanism utilized in this paper	12-13
2.2. Informal nomenclature utilized in this paper	14
2.3. Physiographic provinces of Oregon	17
2.4. Map showing major faults, lineaments, hot springs, and Quaternary volcanic centers relative to zones of anomalously high heat flow in the Cascades	30-31
2.5. Episodes of deformation in some mapped areas of northern and central Cascades	32
2.6. Nepheline-olivine-clinopyroxene-orthopyroxene-quartz quadrilateral	47
2.7. $\text{Na}_2\text{O}+\text{K}_2\text{O}-\text{FeO}^*-\text{MgO}$ ternary diagram	49
2.8. FeO^*/MgO versus SiO_2	50
2.9. FeO^* versus SiO_2	50
2.10. Al_2O_3 versus normative plagioclase	52
2.11. $\text{Na}_2\text{O}+\text{K}_2\text{O}$ versus SiO_2	53
3.1. Location of the Outerson Mountain-Devils Creek map area	72
3.2. Stratigraphy of the Outerson Mountain-Devils Creek area	76
4.1. Location of the Cougar Reservoir map area	93
4.2. Stratigraphy of the Cougar Reservoir area	97
5.1. Location of the Lookout Point map area	120
5.2. Stratigraphy of the Lookout Point area	122
5.3. Stratigraphic section of lavas of Black Canyon	127
6.1. Location of the Swift Creek map area	136
6.2. Stratigraphy of the Swift Creek area	139
7.1. Physiographic provinces of Oregon showing area discussed in this paper	153
7.2. Heat flow in the Cascade Range of Oregon	159

7.3.	Geothermal-gradient, heat-flow, interpreted crustal temperatures, and regional Bouguer gravity values for the western part of the northern Oregon Cascade Range	164
7.4.	Several models of the relationship of hot springs to the heat-flow transition at the Western Cascade-High Cascade boundary .	167

TABLES

1.1.	Heat-flow holes drilled by the Oregon Department of Geology and Mineral Industries in 1979 and 1980 in the central Cascades	3
2.1.	Parameters that distinguish volcanic rocks erupted during various central Oregon volcanic episodes	15
3.1.	Estimated minimum reservoir temperatures and partial analyses from new samples of wells and springs in the Breitenbush KGRA	89
4.1.	Estimated reservoir temperatures of Terwilliger Hot Springs ...	98
7.1.	Estimates of the electrical generation potential of the Oregon Cascade Range	156
A.1.	New K-Ar data, Oregon	185
B.1.	Rock chemistry, Outerson Mountain-Devils Creek area, Marion County, Oregon	186
B.2.	Rock chemistry, Cougar Reservoir area, Lane County, Oregon	188
B.3.	Rock chemistry, Lookout Point area, Lane County, Oregon	191
B.4.	Rock chemistry, Swift Creek area, Lane County, Oregon	193
D.1.	Temperature and heat-flow data for the Oregon Cascades	198

PLATES (in envelope)

1	Index to geologic mapping in the Oregon Cascades at scales larger than 1:250,000
2	Stratigraphic columns of regional interest in the Oregon Cascades
3	Geologic map of the Outerson Mountain-Devils Creek area, Marion County, Oregon
4	Geologic map of the Cougar Reservoir area, Lane County, Oregon
5	Geologic map of the Lookout Point area, Lane County, Oregon
6	Geologic map of the Swift Creek area, Lane County, Oregon
7	Heat-flow map of the Cascade Range of Oregon

CHAPTER 1. INTRODUCTION

By George R. Priest

Oregon Department of Geology and Mineral Industries

This report summarizes investigations of the geology and geothermal resources of the central Cascades of Oregon conducted from 1977 through 1982. The project was funded by the State of Oregon and the U.S. Department of Energy (USDOE) (USDOE Contract EG-77-C-06-1040 and Cooperative Agreement DE-FC07-79ID12044).

A shallow drilling program and geologic mapping project provided data for heat-flow and geologic analysis. In some areas, detailed geologic maps were produced around individual drill sites, so that heat-flow interpretations could be related to local geology (Figure 1.1). Heat flow was calculated by D.D. Blackwell and J.L. Steele of Southern Methodist University, Dallas, Texas. Interpretation and collection of the heat-flow data were accomplished by G.L. Black, Oregon Department of Geology and Mineral Industries (DOGAMI), with the aid of D.D. Blackwell and J.L. Steele (see Black and others, Chapter 7, this volume). Drilling and geologic mapping were primarily conducted by G.R. Priest and N.M. Woller of DOGAMI (see papers by Priest and Woller, Woller and Priest, and Woller, Chapters 3, 4, 5, and 6, this volume). Early phases of the drilling program were supervised by D.A. Hull (DOGAMI) in 1977 and by J.F. Riccio (DOGAMI) in 1979. D.E. Brown (DOGAMI) supervised reconnaissance geologic mapping of the Belknap-Foley and Willamette Pass areas as part of a separate investigation of low-temperature geothermal resources. This paper primarily summarizes the data generated by these workers. Figure 1.1 shows the location of drill holes and map areas, and Table 1.1 lists DOGAMI temperature-gradient holes.

In addition to the above DOGAMI investigations, five separate projects were subcontracted: (1) R.W. Couch of Oregon State University supervised production of gravity and aeromagnetic maps of the Cascades (DOGAMI maps GMS-8 [Pitts and Couch, 1978], 9 [Couch and others, 1978], 15 [Couch and others, 1981b], 16 [Couch and others, 1981c], 17 [Couch and others, 1981a], and 26 [Couch and others, 1982b] and Open-File Report 0-82-9 [Couch and others, 1982a]), exclusive of aeromagnetic

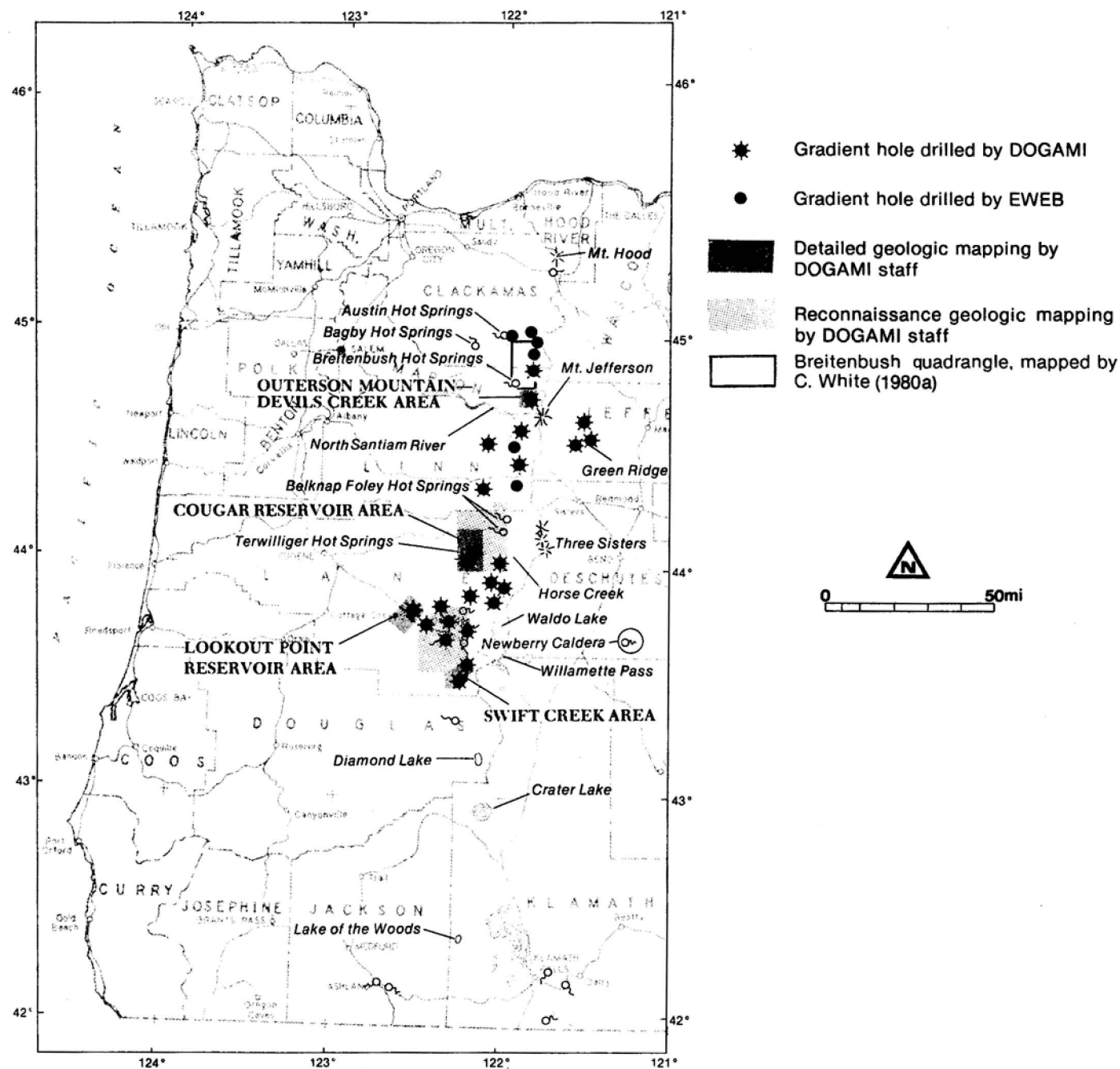


Figure 1.1. Map showing locations of drill holes and areas studied during the central Cascade geothermal project.

Table 1.1. Heat-flow holes drilled in the Oregon Cascades by DOGAMI in 1979 and 1980

Twn/Rng/Sec ⁺⁺	Hole name	Drilled depth (m)
8S/8E/31C	Cub Creek*	142
10S/7E/11Aa	Devils Creek*	154
11S/7E/10Dc	Minto Creek*	122
11S/6E/22Db	Buck Mtn.*	154
11S/10E/5Ac	Castle Rock*	154
12S/9E/1Bc	Green Ridge	154
13S/7E/9Ab	Detroit Road	76
13S/9E/5Ab	Fly Creek*	119
14S/6E/32Dc	Wolf Meadow*	154
17S/5E/8Ac	Walker Creek*	154
17S/5E/20Ba	Rider Creek*	154
17S/6E/25Ad	Mosquito Creek*	154
18S/5E/11Bd	Rebel Creek*	154
19S/6E/8Ba	Elk Creek*	133
19S/5E/27Bc	Brock Creek*	154
19S/4E/29Cc	Christy Creek*	154
19S/6E/25Dc	North Fork*	154
20S/4E/27Dd	Wall Creek*	137
20S/2E/35Ac	Burnt Bridge Cr.*	154
21S/5E/16Ac	Black Creek*	500
23S/5E/8Da	Pinto Creek*	154
24S/5E/18Ca	Tumblebug Creek*	154
21S/3E/17Da	Oakridge City Well**	335 ⁺
21S/3E/26Ca	Hills Creek Dam**	160

* Drilled under contract DE-FC07-79ID12044.

** Drilled under contract DE-FC07-79ET27220.

+ Deepened from 183 m to 335 m.

++ See Appendix C for explanation of township-range location system.

coverage of the north Cascades. Gravity field work and calculations were accomplished primarily by G.S. Pitts and M. Gemperle, with assistance from C.A. Veen and D.E. Bramen. Aeromagnetic field and laboratory work were completed by M. Gemperle, G.G. Connard, and W.H. McLain. The U.S. Geological Survey (USGS) subcontracted the gravity and aeromagnetic work in the central Cascades, while DOGAMI subcontracted gravity surveys in the northern and southern Cascades and an aeromagnetic survey of the southern Cascades. (2) C.W. Field and S.G. Power of Oregon State University completed a study of Western Cascades mining districts to relate older geothermal systems to modern ones. (3) A lineament study of the Cascades was accomplished in two parts. The north Cascades lineaments were described by R. Venkatrishnan, J.G. Bond, and J.D. Kauffman of Geoscience Research Consultants, Moscow, Idaho (DOGAMI Special Paper 12 [Venkatakrishnan and others, 1980]). South Cascades lineaments were studied by C.F. Kienle and C.A. Nelson of Foundation Sciences, Inc., Portland, Oregon, and R.D. Lawrence of Oregon State University (DOGAMI Special Paper 13 [Kienle and others, 1981]). (4) A. Cox and J. Magill of Stanford University conducted a study of paleomagnetism of Western Cascades igneous rocks (DOGAMI Special Paper 10 [Magill and Cox, 1980]). (5) C.M. White, Boise State University, investigated the geology of the Breitenbush Hot Springs quadrangle (DOGAMI Special Paper 9 [White, 1980a]) (Figure 1.1).

Data from the Mount Hood geothermal assessment project (DOGAMI Open-File Report 0-79-8 [Hull and Riccio, 1979], Special Paper 8 [White, 1980b], and Special Paper 14 [Priest and Vogt, 1982]) are also used in this paper to develop a comprehensive geothermal model. For summaries of Mount Hood data, the reader is referred to DOGAMI Special Paper 14 (Priest and Vogt, 1982) and a special issue of the Journal of Geophysical Research (volume 87, number B4) on Mount Hood. DOGAMI Special Paper 8 by C.M. White (White, 1980b) describes the igneous petrology of Mount Hood.

Temperature and heat-flow data from a drilling project (Figure 1.1) conducted by the Eugene Water and Electric Board, Eugene, Oregon, are also summarized here (Black and others, Chapter 7; see also DOGAMI Open-File Report 0-80-12 [Youngquist, 1980]). This drilling project was primarily funded by USDOE with smaller contributions by Southland Royalty Company, Fort Worth, Texas; Sunoco Energy Development Company of Dallas, Texas; and the Eugene Water and Electric Board.

CHAPTER 2. OVERVIEW OF THE GEOLOGY AND GEOTHERMAL RESOURCES

OF THE CENTRAL OREGON CASCADES

By George R. Priest, Neil M. Woller, Gerald L. Black,
Oregon Department of Geology and Mineral Industries,
and

Stanley H. Evans,
University of Utah Research Institute, Salt Lake City, Utah

ABSTRACT

Eruption of voluminous silicic tuffs and lesser volumes of iron-rich intermediate to silicic lavas between 40 and 18 m.y. B.P. and eruption of intermediate calc-alkaline lavas and subordinate tuffs about 18 to 9 m.y. B.P. formed most of the volcanic pile in the central Western Cascades. The axis of volcanism had shifted to the vicinity of the High Cascade province by about 9 m.y. B.P., when more mafic, alkaline, and iron-rich lavas began to erupt. Slight folding in the north-central Cascades also ended by about this time. Widespread north-south- to north-northwest-trending normal faulting accompanied subsidence of the High Cascade axis and uplift of adjacent areas of the central Cascades between 5 and 4 m.y. B.P., as voluminous basaltic lavas began to form a broad platform in the High Cascades. A north-south-trending chain of composite volcanoes developed along the High Cascade axis in the Quaternary as volcanism became slightly more silicic. The youngest composite cones are chiefly andesitic in composition, although basaltic eruptions have continued into the Holocene on the surrounding platform.

Compositional and textural similarity of some of the 9- to 0-m.y. B.P. basalts in the Basin and Range and the Cascades and the contemporaneity of changes in volcano-tectonic events in the Basin and Range and the Cascades suggest that the geologic history of the two areas is closely related. A major change in the plate-tectonic regime about 10 to 8 m.y. B.P. may have affected both areas, resulting in increased extensional tectonic influence in the central Cascades. An additional change in the interaction of lithospheric plates at the end of the Miocene is probably necessary to account for the pronounced

uplift and north-south faulting which occurred 5 to 4 m.y. B.P. in the Cascades.

Occurrence of silicic Quaternary volcanic centers and numerous faults in the Newberry volcano-Three Sisters area are evidence that this area is the best exploration target for shallow high-temperature hydrothermal systems in the Cascades. The entire High Cascade Range has a heat-flow anomaly and is a good exploration target for geothermal resources if permeable reservoir rocks can be delineated.

INTRODUCTION

This paper summarizes the general geology of the central Cascade Range of Oregon with the goal of achieving a viable geologic model to guide future geothermal exploration. One of the most important factors limiting all exploration in the Cascades of Oregon is the lack of accurate detailed geologic maps. Four new detailed geologic maps (see Figure 1.1 of the previous chapter) are presented in the following four papers (Chapters 3 to 6) and are utilized with other data (Plate 1) to develop a volcano-tectonic model for the central Cascades. Geothermal exploration areas based on these geologic and geophysical data are then recommended.

An important conclusion of this study is that the central Cascade Range is probably one of the most attractive areas for geothermal resources in the western United States. Silicic Holocene volcanic centers at South Sister and Newberry volcano, which have erupted numerous times during the last few thousand years, occur in a region with several intersecting fault systems. They may have both high-level heat sources and highly permeable reservoir rocks.

The potential of this area is underscored by the recent discovery of very high temperatures in a diamond drill hole drilled by the U.S. Geological Survey (USGS) at Newberry caldera (Figure 1.1). Measured temperatures of 265° C (509° F) at 932 m (3,057 ft) make this the hottest geothermal well in the northwest (Sammel, 1981). This is much hotter than wells drilled considerably deeper in The Geysers area of northern California, where the world's largest electrical production from a geothermal source is produced from fluids at approximately 232° C (450° F).

The Oregon Cascades are also the site of a regional heat-flow high (Blackwell and others, 1978; Black and others, Chapter 7). Background heat flow, where measured along the margins of the High Cascade physiographic province, is roughly two and one-half times normal crustal heat flow (Blackwell and others,

1978; Black and others, Chapter 7). Electrical-grade geothermal resources may be present within the area of this regional anomaly at depths of a few kilometers. This paper describes geologic environments amenable to hydrothermal circulation and examines the nature of deep-seated heat sources responsible for high regional heat flow in the Cascades.

PREVIOUS WORK

This study draws on a considerable body of previous geological work by numerous scientists working in the central Cascades. Although there are many new data on the central Cascades, the pioneering work by Callaghan (1938), Chaney (1938), Thayer (1936, 1939), Williams (1933, 1935, 1942, 1944, 1953, 1957), and Peck and others (1964) are the foundation for all later studies. Papers by Taylor (1967, 1968, 1973a,b, 1978, 1980, 1981) are important sources on the central High Cascades and Deschutes Basin. Theses by Sutton (1974) on Mount Jefferson and Davie (1980) on Three Fingered Jack include large-scale geologic maps of these important High Cascade cones. Williams' (1935, 1957) and Higgin's (1973) data for Newberry caldera have been recently supplemented by detailed mapping of the volcano by MacLeod (1978a,b), MacLeod and Sherrod (1979), and MacLeod and others (in press). Plate 1 summarizes most of the available geologic map coverage in the Cascades at scales of more than 1:250,000.

Geologic investigations of the Western Cascade province have historically lagged behind those of the High Cascades. The lack of adequate stratigraphic and age control has led to much confusion and disagreement among workers in the province. Steep terrain and heavy colluvial and vegetative cover have generally discouraged workers from mapping in the Western Cascades. Another problem is that some data have been utilized without adequate field studies to draw small-scale generalized maps. Further confusion has been caused because regional sampling programs for K-Ar and petrochemical data seldom have had proper stratigraphic control.

One basic problem in the Cascades is the local nature of most unconformities. Whereas it is possible to find large time gaps between volcanic rock units in local areas, these may not be gaps in volcanism on a regional scale. A series of volcanic centers delineating a particular axis of volcanism need not have overlapping deposits. Regions between centers will have rock sequences with large gaps in the volcanic record recorded as unconformities in numerous local areas. A relatively continuous regional volcanic history can thus be interpreted

as episodic on the basis of incomplete mapping and radiometric dating. Data in the Cascades are still inadequate for detailed conclusions about the periodicity of volcanism, but, as more areas are mapped and sampled, a history of relatively continuous volcanism is emerging for the Neogene.

There is still inadequate detailed map coverage in the Western Cascades, particularly in the southwestern part. Anderson's (1978) map of the upper Clackamas River area, White's (1980a,c) work in the Battle Ax and Breitenbush quadrangles, Dyhrman's (1975) work in the Bagby Hot Springs area, Clayton's (1976) map in the Breitenbush Hot Springs area, and Rollins' (1976) and Thayer's (1936, 1939) maps in the North Santiam drainage are the best data at relatively large scales available in the north-central Western Cascades. Pungrassami (1970) also mapped a small area in the western Detroit Reservoir area. Hammond and others' (1980, 1982) map of the north-central Western Cascades is the best available compilation. The earlier compilations of Wells and Peck (1961) and Peck and others (1964) are more comprehensive but not as detailed as the above maps and lack age control provided by recent K-Ar studies.

Geologic work in Western Cascade areas south of the North Santiam River has been done mainly by economic-geology students on mining districts. None of these theses have focused on the volcanic stratigraphy. Recent volcanic stratigraphic theses by Avramenko (1981) and Flaherty (1981) at the University of Oregon have contributed greatly to knowledge of the structural boundary between the High Cascade and Western Cascade provinces. Both these theses and earlier work by Barnes (1978), Brown and others (1980a), Hammond and others (1980), Taylor (1978, 1980), Thayer (1939), Williams (1957), and White (1980a,c) have helped define the location of the margins of possible central High Cascade axial grabens hypothesized by Allen (1966). Maynard's (1974) work at Lake of the Woods, Naslund's (1977) map of the southernmost High Cascades, and Wells' (1956) map of the Medford quadrangle are among the few large-scale maps of volcanic rocks in the southern Cascades.

There is a great need to update the small-scale compilation maps of Wells and Peck (1961) and Peck and others (1964). New maps in preparation by George W. Walker, Norman S. MacLeod, David R. Sherrod, and James G. Smith of the USGS should provide the needed update.

McBirney and others (1974), White and McBirney (1978), and White (1980a,c) have summarized chemical, isotopic, and radiometric age data on central Cascade rocks. Their syntheses indicate that the central part of the Cascade Range has

been the site of intense episodic volcanism since the Oligocene. They define several episodes of chemically distinct magmatism which occurred synchronously along the length of the Oregon Cascades. Many aspects of their model have been confirmed by Hammond (1979), Hammond and others (1980, 1982), Avramenko (1981), Flaherty (1981) and data of this paper. There are, however, differences between our conclusions and interpretations and those of previous workers, owing primarily to the larger geographic coverage of new maps, new chemical data, and particularly, new K-Ar dates.

GENERAL GEOLOGY OF THE CASCADES

The Cascade Range consists of a thick pile of volcanic and related intrusive rocks which fill a broad north-south- to north-northeast-trending depression in Eocene and older rocks (Peck and others, 1964). Although great thicknesses of volcanic rock accumulated in Oligocene to Miocene time, the volcanic mountain range was not high enough to deplete the prevailing westerly winds of their moisture and thereby create semi-arid conditions in eastern Oregon until Pliocene time (Chaney, 1938; Williams, 1942). In the early Pliocene (5 to 4 m.y. B.P.), rapid uplift and erosion of the central Western Cascades and foundering of the area now occupied by the High Cascades created an elevated mountain range in the western part of the province which caused an effective rain shadow (e.g., see Chaney, 1938; Williams, 1942, 1953; Taylor, 1980; Flaherty, 1981). Deep valleys were rapidly cut into the elevated western part of the range, and by about 4 to 3 m.y. B.P., most of the relief and drainage pattern which characterize the Western Cascade physiographic province were well established (e.g., see Thayer, 1936, 1939; Williams, 1942, 1953; Flaherty, 1981). Most of the present relief on the High Cascade Range did not exist until the Quaternary, when the majority of the High Cascade composite cones were built on a low platform of voluminous mafic Pliocene lavas (e.g., Williams, 1953; Taylor, 1980).

These changes in the physiography of the Cascades were accompanied by changes in the overall composition of the volcanic rocks and the style of tectonic deformation. During the latest Eocene to earliest Miocene, voluminous silicic ash flows and lesser amounts of black, tholeiitic lava and calc-alkaline andesite, dacite, and rhyolite covered all of the area now occupied by the central Western Cascades (e.g., see Callaghan, 1933; Thayer, 1937, 1939; Peck and others, 1964; White 1980a,c). Woller and Priest (Chapter 5) present evidence that some west-northwest-trending lateral faulting occurred prior to

22 m.y. B.P. which affected these early rocks. During the middle Miocene, calc-alkaline andesite, basaltic andesite, and subordinate basalt erupted during a period of gentle folding (Thayer, 1936, 1939; Williams, 1953; Peck and others, 1964; Hammond, 1979; Hammond and others, 1980). Toward the end of the Miocene, between about 9 to 4 m.y. B.P., basalt, basaltic andesite, and subordinate andesite and dacite began to erupt from vents east of most of the earlier Cascade vents. When the volcanism became more mafic, about 9 m.y. B.P., the folding which characterized the middle Miocene central Cascades was replaced by normal faulting along north to northwest trends, and numerous northwest-trending dikes were injected (e.g., see Priest and Woller, Chapter 3, Chapter 4; Avramenko, 1981).

Uplift of the Western Cascades in the early Pliocene was accompanied by additional north- to northwest-trending normal faulting, especially at the present Western Cascade-High Cascade physiographic boundary. Thayer (1936) noted that there was evidence of a 2,000-ft-high, north-south-trending, east-facing escarpment on the eastern Western Cascade boundary along the upper McKenzie River. Later work by Taylor (1973b, 1980), Brown and others (1980a) and Flaherty (1981) has verified that there is a series of north-south-trending fault scarps which create an escarpment of this magnitude along the upper McKenzie River-Horse Creek drainage. Hales (1975) and Taylor (1980) pointed out that the Green Ridge escarpment east of the High Cascades is complementary to the McKenzie scarp, forming a graben on the High Cascade axis, as postulated by Allen (1966). Williams (1942) presented evidence for an analogue to the McKenzie escarpment west of Crater Lake National Park, where old Western Cascades rocks are uplifted to high elevations next to a thick pile of younger rocks erupted within the High Cascade province. The uplift, faulting, and most of the resulting erosional relief on the McKenzie-Horse Creek escarpment occurred over a very short interval between about 5 and 3.4 m.y. B.P. according to Flaherty's (1981) data, and Taylor (1980) concludes that most of the faulting probably occurred between 5 and 4 m.y. B.P.

This major faulting event in the early Pliocene was accompanied by voluminous eruptions of basalt and basaltic andesite in the High Cascades. Highly fluid diktytaxitic basalt flows which dominated the earliest eruptions frequently poured into the western Cascade drainages, while the more silicic lavas were constrained by their viscosity to the low shieldlike platform which was developing on the present site of the High Cascades (e.g., see Taylor, 1980).

By Quaternary time, basaltic andesite composite cones were developing from more explosive activity along the central and western parts of the High Cascade province amid continued effusive eruptions of basalt and basaltic andesite in the platform (Williams, 1953; Taylor, 1980). More silicic composite volcanoes were built in the latter part of the Quaternary at Mount Hood, Mount Jefferson, Mount Bachelor, South Sister, and Mount Mazama, but basaltic eruptions still continued in the surrounding platform (e.g., Williams, 1953; Taylor, 1980). The youngest eruptions in the High Cascades have been chiefly dacitic to rhyodacitic (e.g., at South Sister and Mount Mazama) and basaltic (e.g., the Belknap Crater and other Holocene basalts).

VOLCANIC STRATIGRAPHY

Introduction

A combination of time- and rock-stratigraphic units have traditionally been used for regional stratigraphy in the Cascades (e.g., Wells and Peck, 1961; Peck and others, 1964). Owing to regional changes in the volcanism along the Cascades through time, certain intervals of geologic time are characterized by distinctive rock-stratigraphic units. Ages of volcanic rock have in the past been judged by both radiometric dates and relative degree of alteration, as well as by the tacit assumption that distinctive compositional types of volcanic rock characterize certain geologic times. Data from the present study suggest that the latter assumption is often, though not invariably, justified.

Figure 2.1 and Plate 1 summarize regional and local stratigraphic units defined by various workers in the north-central Cascades and compare them to an informal system of time categories used for this paper (Figure 2.2 and Table 2.1). The system used here provides a basis for discussion and is not intended for formal usage or as a replacement for existing rock-stratigraphic nomenclature. It is based on breaks in time which, from mapping in the central Cascades, appear to correspond to broad changes in the overall composition of volcanic sequences. This system avoids some of the confusion generated by previous usage of regional rock-stratigraphic systems which sought to correlate particular type sections over unrealistically large distances along the Cascades. We also avoid using terms such as "Sardine Formation," whose meaning, in terms of the age of the rocks concerned, is still debated (e.g., see Thayer, 1939; Peck and others, 1964; Hammond and others, 1980; White, 1980a,c). The same is true of the name

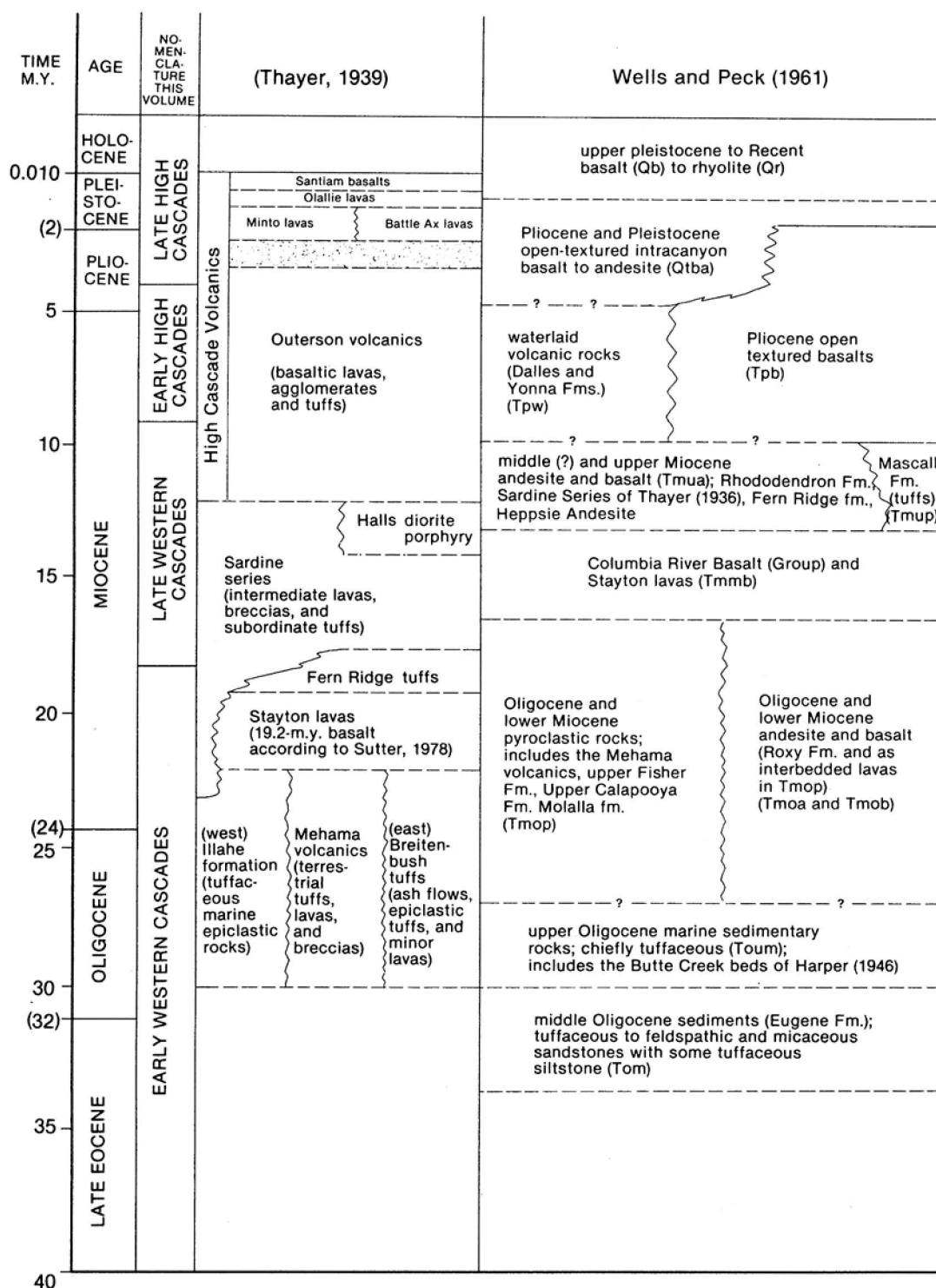
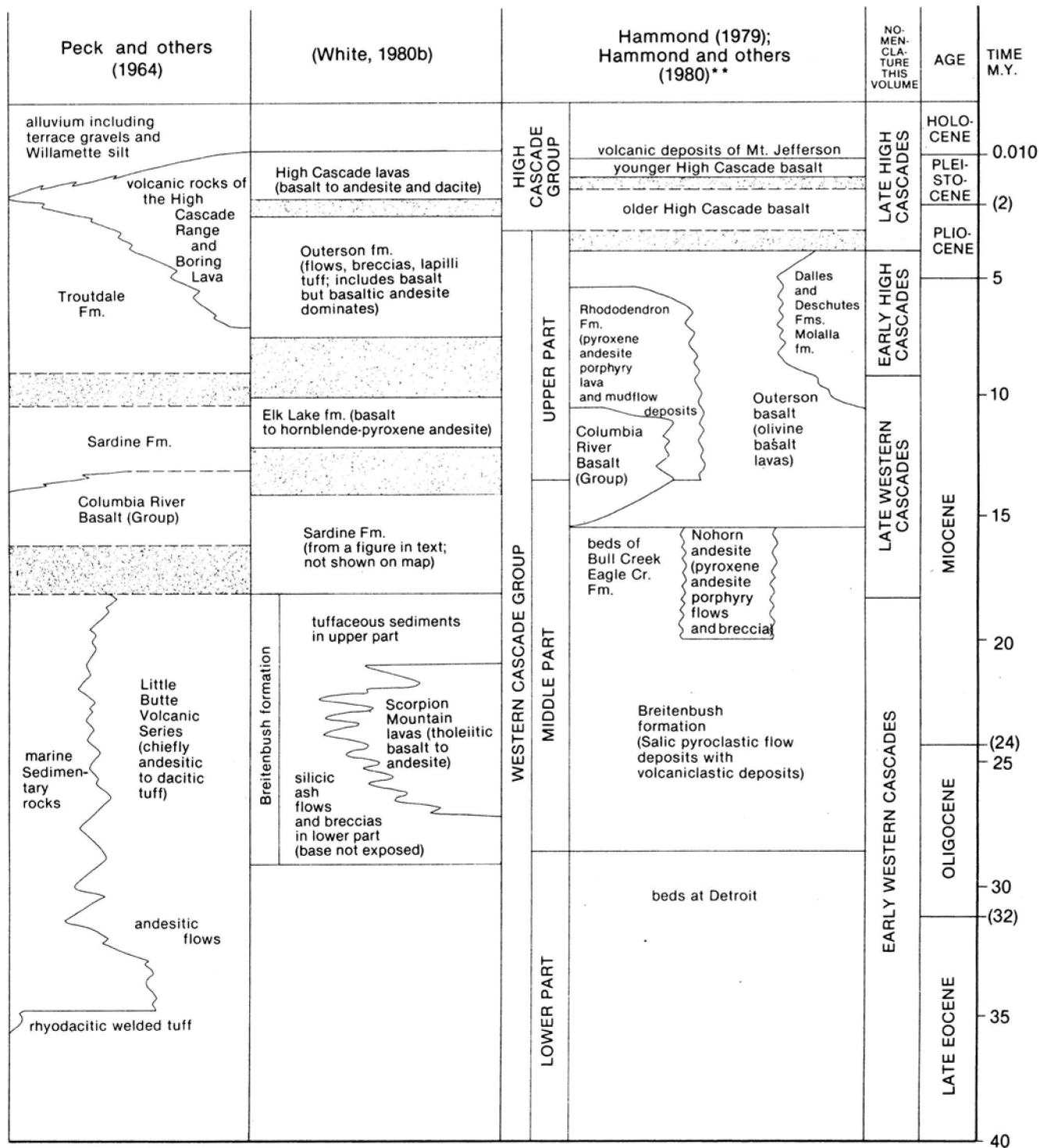


Figure 2.1 (both pages). Regional stratigraphic units used by various workers in the Cascades compared to time categories of distinctive volcanism utilized in this paper. Time limits of stratigraphic units were estimated. Geologic time units are those of Armentrout (1981).



Volcanic episode (± 1 m.y. B.P.)	Volcanic rocks	Correlative rock-stratigraphic units
Late High Cascades (4 to 0 m.y. B.P.)	Chiefly mafic volcanic rocks; some are slightly alkaline high-alumina basalt; commonly highly diktytaxitic in lower part; more silicic in upper part. Includes the High Cascade composite cones. Includes some andesitic, dacitic, and rhyodacitic tuff and lava	High Cascade lavas (McBirney and others, 1974; White, 1980a); High Cascades group (Hammond, 1979; Hammond and others, 1980); upper part of volcanic rocks of the High Cascades and Boring Lavas (Peck and others, 1964).
Early High Cascades (9 to 4 m.y. B.P.)	Chiefly mafic lavas and some interbedded tuffs; many lavas are slightly alkaline olivine tholeiites with diktytaxitic texture; includes some alkali basalt and many compact high-alumina basalts and basaltic andesites. Also includes many andesites and some ash-flow and ash-fall tuff. May be largely absent from the southern Cascades (Smith, 1979).	Uppermost part of Outerson volcanics as mapped by Thayer (1939); uppermost part of Outerson formation as mapped by White (1980a); upper part of Outerson basalt (Hammond and others, 1980); lower part of volcanic rocks of the High Cascades and Boring Lavas (Peck and others, 1964); intermediate series of Avramenko (1981) and Flaherty (1981); probably correlative to Deschutes Formation (Hales, 1975; Taylor, 1981).
Late Western Cascades (18 to 9 m.y. B.P.)	Chiefly intermediate volcanic rocks with common interbedded dacitic tuffs; includes voluminous, highly phyrific two-pyroxene andesite with less basalt, basaltic andesite, and dacitic tuff. Basalts of this group are generally compact and often contain orthopyroxene in the groundmass. This sequence may be very thin or absent in much of the southern Cascades (Smith, 1979).	Sardine series (Thayer, 1936, 1939); Sardine Formation (Peck and others, 1964); Sardine Formation and Elk Lake formation (McBirney and others, 1974; White, 1980a,c); Rhododendron Formation (Hammond, 1979; Hammond and others, 1980, 1982); most of lower part of Outerson volcanics as mapped by Thayer (1939); lower part of Outerson basalt (Hammond and others, 1980).
Early Western Cascades (40 to 18 m.y. B.P.)	Chiefly silicic and tholeiitic volcanic rocks. Interbedded rhyodacitic tuffs and iron-rich tholeiitic basalt, tholeiitic basaltic andesite, and ice-landite with minor rhyodacitic, rhyolitic, and dacitic lavas; local abundant clastic interbeds. This unit contains abundant andesitic lavas in southern Cascades.	Breitenbush tuffs (Thayer, 1936, 1939); Little Butte Volcanic Series (Peck and others, 1964); Breitenbush formation (Hammond, 1979; Hammond and others, 1980); Breitenbush formation and Scorpion Mountain flows (White, 1980a,c).

Figure 2.2. Informal nomenclature utilized in this paper for compositionally distinctive regional episodes of volcanism in the central Cascades. The system is for purposes of discussion only and should not be considered a revision of rock-stratigraphic nomenclature.

Table 2.1 Parameters which distinguish volcanic rocks erupted during various central Oregon volcanic episodes. Andesites, dacites, and tuffs occur in all units and have similar mineralogy and texture in all units. They are not listed if not one of the dominant rock types. cpx = clinopyroxene; opx = orthopyroxene; plag = plagioclase; comp = composition

PARAMETER Age \pm 1 m.y.	EARLY WESTERN CASCADES 40 to 18 m.y. B.P.	LATE WESTERN CASCADES 18 to 9 m.y. B.P.	EARLY HIGH CASCADES 9 to 4 m.y. B.P.	LATE HIGH CASCADES 4 to 0 m.y. B.P.
Characteristic rocks	Rhyodacitic laharc, epiclastic, and ash-flow tuff + silicic tholeiitic lavas and rhyodacite lava	Two-pyroxene andesite + basaltic andesite + dacitic tuff; common autoclastic and epiclastic rocks	Iron-rich basalt + basaltic andesite; some alkaline basalts	Iron-rich basalt + basaltic andesite; some alkaline basalts
Distribution (in Western and High Cascades)	Lower valleys of the Western Cascades	Western Cascade ridges and upper valleys	Western Cascade ridge tops; sides of deepest High Cascade valleys	In High Cascade province and present topographic lows outside the province
Degree of alteration	Moderate to heavy in the tuffs; light to moderate in tholeiitic lavas	Light to moderate in tuffs and andesites; less in basalts	Light to none	Generally none
Dominant alteration (excludes local contact metamorphism)	Zeolite-facies to low-grade propylitic alteration	Low-grade zeolite facies; commonly affects plag and glass	Some alteration of opx + olivine to saponite; plag is fresh	Deuteric only, unless at a volcanic vent
Main area of eruption	Broad area of the Western Cascades	Broad area of the Western Cascades	In and on the margins of the High Cascades	Axis of the High Cascades
Dominant texture of lavas	Compact, aphyric, black tholeiitic lavas and glassy flow-banded rhyolite and rhyodacite	Highly phyrlic to megacrystic andesites with nearly aphyric compact mafic lavas	Slightly phyrlic, compact, gray to black, with some moderately diktytaxitic lavas	Slightly phyrlic, highly diktytaxitic gray to black basalt; compact to slightly diktytaxitic basaltic andesite
Dominant phenocrysts	Rhyodacite = plag + opx; rhyolite = sanidine; tholeiitic lavas = rare plag + altered olivine or clinopyroxene	Dacite = opx + hornblende + plag; andesite = plag + opx + cpx; basaltic andesite = plag + cpx + olivine	Basaltic andesite = olivine + cpx; basalt = olivine	Basaltic andesite = olivine + cpx; basalt = olivine
Dominant groundmass phases	Rhyodacite = altered glass + plag + quartz; rhyolite = altered glass + quartz + alkali feldspar; tholeiitic = pilotaxitic to felty plag + cpx + Fe-Ti oxides	Dacite = hyalopilitic with opx + plag + glass; andesite = pilotaxitic to felty plag + opx + cpx; basaltic andesite = felty to pilotaxitic plag + cpx + Fe-Ti oxide \pm olivine	Basalt andesite = pilotaxitic to felty plag + cpx + minor Fe-Ti oxide; basalt = felty to diktytaxitic plag with subophitic brownish cpx + Fe-Ti oxide \pm olivine	Basaltic andesite = pilotaxitic to felty plag + cpx + minor Fe-Ti oxide; basalt = coarsely diktytaxitic plag with subophitic to ophitic, purplish-brown to brownish cpx + Fe-Ti oxide \pm olivine
Chemical character	Bimodal: calc-alkaline and tholeiitic; both types are quartz-normative	Strongly calc-alkaline	Calc-alkaline to slightly alkaline	Calc-alkaline to slightly alkaline
Most distinctive characteristic	Silicic bimodal comp and consistent alteration	Light to moderately altered calc-alkaline lavas of intermediate composition	Distribution; occurrence of some basalts with Fe-rich comp and diktytaxitic texture	Distribution; highly diktytaxitic basalts; slightly alkaline, Fe-rich comp

"Outerson formation." Data of Priest and Woller (Chapter 3) from the Outerson Mountain area suggest it is largely older than about 6.3 m.y., whereas earlier data placed it between about 6 and 4 m.y. B.P. (e.g., McBirney and others, 1974; White, 1980a,c).

This system also simplifies comparison of widely separated stratigraphic sequences in regional studies. It is particularly useful on compositional diagrams for comparison of units from the major volcanic episodes.

General discussion

The two names "High Cascades" and "Western Cascades" were chosen to conform with previous usage. Mapping of this study and previous work (e.g., Peck and others, 1964; White and McBirney, 1978) indicate that vents in the High Cascade physiographic province and areas immediately adjacent to the province (Figure 2.3) are the sources for most of the latest Miocene and younger volcanic rocks. More silicic volcanic rocks of Oligocene to middle Miocene age characterize much of the Western Cascade physiographic province. Numerous vents of these older rocks in the Western Cascade Range and the supposed absence of lithologically similar rocks east of the High Cascades suggest that the main Oligocene to middle Miocene volcanic axis was in the Western Cascade physiographic province (e.g., Peck and others, 1964; White and McBirney, 1978). There is, however, no proof that Oligocene to middle Miocene vents are not abundant beneath the cover of High Cascade lavas, and some John Day Formation rocks east of the High Cascades are lithologically similar to contemporaneous Western Cascade rocks, according to MacLeod (personal communication, 1982). Spatial separation of the High Cascade and Western Cascade volcanic axes has prompted usage of informal terms such as "volcanic rocks of the High Cascade Range" and "volcanic rocks of the Western Cascade Range" (Peck and others, 1964). Other workers have used terms such as "High Cascades" and "Western Cascades series" or group (e.g., see Hammond and others, 1980; White, 1980c; Avramenko, 1981; Flaherty, 1981). Mapping and numerous K-Ar dates generated for this report (Appendix A) and other recent studies suggest that both the eastward shift or narrowing of the volcanic axis from the Western Cascades to the High Cascades and the change from andesitic to more mafic volcanism occurred between about 10 and 8 m.y. B.P. over large parts of the central Oregon Cascades. A time boundary of 9 m.y. B.P. is a best fit to the current K-Ar data. The two major subdivisions have been further subdivided into "early" and "late" time periods on the basis of

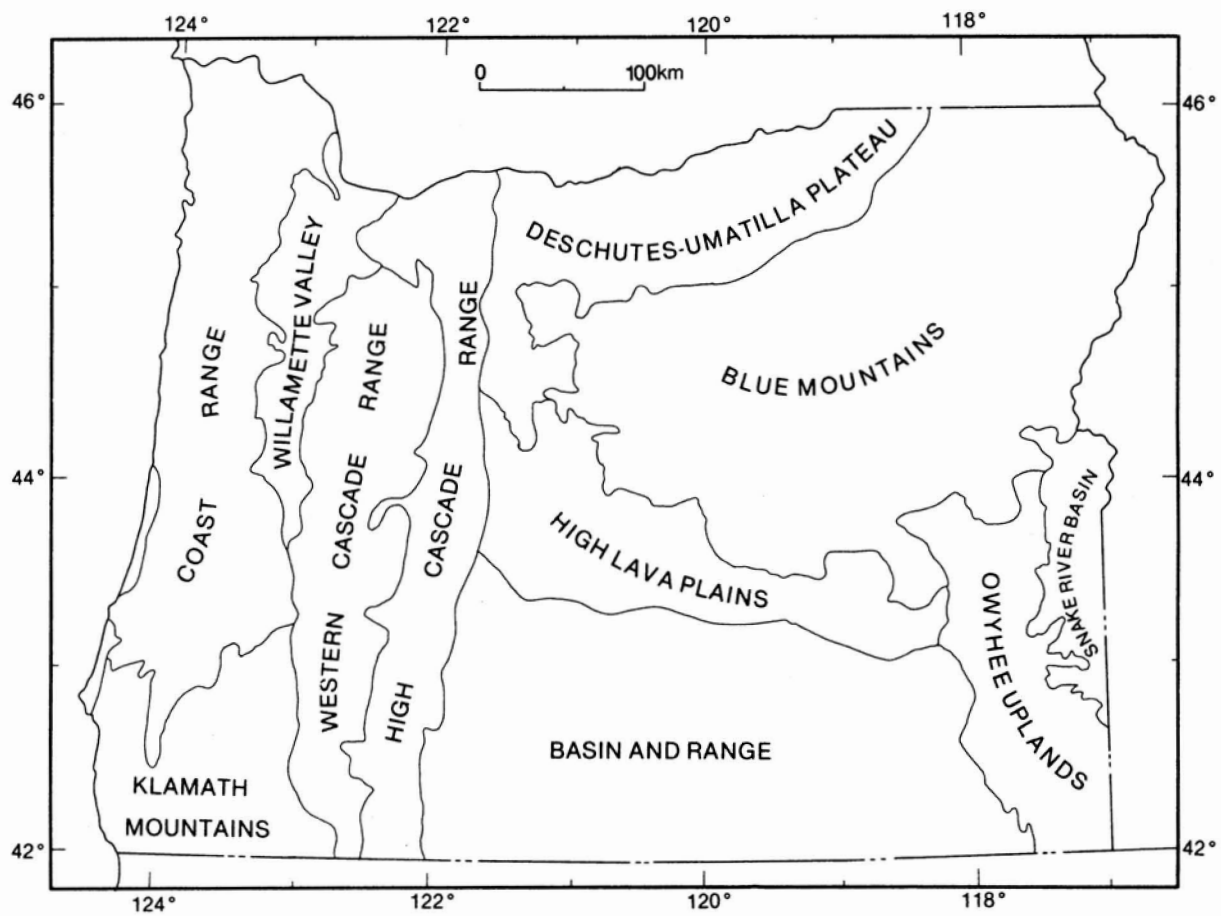


Figure 2.3. Physiographic provinces of Oregon (after Dicken, 1950).

radiometric age data and mappable characteristics of the rocks in each age group.

Early Western Cascade rocks are mostly silicic lavas and tuffs, with fewer mafic flows. These rocks were largely mapped as the Little Butte Volcanic Series by Peck and others (1964), based in part on correlation to the Little Butte Formation of Wells (1956) in the Medford quadrangle. Included in the upper part of this early Western Cascade sequence is a distinctive series of silicic, iron-rich lavas mapped by White (1980a,c) as the Scorpion Mountain lavas. The Scorpion Mountain magma type is probably compositionally unique enough to serve as a mappable unit throughout the central Cascades. It may be that this petrochemical unit and other similar units in younger and older rocks may serve as regional correlation tools when more data are available.

The Oligocene and lower Miocene early Western Cascade rocks are unconformably overlain by middle Miocene lavas and subordinate dacite tuffs. Rocks deposited during the middle Miocene episode are here informally termed volcanic rocks of the late Western Cascades. These rocks have been mapped as Sardine series (Thayer, 1939), Sardine Formation (Peck and others, 1964), and Sardine and overlying Elk Lake formation (White, 1980a,c). The late Western Cascade lavas are predominately highly porphyritic two-pyroxene andesite and fine-grained basalt and basaltic andesite, with typical calc-alkaline chemical composition (i.e., low FeO and high CaO, MgO, and alumina). The erosional unconformity separating the early and late Western Cascade rocks probably spans at least the interval between about 19 and 17 m.y. B.P.; 18 m.y. B.P. has been arbitrarily picked as the boundary between the two volcanic episodes.

Volcanic rocks erupted during the High Cascade episode are generally composed of fresh-appearing basaltic rocks with subordinate amounts of andesite and still smaller amounts of dacite to rhyodacite tuff and lava, all of which erupted within the last 9.0 m.y. Diktytaxitic textures and slightly alkaline, iron-rich compositions are common in the basalts but not as common in the more silicic rocks. Examples of these basalts are the early High Cascade lavas of Tipsoo Butte (see Chapter 4) and late High Cascade lavas at Cupola Rock and Foley Ridge, near McKenzie Bridge (Flaherty, 1981). Although there are some lithologic differences, the early and late High Cascade units are distinguished in the field primarily by the degree to which their distribution is controlled by current topography. The early High Cascade rocks are either in strongly reversed topography or are obviously displaced into lows created by faulting which occurred about 5 to 4 m.y. B.P. These early High Cascade lavas and tuffs

have been called the Outerson formation (e.g., McBirney and others, 1974; White, 1980a,c). Where these early High Cascade rocks are present beneath late High Cascade units in the High Cascade physiographic province, Taylor (1980) informally called them the Plio-Cascades.

The distribution of late High Cascade volcanic rocks is, in contrast, clearly controlled by present topography. The main topographic lows controlling the distribution of late High Cascade lavas in the central High Cascades are a series of grabens which appear to have caused general subsidence of the High Cascade axis relative to adjacent areas between 5 and 4 m.y. B.P. (e.g., see Taylor, 1980). Westward and eastward drainages crossing the horsts on either side of the grabens cut rapidly downward after the early Pliocene faulting and uplift, producing more than a kilometer of erosion over a period of as little as 1.6 m.y. (e.g., Flaherty, 1981; Priest and Woller, Chapter 4). These drainages hold numerous basaltic flows of the late High Cascades. The late High Cascade episode is informally defined as the period between 4 and 0 m.y. B.P. and can be most easily recognized on the margins of the High Cascade physiographic province where the early Pliocene erosion creates a steeply unconformable contact.

Rocks deposited during both the late and early High Cascade episodes have been recognized as a petrogenetically related group by earlier workers. They were grouped together as the "volcanic rocks of the High Cascades" by Thayer (1936, 1939) and Peck and others (1964) after terminology of Callaghan (1933). The two units also correspond to the High Cascade series of Williams (1949) as used by White (1980c). Data of this study suggest that the two units are essentially one compositional type. Because of this close compositional similarity, where the distinction between early and late High Cascade volcanism is not marked by mappable characteristics such as the previously mentioned unconformity, K-Ar dating may be necessary to distinguish between the two units. In such instances the distinction may not be useful.

In the north Cascades around Mount Hood, uplift adjacent to downfaulted areas of the High Cascade axis occurred after 3.0 m.y. B.P. (Priest, 1982). Therefore, faulted, high-standing rocks include late High Cascade units of 3 to 4 m.y. age. Reconnaissance mapping by Smith (1979) in the southern Oregon Cascades suggests that there is no obvious distinction between rocks of early High Cascade and late Western Cascade age, and they are mapped there as one unit. The nomenclature presented here is thus mainly useful in the central Cascades,

particularly in the Western Cascade province where the writers have mapped, and may not be practical in other parts of the Cascades. We anticipate that this informal nomenclature will be replaced by a workable rock-stratigraphic system as detailed map coverage becomes available. The following sections describe the rocks of each of these age groups where they have been mapped in detail in the central Cascades.

Volcanic rocks of the early Western Cascades (40-18 m.y. B.P.)

Early Western Cascade rocks are chiefly ash-flow tuffs, debris flows, lava flows, and epiclastic mudstone and sandstone, with some distinctive siliceous, iron-rich tholeiitic lavas interbedded in the upper part. In the regional mapping of Peck and others (1964), these rocks were generally named the Little Butte Volcanic Series, although the tholeiitic lavas were sometimes mistaken for the Columbia River Basalt Group (e.g., see White, 1980a,c; Lux, 1981, 1982).

In the Breitenbush Hot Springs area, the sequence is represented by moderately altered ash-flow tuff and interbedded epiclastic rocks called the Breitenbush tuff or Breitenbush formation (e.g., Thayer, 1936, 1939; Hammond, 1979; Hammond and others, 1980; White, 1980a,c). The Breitenbush rocks are overlain by a series of black tholeiitic basaltic andesite, icelandite, and iron-rich dacite flows called the Scorpion Mountain lavas by White (1980a,c). No radiometric dates which the writers consider reliable are available for the altered pyroclastic rocks, but ages of 27 to 19 m.y. B.P. have been reported by White (1980a,c) for the Scorpion Mountain magma type in various localities in the central Western Cascades.

In the Belknap Hot Springs-Cougar Reservoir area, moderately altered ash-flow tuffs, laharic tuffs, epiclastic rocks, and subordinate rhyodacitic to dacitic lavas make up the early Western Cascade section. These rocks are called the tuffs of Cougar Reservoir by Priest and Woller (Chapter 4) and are intruded by and overlain with steep angular unconformity by late Western Cascade volcanic rocks. These late Western Cascade rocks have an oldest K-Ar date of 16.3 m.y. B.P. Immediately west of the Cougar Reservoir area, the older tuffs are reportedly intruded by the Nimrod stock, dated by Sutter (1978) at 16.3 ± 0.2 m.y. B.P. (recalculated by Fiebelkorn and others, 1982).

Early Western Cascade rocks also crop out in the Lookout Point Reservoir area where they have been mapped in detail by Woller and Priest (Chapter 5, this volume). Ash-flow tuffs, laharic tuffs, epiclastic rocks, and subordinate

silicic lavas are overlain by and interbedded with a series of tholeiitic lavas similar to the Scorpion Mountain lavas of White (1980a,c). The tholeiitic lavas in the overlying sequence (the lavas of Black Canyon) yielded minimum K-Ar dates of about 22 m.y. B.P. The lavas of Black Canyon are in turn overlain by late Western Cascade lavas whose oldest K-Ar date is 15.9 ± 7.6 m.y. B.P. A slightly altered basaltic andesite flow in the tuffs underlying the Black Canyon rocks yielded a minimum age of 24.7 ± 2.0 m.y.

Sanidine-phyric rhyolitic lavas occur at the top of the early Western Cascade section in the Hills Creek dam area, immediately south of Lookout Point area (e.g., see Brown and others, 1980b). A minimum age of 17.3 ± 0.7 m.y. was obtained on a sanidine separate from a moderately altered rhyolite sample (sample OM-520 of Brown and others, 1980b). The age probably reflects resetting of the K-Ar age by late Western Cascade hydrothermal activity. K-Ar ages of 21.3 ± 1.0 m.y. obtained on dacite from Stone Mountain and 18.7 ± 0.9 m.y. obtained on basalt near Groundhog Mountain (see Brown and others, 1980b) in the Hills Creek Dam area are probably better approximations of the ages of the uppermost rocks of the early Western Cascades section there.

Smith and others (1980) traced a biotite-bearing ash-flow tuff near the base of the early Western Cascades section from the southwestern Cascades to the central Cascades. They obtained a high-quality K-Ar date of 34.9 m.y. B.P. Lux (1982) considers the base of the Little Butte Volcanic Series to be about 40 m.y. B.P. and lists one date of 41.5 ± 0.9 m.y. B.P. Until other data become available, 40 m.y. is here considered to be the older age limit of the early Western Cascade sequence in the central Cascades. The younger age limit is arbitrarily placed at 18 m.y., about 1 m.y. younger than the youngest age obtained for rocks of the Scorpion Mountain magma type and about 1 m.y. older than the oldest dated rocks which probably overlie Scorpion Mountain-type rocks.

Paucity of K-Ar dates in the 19- to 17-m.y. B.P. interval suggests a lull in regional volcanic activity, although this may simply be a reflection of the limited data available. Widespread occurrence of an erosional unconformity with high relief at the top of the early Western Cascades sequence (e.g., discussion of the Sardine-Little Butte contact by Peck and others, 1964) is evidence that this time may have been one of uplift as well. The steep intra-canyon relationships between the 22-m.y. B.P. Black Canyon lavas and underlying silicic tuffs (Woller and Priest, Chapter 5) suggest that this uplift may have

started prior to 22 m.y. B.P.

Volcanic rocks of the late Western Cascades (18-9 m.y. B.P.)

Rocks of the late Western Cascades are chiefly calc-alkaline lavas and debris flows of intermediate composition with subordinate dacitic ash-flow and ash-fall tuff. Basalt and basaltic andesite may be locally abundant, but these mafic lavas rarely reach compositions as iron-rich as the overlying High Cascade lavas or underlying tholeiitic lavas of the early Western Cascades. Peck and others (1964) mapped these rocks as the Sardine series after terminology of Thayer (1936, 1939).

Sardine Mountain in the Breitenbush Hot Springs area is the type locality of the Sardine series of Thayer (1936, 1939). Predominance of andesitic lavas over tuffaceous rocks in this sequence was the feature used by Thayer (1936, 1939) to distinguish these late Western Cascade lavas from the underlying early Western Cascade sequence (Breitenbush tuff). A disagreement has arisen among workers in the area concerning the relative position of the Sardine series of Thayer (1939) and the Breitenbush tuff. The Breitenbush tuff and Sardine series are apparently in fault contact on the western limb of the Breitenbush anticline. It is disagreement on the direction of displacement on this fault and the absence of reliable radiometric data at Sardine Mountain which have caused confusion. White (1980c) shows the lavas of Sardine Mountain as younger than the Breitenbush tuff, whereas Hammond and others (1980) interpret the lavas as older than the tuff. Lavas correlated with the Sardine Mountain lavas by White (1980a,c) have oldest and youngest K-Ar dates of 17.2 and 11.2 m.y. B.P. (White, 1980a,c). They are in turn overlain by a group of andesitic lavas called the Elk Lake formation which erupted between about 11.8 and 9.8 m.y. B.P. (McBirney and others, 1974; White, 1980a,c). Much of the sequence mapped as Elk Lake formation and Sardine Formation by White (1980a,c) is mapped as Rhododendron Formation and the lower part of the Outerson basalt by Hammond and others (1980, 1982).

Mapping for this study (Priest and Woller, Chapter 3) in the Outerson Mountain-Devils Creek area has shown that slightly altered basalts, basaltic andesites, and subordinate andesites found there are probably 9.5 ± 1.2 m.y. B.P. and older. These rocks are, in part, age equivalents to the Elk Lake formation and Sardine Formation of White (1980a,c), as well as the Rhododendron Formation of Hammond and others (1980, 1982). They have been informally named the lavas of Outerson Mountain by Priest and Woller (Chapter 3). The lavas of Outerson

Mountain are overlain by undated andesitic to dacitic nonwelded ash-flow tuffs (the tuffs of Outerson Mountain) which fill a steep paleotopography (e.g., Clayton, 1976; Priest and Woller, Chapter 3). These ash flows are overlain by fresh-appearing early High Cascade mafic and subordinate andesitic lavas whose oldest K-Ar date is 6.3 ± 0.2 m.y. B.P. This date was obtained at the top of Outerson Mountain, where only one flow of early High Cascade lava is present. The late Western Cascade sequence in this area was therefore deposited mainly between about 17.2 and 9.5 m.y. B.P.

The Belknap-Foley area has a late Western Cascade section dominated by megacrystic two-pyroxene andesite with subordinate basaltic andesite and dacite ash-flow and ash-fall tuff. The oldest radiometric date is 16.3 m.y. B.P. on the glassy plug which forms the abutments of Cougar Dam; the youngest reliable date is 8.8 ± 0.3 m.y. B.P. at the top of the section at Lookout Ridge. The sequence is capped by iron-rich diktytaxitic basalts on the east side of Cougar Reservoir (the lavas of Tipsoo Butte) and at Lookout Ridge. These lavas have dates on basal flows of 8.34 ± 0.36 m.y. B.P. at Lookout Ridge and 7.80 ± 0.77 m.y. B.P. at Cougar Reservoir. Flaherty (1981) noted a small unconformity in the late Western Cascade sequence below the uppermost 9.3- to 8.9-m.y. B.P. dacite flows in the Belknap Hot Springs area, although no similar unconformity was noted by Priest and Woller (Chapter 4) to the west at Cougar Reservoir. There is also no evidence of a widespread unconformity between 15 and 11 m.y. B.P. which was noted by McBirney and others (1974) in their study of the region (i.e., between their Sardine and Elk Lake formations). A large volume of lava and tuff at Cougar Reservoir has ages in this interval.

A sequence of two-pyroxene andesite lavas occurring in the Lookout Point area have top and bottom flows dated at 8.3 ± 5.5 m.y. B.P. and 15.9 ± 7.6 m.y. B.P., respectively (Woller and Priest, Chapter 5). At Patterson Mountain, this late Western Cascade section is capped by an early High Cascade basaltic flow dated at 5.81 ± 0.30 m.y. B.P.

In the Swift Creek area, the late Western Cascade sequence is composed of large volumes of both two-pyroxene andesite and basalt to basaltic andesite (Woller, Chapter 6). Although the base of the section is not exposed, the oldest reliable age is about 17.0 ± 0.19 m.y. B.P., and the youngest dated flow is about 13.1 ± 0.6 m.y. B.P. These flows are capped by basal early High Cascade basalts K-Ar dated at 5.56 ± 0.34 m.y. B.P.

Substantial time gaps of 3 to 8 m.y. occur between rocks of the early High

Cascade and late Western Cascade episodes in the Breitenbush, Lookout Point, and Swift Creek areas, but no apparent time gap exists in the Belknap Hot Springs area. It is likely that, whereas local areas have experienced episodic volcanism, the central Cascades region as a whole has had relatively continuous volcanism during late Western Cascade and early High Cascade time. A large number of late Western Cascade volcanic centers, however, occur several kilometers west of early High Cascade volcanic centers (Peck and others, 1964; Priest and Woller, Chapter 4). Both an eastward shift or narrowing of volcanism and a switch to more mafic composition appears to have occurred about 10 to 8 m.y. B.P. A good compromise with the available dates is 9 m.y. B.P. for the top boundary on the late Western Cascade episode. The bottom boundary has been arbitrarily assigned at 18 m.y. B.P., as previously explained.

Volcanic rocks of the early High Cascades (9-4 m.y. B.P.)

Early High Cascade volcanic centers produced voluminous basalts and basaltic andesites and much less abundant andesite lava and dacitic ash-flow and ash-fall tuff. The eruptions occurred from a large area probably mostly within the High Cascade physiographic province. White and McBirney (1978) estimate that volcanic rocks of this episode erupted from an area about twice as broad as the High Cascade physiographic province. Numerous vents for these rocks have been recognized a few kilometers west of the High Cascade province (e.g., Hammond, 1979; Hammond and others, 1980, 1982; White, 1980a,c), and compositionally and temporally similar rocks of the Deschutes Formation were erupted from vents along the central High Cascades and its eastern margin (e.g., Hales, 1975; Taylor, 1973b, 1981). In the Western Cascade physiographic province, early High Cascade rocks are the relatively unaltered mafic to intermediate lavas which cap the highest ridges. These rocks are the extensive ridge-capping units labeled QTba, QTp, Tpb, and QTV on various regional compilation maps of the Western Cascades (e.g., Wells and Peck, 1961; Peck and others, 1964).

In the Breitenbush Hot Springs area, the early High Cascade sequence is chiefly fresh basalt, basaltic andesite, and subordinate andesite flows which occur along ridge tops in the steep Western Cascade terrain. A few of the basalt flows have a somewhat alkaline composition, with olivine in the groundmass. Many of the basalts have ophitic clinopyroxene in the groundmass (e.g., White, 1980a). Examples of these alkaline basalts were described by White (1980a) northwest of Breitenbush Hot Springs (e.g., his sample number 18). The

early High Cascade lavas described by Priest and Woller (Chapter 3) in the Outerson Mountain-Devils Peak area are, however, chiefly basaltic andesites with some basalt and dacite. Priest and Woller (Chapter 3) note that an early High Cascade basalt capping the ridge south of Outerson Mountain contains more abundant groundmass olivine compared to underlying late Western Cascade basalts. The oldest early High Cascade flow so far reliably dated in this area occurs at the top of Outerson Mountain and has a date of 6.3 ± 0.2 m.y. B.P. This flow correlates roughly with the upper Miocene-Pliocene lavas which yielded a date of 6.0 ± 0.9 m.y. B.P. (Priest and Woller, Chapter 3). The youngest date, 3.6 m.y. B.P., was obtained on a lava mapped at Breitenbush Mountain as Outerson formation by White (1980a). The oldest date in late High Cascade lavas is 4.2 ± 0.3 m.y. B.P. (Hammond and others, 1980).

In the Belknap-Foley area volcanic rocks of the early High Cascade episode are iron-rich basalts and basaltic andesites with subordinate andesite and minor tuff which occur at the highest elevations on some Western Cascade ridges. Diktytaxitic texture is common in basalts at the base of the early High Cascade section at Cougar Reservoir (lavas of Tipsoo Butte), although the texture is not as coarsely developed as in basal late High Cascade lavas which occur in the McKenzie River drainage at Foley Ridge and Cupola Rock (e.g., see descriptions by Flaherty, 1981). Some diktytaxitic samples of the lavas of Tipsoo Butte have subophitic clinopyroxene which in thin section is brownish in plain light. The brownish hue and high TiO_2 in whole-rock analyses suggest that the clinopyroxene is titaniferous. Similar titaniferous clinopyroxene was noted in slightly alkaline late High Cascade lavas at Cupola Rock (Flaherty, 1981). A basal flow dated at 7.80 ± 0.77 m.y. B.P. at Tipsoo Butte is overlain by a flow dated 9.4 ± 0.4 m.y. B.P., and a date of 10.2 ± 2.0 m.y. B.P. was at English Mountain on a stratigraphically higher flow (Appendix A). It may be that the mode of eruption or some other factor causes these volatile-rich diktytaxitic basalts to be incompletely degassed of radiogenic argon during cooling. The bulk of K-Ar data obtained by both Flaherty (1981) and this study suggests that a K-Ar date of 8.34 ± 0.36 m.y. B.P. on a basal flow at Lookout Ridge is probably the oldest reliable date for rocks of the early High Cascade episode in this area. The youngest available date is 3.88 m.y. obtained at Lookout Ridge by Sutter (1978), but some doubt about the sample location has been voiced by several workers in the area. The youngest reliable date is 5.0 m.y. B.P., obtained by E. M. Taylor (1981) on a basaltic ash flow near Trailbridge Reservoir. The oldest K-Ar date

in nearby late High Cascade lavas is 3.9 m.y. B.P. (Taylor, 1980).

High-alumina basalt, high-alumina basaltic andesite, and dacitic to rhyodacitic tuffs of the Deschutes Basin (Taylor, 1973b) are probably early High Cascade units, at least in part. Diktytaxitic, iron-rich, slightly alkaline basalts are common in this sequence, although ash-flow and air-fall tuff and epiclastic deposits are also common, especially eastward away from the High Cascades (e.g., see Taylor, 1973b; Hales, 1975; Taylor, 1980). Rimrock basalts of the Deschutes Basin have yielded several K-Ar ages of about 4.8 m.y. (Taylor, 1973b), although an age of 10.7 ± 1.2 m.y. was recently determined on the same or a similar lava by Bunker and others (1982). Basalt flows at the top of the Green Ridge scarp have dates as recent as 5.2 m.y. B.P., and a flow near the top of a fault block on the west side of the Green Ridge fault has a K-Ar date of 4.5 ± 0.4 m.y. B.P. (Hales, 1975). An anomalously old date of 9.2 ± 0.6 m.y. B.P. was also obtained from a basalt from the crest of Green Ridge; hornblende separated from lavas below the basalts yielded a K-Ar date of 8.0 ± 0.6 m.y. B.P. (Hales, 1975). The 8.1-m.y. B.P. date is representative of the oldest part of the sequence. The 9.2-m.y. B.P. date may be another example of excess radiogenic argon noted above in the Belknap Hot Springs area, where anomalously old dates were obtained on early High Cascade lavas. Late High Cascade lavas K-Ar dated at about 2.5 m.y. B.P. bank up against the Green Ridge fault (Armstrong and others, 1975; Hales, 1975). The oldest part of the Deschutes Formation may be as old as 12 m.y. B.P. (Taylor, 1973b), although Taylor (personal communication, 1981) indicated that the base of the part of the formation characterized by iron-rich basalt is probably about 9 m.y. B.P. The part of the Deschutes Formation corresponding compositionally to the volcanic rocks of the early High Cascades was probably deposited between about 9 and 4.5 m.y. B.P.

In the Lookout Point area, one dense basalt near the top of Patterson Mountain yielded a K-Ar age of 5.8 ± 0.3 m.y. A small, locally erupted late High Cascade flow, intracanyon into older rocks in the same area at Armet Creek, was K-Ar dated at 0.56 ± 0.16 m.y. B.P. The High Cascade section as a whole is very thin and unrepresentative in this area owing to the great distance from High Cascade sources.

A thin sequence of compact basalt flows in the Swift Creek area near Diamond Peak caps late Western Cascade basalts of almost identical aspect. The top and bottom flows of this early High Cascade section yielded K-Ar dates of 4.3 ± 0.4 m.y. B.P. and 5.56 ± 0.34 m.y. B.P., respectively. The oldest late High Cascade

flow is an intracanyon diktytaxitic basalt which yielded a K-Ar date of 1.98 ± 0.25 m.y. B.P.

Numerous diktytaxitic basalts capping Western Cascade ridges throughout the area between Lookout Point and Swift Creek have been described by Brown and others (1980b). The diktytaxitic texture is thus common in the region, although lacking in local areas. Where it is absent and where underlying late Western Cascade rocks are nearly unaltered basalts, the contact may be difficult to locate. This was certainly the case at Swift Creek, even though there is about a 7.5-m.y. age difference across the contact.

The bulk of the K-Ar data supports placing the lower time boundary of the early High Cascade episode at about 9.0 m.y. B.P., based chiefly on the Breitenbush and Belknap Hot Springs data. The upper boundary should be placed at about 4 m.y. B.P., based on the uppermost basalt flows at Breitenbush, Green Ridge, and Swift Creek and the lowermost late High Cascade flow dated near Belknap Hot Springs. The data presented here suggest the possibility that if more dates were available from within the High Cascade province (the probable source for much of both the early and late High Cascade rocks), there would be no significant time gaps in the High Cascade volcanism on a regional scale.

Volcanic rocks of the late High Cascades (4-0 m.y. B.P.)

North-south faulting and formation of probable grabens in much of the central Oregon High Cascades between 5 and 4 m.y. B.P. was followed by eruption of voluminous flows of diktytaxitic basalt and basaltic andesite from contiguous shield volcanoes forming a low platform in the High Cascades (Taylor, 1980). These initial basaltic flows reached deep into the Western Cascade province through canyons, some of which were carved into escarpments bounding the grabens. The distribution of these Pliocene to early Pleistocene intracanyon basalts is clearly related to present topographic lows, distinguishing them from similar early High Cascade basalts and basaltic andesites which cap the highest Western Cascade ridges. Basaltic andesite increases in abundance relative to basalt in progressively younger Quaternary flows (Taylor, 1980). The compositionally caused increasing viscosity of these flows restricted them to the High Cascade axis. Basaltic andesite and less abundant andesite, dacite, and rhyodacite form prominent Quaternary composite cones in local areas which, although imposing, are far smaller in volume than coeval basalt and basaltic andesite on the platform (e.g., see Taylor, 1980). Mount Hood, Mount Jefferson, the Three Sisters, Diamond Peak, and Mount Mazama (Crater Lake) are some of the largest composite

cones.

In the Breitenbush Hot Springs area, late High Cascade lavas are chiefly basalt and basaltic andesite flows and cinder cones of very fresh aspect. The distribution of the lavas is obviously controlled by existing topography. The volcanic vents often display original volcanic landforms which are preserved with little erosional modification. The oldest flow in this sequence dated by White (1980a,c) is 1.97 ± 0.27 m.y. B.P.; Hammond and others (1980) list a 4.2 ± 0.3 -m.y. B.P. date on a basal High Cascade tephra deposit. Some of the youngest rocks in this area are post-glacial debris flows from Mount Jefferson and volcanic flows around Ollalie Butte (Hammond and others, 1980).

In the Belknap Hot Springs area, north-south- to northwest-trending faults drop the High Cascade province down relative to uplifted areas of the Western Cascades. These faults were first noted by Thayer (1936) and Taylor (1980) and mapped in reconnaissance by Brown and others (1980a). They were later verified by detailed mapping of Flaherty (1981) and Avramenko (1981). A thick sequence of Pliocene basalt, which Jan (1967) and Flaherty (1981) found to be anomalously alkali-rich, banks up against these east-facing fault scarps. The best examples of these alkali-rich basalts occur at Cupola Rock (Flaherty, 1981) and Scott Creek (Jan, 1967). The Scott Creek sequence is particularly interesting, since it contains pillow basalts indicative of lakes (Jan, 1967) which may have been temporarily dammed by lava along the fault scarps (Taylor, 1980). The basal basalts are highly diktytaxitic and, where alkali-rich and nearly holocrystalline, have purplish-brown titaniferous clinopyroxene in the groundmass (Flaherty, 1981). The sequence has more basaltic andesite at higher levels, and the diktytaxitic texture becomes less common in the more siliceous flows. The oldest date so far obtained is about 3.9 m.y. B.P., and the youngest eruptions are those which occurred from Belknap Crater about 1,500 yr ago (Taylor, 1968, 1980).

The late High Cascades are represented in the Lookout Point area by only two flows (see Chapter 5). The High Prairie flow, a diktytaxitic basalt flow dated at 11.01 ± 0.15 m.y. B.P. (Sutter, 1978), flowed from the High Cascades down the North Fork of the Middle Fork of the Willamette River. Woller and Priest (Chapter 5) and others question the date that Sutter obtained on this flow. The sample location indicated by Sutter had only glacial debris overlying the flow. The Armet Creek basaltic andesite flow was dated at 0.56 ± 0.16 m.y. B.P. and erupted from a local vent at the head of the creek a few kilometers northeast of Lookout Point Reservoir (Woller and Priest, Chapter 5).

The late High Cascade sequence in the Swift Creek area is composed chiefly of intracanyon diktytaxitic and compact basalt flows which appear to have erupted from the vicinity of Diamond Peak (Woller, Chapter 6). The oldest flow yielded a K-Ar date of 1.98 ± 0.25 m.y. B.P.; the youngest dated flow had a K-Ar date of 0.17 ± 0.48 m.y. B.P.

As explained in the previous section, the lower boundary of the late High Cascade episode is 4.0 m.y. B.P. The youngest High Cascade eruptions in Oregon were at Mount Hood in 1859 and 1865 A.D. (Crandell, 1980).

STRUCTURAL GEOLOGY

Introduction

The central Oregon Cascades have numerous lineaments and known structures which strike northwest, northeast, and north-northwest to north-south (e.g., see Peck and others, 1964; Venkatakrishnan and others, 1980; Kienle and others, 1981). Few of these lineations and structures have been mapped in detail, so only tentative conclusions can be made on the overall history of deformation in the Cascades. This section will present what is known about the structure from geologic mapping and suggest some possible interpretations of the limited data base. Various major lineations of Lawrence (1976) and some mapped faults and Quaternary volcanic centers are shown in Figure 2.4. Figure 2.5 illustrates schematically some periods of faulting and folding in various mapped areas in the northern and central Cascades.

North-south and north-northwest-trending faults

North-south faults thus far mapped are concentrated along the eastern margin of the Western Cascade physiographic province (Figure 2.4). Williams (1942) inferred from the linearity of the High Cascade-Western Cascade boundary that it was fault controlled. These faults bound blocks which drop the High Cascade province down relative to adjacent areas at Mount Hood (Williams and others, 1982; Priest, 1982; Priest and others, 1982a), Green Ridge (Hales, 1975), the McKenzie River-Horse Creek area (Taylor, 1973a; Brown and others, 1980a; Avramenko, 1981; Flaherty, 1981), Cougar Reservoir (Priest and Woller, Chapter 4), possibly the Walker Rim area (Wells and Peck, 1961), the Mount Bailey-Diamond Lake area (Barnes, 1978), and possibly Lake of the Woods (Maynard, 1974). Williams (1942) inferred from the high elevation of the Western Cascades west of Crater Lake relative to High Cascade outcrops to the east that there was a major fault scarp

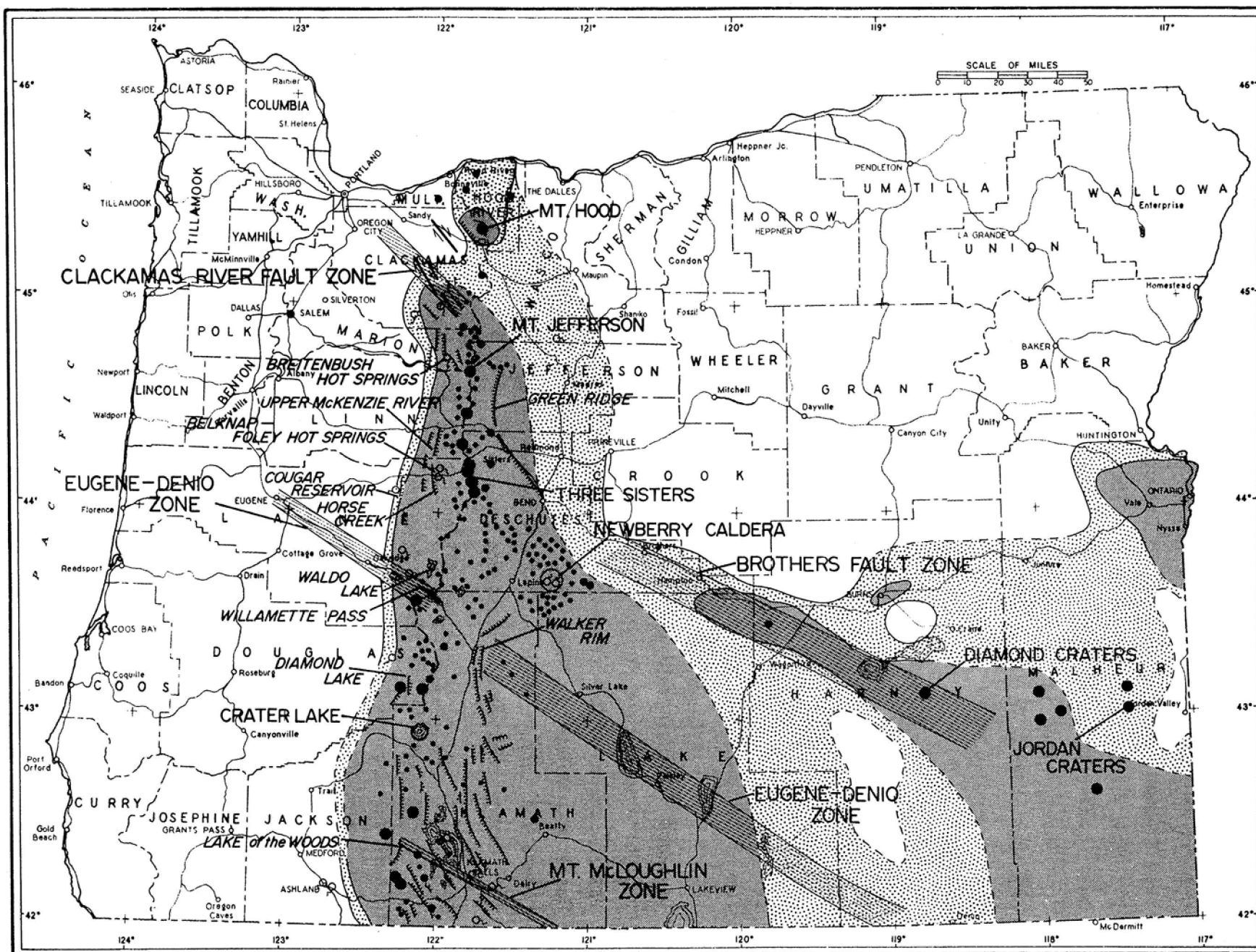


Figure 2.4 (facing page). Map showing some major faults, lineaments, hot springs and Quaternary volcanic centers relative to zones of anomalously high heat flow in the Cascades and adjacent areas of Oregon. Geologic data are from Wells and Peck (1961), Hales (1975), Peterson and others (1976), Walker (1977), Barnes (1978), Beeson and Moran (1979), Brown and others (1980a), Hammond and others (1980), Avramenko (1981), Flaherty (1981), Priest and others (1982), and Beeson and others (in preparation). Heat-flow data are from Blackwell and others (1978) and Black and others (Chapter 7).

<u>Dark gray</u>	= heat flow over 100 mW/m^2
<u>Light gray</u>	= heat flow between 100 mW/m^2 and 80 mW/m^2
<u>Hachured lines</u>	= mapped normal faults, hachured on the downthrown side. Only faults in or closely adjacent to areas of high heat flow in the Cascades are shown; areas west of the high-heat-flow zone tend to have fewer well-defined fault scarps, partly because less mapping has been done in those areas and possibly also because the faulting is older.
<u>Line with offset arrows</u>	= lateral fault showing relative displacement.
<u>Solid dots</u>	= Quaternary volcanic centers. Size of dot is crudely related to the size of the volcanic center relative to other centers. Many more centers exist than are shown, particularly in the High Cascades, but scale does not allow more detail:
<u>Large circles</u>	= calderas (diameter = actual diameter).
<u>Diagonal-line pattern</u>	= major northwest-trending lineations; names are from Lawrence (1976); Clackamas River fault zone is from Anderson (1978) and Beeson and others (1982).
<u>Open circle with curved line</u>	= thermal springs in and adjacent to the Cascades.

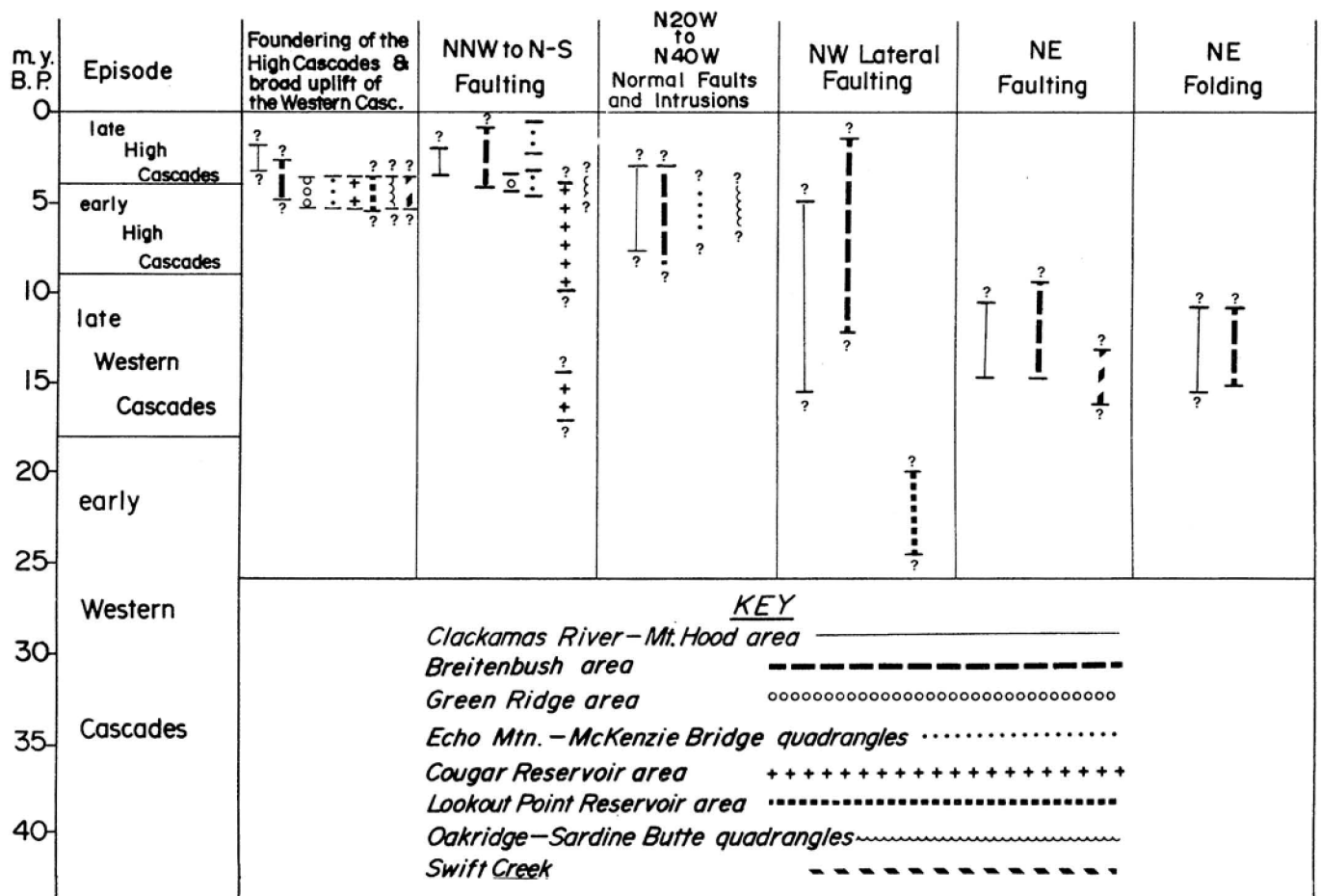


Figure 2.5. Episodes of deformation in some mapped areas of the northern and central Cascades. Data from Hales (1975), Hammond and others (1980), Taylor (1980), White (1980a,c), Avramenko (1981), Flaherty (1981), Priest and Woller (Chapters 3 and 4), Woller and Priest (Chapter 5), and Woller (Chapter 6).

on the east boundary of the Western Cascades there. North-south faults have also been mapped in the upper Breitenbush Hot Springs area (Hammond and others, 1980; White, 1980a,c). Whereas the Breitenbush faults have a complex pattern of displacement, it is possible that net subsidence of the High Cascade axis relative to adjacent uplifted areas has occurred there also (Thayer, 1936, 1939; White, 1980c), although Rollins (1976) and Hammond and others (1982) found no evidence of this. Similar unmapped faults may be manifested by lineations following the western boundary of the High Cascade province from Horse Creek to Crater Lake (e.g., see Venkatakrishnan and others, 1980; Kienle and others, 1981). Steep east-dipping gravity gradients on both Bouguer and residual anomaly maps bound the High Cascade province along a north-south zone (Couch and others, 1978; Pitts and Couch, 1978; Pitts, 1979) and have been interpreted to be the result of faults (e.g., Pitts, 1979; Priest and others, 1980; Flaherty, 1981).

The amount of downward displacement on the High Cascade axis relative to adjacent areas east and west of the axis is at least several hundred meters in most places and may exceed 1 km in the central Cascades. On the west side of Mount Hood the Columbia River Basalt Group (CRBG) is displaced downward in the Old Maid Flat area (Beeson and Moran, 1979; Beeson and others, in preparation), and at least another 400 m of down-to-the-east displacement probably occurs on a northwest-trending fault at Old Maid Flat (Priest and others, 1982a). At least 600 m of down-to-the-west movement has been estimated on the Hood River fault east of Mount Hood (N. M. Woller, unpublished mapping). White (1980c) estimates that the Mount Jefferson block has subsided about 750 m on north-south-trending faults in the Breitenbush Hot Springs area relative to uplifted adjacent areas. Hammond and others (1982), however, do not see any evidence for this subsidence. Hales (1975) and Taylor (1980) estimate that the same block is displaced downward on the Green Ridge boundary fault by at least 900 m. Taylor (1980) emphasizes that the Mount Jefferson-Three Sisters block may have subsided much more than 900 m and argues that no uplift or tilting is necessary to explain the attitude of rocks in the Green Ridge block. Down-to-the-east faults occur on the west side of the Three Sisters area along the Horse Creek-McKenzie River fault zone, where about 620 m of displacement occurs (Flaherty, 1981). Sixteen kilometers west of Horse Creek, the Cougar Reservoir fault zone has at least 152 m of similar displacement (Priest and Woller, Chapter 4). Barnes (1978) shows north-south to north-northeast, down-to-the-east faults which bound the west side of the High Cascade province. A fault analogous to the fault on the west side of Diamond

Lake also occurs west of Lake of the Woods in the southern Cascades (Maynard, 1974). In view of the large number of north-south volcanic vent alignments in the central High Cascades, it is possible that additional north-south faults are buried by late High Cascade lavas within the High Cascade province, although these alignments could be passive features controlled by the orientation of the regional stress field (e.g., see Nakamura, 1977).

Although stratigraphic offsets prove large dip-slip displacements, some horizontal and near-horizontal slickensides on the north-south-trending faults show that some lateral movement has also occurred. Beeson and Moran (1979) and Beeson and others (in preparation) found subhorizontal slickensides on the Hood River fault zone bounding the Mount Hood subsidence block on the east, although Woller (unpublished detailed mapping) found only slickensides raking 90° on this zone in an adjacent area. Priest and Woller (Chapter 4) noted horizontal slickensides on splinters of the Cougar Reservoir fault above Cougar Dam.

Age of north-south and north-northwest-trending faults

Most of the movement on major north-south-trending faults in the central Cascades occurred during the early Pliocene, although older and younger displacements have been documented in various places. Most offset on faults bounding the central High Cascade province occurred between 4 and 5 m.y. ago (e.g., Hammond and others, 1980; Taylor, 1980). Faults in the upper McKenzie River area which bound the western side of the central High Cascades block had last movements between 1.0 and 0.7 m.y. B.P., although large movements also occurred during the early Pliocene (Avramenko, 1981). North-south- to northwest-aligned Holocene basaltic vent strings associated with the Belknap Crater-Nash Crater-Sand Mountain eruptions west of the Three Sisters suggest that the north-south-trending faults may still be active enough to channel magma to the surface. As previously mentioned, however, there is no documented example of faults cutting these Holocene deposits, and the vent alignments could be a passive product of the orientation of the regional stress field (e.g., see Nakamura, 1977).

The oldest documented north-south fault in the central Cascades is probably the Cougar Reservoir fault. The fault appears to control a 16.3 ± 1.8 m.y. B.P. glassy dacite intrusion which is strongly elongated north-south (Priest and Woller, Chapter 4). Dikes filled with both magmatic material and explosion breccias occur within the intrusion following northwest- to north-northwest-trending shears and fissures. The fault, however, also offsets lavas dated at

13.2±0.7 m.y. B.P. by at least 152 m, so considerable movement younger than 13.2 m.y. B.P. has also occurred. Stratigraphic relationships between early High Cascade lavas and the Cougar fault suggest that the fault may have had major movement prior to 7.8 m.y. B.P. and during the period between 7.8 and about 5.0 m.y. B.P. (Priest and Woller, Chapter 3). It is not known whether additional offset occurred during the 5- to 4-m.y. B.P. faulting episode which occurred at Horse Creek to the east, but there is little topographic evidence for such displacement at Cougar Reservoir (see Chapter 4; Plate 4). In any case, the Cougar fault does not cut Pleistocene gravels where they cap the shear zone in one locality.

Northwest-trending faults with lateral movement

A N. 40° W.-trending right-lateral fault zone at the Clackamas River (Anderson, 1978) and three major N. 60° W.-trending lineations (Lawrence, 1976) intercept the High Cascade axis (Figure 2.4). The Clackamas River fault zone is interpreted by Beeson and Moran (1979) and Beeson and others (in preparation) to be an extension of the Brothers fault zone (Figure 2.4) of Lawrence (1976). The Brothers fault zone is also thought to be a zone of right-lateral shear bounding the Basin and Range province (Lawrence, 1976). Davis (1981), however, argues that there is evidence of left-lateral shear. It is also apparent that all of the mapped faults in the Brothers zone are largely, if not completely, dip-slip (e.g., Walker, 1977). The Green Ridge-Tumalo fault (e.g., see Peterson and others, 1976) has been interpreted as the deflection of the northwest-trending Brothers fault zone into the north-south High Cascade trend (Lawrence, 1976). Northwest-trending faults with right-lateral oblique slip displacement in the Breitenbush area (White, 1980a,c), may be part of the overall Clackamas River-Brothers fault system postulated by Beeson and Moran (1979) and Beeson and others (in preparation).

The Eugene-Denio zone of Lawrence (1976) is a lineament which appears to cross the High Cascade axis in the Willamette Pass-Diamond Peak area (Figure 2.4). Parts of this lineation in the Western Cascades were mapped by Woller (Chapter 6) adjacent to the High Cascades, by Brown and others (1980b) in the Oakridge-McCredie Hot Springs area, and by Woller and Priest (Chapter 5) in the Lookout Point Reservoir area (see Figures 1.1 and 2.4 for locations). Northwest-trending faults were mapped or inferred in all of these areas. In the Lookout Point area, numerous northwest- to west-northwest-trending shear zones with subhorizontal slickensides were found in early Western Cascade tuffaceous rocks. Oblique-slip

shear zones were found in the Swift Creek area. On the east side of the High Cascades, the Eugene-Denio zone appears as a series of northwest-trending faults which cut across the Walker Rim (e.g., see Wells and Peck, 1961; Kienle and others, 1981). Kienle and others (1981) inferred from photogeologic analysis that some of these faults have right-lateral strike-slip displacement; however, MacLeod (personal communication, 1982) found no evidence of lateral displacements. All mapped faults in the Eugene-Denio lineament in the Basin and Range appear to have chiefly or entirely dip-slip displacement (e.g., Walker, 1977).

Although some authors (e.g., Lawrence, 1976) have inferred that there is some lateral offset of the High Cascade axis across the Eugene-Denio zone, Wolter (Chapter 6) found no evidence to support this hypothesis. Basalts mapped by Wells and Peck (1961) and Peck and others (1964) as High Cascade units south of the Eugene-Denio lineament in the Swift Creek area are actually the lower part of the late Western Cascade sequence. This changes the inferred Western Cascade-High Cascade boundary to the vicinity of Diamond Peak (Figure 2.4) and largely eliminates any lateral offset of this boundary relative to areas north of the Eugene-Denio zone.

The Mount McLoughlin zone of Lawrence (1976) is a poorly defined lineation which terminates at the High Cascades near a north-south trending fault mapped by Maynard (1974). No lateral faults have been described in this zone.

There is no evidence that any of the major lineations shown on Figure 2.4 are unique zones of faulting in the Western Cascades. Further mapping will probably reveal numerous lateral fault zones parallel to the ubiquitous N. 40°-60° W. lineaments noted by Venkatakrishnan and others (1980) and Kienle and others (1981). It may be fortuitous that the Clackamas River and the Willamette River have created well-defined lineaments, whereas other major rivers have followed zones of weaknesses with other trends.

Age of northwest-trending faults with lateral movement

Beeson and Moran (1979) show that some documented movement on the Clackamas River fault zone is younger than the Sardine Formation of Peck and others (1964), although Beeson and others (in preparation) indicate that a fault scarp parallel to the Clackamas River may have acted as a barrier to the Grande Ronde Basalt. Lux's (1982) radiometric dates on Grande Ronde Basalt in western Oregon indicate that it erupted over a short time span about 15.3 ± 0.4 m.y. B.P. The Clackamas River wrench fault was thus probably active prior to 15.3 m.y. B.P. Hammond and

others (1980) inferred from mapping in the Clackamas River-Breitenbush Hot Springs area that northwest-trending oblique-slip faults began movement about 12 m.y. B.P. and remained active during later episodes of more northerly-trending faulting. White (1980a) infers that some of these northwest-trending oblique-slip faults in the Breitenbush Hot Springs area have displaced Pleistocene units. There appears to be evidence of a long history of northwest-trending lateral to oblique-slip faulting in the northern Oregon Cascades from before 15.3 m.y. B.P. to Pleistocene times.

Mapping by Woller and Priest (Chapter 5) in the Lookout Point area, Brown and others (1980b) in the Oakridge-McCredie Hot Springs area, and Woller (Chapter 6) in the Swift Creek area has revealed no northwest-trending lateral faults younger than about 5.5 m.y. B.P. in the Western Cascade segment of the Eugene-Denio lineament. Although a few small lateral shears were found in the 22-m.y. B.P. lavas of Black Canyon in the Lookout Point area, there was no obvious lateral offset of a paleocanyon filled with these lavas, even though the paleocanyon crosses the Willamette River portion of the Eugene-Denio zone at right angles (see Chapter 5). Northwest- to west-northwest-trending lateral shear zones are, however, abundant in tuffs underlying the lavas of Black Canyon (Chapter 5). As mentioned previously, the tuffs have a minimum age of 24.7 ± 2.0 m.y. B.P. and may be somewhat older. Brown and others (1980b) found no similar shears in early High Cascade lavas which apparently follow paleocanyons parallel to the Eugene-Denio lineament. Within the Eugene-Denio lineament, Woller (Chapter 6) found some northeast- and northwest-trending shear zones cutting late Western Cascade lavas, but some of these shears were overlain by undeformed late Western Cascade lavas. In the same area, Woller (Chapter 6) also inferred a pre-5.5 m.y. B.P. fault roughly parallel to the Eugene-Denio zone at Pinto Creek.

On the east side of the Cascades, northwest-trending faults within the Eugene-Denio lineament cut lavas mapped as Quaternary-Tertiary volcanic rocks by Wells and Peck (1961). These rocks are probably of early High Cascade age (MacLeod, personal communication, 1982), but none of these faults have any documented lateral displacement (e.g., see Walker, 1977).

It appears that there is evidence of a long history of lateral movement on northwest-trending faults in Clackamas River-Breitenbush area, perhaps starting before 15.3 m.y. B.P. and continuing into Pleistocene time. Similar movements in the area of the Eugene-Denio lineament had largely ceased prior to 22 m.y. B.P. A few minor oblique-slip faults in 22-m.y.-old rocks in the Lookout Point

area, however, indicate that some small lateral movements occurred in the post-22-m.y. B.P. period, although dip-slip faulting was dominant.

N. 20°-40° W. normal faults and intrusives

Numerous dikes and normal faults with trends between N. 20° W. and N. 40° W. occur in the Western Cascades. Peck and others (1964) noted that northwest-trending faults are the dominant structures in the Cascades and cited several examples of them including youthful normal faults which cut late High Cascade rocks south of Crater Lake. Callaghan and Buddington (1938) also noted that mineralized veins and intrusive rocks of the Western Cascade episode tended to preferentially follow northwest-trending structures. Only a small percentage of these faults and dikes have been documented in the central Western Cascades because of a lack of detailed mapping.

N. 20°-40° W.-trending faults with both normal and lateral offsets are common in the Clackamas River-Mount Hood area (Beeson and Moran, 1979; Beeson and others, in preparation). The faults are interpreted by Beeson and others (in preparation) as the result of an overall system of right-lateral wrenching along a N. 45° W. trend.

Reconnaissance maps of the Breitenbush area (White, 1980a,c; Hammond and others, 1980, 1982) show numerous N. 20°-40° W. normal faults which appear to be terminated by north-south faults (Hammond and others, 1982). Priest and Woller (Chapter 3) found two small N. 30°±10° W.-trending normal faults which displace only uppermost late Western Cascade tuffs. These small faults are parallel to nearby early High Cascade basaltic andesite dikes (see Chapter 4).

Avramenko (1981) noted swarms of early High Cascade dikes and a few parallel normal faults with an average trend of N. 30° W. in the Echo Mountain quadrangle in the upper McKenzie River area. Brown and others (1980a,b) show numerous northwest-trending normal faults in Western Cascade rocks on reconnaissance maps of the McKenzie River, Sardine Butte, and Oakridge quadrangles. Many of these faults are shown cutting early High Cascade units.

Age of N. 20°-40° W. normal faults and intrusives

Data on the age of N. 20°-40° W. faults is, for the most part, lacking; however, the previously mentioned reconnaissance maps show these faults cutting early High Cascade units in numerous places (e.g., see Brown and others, 1980a,b; Hammond and others, 1982). No definite age estimates for the N. 20°-40° W. faulting in the Clackamas River-Mount Hood area are known, but the faults do cut the

Columbia River Basalt Group and overlying late Western Cascade units (Beeson and Moran, 1979; Beeson and others, in preparation). Hammond and others (1982) note on their reconnaissance map that some of these faults have had recurrent movement into late High Cascade time in the Breitenbush area. The two small faults mapped in detail in the same area by Priest and Woller (Chapter 3) appear to have moved in the interval between about 9.5 and 6.3 m.y. B.P. Peck and others (1964) and Naslund (1977) noted that the northwest-trending faults in the southern Cascades cut late High Cascade units. Naslund (1977) showed examples of these faults cutting lavas erupted within the last normal polarity epoch (i.e., within the last 770,000 yr).

The northwest-trending faults seem to have chiefly begun movement sometime prior to the north-south-trending faults, probably during the beginning of early High Cascade time. Observations of Callaghan and Buddington (1938), however, suggest that older intrusive rocks of the Western Cascade episode also followed northwest-trending structures. Movement on these faults has apparently been recurrent into late High Cascade time.

Northeast-trending faults

Although there are many northeast-trending photogeologic and geophysical lineations in the Cascades (e.g., see Venkatakrishnan and others, 1980; Kienle and others, 1981; various geophysical studies by Couch, Gemperle, Pitts, McLain, and Veen), there are fewer northeast-trending faults verified by geologic mapping than faults with other trends. Some northeast-trending reverse faults occur in northeast-trending folds in the Mount Hood area (Beeson and Moran, 1979; Vogt, 1979, 1981; Beeson and others, in preparation). Northeast-trending faults also occur in the Breitenbush Hot Springs area where both lateral and normal movements have occurred (e.g., Hammond and others, 1980; White, 1980a,c). Northeast-trending shear zones with slickensides indicating some lateral displacement occur in the Swift Creek area at Pinto Creek (Woller, Chapter 6). Barnes (1978) notes that a northeast-trending dip-slip fault mapped by Wells (1956) in the Medford quadrangle continues into the Diamond Lake area.

Age of northeast-trending faults

Most northeast-trending faults appear to be middle to late Miocene in age, although younger faults with this trend also occur. Provided generalizations about the age of folds in the Mount Hood area apply to the intimately associated northeast-trending faults, the faults began movement during the time of formation

of the Grande Ronde Basalt of the Columbia River Basalt Group about 15.3 m.y. B.P., but the youngest movement on these faults is not well constrained (e.g., see Beeson and Moran, 1979; Beeson and others, in preparation). Northeast-trending faults in the Breitenbush Hot Springs area are associated with middle to late Miocene folds, and some of these faults cut the 11.8- to 9.8-m.y. B.P. Elk Lake Formation (White, 1980a). Some small northeast-trending shear zones in the Swift Creek area are between 17 and 5.5 m.y. in age (Woller, Chapter 6). Barnes (1978) shows that northeast-trending faults near Diamond Lake cut late High Cascade lavas of Mount Bailey. He relates these faults to the response of northeast-trending Klamath Mountain structures to High Cascade extension. Similar young extensional faults follow northwest and north-south trends in the same area (Barnes, 1978).

Folds

Folds chiefly occur in Western Cascade rocks in the northern part of the Oregon Cascades. Northeast-trending folds with local thrust-faulted limbs occur in the Mount Hood-Columbia Gorge area (Hodge, 1938; Beeson and Moran, 1979; Beeson and others, in preparation). Along the North Santiam River, north-northeast to northeast-trending folds have been described and named by Thayer (1936), from west to east, the Mehama anticline, Sardine syncline, and Breitenbush anticline. Wells and Peck (1961) and Peck and others (1964) mapped these and related folds throughout much of the northern Oregon Western Cascades, but Hammond and others (1980, 1982) show these folds as small disjointed structures extending only a few kilometers in any one area. Most of these folds have limbs dipping less than 20° , although limbs of the Breitenbush anticline locally dip as much as 60° (e.g., Peck and others, 1964; White, 1980a,c). No evidence for this anticline was found to the south in the Cougar Reservoir area (Priest and Woller, Chapter 4).

Flaherty (1981) measured easterly dips of 7° - 10° in late High Cascade lavas of Cupola Rock near Belknap Hot Springs. He interprets this as evidence of subsidence along the High Cascade axis. Most cross sections drawn on regional geologic maps also infer a broad synclinal structure under the High Cascades (e.g., see Wells and Peck, 1961; Peck and others, 1964).

Although folding in the North Santiam drainage and areas north of the Clackamas River is well documented, the gentle dips which Wells and Peck (1961) and Peck and others (1964) interpret as folds in areas to the south could be explained by local tilting of or compression between fault blocks and, in some

cases, by depositional dips. Preliminary interpretations by G. W. Walker (personal communication, 1982) indicate no evidence of folding due to regional compression. Further detailed mapping is necessary to document the regional folds shown by Wells and Peck (1961) and Peck and others (1964).

Age of folds

Most folds in the central Oregon Cascades are probably middle to late Miocene in age, although there is some evidence that slight early Pleistocene downwarping of the High Cascades may have occurred. As previously mentioned in the section on northeast-trending faulting, folding in the Mount Hood area had probably begun by about 15.3 m.y. B.P., but the youngest folding is not well constrained (e.g., see Beeson and Moran, 1979; Beeson and others, in preparation). Similar folding in the Breitenbush Hot Springs area occurred between 15 and 11 m.y. B.P. (White, 1980a,c). Folding hypothesized by Flaherty (1981) in the Belknap Hot Springs area ended between 8.9 and 7 m.y. B.P., although slight subsidence along the High Cascade axis may have caused 3.4- to 2.0-m.y. B.P. lavas near McKenzie Bridge to be tilted toward their easterly source areas (Flaherty, 1981). Inferred folds in the Willamette Pass area appear to affect early and late Western Cascade rocks, but no obvious folds occur in early High Cascade units (e.g., see Wells and Peck, 1961; Peck and others, 1964; Brown and others, 1980b).

Structural interpretations and speculations

The general pattern of northwest, northeast, and north-south lineations and mapped structures in the Cascades can be explained by a stress field with a horizontal north-south to north-northwest maximum compressive stress, a horizontal east-west minimum stress axis, and a vertical intermediate stress axis, according to Venkatakrishnan and others (1980) and Kienle and others (1981). The northwest-trending lateral faulting along the Clackamas River and similar shears in the Lookout Point Reservoir area could be caused by this stress regime. Likewise, north-south to north-northwest normal faults could also be accommodated because they are parallel to the maximum stress axis and perpendicular to the minimum compressive stress axis. These extensional faults could, however, just as easily be explained by east-west extension with maximum compressive stress axis vertically oriented.

It is difficult to account for the north-northeast-trending folds in the Breitenbush area by simple north-south to north-northwest compression; presumably

some local compression in a west-northwest to east-southeast direction would be necessary to cause the folds. It is also difficult to obtain the northeast-trending folds and associated thrust faults north of the Clackamas River from simple north-south compression unless local stresses associated with the right-lateral wrench faults have somehow produced the folds (Beeson and Anderson, personal communication, 1982).

One problem with the assumption that the regional stress regime has remained more or less constant during the Neogene (and perhaps earlier) is the change in both volcanism and style of deformation which occurred between late Western Cascade time and High Cascade time. About 10 to 8 m.y. B.P., mafic lavas began to dominate eruptions, and the focus of volcanism became limited chiefly to the eastern part of the Cascades. Northeast to north-northeast folding in the Breitenbush Hot Springs-North Santiam River area had terminated by about this same time. About 4 to 5 m.y. ago, a widespread north-south faulting event caused large areas of the central High Cascade axis to be displaced downward relative to uplifted areas of the Western Cascades (e.g., Thayer, 1936, 1939; Williams, 1942, 1953). A period of very rapid downcutting of the Western Cascades then occurred, producing most of the present kilometer or so of relief in about 1.6 to 3 m.y. (e.g., Flaherty, 1981). North-south faulting continued in the central Cascades, but not on the scale of that in this 5- to 4-m.y. B.P. interval. Perhaps equally important is the abrupt restriction of High Cascade volcanism to the present area of the High Cascade physiographic province--the boundaries of which correspond in some places to the prominent north-south-trending faults. Such abrupt changes in rate and style of deformation and accompanying changes in volcanism are most likely the result of equally abrupt changes in the stress regime resulting from changes in the interaction of major lithospheric plates. Changes in the direction spreading on the Juan de Fuca Ridge between 7 and 4 m.y. B.P. and possible partial coupling of the Juan de Fuca plate with the North American plate in this interval (Atwater, 1970) may have caused these changes in deformation and volcanism. It may also be significant that Atwater's (1970) models require a change in direction of plate motion of 20° about 10 m.y. B.P. The reorganization of plate boundaries which caused the opening of the Gulf of California about 5 to 4 m.y. B.P. (Atwater, 1970) may also have had some influence on the Cascade stress regime.

The cessation of folding in the North Santiam River area and beginning of dominantly mafic volcanism throughout much of the central Cascades between

about 10 and 8 m.y. B.P. may have been caused by increased extensional stresses. N. 30° W.-trending early High Cascade dikes in the Echo Mountain area (Avramenko, 1981) could be explained by minimum compressive stress in an east-northeast direction or by fissures and small faults following pre-existing structural trends. Callaghan and Buddington (1938) point out that most intrusives of a variety of ages in the Western Cascades follow northwesterly trends. Early High Cascade volcanism in the Outerson Mountain area was preceded in the interval between 9.5 and 6.3 m.y. B.P. by N. $30^{\circ}\pm 10^{\circ}$ W. normal faulting, according to Priest and Woller (Chapter 3). This would lend support to the hypothesis that the minimum compressive stress was reoriented to about N. $60^{\circ}\pm 10^{\circ}$ E. during the change from the late Western Cascade to early High Cascade volcanic episodes. In the Cougar Reservoir area, early High Cascade volcanism may have been immediately preceded by or contemporaneous with north-south normal faulting indicative of east-west extension. A great deal of mapping must be done before the details of early High Cascade deformation can be determined.

The major north-south normal faulting which immediately preceded eruption of the diktytaxitic basalts characteristic of the lower part of the late High Cascade section is probably best explained by an abrupt increase in east-west extension about 5 to 4 m.y. B.P. This increase in extension correlates with general uplift of the central Western Cascades at about the same time. Fault-plane solutions for earthquakes in the region suggest current east-west extension (Couch and Lowell, 1971). Beeson and Moran (1979) favor similar uplift of the Mount Hood region prior to formation of the Hood River fault and downdropping of the block immediately adjacent to the Mount Hood volcano.

Another factor which may influence the style of deformation in the Cascades is the relative strength of various parts of the crust. The high heat flow characteristic of the High Cascades province should cause the High Cascade crust to be more plastic and less rigid. If faulting is concentrated in areas of weak crust, especially where thermally weakened crust is adjacent to cooler crust, this might explain the poorly defined aspect of structures and lineations in the cooler Western Cascade crust relative to that of areas to the east. For example, compare the density of well-defined faults and lineaments noted by Kienle and others (1981) in the Western Cascades versus that in the High Cascades and Basin and Range province. Concentration of well-defined fault scarps on the margins of the highest part of the High Cascade heat-flow anomaly of Blackwell and others (1978) and Black and others (Chapter 7) might also be explained by

this hypothesis (see Figure 2.4). Elevated temperatures in the upper crust in the Klamath Lake area, postulated from Curie-point isotherm studies of McLain (1981), may cause general downfaulting along the High Cascade axis postulated by Allen (1966) to appear to merge with the northern end of the Klamath graben (Figure 2.4). The Tumalo and Walker Rim faults both appear to swing toward the very hot crust which must underlie Newberry volcano (Figure 2.4). Likewise, concentration of lateral faults in the Clackamas River area may reflect interaction between somewhat cooler crust to the north and hotter crust to the south of the Clackamas River (Figure 2.4). The margins of a local heat-flow anomaly (Figure 2.4) associated with Mount Hood are also associated with a late Pliocene(?) fault at Old Maid Flat (Priest and others, 1982a) and with the Hood River fault. The youthful age of the Hood River fault (less than 3 m.y. B.P.) compared to the large 5- to 4-m.y. B.P. faults in the central Cascades might correlate with the age of this local heat-flow anomaly which, in turn, probably correlates with the age of volcanism at the Mount Hood volcano. The apparent decrease in the density of well-defined faults and lineaments into the Western Cascades could also be a function of the paucity of detailed mapping and the difficulty of forming long-lived scarps in the soft tuffaceous rocks which underlie many areas of the rain-drenched western slopes of the Cascades.

The above hypothesis implies that the western Oregon lithosphere south of the Clackamas River fault zone and east of the faults concentrated at the westernmost edge of the High Cascade heat-flow anomaly may have acted as a relatively stable block or microplate. Crustal spreading in the Basin and Range province to the east has, according to paleomagnetic models of Magill and Cox (1980), rotated western Oregon about 25° in a clockwise manner during the last 25 m.y. B.P. The axis of rotation in their model is in southern Washington. If the boundaries of this relatively undeformed microplate were governed by relative heat flow in the past, as they may be now, then rotation of the Western Cascades lithosphere across a north-south zone of magma generation, possibly a north-south subduction zone, could explain the migration of both active volcanism and tectonic deformation from the Western Cascades toward the present High Cascades during the Neogene. The north-south- and northwest-trending faulting which affected the Cascades in the last 10 m.y. could thus be considered to be a manifestation of Basin and Range spreading.

The discontinuous nature of faulting and folding episodes in the Cascades, however, are incompatible with a constant rate of rotation and spreading

throughout the last 25 m.y. It is more likely that an acceleration of Basin and Range spreading occurred between about 10 and 8 m.y. B.P., coincident with the beginning of High Cascade mafic volcanism and the switch to the easterly position of the volcanic axis. It was also at about this time that the current Basin and Range topography became well defined (Stewart, 1978). This is also the approximate beginning of eruption of diktytaxitic to compact high-alumina olivine tholeiites in the Basin and Range of Oregon (Hart, 1982) and the beginning of westward migration of rhyolitic volcanism from easternmost Oregon along the northern margin of the Basin and Range (MacLeod and others, 1975). Compositional similarities of high-alumina basalts erupted from the High Cascades in the last 9 m.y. to basalts of this age in the Basin and Range (see the following sections) further suggest that a similar modification of the composition of magmas generated in both the Basin and Range and the Cascades occurred during this time interval. The overall change in tectonism and volcanism may be the result of the previously mentioned plate geometry.

There are many other models which can explain the structural features of the Cascades. Until much more detailed geologic mapping and radiometric data are available to constrain the number of possible models, it is impractical to list them all. Time spent inventing models is probably better spent in the field and laboratory generating data.

PETROCHEMISTRY

Introduction

Numerous rocks have been chemically analyzed from each of the four map areas studied in detail for this report (see Appendix B). These analyses are by no means a comprehensive representation of the Western and High Cascade sequences, but the compositional fields of these samples and selected analyses from the literature are probably typical of the range of compositions in other areas.

Compositional fields from the literature are shown on various diagrams for comparison. Some samples of alkali-rich High Cascade mafic lavas from the literature have been plotted on compositional diagrams to illustrate this petrologically important group of rocks. It is beyond the scope of this report to show all the available literature data.

Analytical methods

All rocks, except those from the Devils Creek area; Swift Creek samples

P-604, TMO, P-509, P626, and P-PHL; Rider Creek samples Ri-22, Ri-46, Ri-60, and LB; and Lookout Point sample BB-PPAT were chemically analyzed by standard atomic absorption methods at the University of Oregon (Christine McBirney, analyst). The samples noted above were analyzed by standard induced argon-coupled plasma techniques at the University of Utah Research Institute, Salt Lake City, Utah (Ruth Kroenman, analyst). All samples are listed in Appendix B with locations.

Recalculation of data

Where specific oxide percents are listed in the text or on the chemical diagrams, the value is from an analysis which has been recalculated to a 100-percent total without volatiles and with all iron as Fe^{+2} . This applies to this chapter and all following chapters. This recalculation removes some variations caused solely by weathering and low-grade metamorphism.

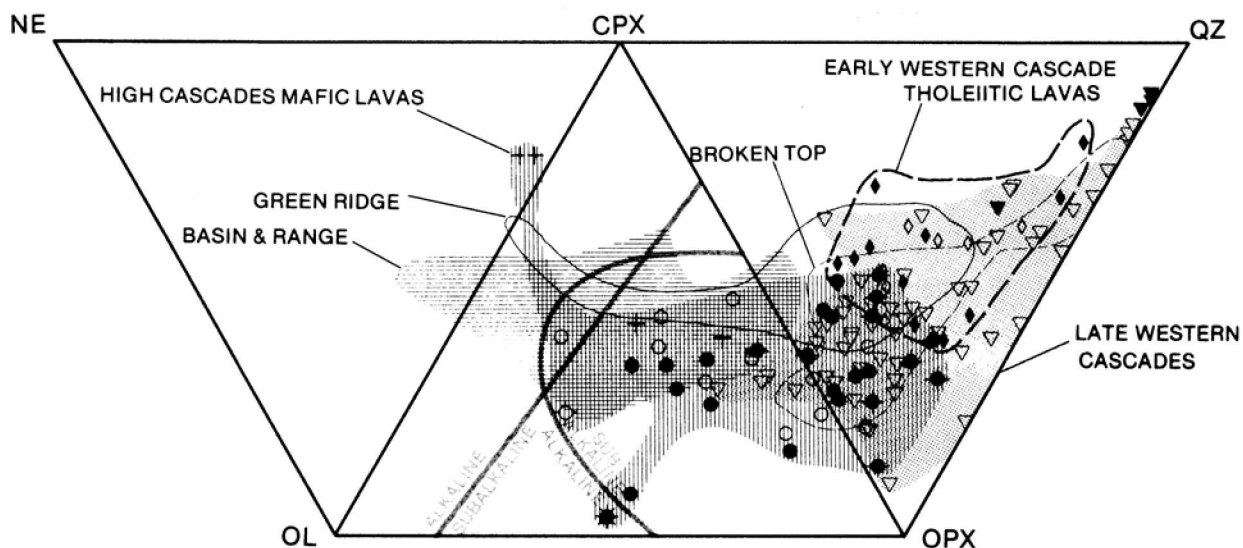
Normative mineral compositions have been calculated using an oxide analysis which has been recalculated to a 100-percent total without volatiles and with $\text{Fe}_2\text{O}_3/\text{FeO}$ in a weight ratio of 0.31 (molecular ratio of $\text{Fe}^{+3}/\text{Fe}^{+2}$ of 0.28). CIPW norms are listed in Appendix B, but the compositional diagrams utilize cation norms (e.g., see recommendations of Irvine and Baragar, 1971, p. 526).

Nomenclature

Volcanic rocks are named in this and following chapters primarily by means of a simple system based on SiO_2 (silica) of recalculated analyses (see previous section). The following rock names apply to rocks with the silica contents in the designated ranges:

1. Silica less than 53 percent = basalt.
2. Silica between 53 and 57 percent = basaltic andesite.
3. Silica between 57 and 63 percent = andesite.
4. Silica between 63 and 70 percent = dacite.
5. Silica more than 70 percent = rhyodacite.

Rocks with silica contents of more than 70 percent and which have K_2O greater than 4 percent are termed "rhyolite" rather than rhyodacite. Basalts which are not nepheline normative are nevertheless classified as "alkaline" if they plot in the smaller alkaline field on Chayes' (1965, 1966) normative clinopyroxene-olivine-orthopyroxene ternary diagram and "subalkaline" if they plot in the smaller subalkaline field (see Figure 2.6). Samples which plot in the borderline area on Chayes' (1965, 1966) diagram are termed "slightly alkaline." Nepheline-normative basalt is termed "alkali basalt." Rocks which are iron-rich enough to

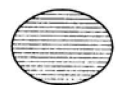


LEGEND FOR COMPOSITIONAL DIAGRAMS

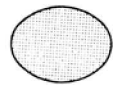
- Late High Cascade sample of this study
- Early High Cascade sample of this study
- ◊ Plio-Cascade sample of Maynard (1974)
- + Cascades Formation sample of Jan (1967) along Scott Creek
- ◆ Mafic lavas of Devils Canyon of Barnes (1978)
- ★ Alkali-rich sample of Outerson Formation from White (1980 a)
- ▽ Late Western Cascades sample of this study
- ◆ Scorpion Mountain lavas sample of White (1980 a, c)
- ◇ Lavas sampled in this study which are correlative to the Scorpion Mountain lavas. All samples but two are from the lavas of Black Canyon at Lookout Point Reservoir. The other two samples are from the lavas of Hardesty Mountain (Lookout Point Reservoir) and the tuffs of Cougar Reservoir
- ▼ Non-tholeiitic early Western Cascades sample of this study. Samples suffer from slight hydrothermal alteration in most cases



Field of composition for early and late High Cascade mafic lavas (less than 58% silica)



Field of composition for 9 to 0 m.y. B.P. Basin and Range lavas of Hart (1981)



Full field of composition for late Western Cascade samples of this study



Field of composition for Broken Top volcano; includes only samples from the flanks of the volcano. Data taken from Taylor (1978)



Field of composition for early High Cascade mafic lavas of Green Ridge (SiO_2 less than 58%). Data is from Hales (1975)



Field of composition of the diamond-shaped symbols above. Shows the range of composition of early Western Cascade tholeiitic lavas

Figure 2.6. Nepheline-olivine-clinopyroxene-orthopyroxene-quartz quadrilateral. NE = nepheline; OL = olivine; CPX = clinopyroxene; OPX = orthopyroxene; QZ = quartz. The subalkaline-alkaline boundaries are those of Chayes (1965, 1966).

plot in the tholeiitic field of Irvine and Baragar's (1971) AFM diagram (Figure 2.7) are termed "tholeiitic " if not alkaline as defined in Figure 2.6. The term "icelandite" is used for andesites which plot in the tholeiitic field of Figure 2.7. The term "high-alumina basalt" is used for basalts with Al_2O_3 over about 17 percent (e.g., see recommendations of Carmichael and others, 1974, p. 33).

Methods of comparison

Compositional variation diagrams utilizing simple oxides and normative mineral values will be used to compare and contrast groups of rocks from the Western Cascade, High Cascade, and Basin and Range provinces. The Cascade samples are from this study and literature values, while the Basin and Range samples are samples of eastern Oregon basalts of Hart (1982) K-Ar dated between about 9 and 0 m.y. B.P. In no case are the number of samples or size of compositional fields to be considered related to the volume of the rock units.

Because some processes of differentiation tend to lead to silicic magmas of similar eutectic or thermal minimum compositions, it is often more profitable to compare the compositions of mafic volcanic rocks which tend to reflect fundamental differences in parent magmas. The differentiation causes silicic rocks from all of the different groups to completely overlap one another, producing considerable clutter on the diagrams. In order to reduce this clutter, lavas with more than 58 percent SiO_2 from High Cascade, Green Ridge, and Basin and Range units will be excluded from the diagrams so that compositions of the dominantly intermediate to silicic Western Cascade samples can be shown. The complete compositional spread of samples from the flanks of Broken Top volcano in the High Cascades will also be shown to illustrate a complete High Cascade magma series (data taken from Taylor, 1978).

Useful compositional parameters for mafic rocks are the degree of alumina, iron, and alkali enrichment of differentiation series. These parameters are sensitive indicators of petrogenesis (e.g., see discussions by Yoder and Tilley, 1962; O'Hara, 1965; Green and Ringwood, 1968; Ringwood, 1975; Yoder, 1977). The iron enrichment relative to magnesium content can be shown by a plot of SiO_2 versus FeO^*/MgO (FeO^* = all iron recalculated to Fe^{+2}) and on the previously mentioned AFM diagram (Figures 2.8 and 2.7, respectively). Total iron enrichment is best shown on an FeO^* versus SiO_2 diagram (Figure 2.9). Alumina content is shown on the Al_2O_3 versus normative plagioclase diagram of Irvine and Baragar

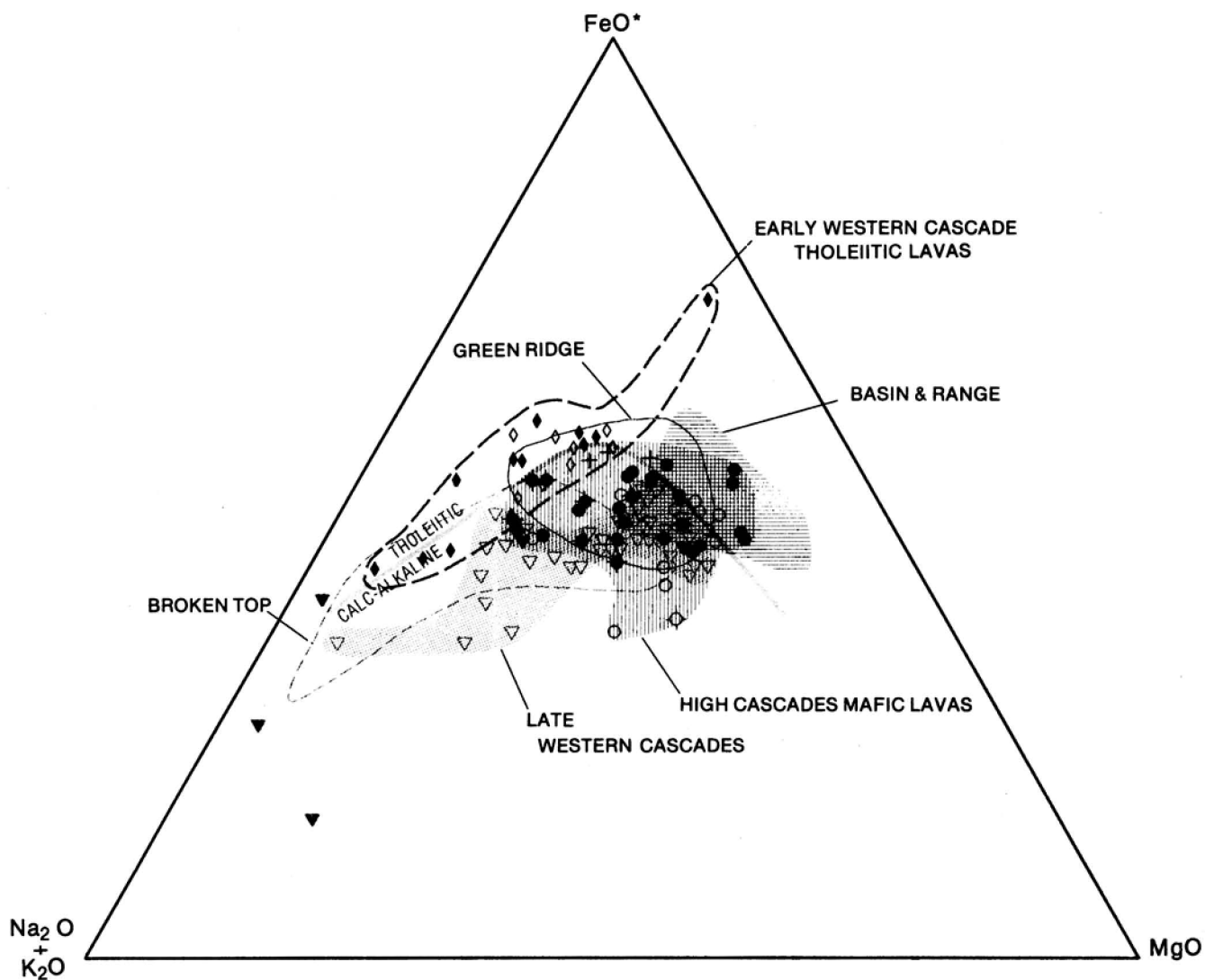


Figure 2.7. $\text{Na}_2\text{O}+\text{K}_2\text{O}-\text{FeO}^*-\text{MgO}$ ternary diagram. The tholeiitic-calc-alkaline boundary is taken from Irvine and Baragar (1971). FeO^* = all iron recalculated to Fe^{+2} ; other symbols as in Figure 2.6.

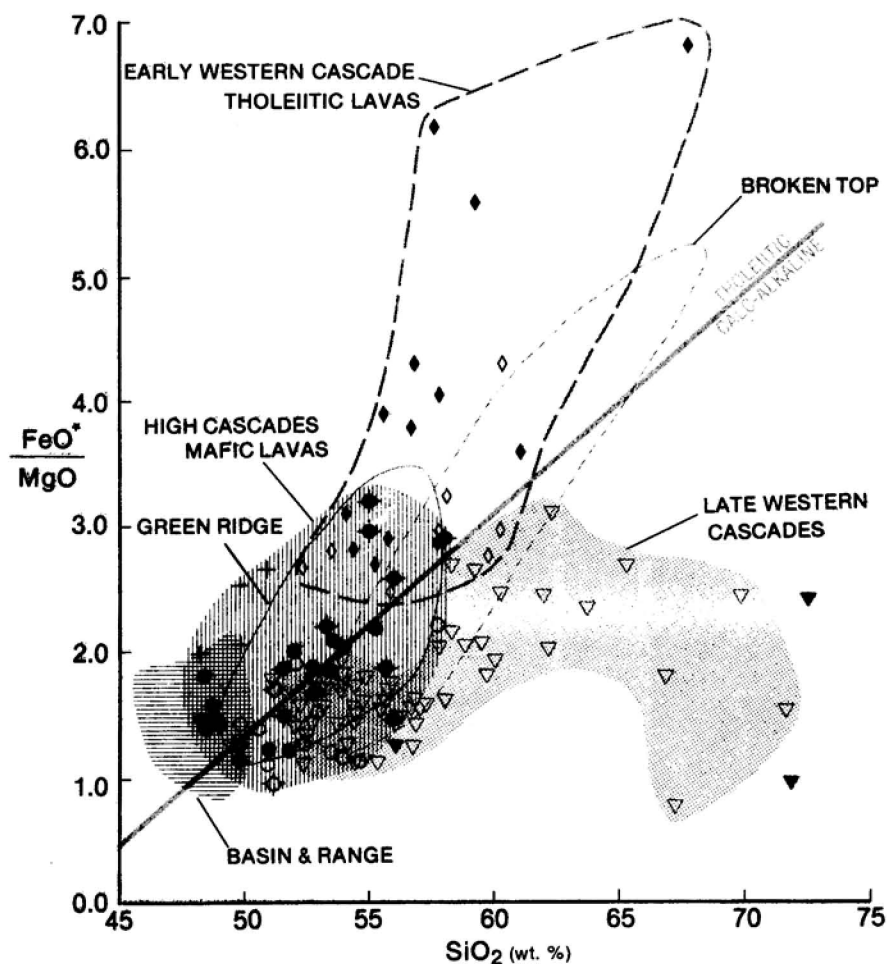


Figure 2.8. FeO^*/MgO versus SiO_2 with Miyashiro's (1974) boundary between the calc-alkaline and tholeiitic compositional fields. FeO^* = all iron recalculated to Fe^{+2} . See Figure 2.6 for explanation of other symbols.

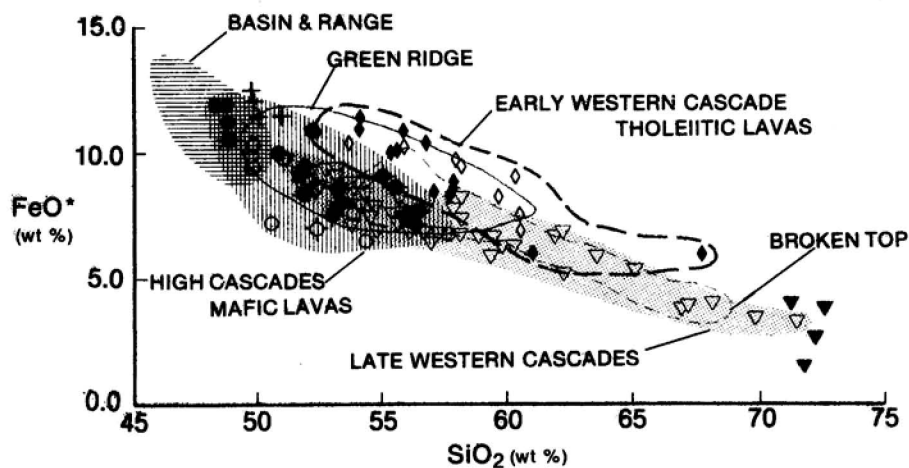


Figure 2.9. FeO^* versus SiO_2 . FeO^* = all iron recalculated to Fe^{+2} ; symbols as in Figure 2.6.

(1971) Figure 2.10. The alkalinity is best shown by the amount of total alkalis versus the silica content (Figure 2.11) or as the amount of silica saturation in the previously mentioned diagram of Figure 2.6.

The samples presented here will be compared to fields of composition of samples from other parts of the world by means of lines separating major types of differentiation series. Kuno (1966) described a suite of tholeiitic lavas from the outer margins of the Japanese volcanic arc which differ in composition from more alkaline and aluminous lavas in the main central part of the arc which he called the high-alumina basalt series. Both of these suites differ strongly from alkaline back-arc lavas, which he termed the alkali basalt series. MacDonald and Katsura (1964) described similar alkali and tholeiitic basalt differentiation series in the Hawaiian Island chain but did not recognize the high-alumina basalt type noted by Kuno in the subduction-related island-arc terrane. Miyashiro (1974) plotted numerous island-arc differentiation series and arbitrarily split them on the FeO^*/MgO versus SiO_2 diagram into iron-rich "tholeiitic" and iron-poor "calc-alkaline" series (Figure 2.8). Irvine and Baragar (1971) similarly divided basaltic suites into iron-rich, alumina-poor "tholeiitic" fields and iron-poor, alumina-rich "calc-alkaline" fields on the AFM and alumina versus normative plagioclase plots (Figures 2.7 and 2.10). Irvine and Baragar's fields took into account tholeiitic compositions from the ocean basin and continental flood basalts which tend to be very iron-rich and alumina-poor compared to subduction-related island-arc suites.

All of the above systems were designed to deal with mafic rock series and produce definitions of "calc-alkaline" appreciably different from the original definition by Peacock (1931). Peacock designated a differentiation series "calc-alkaline" if it had samples with $\text{alkalies}/\text{CaO} = 1.0$ at SiO_2 contents between 56 and 61. It is now recognized that subduction-related, mature island arcs and continental margin arcs typically have iron-poor differentiation series with Peacock indices in this range.

The other methods of defining "calc-alkaline" are distinctly easier to apply than Peacock's method, since they do not necessarily require that a complete spectrum of comagmatic differentiates be available. The other methods are also more applicable to mafic magmas, which are of principal interest here.

Comparisons

Whereas there is considerable compositional overlap between all of the Cascade units, there are some overall compositional differences, particularly

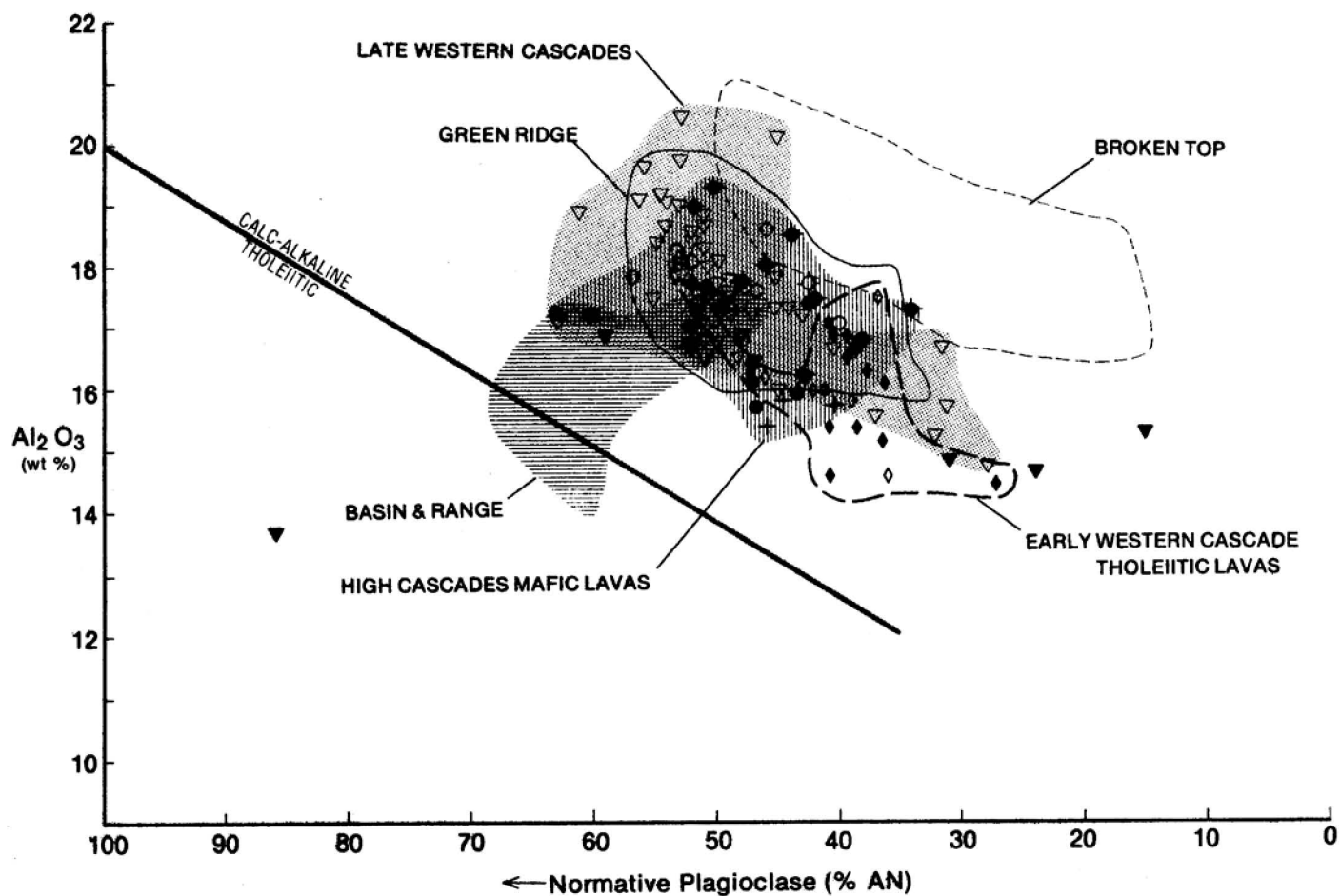


Figure 2.10. Al_2O_3 versus normative plagioclase (AN = anorthite). The calc-alkaline-tholeiitic field boundary is from Irvine and Baragar (1971); other symbols as in Figure 2.6.

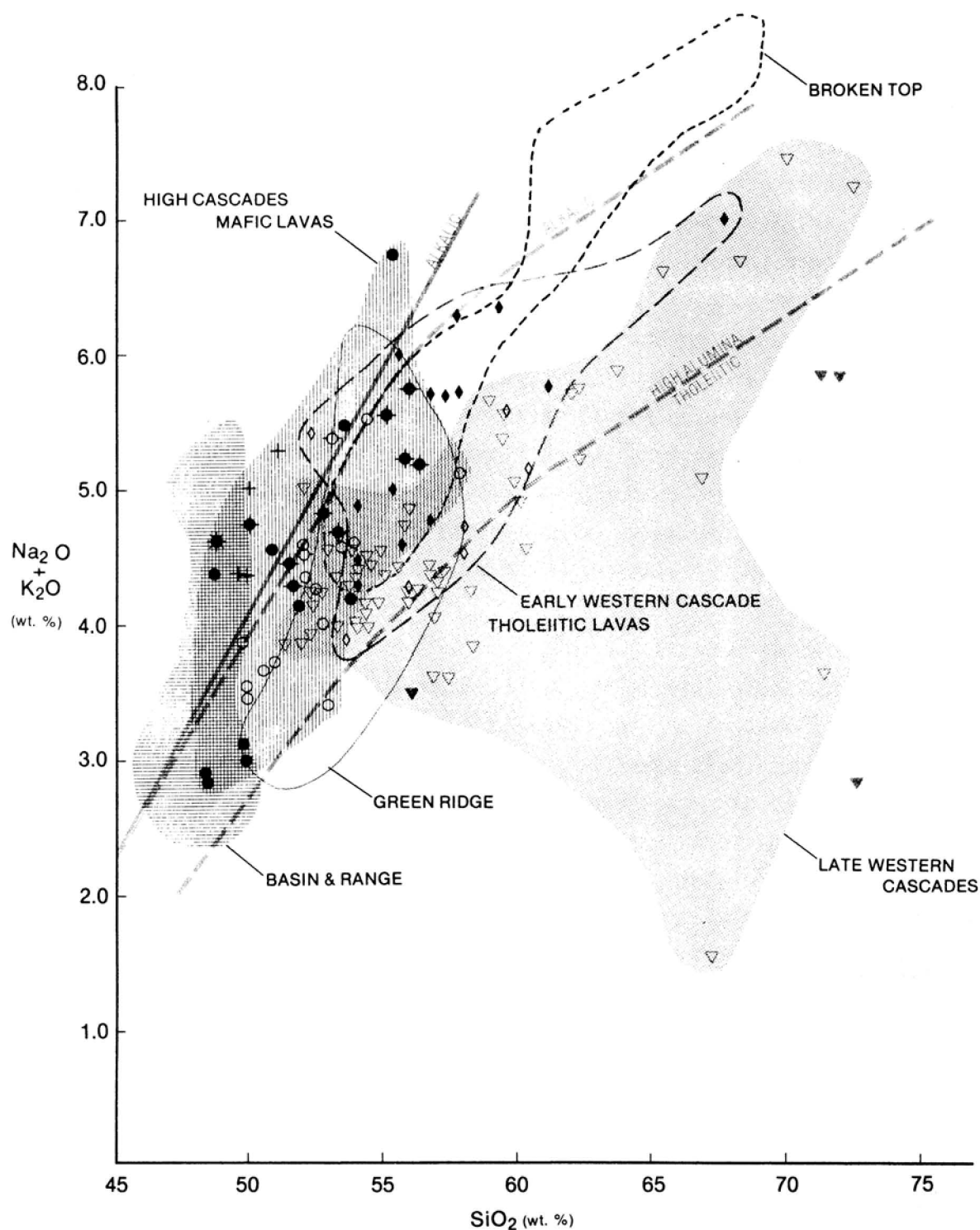


Figure 2.11. $\text{Na}_2\text{O} + \text{K}_2\text{O}$ versus SiO_2 with the alkali basalt and tholeiitic basalt fields of Macdonald and Katsura (1964) for Hawaiian island rocks. Also shown are the boundaries of the alkali basalt, high-alumina basalt, and tholeiitic basalt fields of volcanic rocks of the Japanese arc (Kuno, 1966). Other symbols as in Figure 2.6.

between the mafic end members. In the extremes of their compositional range, the High Cascade basalts tend to be somewhat less silicic and richer in alkalis than the Western Cascade basalts. Lavas from the early Western Cascade tholeiitic series (the Scorpion Mountain magma type) which have been plotted on the diagrams are from mapped areas in the upper part of the sequence and have SiO_2 contents no lower than 52.4 percent (e.g., sample BB-30, Appendix B). Newly received data from a thesis by Lux (1981) on the lower part of the early Western Cascade sequence show that that part of the tholeiitic series has SiO_2 between about 49.8 and 52.0 percent (recalculated volatile-free). All of the analyzed tholeiitic series samples are, however, quartz normative (e.g., Figure 2.6; Lux, 1981), whereas many late Western Cascade basalts and, particularly, High Cascade basalts are commonly somewhat undersaturated with respect to quartz. Aside from the Basin and Range compositional field, only the High Cascade samples plot into the alkaline compositional space on Figure 2.6 (see also Figure 2.11).

The late Western Cascade sequence is iron-poor relative to both the early Western Cascade tholeiitic lavas and the High Cascade lavas (Figures 2.7, 2.8 and 2.9). Late Western Cascade rocks are strongly calc-alkaline on all of the diagrams which show calc-alkaline fields. Calc-alkaline lavas and tuffs are also common in the early Western Cascade sequence (e.g., see Lux, 1981), although few of these rocks were collected in this study. All of the High Cascade compositional fields completely overlap the late Western Cascade fields. Iron-poor calc-alkaline rocks are thus very common in all of the Cascade units, and a general calc-alkaline composition is characteristic of Cascade rocks erupted throughout the last 40 m.y. Differences in the range of compositions within each group of rocks, however, is consistent and may be related to important differences in petrogenesis.

The fields of composition for the mafic lavas of the southeastern Oregon Basin and Range do not overlap the Western Cascade compositional fields at all, yet the High Cascade fields overlap both the Western Cascade and Basin and Range fields. Were samples from parts of the Basin and Range near the Cascades included in the Basin and Range field, for example, Newberry volcano (Higgins, 1973) or the Yamsay Mountain complex (Hering, 1981), there would be a great deal of overlap with Western Cascade compositions, because the Basin and Range volcanic centers near the Cascades, while having many compositional dissimilarities, also have a significant amount of calc-alkaline rock of intermediate

composition. Because the petrologic interpretation and tectonic setting of the volcanoes near the Cascades is probably complex, these data were excluded to facilitate comparison of Cascade rocks to rocks unquestionably generated within an area of Basin and Range tectonism free of any effects of past or present Cascade processes. With this in mind, it is apparent from the compositional plots that the most mafic lavas of both the early and late High Cascade episodes have many attributes of contemporaneous Basin and Range basalts including:

1. Moderate iron enrichment.
2. Moderate alkali enrichment with some nepheline normative basalt.

In terms of Kuno's (1966) fields of composition for island-arc rocks, both the Basin and Range and the most mafic and most alkaline of the High Cascade basalts are similar to Kuno's back-arc alkali basalt series (e.g., Figure 2.11). Alkali basalts occur in both the late and early High Cascade sequences. Nepheline normative basalts were collected by Jan (1967) from late High Cascade units in the Scott Creek drainage north of Belknap Hot Springs, and a slightly nepheline normative sample of early High Cascade basalt from Green Ridge was analyzed by Hales (1975). Most nepheline normative samples from the Basin and Range erupted contemporaneously with the late High Cascade episode in the late Pliocene to Holocene (e.g., see Hart, 1982).

The textures of many of the 9- to 0-m.y. B.P. Basin and Range basalts also resemble the High Cascade basalts. Both groups have abundant diktytaxitic lavas with colored subophitic to ophitic clinopyroxene. The most mafic end members of both groups also frequently have olivine in the groundmass and show no reaction relationship of olivine with pyroxene. Examples of High Cascade lavas of this type include the late High Cascade Cupola Rock lavas of Flaherty (1981), early High Cascade basalts collected by White (1980a,c) in the Breitenbush area, and some samples of the early High Cascade lavas of Tipsoo Butte at Cougar Reservoir (Priest and Woller, Chapter 4).

The Western Cascade tholeiites generally show no alkaline tendencies and plot in fields characteristic of primitive to mature island-arc series (i.e., the tholeiitic and high-alumina fields, respectively, shown in Figure 2.11). The early Western Cascade tholeiitic series is similar in composition to the island-arc tholeiitic series characteristic of the outer margin of the Japanese arc on Kuno's (1966) diagram (Figure 2.11). The late Western Cascade mafic lavas plot instead in the high-alumina basalt series, typical of the main part of the mature andesitic arc in the Japanese islands (Figure 2.11).

Most of the Cascade basalts plotted here have alumina contents greater than 17 percent and can be called high-alumina basalt (see nomenclature section and Figure 2.10). A large number of the Basin and Range basalts of Hart (1982) are also high-alumina by this definition, although many have alumina less than 17 percent (Figure 2.10). Hart's (1982) average Al_2O_3 for his "high-alumina olivine tholeiite" was 17.02 percent (his Table 3.11, p. 158), indicating that the average sample is a borderline high-alumina basalt by the nomenclature of Carmichael and others (1974). Hart (1982) used Yoder and Tilley's (1962) definition of olivine tholeiite (i.e., a basalt which is neither quartz nor nepheline normative but which has significant olivine and hypersthene in the norm). By this definition, most High Cascade basalts are olivine tholeiites and the early and late Western Cascade basalts are chiefly tholeiite to quartz tholeiite. This is a result of the high silica saturation characteristic of rocks of the Western Cascade episode (e.g., see Figure 2.6). Using both the classification of this paper and Yoder and Tilley's (1962) classification, the Basin and Range basalts are best described as alkaline olivine tholeiite to high-alumina alkaline olivine tholeiite; High Cascade basalts are alkaline to sub-alkaline high-alumina olivine tholeiites; the Western Cascade basalts are sub-alkaline high-alumina olivine tholeiite to high-alumina quartz tholeiite.

One feature not shown on the diagrams is the bimodal nature of the southeastern Oregon sequence (Basin and Range). In addition to the basalts, Basin and Range volcanic assemblages typically contain a large volume of highly silicic lavas and tuffs which are also very alkali-rich, primarily because of high Na_2O . This has given rise to such names as "soda rhyolite" to describe these silicic rocks. This bimodal basalt-rhyolite assemblage is typical of other parts of the Basin and Range province as well (e.g., Christiansen and Lipman, 1972). Whereas volcanic rocks of intermediate composition occur in the Basin and Range sequence, particularly in the westernmost part of the province, both the High Cascade and Western Cascade sequences contain a much larger volume of intermediate lavas and tuffs of andesitic to dacitic composition. This assemblage of mafic and intermediate rocks is typical of subduction-related volcanism on island arcs and continental margins throughout the world (e.g., Dickinson and Hatherton, 1967).

To summarize, the Cascade sequence is fundamentally calc-alkaline in character but has changed in composition through time. The early Western Cascade rocks are chiefly iron-rich quartz normative basalt to dacite and iron-poor calc-alkaline andesite to rhyodacite with a large proportion of iron-poor dacite to rhyodacite tuff. The late Western Cascade sequence is free of the

iron-rich, tholeiitic differentiates but has a large volume of calc-alkaline basalt to andesite and a smaller volume of dacitic tuff. In both early and late High Cascade time a larger proportion of basalt erupted than in earlier times and the range of basalt compositions reached compositions more alkaline and silica-poor than earlier basalts. The High Cascade basalts tend to have FeO^* and FeO^*/MgO somewhat higher than late Western Cascade basalts but lower than the early Western Cascade tholeiites. The most alkaline and least silicic of the High Cascade basalts resemble high-alumina olivine tholeiites erupted contemporaneously in the Basin and Range province of southeastern Oregon.

The Cascade volcanic rocks resemble volcanic rocks erupted from subduction-related island-arc terranes. The iron-rich early Western Cascade lavas resemble island-arc tholeiites from the early stages of island-arc development and tholeiites erupted on the outer margin of island arcs. The late Western Cascade lavas resemble the rocks of Kuno's (1966) high-alumina basalt series which characterize the mature stage of island-arc development in the central part of an island arc. The High Cascade rocks have characteristics of both the high-alumina basalt series and Kuno's (1966) alkali basalt series characteristic of back-arc areas.

SPECULATIONS ON THE TECTONIC SETTING OF VOLCANIC EPISODES FROM COMPOSITIONAL EVIDENCE

Introduction

It is beyond the scope of this paper to quantitatively evaluate possible petrologic models which might generate the volcanic rocks of the Cascades. In order to adequately treat petrogenesis in a quantitative manner, it is necessary to have much more data, especially trace-element and isotopic data on individual volcanic centers. This would allow detailed modeling of comagmatic rock series. Approximate pressures, temperatures, and the fugacities of H_2O and O_2 of magmas at the site of last equilibration in the crust or mantle can be estimated using microprobe data (e.g., see Carmichael and others, 1974). Unfortunately, neither microprobe nor adequate trace-element data are available from this study to quantitatively test partial melting or differentiation models. Even with additional data, it is likely that the study would yield a large number of petrologic models related to a variety of tectonic processes.

It is nevertheless important that some petrologic speculation be developed, if for no other reason than to generate enough lively debate to encourage good

quantitative studies of central Cascade volcanism. A few observations and assumptions will be made, which themselves are speculative, in order to provide a basis for the discussion:

1. The composition of volcanic rocks is chiefly a function of the following variables:
 - (a) The mineralogy and chemical composition of source rocks
 - (b) Conditions of partial melting (T , P , f_{O_2} , f_{H_2O} , percent melting)
 - (c) Path and rate of rise of magmas to the surface. These factors are important controls on the degree and conditions of equilibration of the magma with various wall-rock compositions and the amount of differentiation by crystal settling, vapor-phase transport, and other processes.
2. Since high rates of magma generation are commonly associated with active tectonic processes such as subduction and extensional faulting, it is likely that tectonic and petrogenetic processes are intimately related.
3. Although far from perfect, there nevertheless is a correlation between specific compositional types of volcanic rock and specific tectonic environments.
4. Observations 2 and 3 imply that tectonic processes very often have a characteristic effect on one or more of the variables of observation 1. This, in turn, implies that the composition of volcanic rocks may be used as a clue to the tectonic environment which prevailed when they were erupted.
5. It is apparent that composition of volcanic rocks does not represent proof of tectonic environment, because any of the variables of observation 1 can probably be duplicated in a number of tectonic environments under special circumstances. For example, a mantle source might be altered by subduction processes in such a way that calc-alkaline melts could be derived from it. The same source could then be tapped by some unrelated process in a different tectonic environment. The following models must be considered only unproven hypotheses.

Early Western Cascade episode

The early Western Cascade tholeiitic series (the Scorpion Mountain magma type) consistently plots in the compositional fields of island-arc tholeiite (e.g., Figure 2.11), although White (1980c) points out that trace-element abundances of the Scorpion Mountain rocks are more similar to tholeiitic series from

orogenic continental margins. The few available analyses of silicic rocks from the early Western Cascades are similar to calc-alkaline silicic fields on all of the chemical diagrams considered here. Island arcs in the initial stages of development typically erupt voluminous, relatively iron-rich basalts (Jakes and White, 1972). Island arcs overlying continental crust are characterized by the eruption of voluminous silicic rocks chiefly in the form of ash flows and falls (e.g., see Jakes and White, 1969; Carmichael and others, 1974). The early Western Cascade volcanic series may represent the early stages of development of a subduction-related volcanic arc in an area underlain by significant continental crust, because the series has tholeiitic lavas similar to primitive island arcs and voluminous silicic tuffs typical of island-arc terranes underlain by continental crust.

Late Western Cascade episode

The late Western Cascade rocks have compositions typical of mature andesitic volcanic arcs. Andesitic volcanism of this kind is very commonly associated with areas of active subduction which have had well-developed subduction regimes for some time (e.g., Jakes and White, 1969). The late Western Cascade volcanism may be the result of partial melting which occurred in a maturing subduction regime initiated during early Western Cascade time.

High Cascade episode

The High Cascade and Basin and Range volcanic series have chemical affinities to both the back-arc alkali basalt series and the high-alumina volcanic series on Kuno's (1966) diagrams. The Basin and Range basalts are part of a bimodal basalt-rhyolite assemblage which is typical of the extensional Basin and Range tectonic regime throughout the western United States (e.g., Christiansen and Lipman, 1972). The High Cascade sequence, however, has a significant volume of intermediate volcanic rocks and has been characterized by eruption from a linear, north-south-trending volcanic axis with numerous composite cones. The overall composition and distribution of the High Cascade sequence, as well as the current heat-flow regime (e.g., Blackwell and others, 1978), are thus more typical of a subduction-related arc than of a broad extensional province such as the Basin and Range. Plate-tectonic models of Atwater (1970) and Atwater and Molnar (1973) also require subduction in the central Oregon High Cascades during the Neogene.

The definite compositional and textural affinities of contemporaneous High

Cascade and Basin and Range basalts, however, argue for a petrogenesis for High Cascade magmas which is also partially related to processes which generate Basin and Range magmas. It is highly unlikely that eruption of alkaline high-alumina basalts in both the High Cascades and a large area of the Basin and Range beginning between 10 and 8 m.y. B.P. could be sheer coincidence.

The linkage of some High Cascade volcanic processes to processes operative in the Basin and Range province is central to understanding the nature of High Cascade volcanism. Similarities in composition and probably in petrogenesis between late High Cascade mafic lavas and mafic lavas of the eastern Oregon Basin and Range were first noted by Taylor (1980) and more completely discussed in a later study by Flaherty (1981). Priest and others (1981) pointed out both the chemical and textural affinity of early High Cascade basalts to the eastern Oregon basalts. All of these workers concluded that basaltic magmatism in the Cascades may have been affected by partial melting processes linked to Basin and Range-like extensional tectonism.

Petrologic arguments of Flaherty (1981) suggest that extensional faulting may be necessary to explain the eruption of early High Cascade basalts. He shows that compositions of mafic end members of early High Cascade lavas in the Belknap Hot Springs probably last equilibrated at about 10 kb (30-km depth). He calls on crustal extension during early High Cascade time to bring these magmas rapidly to the surface without extensive re-equilibration and differentiation at shallower levels. Similar arguments for rapid ascent to the surface were advanced by him for late High Cascade basalts.

The previously discussed cessation of middle Miocene folding between about 7 and 11 m.y. ago is evidence that more extensional crustal conditions began to affect the Cascades during early High Cascade time. Occurrence of numerous northwest-trending early High Cascade mafic dikes and normal faults at this time is additional evidence of relatively extensional crustal conditions (e.g., see the section on N. 20°-40° W. normal faults and intrusives).

The switch to more crustal extension and change to more mafic volcanism probably corresponds to a major change in the plate-tectonic regime about 9 m.y. B.P. Between about 10 and 8 m.y. B.P., a change in the direction of Basin and Range spreading probably occurred (Zoback and Thompson, 1978), and Atwater (1970) infers from the geometry of oceanic-plate movements that the direction of plate convergence may also have changed at about this same time.

Extensive normal faulting and local formation of north-south-trending

grabens along the central High Cascade axis during the last 4 to 5 m.y. is conclusive evidence that late High Cascade volcanism is also closely related to a time of crustal extension. As previously mentioned, focal mechanism studies of Couch and Lowell (1971) also indicate that the current stress regime has the minimum compressive stress axis oriented approximately perpendicular to these north-south-trending faults.

Conclusions

The compositional data favor a tectonic history for the Cascades which includes three major stages:

1. Initial formation and development of a subduction zone between about 40 and 18 m.y. B.P. This early Western Cascade episode was characterized by eruption of magmas similar to those evolved from primitive island arcs or shallow subduction on the outer margins of mature island arcs.
2. Maturation of the subduction zone continued between about 18 and about 9 m.y. ago. This late Western Cascade period was characterized by eruption of calc-alkaline andesite and high-alumina basalt typical of mature island arcs over well-developed active subduction zones.
3. Modification of the pattern of structural deformation between 10 and 8 m.y. B.P. probably caused eruption of magmas more mafic and alkaline than previous magmas. The most mafic basaltic lavas of this High Cascade episode of magmatism resemble back-arc lavas of island arcs and even more closely resemble contemporaneous basalts of the Oregon Basin and Range province. The structural modification probably involved increased extensional deformation related to Basin and Range spreading. Continued eruption of magmas similar to the late Western Cascade magmas, presence of a north-south-trending line of composite calc-alkaline volcanoes, and existence of heat-flow patterns typical of subduction zones argue for continued operation of an active subduction zone beneath the High Cascade province.

KNOWN AND PROBABLE HYDROTHERMAL SYSTEMS

Fifteen thermal springs with temperatures above 20° C are known in the Cascade physiographic province (Figure 2.4). Most of the springs are concentrated along the margin of the Western Cascade province in the deepest valleys. Many of the springs in the northern and central Oregon Cascades are associated with

mapped faults. The main springs in Ashland, Oregon, probably related to Cascade hydrothermal systems, are in the 30°-C to 34°-C range and rise along the contact between the Ashland pluton and surrounding sedimentary rocks (Elliot and others, 1981). The four hottest springs in the Cascades, excluding the fumaroles at the Mount Hood vent, are Austin (Carey) Hot Springs (86° C), Breitenbush Hot Springs (92° C), Belknap Hot Springs (86.7° C), and Foley Hot Springs (80.6° C) (Mariner and others, 1980). These springs have estimated mean reservoir temperatures of between 99° C and 125° C, based on various chemical geothermometers calculated from the concentrations of Na, K, Ca, Mg, and Si (Brook and others, 1978). Reservoir temperatures of 181° C and 195° C have been estimated from sulfate water isotope data for Austin and Breitenbush Hot Springs, respectively (Brook and others, 1978).

The Belknap-Foley-Bigelow hydrothermal system is apparently controlled by eastern boundary faults of the uplifted Western Cascade block (see the section on north-south faults). Similar north-south-trending faults are associated with Terwilliger Hot Springs at Cougar Reservoir and with Breitenbush Hot Springs (Figure 2.4). The youthful age of these north-south faults and their position perpendicular to the minimum compressive stress axis in the Cascades (see structural geology section) probably promote fracture permeability which, in turn, allows deep circulation of meteoric water. Because these faults are concentrated in thermally weakened crust of the High Cascade heat-flow anomaly, meteoric water can reach quite high temperatures at relatively shallow depths. The hottest springs could reach their calculated reservoir temperatures at about 2 to 3 km according to heat flow and gradients measured by Blackwell and others (1978) and Black and others (Chapter 7). Taking the Breitenbush Hot Springs area as a typical example, a temperature-gradient hole at Devils Creek yielded a terrain-corrected gradient of 72.6° C/km, which means that temperatures of about 200° C could be encountered at about 2.74 km (Priest and others, 1982). If temperatures such as this occur at drillable depths within most of the central High Cascade heat-flow anomaly, the entire central High Cascade area is a good target for high-temperature thermal fluids. The problem facing exploration in the Cascades is not adequate temperatures but adequate permeability required to produce significant fluids. This problem will be addressed in the next section on reservoir rocks.

Superimposed on the high regional heat-flow pattern, there likely are local small anomalies of even higher heat flow at and near Holocene volcanic vents.

A good example is Mount Hood, which is associated with a local anomaly at least 20 mW/m^2 higher than the surrounding background heat flow of the High Cascades (Steel and others, 1982; Black and others, Chapter 7; see Figure 2.4). The increase in heat flow over background is no doubt quite extreme near fumaroles of the Crater Rock plug dome which is still cooling from eruptions about 200 yr B.P. (Crandell, 1980). Similar high heat flow and possible high-temperature hydrothermal systems could occur at other Holocene volcanic centers such as Mount Jefferson, the Three Sisters, and Crater Lake. All of these volcanic centers have erupted significant volumes of andesitic to dacitic magma. Silicic magmas, because of their high viscosity, tend to form large shallow plutonic bodies which can drive hydrothermal convection systems. These volcanoes, then, have a good chance of being underlain by shallow plutonic bodies.

Although not in the High Cascades, Newberry volcano is probably the best example of a silicic volcanic center with a high-temperature hydrothermal system. Fluids with temperatures of 265°C were found at the bottom of a 932-m-deep drill hole near a 1,300-yr B.P. rhyodacite flow in the summit caldera (Samuel, 1981). Taylor (1981) has described a broad silicic volcanic highland 32 km (20 mi) wide located in the Three Sisters area adjacent to Newberry volcano. Existence of numerous late Pliocene ash flows with probable source areas near or in this highland (Taylor, 1981) is evidence that calderas similar to the one at Newberry might also occur in the Three Sisters area. It is thus quite possible that the Three Sisters area may harbor high-temperature hydrothermal systems similar to the one at Newberry.

Most of the Three Sisters highland, except for the part adjacent to Century Drive south of Broken Top volcano, is in a wilderness area, and therefore development of the highland is not likely. The same is true of the Mount Jefferson and Crater Lake areas--the former is in wilderness and the latter is a national park. Recent investigations of the USGS have revealed warm springs in the bottom of Crater Lake indicative of active hydrothermal circulation (Williams and von Herzen, 1982), and the caldera is very young. Exploration in areas near Crater Lake, but outside of the park boundary, might be worthwhile.

Although it is not normally considered part of the Cascades, the Klamath Falls hydrothermal system may be closely related to the High Cascades. As previously discussed, the Klamath graben may be an extension of High Cascade graben structures into a zone of very high heat flow inferred from Curie-point isotherm studies by McLain (1981). McLain (1981) estimated from aeromagnetic data that

the Mount McLoughlin-Klamath Lake area has heat flow between 130 and 160 mW/m² and a depth to the 580° C Curie-point isotherm of between 4 and 6 km below sea level. He also points out that the Curie point could be as low as 300° C, which would yield calculated heat flow of approximately one-half of the 130- to 160-mW/m² values. He, however, feels the latter possibility is unlikely in view of modeling constraints posed by the probable mineralogy of local crustal rocks. Absence of a reliable knowledge of the composition of crustal rocks at 4- to 6-km depth is, however, a serious problem for interpretation of McLain's (1981) data. McLain (1981) also points out that Newcomb and Hart (1958), Peterson and Groh (1967), and Peterson and McIntyre (1970) all postulate that the heat source for the Klamath Falls hydrothermal system lies to the northwest, approximately within the Mount McLoughlin-Klamath Lake area.

Sammel (1980) suggested that hydrothermal systems at Klamath Falls have reservoir temperatures of about 150° C, based on various Na, K, Ca, Mg, and Si geothermometers. Sulfate-water isotope geothermometers give estimated reservoir temperatures of about 190° C for some hot springs of the Klamath Falls area (Brook and others, 1978). Sammel (1980), while noting that much of the shallow heat in the Klamath basin had been redistributed by hydrothermal circulation, estimated that the average heat flow is about 83.6 mW/m². Sammel (1976) and Sass and Sammel (1976) concluded that background heat flow is about 60 to 70 mW/m², with background gradients of 30° to 40° C. These estimates were much lower than Sammel's (1980) estimate and the average of 84 to 117 mW/m² estimated by Blackwell and others (1978). Blackwell and others (1978) estimated an average gradient of 100° to 150° C/km for lake sediments and 50 to 100° C/km in basalts of the area. The estimates of Blackwell and others (1978) are preferred, since they are more in line with Sammel's (1981) estimate and the 80 to 160 mW/m² estimated for the entire Klamath basin by McLain (1981).

Using these temperature gradients and heat-flow values, it is possible to make crude estimates of the depths to which meteoric water would have to circulate to reach various temperatures. In order to reach temperatures of 200° C in the Mount McLoughlin-Klamath Lake heat-flow anomaly of McLain (1981), circulation would probably only need to reach to depths of 2 to 3 km. It would be very surprising if meteoric water could not penetrate to these depths, in view of the numerous youthful, relatively undissected fault scarps (e.g., Kienle and others, 1981) and continuing seismic activity in the region (e.g., see seismic data of Couch and Lowell, 1971). Drilling and heat-flow measurement should be pursued

throughout the Klamath basin with particular emphasis on the Mount McLoughlin-Klamath Lake area to establish the details of hydrothermal circulation. Shallow temperature probing of Klamath Lake and other lakes in the southern Cascades might be a possible low-cost exploration technique worthy of study.

POTENTIAL RESERVOIR ROCKS FOR HYDROTHERMAL CIRCULATION

Most lavas and other brittle rocks in the Cascades probably have sufficient fracture permeability to allow movement of hydrothermal fluids where the rocks are intercepted by youthful fault zones, particularly the north-south faults (i.e., see the previous section). Priest and others (1982), however, found that andesitic to dacitic lavas, flow breccias, and debris flows of late Western Cascade and older rocks in the Mount Hood area tend to be very reactive during even low-grade zeolite-facies metamorphism, causing almost complete loss of permeability. Their findings suggest that Miocene tholeiitic basalts and silicic intrusive rocks with extensive open fractures may be prevented from receiving meteoric water by overlying impermeable altered andesitic to dacitic rocks of the late Western Cascades episode. The permeability of intrusive rocks is not only supported by the studies of diamond core made by Priest and others (1982) but by evidence of extensive downflow in temperature-gradient holes drilled into intrusions around Mount Hood (e.g., Steele and others, 1982). Evidence of upflow within the outer margins of the Ashland pluton (see previous section) is additional evidence that intrusive rocks tend to be permeable.

Free movement of ground water through most High Cascade lavas (i.e., lavas less than about 9 m.y. B.P.) is indicated by the highly irregular, low-temperature gradients and abundant ground water encountered in these rocks during drilling of temperature-gradient holes (e.g., see Blackwell and others, 1978; Youngquist, 1980). Unfortunately, whereas the lavas tend to be laterally permeable, impermeable intervening fine-grained pyroclastic and epiclastic rocks tend to limit vertical permeability. Blackwell and others (1982) found that there was very little vertical communication between aquifers in the Mount Hood volcano. Sammel (1981) found numerous aquifers with widely varying temperatures at Newberry volcano. These wide temperature variations would be unlikely if there were much vertical exchange between the aquifers. It is probably essential that vertical pathways be present whereby meteoric waters are able to percolate deeply enough to reach deeply buried rocks with high temperature. Previously mentioned fault zones adjacent to grabens along the High Cascade axis

and in the Klamath Lake area probably conduct water to deeply buried rocks. Caldera faults at Newberry volcano and Crater Lake probably provide conduits for intracaldera circulation systems.

The actual edifices of the High Cascade composite cones are probably not good geothermal targets, although economic hydrothermal systems may exist in older rocks beneath the volcanoes, especially if silicic magmas have intruded into the upper crust. Water may simply run off rapidly at shallow levels through the radially dipping flank flows without deep circulation if vertical aquifers such as faults are not present in the cones. Even if moderately deep circulation occurs in the volcanoes, the heavy rate of precipitation in the Cascades may cause ground-water flushing of heat from the systems to be so rapid that high-temperature hydrothermal systems may not have long lives. There is also no evidence of other than very small intrusions within the cones. Careful hydrologic analysis and drilling of the composite cones must be accomplished to evaluate these variables. Results from drilling at Mount Hood (Steele and others, 1982) have not been encouraging.

Vertical conduits for penetration of meteoric water are also essential in Western Cascade terranes in order to provide pathways through the impermeable andesitic and tuffaceous units. Youthful fault zones commonly occur in the Western Cascade Range in areas of high heat flow within and along the margins of the High Cascades heat-flow anomaly (see Figure 2.4 and the section on structural interpretation). These faults may provide pathways for deeply circulating fluids to reach tholeiitic lavas and plutonic rocks which may serve as reservoirs at depth. Likewise, intrusions which crop out at the surface may provide similar conduits for deeply circulating waters. Exploration in the Western Cascades should be aimed at the faults and plutonic contacts where they lie in the High Cascade heat-flow anomaly.

Areas which are likely to have much-enhanced vertical permeability in all types of terrain are intersections of major fault zones. The most likely such intersections are in areas where the major northwest- and northeast-trending faults intercept north-south-trending faults of the High Cascades. The largest intersection of this type occurs where the Brothers fault zone intercepts the High Cascade axis in the Newberry-Three Sisters area. The high density of volcanic centers in this area (Figure 2.4) are likely the result of numerous pipelike conduits created by fault and fracture intersections. The location of some of these buried structures can probably be inferred from lineations in

the pattern of volcanic vents, although, as previously mentioned, such alignments may be a passive reflection of regional stresses and not actual faults (e.g., see Nakamura, 1977). Intersections of volcanic-center lineations, where they are the extensions of mapped faults, may be sites of unusually high permeability.

The Walker Rim is another area which has evidence of numerous fault intersections. Northwest-trending faults of the Eugene-Denio lineament trend toward north-south- and northeast-trending faults which bound the east side of a graben on the eastern margin of the central High Cascades (Figure 2.4). These faults cut lavas of early High Cascade age (MacLeod, personal communication, 1982) and may be sufficiently youthful to have significant fracture permeability. Although the northwest-trending faults are probably older where the Eugene-Denio lineament strikes the west side of the High Cascades (e.g., see Woller, Chapter 6), that area may have some enhanced permeability as well.

The Mount McLoughlin lineament and Clackamas River fault zone may locally provide similar fault intersections where they reach the High Cascade province (Figure 2.4). Upon reaching the High Cascade axis, most of the northwest-trending faults in these zones, however, appear to swing into rough parallelism with the north-south faults. Further mapping will be necessary to make certain that intersections do in fact occur both in these areas and in other areas with intersecting lineament patterns.

RECOMMENDED GEOTHERMAL EXPLORATION TARGETS

The best regional target for geothermal resources in Oregon is the High Cascade province south of the Clackamas River wrench-fault zone. Potential for development of geothermal resources is highest where fracture permeability and heat flow are at a maximum. Major intersections of youthful faults with sites of Holocene volcanism or with other faults are the best exploration sites. North-south-trending faults may have more open fractures, since they are parallel to the major compressive stress axis discussed previously. Volcanic centers containing abundant silicic rocks are most favorable because they are frequently underlain by shallow plutonic bodies.

The Three Sisters-Newberry volcano area is the best exploration site in the Cascades because it meets all of the above criteria. Pliocene to Quaternary faults with northeast, northwest, and north-south strikes converge in this area (e.g., Wells and Peck, 1961; Peterson and others, 1976), and silicic volcanic

centers occur both at South Sister, where there is a broad silicic highland 24 km in diameter (Taylor, 1980), and at Newberry volcano (MacLeod and others, 1981). A gravity anomaly, possibly associated with a silicic plutonic complex, covers an area of 275 km² at Newberry volcano (Williams and Finn, 1981; Black, 1982). The potential at Newberry is underscored by recent discovery of thermal temperatures and possible fluids at 265° C at a depth of 932 m (3,057 ft) in the caldera (Sammet, 1981).

Other secondary targets include the following areas where fracture permeability is combined with heat flow high enough for temperatures greater than 175° C within 3 km (9,843 ft) of the surface (i.e., within the highest heat-flow area of Figure 2.4):

1. All north-south-trending faults in the High Cascades and areas immediately adjacent to the High Cascades. Mapped faults of this type include margins of the High Cascade province at the upper McKenzie River (Avramenko, 1981), Belknap Hot Springs (Brown and others, 1980a; Flaherty, 1981), the Green Ridge-Tumalo fault zone (Hales, 1975; Peterson and others, 1976), possibly Diamond Lake (Barnes, 1978), the Walker Rim (Wells and Peck, 1961), and Lake of the Woods (Maynard, 1974). Other areas with lineations on strike with these mapped faults are also good targets (see Allen, 1966; Venkatakrisnan and others, 1980; Kienle and others, 1981). Some of the most interesting lineations are north-south-aligned volcanic centers which occur in numerous areas (e.g., Taylor, 1980; Figure 2.4).
2. Northwest-trending faults that parallel Basin and Range trends in the southern Cascades may also be good targets (e.g., see Naslund, 1977; Kienle and others, 1981). The Klamath Lake area is probably one of the best prospects. Even though it is part of the Basin and Range physiographic province, it is so closely adjacent to the High Cascades that it probably shares many geological and heat-flow characteristics with the High Cascades. This is supported by recent Curie-point isotherm studies which show that there may be very high heat flow under the Mount McLoughlin-Klamath Lake area (McLain, 1981).
3. The intersection zone of northwest-trending faults of the Eugene-Denio lineament with north-south- and northeast-striking faults of the Walker Rim may be an area of unusually high fracture permeability (e.g., see Wells and Peck, 1961; Kienle and others, 1981). Similar intersection

zones may occur where the Eugene-Denio lineament meets the Cascade axis in the Western Cascades and at the intersection of the Clackamas River and Mount McLoughlin zones with the High Cascade axis. Other intersecting lineament patterns within the High Cascade heat-flow anomaly should also be mapped to determine if faults are in fact present.

CONCLUSIONS

The central Oregon Cascades has been the site of eruption of abundant volcanic rocks for the last 40 m.y. Eruption of voluminous silicic tuffs and lesser volumes of iron-rich mafic to silicic lavas characterize the 40- to 18-m.y. B.P. early Western Cascade episode. Typical calc-alkaline lavas and subordinate tuffs of intermediate composition erupted during the late Western Cascade episode between about 18 and 9 m.y. B.P. Cessation of minor local folding in the north-central Cascades and beginning of eruption of volcanic rocks more mafic, alkaline, and iron-rich than the late Western Cascade rocks occurred about 10 to 8 m.y. B.P. The axis of volcanism shifted at this time toward the east, close to the present High Cascade axis. Widespread north-south to north-northwest normal faulting accompanied subsidence of the High Cascade axis relative to uplifted adjacent areas of the central Cascades, especially the uplifted Western Cascade block, between about 5 and 4 m.y. B.P. A north-south-trending chain of composite volcanoes has developed along the High Cascade axis in Quaternary time amid continuing eruptions of basaltic lavas on top of the platform formed of Pliocene mafic lavas. The overall composition of the 4- to 0-m.y. B.P. sequence has become slightly more silicic with time.

Compositional and textural similarity of some basalts erupted in the Basin and Range province and the central Cascades during the last 9 m.y. leads to the speculation that extensional tectonic processes characteristic of the Basin and Range province may have modified the probably subduction-related central Cascade volcanism. Changes in the Basin and Range which also began at about 10 to 8 m.y. B.P. include:

1. Beginning of westward migration of silicic volcanism from east of the Harney Basin across the High Lava Plains-Basin and Range provinces (Macleod and others, 1975).
2. Beginning of eruption of high-alumina, often diktytaxitic, olivine tholeiites (Hart, 1982).
3. The present physiography of the Basin and Range province became well

defined (Stewart, 1978).

4. The direction of Basin and Range spreading may have changed (Zoback and Thompson, 1978).

The contemporaneity of these events with a major change of Cascade volcanism further suggests that the volcano-tectonic history of the Cascades and the Basin and Range province are closely linked.

The westward migration of silicic volcanism from the Basin and Range culminated in eruption of voluminous silicic volcanic rocks during the last 700,000 yr at Newberry volcano (MacLeod and others, 1981). Silicic Quaternary volcanism in the Three Sisters area adjacent to Newberry volcano (Taylor, 1980) makes the Three Sisters-Newberry volcano area a likely location for high-level plutonic bodies and shallow high-temperature geothermal systems. Numerous northeast-, northwest-, and north-south-trending faults and volcanic vent alignments in the same area are evidence that significant fracture permeability may also be present at depth. These factors make the Three Sisters-Newberry volcano area the best geothermal exploration target in the Oregon Cascades. The entire High Cascade province and a significant part of the Western Cascade Range have very high regional heat flow.

Where faults or Holocene volcanic centers occur, economically exploitable hydrothermal systems may be present. Hot springs along the Western Cascade—High Cascade physiographic boundary are the surface manifestations of the hydrothermal systems related to the regional heat-flow anomaly associated with the High Cascades.

ACKNOWLEDGEMENTS

The study was supported by the U.S. Department of Energy. George W. Walker of the USGS, Paul E. Hammond and Marvin H. Beeson of Portland State University, and Brian H. Baker of the University of Oregon reviewed an early summary of the paper. Norman S. MacLeod of the USGS reviewed the entire volume and provided numerous valuable critical comments. The helpful criticism of these workers, as well as of Donald A. Hull and John D. Beaulieu of the Oregon Department of Geology and Mineral Industries, is appreciated.

CHAPTER 3. PRELIMINARY GEOLOGY OF THE
OUTERSON MOUNTAIN-DEVILS CREEK AREA, MARION COUNTY, OREGON
By George R. Priest and Neil M. Woller,
Oregon Department of Geology and Mineral Industries

ABSTRACT

The Outerson Mountain-Devils Creek area was the site of mafic and subordinate andesitic to dacitic volcanism from about the middle Miocene (older than 11.5 m.y. B.P.) to about 4.8 m.y. B.P. Eruptions of basalt gave way to increasing quantities of basaltic andesite and subordinate andesite in the first phase of activity during eruption of the lavas of Outerson Mountain. The final eruptions of the lavas of Outerson Mountain occurred about 9.5 \pm 1.3 m.y. B.P. Between about 9.5 and 6.3 m.y. B.P., several small dacitic to andesitic ash flows (the tuffs of Outerson Mountain) were erupted from nearby sources, probably to the west or northwest. They were cut by two small, down-to-the-west, N. 30° W.-trending normal faults and then capped by basalt and basaltic andesite flows near Outerson Mountain about 6.3 m.y. B.P. At about the same time, basaltic andesite and dacite erupted from vents in the Spire Rock-Triangulation Peak area.

Heat flow in the area may be high enough to provide temperatures of about 200° C at about 2.7 km. It is not known if adequate fluids and permeable rock units exist at this depth. It is, however, possible that areas adjacent to the two mapped faults may not retain significant fracture permeability, because no new movement has probably occurred on the faults since at least 6.3 m.y. B.P. Areas adjacent to more youthful faults near the map area probably have a better chance of having significant fracture permeability.

INTRODUCTION

The Outerson Mountain-Devils Creek area lies in the Western Cascade physiographic province about 7 km (2.4 mi) southeast of Breitenbush Hot Springs (Figure 3.1). Local relief in the Devils Creek valley is about 620 m (2,034 ft). The South Fork of the Breitenbush River lies about 1.9 km (1.2 mi) north of Devils Creek. The area is characterized by steep, mature topography and poor bedrock exposure. A preliminary geologic map of about 15.5 km² (6 mi²) was produced at a scale of 1:24,000 (Plate 3).

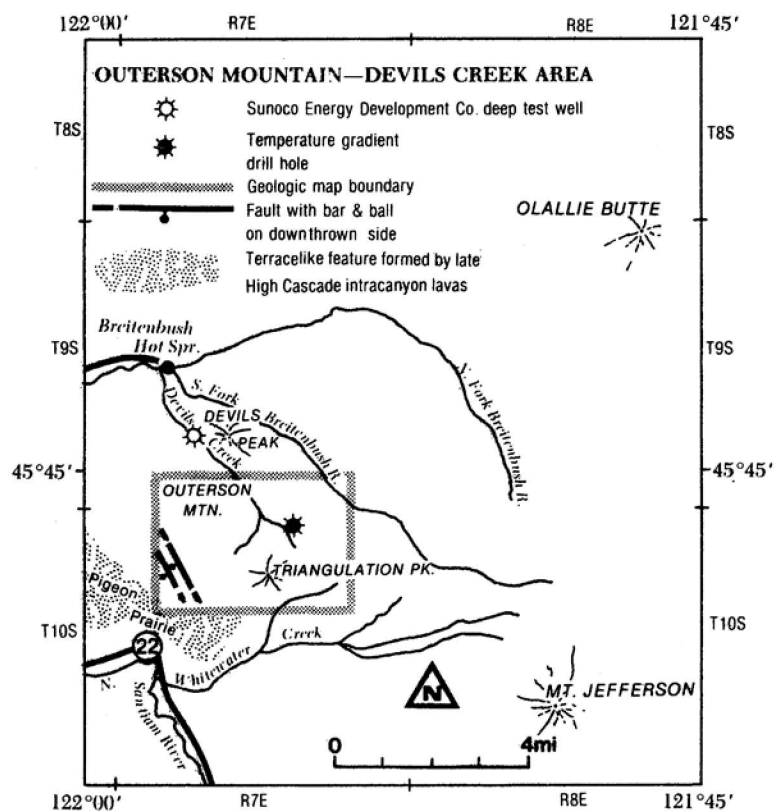


Figure 3.1. Location of the Outerson Mountain-Devils Creek map area and other localities mentioned in the text.

The area was partially mapped during drilling of a 152-m-deep temperature-gradient hole in 1979 in order to interpret the heat-flow data from the well. Additional mapping was completed in 1981. The area was also investigated in order to understand the stratigraphy of a group of rocks at Outerson Mountain called the Outerson formation by White (1980a,c) and the Outerson basalt by Hammond and others (1980, 1982). These names have been used for regional stratigraphic nomenclature in the central Cascades (e.g., McBirney and others, 1974; Taylor, 1980). The area has also recently become important because it was the site of a deep geothermal test well drilled by Sunoco Energy Development in the fall of 1981 on Devils Creek (Figure 3.1). This well was scheduled to reach a depth of 2,743 m (9,000 ft), which would make it the deepest well in the Cascades.

Specific goals of the project were to (1) locate faults which might influence the circulation of hydrothermal waters, and (2) decipher a mass of conflicting geologic data which have been generated by numerous previous workers who have mapped in the area. K-Ar data (Appendix A) generated by Stanley Evans of the University of Utah Research Institute were particularly helpful with respect to the latter goal.

Because of time limitations, it was not possible to complete all of the needed detailed geologic mapping. The small amount of mapping completed should be considered very preliminary. In order to resolve the most critical problems in the area, a detailed geologic map from Sardine Mountain to Mount Jefferson should be completed. Hopefully, the small amount of data presented here will aid in the overall effort.

PREVIOUS WORK

The study area is partly or entirely included in geologic maps by six different workers. Stratigraphic columns for these maps are presented on Plate 1.

The area was first mapped by Thayer (1936, 1939) during his mapping of the North Santiam River drainage. Thayer (1939) mapped all of the area as the Outerson volcanics, which he termed the oldest formation of the High Cascade series. He recognized that the rocks in the area were a varied assemblage of mafic lavas, flow breccias, and tuffs.

On the geologic map of western Oregon, the map area is shown as Pliocene-Pleistocene basalt and andesite (QTba), with a mafic intrusion (QTim) on the south flank of Outerson Mountain. The regional geologic map of Peck and others (1964) shows the area as Quaternary-Tertiary basalt and andesite (QTv), with a

volcanic plug (QTa) in the same locality as unit QTim on Wells and Peck's (1961) map. The location of the intrusive rocks on both maps is a large exposure of gray ash-flow tuff with a very small dike intruding it.

Clayton (1976) next mapped most of the area as part of his master's thesis. His map included a much larger area than the area on Plate 3 and encompassed Breitenbush Hot Springs. He recognized seven rock units in the area but had no radiometric age data and no chemical analyses of rock units. Two of his units, the Lake Leone sediments and the Outerson tuff, were not found in the mapped area but are present outside it. Differences between the nomenclature adopted here and Clayton's (1976) names are a result of differences in placement of rock-unit boundaries. This is discussed in detail in the following sections.

The northern edge of Rollins' (1976) master's thesis map overlaps the study area. Rollins split the rocks cropping out in the overlap zone into three units and showed the detailed distribution of dikes and plugs in the area. The distribution of dikes and plugs in the Triangulation Peak area on Plate 3 has been taken directly from his map. Rollins (1976) did extensive chemical and petrographic analysis of rock units but had no radiometric data. There are also some differences between the separation of mappable rock units between this study and Rollins' study, and his larger map area included units to the south which are both older and younger than units in the Outerson Mountain area.

Hammond and others (1980) published a compilation map which combined all of the units recognized by Rollins (1976) and Clayton (1976) into two major units, the Outerson basalt (To) and overlying older High Cascade basalt (QTb). This map also shows some of the local intrusive rocks and includes some inferred faults not recognized by previous workers. The inferred faults were not found in this study, but the general age relationships inferred by Hammond and others (1980, 1982) are similar to those found here. Hammond and others (1980, 1982) had access to new K-Ar data from their own study and work of Sutter (1978) and White (1980a,c).

White (1980c) mapped the area as part of his doctoral dissertation. His map covers a much larger area, and the Outerson Mountain-Devils Creek area was not the focus of his research. Consequently, he made no attempt to do detailed volcanic stratigraphy in the Outerson Mountain area, although he did add several new chemical analyses and summarized all of the available radiometric dates. He combined the units of the Outerson Mountain area into two major units, the Elk Lake-Sardine Formations (undifferentiated) (Tes) and Plio-Pleistocene lavas (undifferentiated)

(QTb). White (1980c) also showed the distribution of some of the local intrusive rocks. The units and faults of Hammond and others (1980) and White (1980c) do not closely correspond to one another in the study area.

In his map of the Breitenbush quadrangle, which includes the north side of the study area, White (1980a) used somewhat different terminology than in his (1980c) dissertation. He also mapped some faults through to the boundary between his (1980a) map and the map from this report which do not extend as far south on his (1980c) dissertation map. Because the Breitenbush quadrangle extends well east of White's (1980c) dissertation map, the (1980a) Breitenbush map was able to show structures and rock units of the High Cascade province. A significant finding of White's (1980a) study was an inferred north-south-trending fault which separates a thick section of young High Cascade rocks to the east from older rocks to the west. The fault projects just east of the present study area and may be the western boundary of a major graben along the High Cascade axis. Neither Hammond and others (1980) nor Hammond and others (1982) show this fault. Further detailed mapping should be done to resolve this problem.

The 1:62,500-scale map of Hammond and others (1982) shows the geology for a large area from the Clackamas River to the North Santiam River. Contacts on this map within the area of Plate 3 correspond closely with those of Clayton (1976), although there are a few additional faults and some differences in the contacts and the names assigned to the units. The absolute ages of units are similar to ages inferred by Hammond and others (1980).

STRATIGRAPHY

Introduction

The area is dominated by mafic lavas of the late Western Cascade and early High Cascade volcanic episodes, the lavas of Outerson Mountain (Tmo) and the upper Miocene-Pliocene lavas (Tmp), respectively. A thin ash-flow-tuff sequence, the tuffs of Outerson Mountain (Tmt), lies between the two lava units in the southwestern part of the map area. Figure 3.2 summarizes the stratigraphic units of the study area.

Absolute ages of the mafic lavas are based on three new K-Ar dates (see Appendix A) and on three previously published K-Ar dates of Sutter (1978) and White (1980c). Locations of the previously published dates plotted on Plate 3 are those of White (1980c) and White (personal communication, 1982). K-Ar dates

Figure 3.2. Stratigraphy of the Outerson Mountain-Devils Creek area

Nomenclature used in this report	Unit	K-Ar dates m.y. B.P.	Maximum thickness	Lithology and comments
Volcanic rocks of the early High Cascades	Upper Miocene-Pliocene lavas (Tmp)	4.8±0.2 6.3±0.2 6.0±0.9	242 m (794 ft)	Fine-grained gray basaltic andesite to basalt, plagioclase-phyric basaltic andesite, orthopyroxene dacite(?), and near-vent agglutinate.
	Subvolcanic intrusive rocks (Tmi)	5.7±0.1 (S; W)* 11.5±0.2 (S; W)*	---	Dikes and plugs of basaltic to dacitic lava. Some dikes were probably emplaced during late Western Cascade time.
Volcanic rocks of the late Western Cascades	Tuffs of Outerson Mountain (Tmt)	---	Maximum exposed thickness of ash flows: 5th: 18.3 m (60 ft) 4th: 85.3 m (280 ft) 3rd: 9.1 m (30 ft) 2nd: 9.1 m (30 ft) 1st: 48.8 m (160 ft)	Five ash-flow tuff units with interbedded epiclastic and probable surge deposits. Most exposures have incomplete sections averaging about 91 m (300 ft) thickness. Pumice from the 4th ash flow is low-silica andesite; all others have dacite pumice.
	Lavas of Outerson Mountain (Tmo)	9.5±1.3 5.3±0.6	372+ m (1,220+ ft)	Moderately phyric olivine-bearing high-silica basalt to andesite with abundant partially palagonitized surge deposits, aa flows, and cinder deposits. Lower part moderately altered and more mafic; upper part less altered and more silicic. Base is not exposed but probably corresponds to the base of Rollins' (1976) Grizzly Creek lavas.

*W = White (1980c), recalculated by Fiebelkorn and others (1982).

*S = Sutter (1978), recalculated by Fiebelkorn and others (1982).

of Sutter (1978) have been recalculated by Fiebelkorn and others (1982) to conform to currently accepted abundance and decay constants.

Rock names have been assigned according to the chemical classification of Priest and others (Chapter 2) from analyses listed in Appendix B and from previously published data. Locations of all samples analyzed in this study and previous studies are shown on Plate 3.

Volcanic rocks of the late Western Cascades

Lavas of Outerson Mountain (Tmo): Moderately phyric olivine basaltic andesite (53-58 percent SiO₂) and high-silica olivine basalt (51-53 percent SiO₂) make up 95 percent of the unit. Some two-pyroxene andesite is interbedded at the top of the sequence. The sequence becomes more silica rich upward.

Differing eruptive modes have generated lavas, flow breccias (autobreccias), cinders, scoria, partially palagonitized cinders, and palagonite tuffs. The partially palagonitized cinders and palagonite tuffs have bedding with dips up to 50° which reflect high initial dips characteristic of tuff cones. The palagonite tuffs probably developed when mafic magma encountered ground water. Fragmentation and quenching of the magma produced sideromelane cinders, ash, and scoria which were steam-blasted as wet slurries down the sides of the tuff cones. These deposits are most common in the upper part of the sequence on the eastern flank of Outerson Mountain. Because they are laterally discontinuous and chemically related to the enclosing lavas, these surge deposits have not been mapped separately.

The olivine basalt lavas, when holocrystalline, have an intergranular to subophitic texture with randomly oriented plagioclase laths, clinopyroxene, and Fe-Ti oxides. Phenocrysts vary in size from about 1.0 mm to 0.2 mm and consist of chiefly subhedral plagioclase (1-30 percent) and olivine (2-5 percent). Hypohyaline lavas have an opaque black tachylitic glass intersertal between randomly oriented plagioclase laths. Phenocrysts are similar to phenocrysts of the holocrystalline samples. Olivine in the lower part of the section is invariably altered to highly birefringent greenish phyllosilicates, probably saponite or serpentine, and commonly has a reddish hematite rim. Olivine in the upper part of the section is commonly altered to iddingsite and is unaltered in a few uppermost flows. The olivine basalts are most abundant in the lower part of the section. About 152 m of olivine basalt was encountered in the Devils Creek temperature-gradient hole. Olivine basalt is not as common in the upper part of the section

but locally occurs as massive and bedded hyaloclastic deposits.

Basaltic andesite is the dominant rock type in the upper part of the section and looks megascopically identical to the basalt. In thin section, however, the basaltic andesite, when holocrystalline, has a moderate amount of orthopyroxene in the groundmass, sometimes in ophitic intergrowth with plagioclase. A few samples have very minor orthopyroxene phenocrysts with anhedral olivine having embayments and, in one sample, pyroxene rims. Olivine is present as a phenocryst phase in all of the samples.

Andesite was noted only in the upper 150 m of the section, and none was found in the lowest 152 m of the section in the Devils Creek drill hole. The andesite appears megascopically similar to the basalt and basaltic andesite but contains clinopyroxene and orthopyroxene phenocrysts rather than olivine. The andesite forms rehealed autobreccias with 1- to 2-mm-long phenocrysts of plagioclase (8-10 percent), orthopyroxene (1-4 percent), and clinopyroxene (1 percent) set in a hyalopilitic groundmass of devitrified glass. Orthopyroxene is commonly slightly to completely altered to saponite.

The lavas of Outerson Mountain look remarkably homogeneous in outcrop in spite of the wide range of compositional types. The lavas are cliff-forming, reddish-gray to dark-gray units with interflow autobreccias and minor epiclastic rocks, both of which form lower angle slopes. Bedded and massive hyaloclastic deposits locally form "hoodoos," but also, more commonly, gentle slopes. They have a red-brown to dark-gray color where not palagonitized and yellow-brown color where palagonitized. Dark-gray scoria, cinders, and lithic fragments in the surge deposits are commonly suspended in a wholly or partly palagonitized ash matrix. Reddish cinder deposits also occur locally.

The upper contact of the lavas of Outerson Mountain in the Outerson Mountain area has been placed below the tuffs of Outerson Mountain, which are capped by basaltic andesites dated at 6.3 ± 0.2 m.y. B.P. The upper contact in the Triangulation Peak area has been placed at about the 4,640-ft elevation, based on a change in the relative freshness of the rocks. A sample from near the top of the overlying sequence of lavas yielded a K-Ar date of 6.0 ± 0.9 m.y. B.P. The upper contact at Devils Peak was placed between a flow dated by Sutter (1978) at 4.8 ± 0.2 m.y. B.P. and a basaltic andesite flow dated at 9.5 ± 1.3 m.y. B.P. The contact at Devils Peak also falls at about 4,640 ft. There is, however, less evidence of a sharply defined break in the freshness of the rocks across the Devils Peak contact. The lower contact of the lavas of Outerson Mountain is not

exposed in the map area, but 152 m (500 ft) of the unit was penetrated in a drill hole collared at 3,920-ft elevation. The thickness is thus at least 372 m (1,220 ft). The lower part of the sequence must be older than a basaltic sill (White, personal communication, 1981) intruding the lavas of Outerson Mountain at about 3,700-ft elevation at Devils Creek. The sill yielded a date of 11.5 ± 0.2 m.y. B.P. (Sutter, 1978; White, 1980c). The lavas of Outerson Mountain are thus about 9.5 m.y. in age in the upper part and older than 11.5 m.y. in the lower part. A sample dated from the 440-ft level in the drill hole yielded an date of 5.3 ± 0.6 m.y. B.P., but this sample was probably affected by alteration which altered olivine phenocrysts to greenish phyllosilicates.

The upper 366 m (1,200 ft) of the lavas of Outerson Mountain are equivalent to Rollins' (1976) Nan Creek volcanics; the lower 152 m (500 ft) is probably equivalent to Rollins' (1976) Grizzly Creek lavas. Clayton (1976) mapped most of the lavas of Outerson Mountain as the Outerson lava and breccia, but he included some surge and autobrecciated units in the uppermost part of the section in his Cheat Creek sediments which correspond to the upper part of the Rhododendron Formation of Hammond and others (1982). Clayton (1976) also mapped 150 m of the section northeast of Outerson Mountain as the Triangulation Peak volcanics, which correspond to the older basalt and basaltic andesite of Hammond and others (1982). The lavas of Outerson Mountain are included within the larger Outerson basalt unit of Hammond and others (1980) which also includes overlying ash flows of the tuffs of Outerson Mountain. White (1980a) mapped the lavas of Outerson Mountain as Plio-Pleistocene lavas and the underlying Elk Lake formation. Thayer (1939) mapped the lavas of Outerson Mountain and the overlying units of the map area as Outerson volcanics. Wells and Peck (1961) included the unit of Thayer (1939) in their unit QTba which is equivalent to the unit QTV of Peck and others (1964).

Tuffs of Outerson Mountain (Tmt)

Five small, nonwelded andesitic to dacitic ash-flow tuffs and some interbedded epiclastic and surge deposits crop out on the unnamed ridge on the southwest side of Outerson Mountain. These ash flows, here informally named the tuffs of Outerson Mountain, occur in the area between Triangulation Peak and Skunk Creek where they fill an irregular erosional surface cut in the underlying lavas of Outerson Mountain (Plate 3). No flow directions were obtained in this study, but Clayton (1976) noted in exposures of the fourth ash-flow from the bottom that "alignment and blockage of some scoriaceous fragments indicate that flow direction was to

the southeast." The large size and abundance of lithic fragments in many of the ash flows indicate a nearby source. The tuffs are capped by a basaltic andesite flow and cut by two small, northwest-trending normal faults. The faults were recognized by offsets of the lower contact of the tuffs. The potential usefulness of these tuff marker units within the rather monotonous sequence of dark-gray lavas which crop out over most of the study area requires that the tuffs be carefully described.

The lowest ash flow is a cream-colored rock composed of about 20 percent andesitic lithic fragments, 20 percent dacitic (67.0 percent SiO_2) pumice lapilli, and 60 percent ash (see sample DC-103, Appendix B). The pumice is slightly flattened in some parts of the ash flow, although no evidence of welding of glass shards was apparent. The pumice contains about 2 percent plagioclase and 1 percent orthopyroxene in 1-mm and smaller crystals. The glass is entirely altered to smectite. The unit reaches a maximum thickness of about 49 m (160 ft) near Cheat Creek and is the only tuff unit exposed there. This ash flow may correspond to the majority of Rollins' (1976) Cheat Creek beds.

The second ash-flow tuff is a light-yellowish-gray lapilli tuff with about 50 percent light-gray andesitic (61.9 percent SiO_2) pumice lapilli, 30 percent ash, and 20 percent andesitic lithic fragments (see sample DC-104, Appendix B). Pumice from the unit contains about 2 percent plagioclase, 1 percent clinopyroxene, and less than 1 percent orthopyroxene in crystals of 1-mm and smaller size. This is a minor unit in the area, cropping out only in a few places on forest road 2233-650, where it is about 9 m (30 ft) thick.

The third ash flow is also a yellowish-gray unit, similar in appearance to the second ash flow, but it contains lighter colored pumice and numerous small obsidian fragments. No other ash flow in the sequence has as many of these obsidian fragments. The third ash flow is composed of about 36 percent dacitic (65.2 percent SiO_2) pumice lapilli, 55 percent ash, 6 percent andesitic lithic fragments, 2 percent obsidian fragments, and 1 percent cinders (see sample DC-105, Appendix B). The pumice is nearly aphyric, with less than 1 percent plagioclase and pyroxene phenocrysts of 1-mm and smaller size. This is also a minor unit, cropping out with the second ash flow along forest road 2233-650, where it reaches a thickness of about 9 m (30 ft).

The fourth ash-flow unit in the sequence is the thickest and most distinctive of the five tuff units. It is a medium-gray nonwelded tuff with at least one and probably more partings, as well as a crudely bedded basal surge facies.

It is composed of about 15 percent yellowish to gray pumice lapilli (58.1 percent SiO_2), 55 percent gray ash, 30 percent gray to black lithic lapilli, and very minor small obsidian chips (see sample DC-107, Appendix B). Numerous dark-gray scoriaceous lapilli occur in the lithic fraction. The unit is about 49 m (160 ft) thick in most places but reaches a thickness of about 85 m (280 ft) on the southwest side of Outerson Mountain, where it fills a paleocanyon which cuts through all of the underlying ash flows into soft autobreccias and palagonitic surge deposits of the underlying lavas of Outerson Mountain. The paleocanyon appears to trend roughly west-northwest.

Because of the similarity in overall aspects of the fourth tuff unit and massive units in the underlying hyaloclastic deposits of the lavas of Outerson Mountain, most workers (e.g., Clayton, 1976; Hammond and others, 1982) have mapped them as one unit. The steeply unconformable lower contact and andesitic composition of the fourth ash flow distinguish it from the more mafic hyaloclastic deposits. The presence of several meters of crudely bedded surge material in the lower part of the fourth ash flow in the paleocanyon, however, make locating the contact very difficult where it is in contact with surge deposits of the lavas of Outerson Mountain. It may be that the initial stage of eruption of the fourth ash-flow tuff included fragmentation in ground water, forming hyaloclastic surge deposits no different in aspect from similar hyaloclastites in the underlying rocks. Subtle bedding in the lower part of the individual ash flows within the ash-flow sheet may represent additional stages of surge deposition.

The fifth ash flow in the sequence is very poorly exposed in one outcrop near the top of the ridge southwest of Outerson Mountain. The ash flow crops out above the fourth ash flow but below a capping basaltic andesite lava. The unit is composed of 25 percent cream-colored dacitic (69.8 percent SiO_2) pumice lapilli, 65 percent tan-colored ash, and about 10 percent dark-reddish-gray lithic fragments (see sample DC-109B, Appendix B). The pumice is slightly devitrified and contains about 2 percent plagioclase and 1 percent orthopyroxene averaging 0.3 mm in length. The pumice is somewhat flattened, but there is no evidence that the glass shards were welded. The unit has an estimated thickness of 18 m (60 ft). The fifth ash flow closely resembles the first ash flow but has a more yellowish color and considerably less crystal component in the ash-size fraction.

The fourth-erupted ash-flow unit of the tuffs of Outerson Mountain is overlaid by a basaltic andesite lava at Outerson Mountain which yielded a K-Ar date of 6.32 ± 0.2 m.y. B.P. The uppermost dated lava flow in the underlying lavas of

Outerson Mountain is 9.5 ± 1.3 m.y. in age.

The first-erupted ash flow and associated epiclastic rocks are equivalent to Rollins' (1976) Cheat Creek beds. The thick, dark-colored andesitic ash-flow sheet (the fourth-erupted tuff unit) was described by Clayton as his beds of Cheat Creek and was mapped by him to include some hyaloclastic deposits of the underlying lavas of Outerson Mountain. The name Cheat Creek is not used in this report because a much more complete section is available near Outerson Mountain. Hammond and others (1982) combined the sequence of hyaloclastic basaltic tuffs, autobreccias, and andesitic lavas which occur in the upper 150 m of the lavas of Outerson Mountain on the east flank of Outerson Mountain with the tuffs of Outerson Mountain as his Rhododendron Formation. On small-scale reconnaissance maps, the tuffs of Outerson Mountain have been grouped with the Pliocene-Pleistocene lavas of White (1980c), the Outerson basalt of Hammond and others (1980), unit QTv of Peck and others (1964), and unit QTba of Wells and Peck (1961). Thayer (1939) mapped these rocks as part of his Outerson volcanics.

Volcanic rocks of the early High Cascades

Upper Miocene-Pliocene lavas (Tmp): Owing to a paucity of lithologic data on and detailed mapping of rocks capping the lavas and the tuffs of Outerson Mountain, all rocks inferred to be younger than the Outerson Mountain units but older than the intracanyon late High Cascade units are grouped as upper Miocene-Pliocene lavas (unit Tmp, Plate 3). These rocks include a variety of lithologies which may be subdivided when more mapping is completed.

The most common rock type is olivine-bearing basaltic andesite lava, although some orthopyroxene-bearing andesite or dacite probably makes up northerly-dipping, near-vent agglutinate and agglomerate deposits which form the top of the sequence at Triangulation Peak. A distinctive basalt flow with groundmass olivine more abundant than in any of the underlying lavas of Outerson Mountain crops out with a contiguous feeder dike southwest of Outerson Mountain (Plate 3). Unlike most of the lavas in the underlying lavas of Outerson Mountain, the upper Miocene-Pliocene sequence has very little evidence of alteration and, where it is present, olivine is fresh or only slightly iddingsitized. Olivine, particularly in the lowermost part of the sequence, is commonly altered to greenish phyllosilicates in the lavas of Outerson Mountain but never in the upper Miocene rocks. It is, however, a difficult problem to pick the contact between the two units, particularly at Devils Peak where the uppermost part of the lavas of Outerson Mountain become gradationally fresher upward. In that area, as previously

explained, the contact is placed between a flow dated at 9.5 ± 1.3 m.y. B.P. and a flow dated by Sutter (1978) at 4.8 ± 0.2 m.y. B.P.

Two K-Ar dates were obtained on the upper Miocene rocks for this study. A date of 6.3 ± 0.2 m.y. B.P. (63 percent radiogenic argon) was obtained on a small flow capping the tuffs of Outerson Mountain at Outerson Mountain. A sample from the upper part of the sequence west of Triangulation Peak yielded a K-Ar date of 6.0 ± 0.9 m.y. B.P. (9 percent radiogenic argon).

These rocks were mapped in the vicinity of Triangulation Peak as the Triangulation Peak volcanics by Clayton (1976) and the Triangulation Peak lavas by Rollins (1976). They also correspond to the Collawash volcanics mapped by Clayton (1976) in the Devils Peak area. The rocks were mapped as older basalt and basaltic andesite by Hammond and others (1982). On small-scale reconnaissance maps, the upper Miocene-Pliocene lavas have been combined with White's (1980c) Plio-Pleistocene lavas and were mapped as unit QTV (Peck and others, 1964; Hammond and others, 1980) and unit QTba (Wells and Peck, 1961). Thayer (1939) included them in the upper part of his Outerson volcanics.

Subvolcanic intrusive rocks (Tmi)

Basaltic to dacitic dikes are abundant throughout the area. Many of these dikes were probably feeders for local lava flows. A hornblende andesite dike occurs on the north side of Devils Creek, and dacite dikes occur around the Triangulation Peak area. The plug at Spire Rock cuts the upper Miocene-Pliocene lavas and is a high-silica hypersthene dacite with 68.8 percent SiO_2 (see data of Rollins, 1976). A dacite dike on the south flank of Outerson Mountain cuts the uppermost lavas of Outerson Mountain. This dike yielded a K-Ar date of 5.8 ± 0.1 m.y. B.P. (7.1 percent radiogenic argon) and had about 65.8 percent SiO_2 according to White (1980c). A hand sample of this dike, however, appears to be a basaltic andesite, so this casts doubt on the location of the sample. A basaltic andesite (54.3 percent SiO_2) sill in the middle part of the lavas of Outerson Mountain yielded a K-Ar date of 11.5 ± 0.2 m.y. B.P. (10.9 percent radiogenic argon) according to data of Sutter (1978) and White (1980c).

The intrusive rocks have not been examined petrographically in this study. Rollins (1976) describes five separate dacite plugs in the Outerson Mountain-Triangulation Peak area as being petrographically identical. He describes them as being glomeroporphyritic with subhedral plagioclase (5 percent) and hypersthene (2 percent) phenocrysts. The hypersthene phenocrysts are associated with large, granular masses of magnetite. The groundmass is composed of extremely

fine-grained plagioclase and disseminated magnetite.

Rollins (1976) described the petrography of numerous basaltic andesite dikes which are common in the lower part of the stratigraphic section. These rocks have 0.75-mm phenocrysts of subhedral plagioclase (An₅₄) and anhedral olivine (2V near 90°). Olivine phenocrysts are about 5 percent of the rock and are commonly partially or completely altered to either celadonite or hematite and magnetite. The phenocrysts are set in a groundmass of fine-grained plagioclase, clinopyroxene, and magnetite. SiO₂ contents range from 53 to 57 percent.

Most of the intrusions are probably late Miocene in age and correspond to subvolcanic intrusive units mapped by other workers in the area. They correspond to the Plio-Pleistocene dikes and plugs of Clayton (1976) and White (1980c) and are equivalent to unit QT_{im} of Wells and Peck (1961) and unit QT_a of Peck and others (1964).

Volcanic rocks of the late High Cascades

No lavas of late High Cascade age (4 to 0 m.y. B.P.) occur in the map area, but a sample of basalt from the uppermost Pigeon Prairie lavas on the southern boundary of the map area was chemically analyzed (sample PP in Appendix B). This flow is a slightly diktytaxitic basalt (49.4 percent SiO₂) with about 2 percent subhedral to anhedral olivine (0.6 mm) and about 1 percent subhedral plagioclase (0.4 to 1.5 mm) phenocrysts set in a pilotaxitic groundmass of plagioclase with intergranular clinopyroxene and Fe-Ti oxide. Flows of the Pigeon Prairie lavas are deeply intracanyon into all bedrock units of the study area. They are also intracanyon into a sequence of older late High Cascade lavas, the Minto Mountain lavas (e.g., see Rollins, 1976). The distribution and morphology of both the Pigeon Prairie and Minto Mountain lavas suggest that they originated from sources in the High Cascade province (Rollins, 1976). No radiometric date is available for these rocks, but they are younger than the lavas dated at 4.8 m.y. B.P. at Devils Peak (see Sutter, 1978; White, 1980c). Intracanyon flows in this same geologic setting in other parts of the Cascades are generally less than about 4.0 m.y. B.P. in age (Priest and others, Chapter 2).

STRUCTURAL GEOLOGY

Folds and regional tilting

The area lies on the eastern limb of the north-northeast-trending Breitenbush anticline of Thayer (1939). Where not adjacent to faults, dips in a few

thinly bedded epiclastic units in the tuffs of Outerson Mountain vary between 5° and 8° to the east-northeast. Working in a wider area, Rollins (1976) measured dips of about 10° to the southeast within rocks older than his Minto lavas. The Minto lavas are intracanyon lavas of the early part of the late High Cascade sequence. Clayton (1976) measured 5° to 15° dips in the sediments within the lavas of Outerson Mountain and inferred an angular unconformity between these lavas of Outerson Mountain and the overlying tuffs of Outerson Mountain; Rollins (1976) came to similar conclusions. Clayton, however, also found evidence of tilting of a few degrees in late High Cascade lavas. It is difficult to differentiate such small dips from depositional dips in lavas, so Clayton's (1976) observations on the late High Cascade lavas are probably questionable. No evidence of tilting could be demonstrated in the upper Miocene-Pliocene lavas. Slight regional eastward tilting, perhaps related to folding on the Breitenbush anticline, probably ended prior to extrusion of the early High Cascade lavas at Outerson Mountain and Triangulation Peak (i.e., before about 6.3 m.y. B.P.).

Faults

Two small, northwest-trending faults are exposed on the south slope of the ridge southwest of Outerson Mountain. Strikes and dips on these faults are not well constrained owing to irregularities of the fault planes, but both appear to trend about N. 30° W. $\pm 10^{\circ}$ and dip between 72° and 89° to the west. Slickensides on the westernmost fault rake at 90° within the fault plane. The tuffs of Outerson Mountain are offset about 30 m (100 ft) down to the west at each fault. Tilting and minor shearing which affect the tuffs of Outerson Mountain adjacent to these faults do not appear to affect the overlying upper Miocene-Pliocene lavas (T_{mp}). A feeder dike of unit T_{mp} trends N. 30° W. and may follow a small shear or fracture zone associated with the other N. 30° W. faults. The faulting probably took place between 9.5 m.y. B.P., the date of the uppermost lavas of Outerson Mountain, and 6.3 m.y. B.P., the oldest date on the upper Miocene-Pliocene lavas.

Hammond and others (1980) show a northwest-trending and a northeast-trending fault between Outerson Mountain and Triangulation Peak. The oldest ash flow of the tuffs of Outerson Mountain forms a topographic low between the two peaks, but the ash flow is nowhere offset by faults in this low. They also recognized one of the northwest-trending faults noted on Plate 3.

Hammond and others (1982) show five north-south- to northwest-trending

faults in the study area. Only one of these faults closely matches the faults shown on Plate 3.

Thayer (1936, 1939) hypothesized that a 2,000-ft-long, east-facing fault scarp extended N. 10° E. from the eastern side of Mount Bruno (south of Plate 3) beneath Outerson Mountain, to Collawash Mountain (north of Plate 3) prior to burial by "Pliocene" lavas. Following the contact of these "Pliocene" lavas with older rocks, he estimated an eastward slope on the scarp of "500 ft per mile in Mount Bruno" and "1,500 ft per mile in Collawash Mountain."

White (1980a) shows some down-to-the-east, north-south faults east and southeast of Collawash Mountain which offset his Outerson Formation down to the east. One of these faults cuts High Cascade lavas younger than 2 m.y., according to White's (1980a) map. Whereas Thayer (1936, 1939) hypothesized a single fault scarp dipping toward the east, White (1980a) shows a complex series of step faults at Collawash Mountain. There is no evidence of this fault scarp at Outerson Mountain where Thayer (1936, 1939) believes it is buried by these Outerson volcanics (part of his "Pliocene" lavas).

Rollins (1976) shows his Nan Creek and underlying Grizzly Creek lavas (upper and lower part, respectively, of the lavas of Outerson Mountain on Plate 3) wedging out against a western highland of Breitenbush tuff at Bruno Mountain. Rollins (1976), however, interpreted this highland of Breitenbush tuff as an erosional unconformity rather than a fault scarp.

Hammond and others (1980, 1982) show no large down-to-the-east faults along the trend of Thayer's (1936, 1939) "Cascade fault." Hammond and others (1982), instead, show most contacts between major sequences dip toward the east in the southern part of their map area (near Mount Bruno) and are completely faulted by northwest-trending faults in the northern and central part of the area (Collawash Mountain and the Clackamas River). They concluded that there is no evidence that a large down-to-the-east fault separates the High Cascade Range and Western Cascade Range in their area.

One problem which may have led Thayer (1936, 1939) astray in the Outerson Mountain-North Santiam River area is that he assumed that all of the basaltic lavas exposed there were younger than his Sardine series, whereas, in reality, the lavas of Outerson Mountain are probably time-equivalent to many of the rocks he mapped as Sardine series. The unconformity he and Rollins (1976) mapped at Bruno Mountain is actually the erosional break between the early and late Western Cascade sequences rather than the contact between the rocks erupted between the

Western Cascade and High Cascade volcanic episodes. Presumably, this same unconformity was the one Thayer was referring to in areas farther north as the Cascade scarp, although this may not be the case at Collawash Mountain. Hammond and others (1982) show only mafic lavas at Collawash Mountain, so it is difficult to be sure of what Thayer was referring to there, unless it was the steeply east-dipping contact which Hammond and others (1982) show between their basalt of Outerson Mountain (To) and their older basalt and basaltic andesite (QTb). This is essentially the same contact which White (1980a) shows as a series of down-to-the-east step faults. The Collawash Mountain area clearly needs some detailed mapping to determine whether it is, in fact, one outcrop of the scarp of a fault system analogous to the one hypothesized by Thayer (1936, 1939). Recognition of this structure in the Breitenbush area will depend on the ability to discriminate between older and younger mafic lavas--a task which will be very difficult, if not impossible, without tight control from radiometric age determinations. If there is a "Cascade fault" in the Breitenbush area analogous to the one in the Horse Creek-upper McKenzie River area (e.g., Avramenko, 1981; Flaherty, 1981), then it will have moved chiefly during the interval between 5 and 4 m.y. B.P. and will probably be found east of high-standing outcrops of rocks older than this. Areas east of Plate 3 would be logical localities for this structure, if it is present.

Conclusions

The area has been dominated by mafic volcanism from before 11.5 m.y. B.P. to at least 4.8 m.y. B.P., although subordinate amounts of andesite and dacite erupted toward the end of both the late Western Cascade and early High Cascade episodes.

The late Western Cascade episode began with effusive eruptions of high-silica basalt, but basaltic andesite dominated later eruptions. Near the close of the late Western Cascade episode, phreatic eruptions occurred when mafic magmas encountered surface water and ground water. Numerous andesite and basaltic andesite flows and autobreccias erupted between the explosive eruptions. Sometime between 9.5 and 6.3 m.y. B.P., eruptions of dacitic to andesitic ash flows (the tuffs of Outerson Mountain) occurred from a nearby vent, possibly to the northwest or west. These ash flows represent the culmination of the tendency toward more highly evolved, silicic eruptions in the latter part of the late Western Cascade episode.

Following a period of N. 30° W.-trending normal faulting, basaltic andesite

lavas began to erupt about 6.3 m.y. B.P. These lavas continued to erupt until about 4.8 m.y. B.P. Sometime in the latter part of this early High Cascade episode, andesitic to dacitic lavas erupted from the Triangulation Peak area. Numerous dacitic plugs and dikes in that area are the subvolcanic equivalents of this closing phase of the early High Cascade episode.

Following a period of substantial uplift and erosion, basaltic lavas from the High Cascades to the east flowed down a deep canyon south of the study area. These basalts are more mafic than previously erupted lavas and are often diktytaxitic. This late High Cascade episode of activity probably occurred within the last 4 m.y.

GEOTHERMAL RESOURCES

The study area is located adjacent to the southern margin of the Breitenbush Hot Springs Known Geothermal Resource Area (KGRA). The KGRA boundary runs east-west through Devils Peak. The KGRA is predominantly on U.S. Forest Service land, although areas around the hot springs are privately owned. Several springs have temperatures up to 92° C and discharge at about 3,400 l/min (Brook and others, 1979). Brook and others (1979) estimate reservoir temperatures from chemical geothermometry of 99° to 149° C, with a mean temperature of $125 \pm 10^\circ$ C.

Table 3.1 lists some analyses of well and spring samples collected for this study. The various minimum reservoir temperatures are similar to those calculated by Brook and others (1979), although the range goes to somewhat higher temperatures (e.g., 171° C for the silica geothermometer). The high silica values obtained here may, in part, be due to two factors: firstly, both samples which yielded high SiO₂ were from unfiltered samples acidified with ten drops of dilute hydrochloric acid. It is possible that some suspended silica-bearing material was partially dissolved by the acid, enhancing the SiO₂, although some other samples treated in this fashion did not yield high SiO₂ (Table 3.1). Also, silica was actively precipitating from the sample of boiling well water taken in 1980, and silica gel was removed from the filter paper. This filtered 1980 sample yielded a relatively low SiO₂ content of 116 ppm compared to the 175- and 173-ppm values obtained on the unfiltered samples. It may be that the unfiltered samples are more representative in that silica gel was not removed by filtering. The second factor which might have caused one of the two high SiO₂ values is the fact that one of the samples was taken from an artesian well rather than a surface spring. If there is less time for re-equilibration in a rapidly flowing

Table 3.1. Estimated minimum reservoir temperatures and partial analyses from new samples of wells and springs in the Breitenbush Known Geothermal Resource Area (KGRA). Calculations were made according to methods of Fournier and Rowe (1966), Fournier and Truesdell (1973), Fournier (1979), and Mariner and others (1980).

	Wellhead	Spring	Wellhead	Wellhead	Wellhead	Spring
Collection date	1980	12/79	2/23/78	2/10/78	2/10/78	?
Temperature	97.8	98.0	110.0	?	?	81.0
Filtered	Yes	No	No	No	No	?
SiO ₂ (ppm)	116	175	44.2	96	173	128.6
Li (ppm)	1.5	1.78	0.03	1.41	1.9	0.0
Na (ppm)	600	651.0	85.5	675	690	707.4
K (ppm)	27	15.5	8.9	20	34	31.5
Ca (ppm)	81	103.0	21.7	77	90	96.6
Mg (ppm)	< 0.5	1.51	0.8	< 0.5	0.8	1.8
*Si (conductive)	145	171	96	135	170	152
*Si (adiabatic)	140	161	98	131	160	145
*Si (chalcedony)	120	149	66	108	148	127
*Si (amorphous)	25	48	19	15	47	30
*Si (cristobalite)	95	121	46	84	120	101
*Na-K	125	92	178	102	130	124
*Na-K-Ca 4/3 β	125	(98)	(92)	116	134	129
*Na-K-Ca 1/3 β	150	121	170	133	(155)	(150)
*Mg-corrected Ka-K-Ca		100	64	---	105	137

*Minimum reservoir temperature in °C.

well than in a spring, then the well sample may be more representative of the water at depth. Additional sampling needs to be done using various filtering and acidification procedures to determine the actual SiO_2 content of the water.

There are no hot springs in the immediate area of Plate 3, but there is evidence of a relatively high geothermal gradient. A 152-m well which was drilled specifically for temperature-gradient measurement had a bottom-hole temperature of 16.3°C and a relatively high gradient of 83.5°C/km . When this gradient is corrected for terrain and microclimate effects, it reduces to 72.6°C/km , with a calculated heat flow of 2.43 HFU (Black and others, Chapter 7; number T10S/R7E/11Aa, Appendix D). A gradient of this magnitude persists to 600 m about 21 km to the south in another drill hole at approximately the same distance west of the High Cascade axis as the Devils Creek hole (see number T12S/R7E/9Da, Appendix D). It is thus likely that the Devils Creek gradient also persists to at least this depth and represents conductive background heat flow. A heat flow of 2.43 HFU places the Devils Creek area within the main part of the High Cascade heat-flow anomaly of Blackwell and others (1978).

In the fall of 1981, Sunoco Energy Development drilled a deep test well about 1.2 km north of the map area of Plate 3 (SE1/4, sec. 28, T. 9 S., R. 7 E.). The well was targeted to 2,743 m (9,000 ft); the final drilled depth and results of testing are confidential. If the terrain-corrected gradient at Devils Creek persisted to 2,743 m, a temperature of about 200°C would be expected (Priest and others, 1982b).

One problem with deep test wells in the Outerson Mountain-Devils Creek area and other areas underlain by rocks of the Western Cascade volcanic episode is that these rocks may not be permeable, or, if permeable, may not have fluids, even though adequate temperatures can probably be found at depth. For example, the 1,837-m (6,027-ft) Old Maid Flat 7A well near Mount Hood encountered no significant fluids even though the bottom-hole temperature was almost exactly what was predicted from shallow drilling (e.g., see Priest and others, 1982a). Location of fluid, not temperature prediction, is the most difficult problem facing the geothermal explorationist in Western Cascade volcanic terranes.

Fault zones and fractured rocks adjacent to fault zones may provide avenues for circulation of meteoric waters to great depth. These zones may thus be good exploration targets. Fracture permeability can, however, be eliminated by rock alteration during diagenesis and metamorphism, unless refracturing of the rocks occurs. Areas adjacent to youthful fault zones are thus probably better

exploration targets than areas associated with older faults. Because faults in the map area probably became inactive before about 6.3 m.y. B.P., it is possible that the fracture permeability associated with them has been considerably reduced by metamorphic effects. The faults noted by White (1980a,c) and Hammond and others (1980, 1982) which displace more youthful rock are probably better targets.

It is possible that some nonreactive permeable rock unit may lie at sufficient depth to provide a stratigraphic reservoir for thermal fluids. The reservoir characteristics and stratigraphy of the older rocks in the area are insufficiently well known to evaluate this possibility.

CHAPTER 4. GEOLOGY OF THE COUGAR RESERVOIR AREA,

LANE COUNTY, OREGON

By George R. Priest and Neil M. Woller,
Oregon Department of Geology and Mineral Industries

ABSTRACT

Volcanic rocks of the early and late Western Cascade sequences crop out at Cougar Reservoir west of a major north-south fault zone, the Cougar fault. Volcanic rocks of the late Western Cascades and early High Cascades crop out on the east block of the Cougar fault. A drill hole on the east block revealed that at least 152 m of down-to-the-east movement has occurred on the fault and that the dip on the fault plane is greater than 73° to the east. The fault cuts late Western Cascade units dated by K-Ar at 13.2 m.y. B.P. (lavas of Walker Creek). Pleistocene outwash gravels that overlie the fault zone are not offset. Stratigraphic arguments suggest that 366 m to possibly more than 1,033 m of down-to-the-east movement may have occurred. The fault may have displaced rocks in the area roughly at the time of intrusion of a 16.2-m.y. B.P. dacite plug. Early High Cascade lavas which began to flow into the area between about 8.3 and 7.8 m.y. B.P. were probably prevented from flowing west by the scarp of the Cougar fault. It is possible that displacements may have occurred during a period of extensive north-south faulting between about 3.4 and 5.0 m.y. ago, although absence of an obvious current topographic scarp suggests that such displacements, if they occurred, were small.

Slight southward tilting of the area may have occurred during late Western Cascade time between about 13 and 9 m.y. B.P. A major period of nondeposition and erosion developed a topography with at least 366 m of relief between early and late Western Cascade time. A period of rapid erosion and uplift produced about 1 km of relief in the area between 5.0 and 3.4 m.y. B.P.

INTRODUCTION

Cougar Reservoir is located on the South Fork of the McKenzie River between the towns of Blue River and McKenzie Bridge (Figure 4.1). The area is about 80 km (50 mi) east of Eugene on Highway 126.

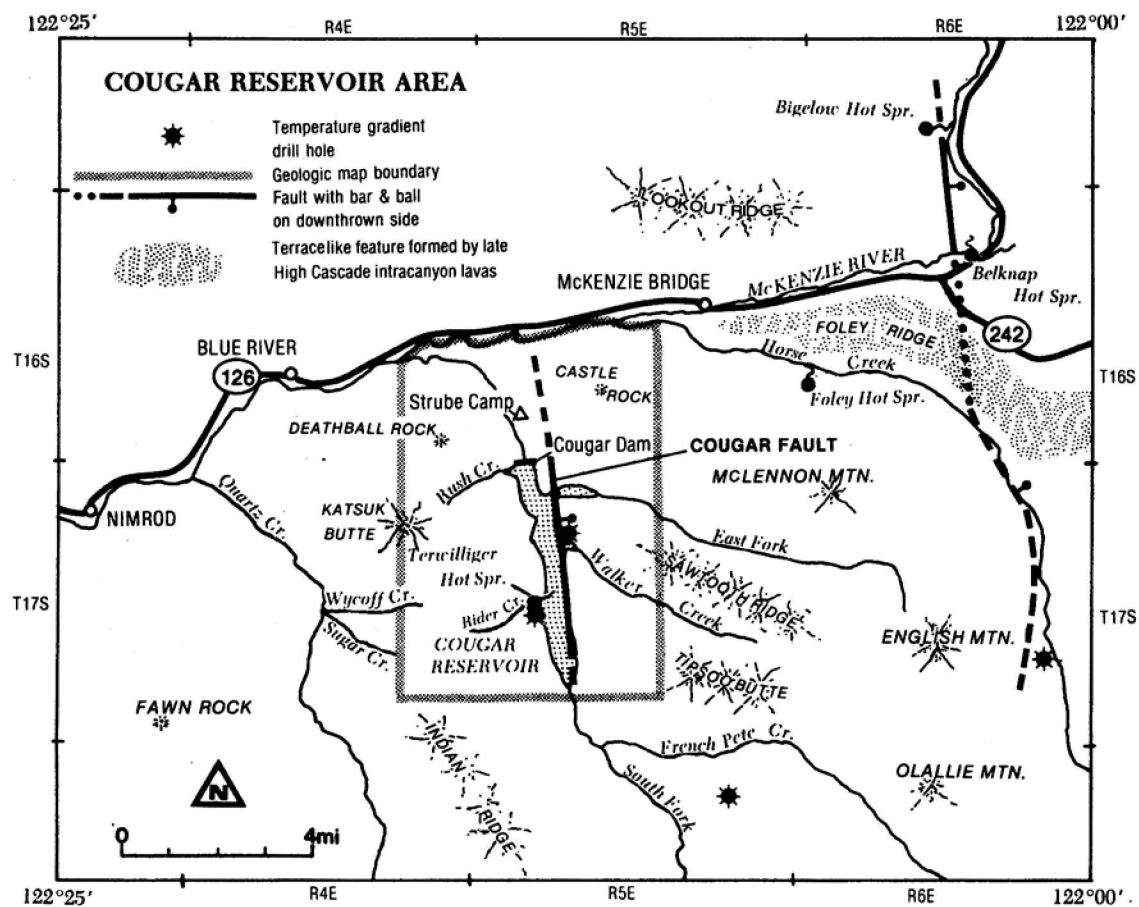


Figure 4.1. Location of the Cougar Reservoir map area and other localities mentioned in the text.

The area is in steep, mature topography of the Western Cascade physiographic province. The northern boundary of the area is the McKenzie River, which runs almost east-west. The central part of the area is dominated by the north-south-trending V-shaped valley of the South Fork of the McKenzie River. Cougar Dam forms a 9.1-km (5.7-mi)-long lake on the South Fork. Local relief is about 1,036 m (3,400 ft).

Geologic mapping at a scale of 1:24,000 was undertaken to define structures and rock units which control the local hydrothermal systems (see Plate 4). The area is only a few kilometers west of the Belknap-Foley KGRA. There is one local thermal spring, Terwilliger Hot Springs, where water at about 44° C issues from fractured andesitic lavas on the west side of Cougar Reservoir at Rider Creek. Other workers, including Bowen and others (1978) and Brown and others (1980a) have noted another thermal spring located under what is now Cougar Reservoir. The earliest reference to this spring comes from Waring (1965), who mentions a warm spring 12.9 km (8 mi) southwest of McKenzie Bridge. This reference, however, fails to mention Terwilliger Hot Springs. Bowen and others (1978) referred to this "drowned" spring as "Cougar Reservoir" hot spring, while a second spring called "Ryder" hot spring was inferred to be at the site of Terwilliger Hot Springs. No spring was noted by geologists of the U.S. Army Corps of Engineers at the site of "Cougar Reservoir" hot spring when constructing Cougar Dam. The mislocation of Terwilliger Hot Springs and the deletion of the correct name for the hot spring in Waring's (1965) compilation have probably created this confusion. The only known hot spring in the area is Terwilliger Hot Springs.

PREVIOUS WORK

Many workers have mapped near the Cougar Reservoir area, but only reconnaissance mapping of Wells and Peck (1961) and Peck and others (1964) was available prior to mapping by the writers. The writers contributed the Cougar Reservoir portion of the larger reconnaissance map of Brown and others (1980a), but the present 1:24,000-scale map (Plate 4) represents a considerable refinement of the 1:62,500-scale map of Brown and others (1980a).

Wells and Peck (1961) mapped the entire area as unit Tmua, middle and upper Miocene andesite roughly equivalent to the Sardine series of Thayer (1936, 1939). Peck and others (1964) mapped the entire area as Sardine Formation, except for a small area of the older tuffaceous rocks at Cougar Dam. Peck and others (1964)

mapped the tuffaceous rocks as Little Butte Volcanic Series (Tlt). Neither Wells and Peck (1961) nor Peck and others (1964) show faults in the area.

Relative to these earlier maps, the present map shows a much larger outcrop area of the older tuffaceous sequence, here informally called the tuffs of Cougar Reservoir. It also shows extensive outcrops of upper Miocene early High Cascade basalts, the lavas of Tipsoo Butte, which cap the ridges east of Cougar Reservoir. The present map shows a large north-south-trending fault along the East Fork of the McKenzie River and other smaller subsidiary faults not shown on earlier maps. Earlier maps show a general easterly dip to the Western Cascade sequence, but only a very slight (7°) southerly dip was recognized in the present study. The easterly dip of the sequence in the earlier maps was used as evidence of a regional anticline in the area (the Breitenbush anticline). The dominance of rocks younger than the Little Butte Volcanic Series on the limbs of this structure and the dominance of the Little Butte Volcanic Series on the axis was used as evidence for existence of an anticline. Our work suggests that younger rocks dominate east of the presumed anticlinal axis principally because of down-to-the-east step faulting along a north-south trend.

GEOLOGIC HISTORY

During early Western Cascade time (40 to 18 m.y. B.P.), the area was the site of intense silicic volcanism, principally in the form of large tuffaceous, pumice-poor, lithic-fragment-rich lahars (tuffs of Cougar Reservoir). Although some ash-flow tuffs, rhyodacite, and iron-rich andesite lavas occur in the sequence, laharic tuffs and interbedded epiclastic sandstones and mudstones dominated the volcanic pile. Between about 22 m.y. B.P.(?) and about 14 m.y. B.P., a steep topography formed with at least 365 m (1,200 ft) of relief. Andesitic lavas (andesites of Walker Creek), dacitic ash-flow tuffs and lapilli and ash-fall tuffs (tuffs of Rush Creek and tuffs of Tipsoo Butte), basaltic flows (basaltic lavas of the East Fork), and numerous andesitic to dacitic plugs (dacite intrusive of Cougar Dam and other andesitic intrusions) invaded the area during late Western Cascade time about 16.2 to 8.9 m.y. B.P. These rocks buried the earlier topography to a depth of at least 471 m (1,545 ft). The late Western Cascade sequence was then capped by iron-rich diktytaxitic basalts (lavas of Tipsoo Butte) during early High Cascade time (about 8.3 to 5.1 m.y. B.P.). These early High Cascade flows filled a topography with very little relief and flowed in from sources to the east.

Between about 5.1 m.y. B.P. and 2.0 m.y. B.P., the area was deeply dissected by the current drainage system, and numerous mudflows poured off the steep slopes. Later, in the Pleistocene, glacial outwash deposits covered the floor of the valley of the East Fork. Steep slopes in the area are very unstable and form large landslides where underlain by late Western Cascade tuffs. These landslides and glacial outwash deposits are being downcut, as is the bed rock, by current streams.

The major structure in the area is the north-south-trending Cougar fault zone, which offsets rocks with a minimum age of about 13 m.y. by at least 152 m (500 ft) and probably by more than 366 m (1,200 ft). The relative motion on the fault is down to the east. North-south elongation of the 16.2-m.y. B.P. dacite intrusion of Cougar Dam along splinters of the Cougar fault suggests that the fault may have been active during initial late Western Cascade volcanism. Breccia dikes and magmatic dikes along northwest-trending subsidiary faults and fissures within the Cougar Dam intrusive also suggest that the faulting and volcanism were concurrent. Slight tilting of the Western Cascade sequence about 7° or less to the south probably occurred during late Western Cascade time.

STRATIGRAPHY

Introduction

Volcanic rocks of the early and late Western Cascades and early High Cascades dominate the area (see Priest and others, Chapter 2, for definitions of these units). Ages have been assigned by K-Ar dating of the tops and bottoms of major sequences where possible. A total of eleven K-Ar dates were determined by Stanley Evans of the University of Utah Research Institute from rocks collected within the map area and at Lookout Ridge north of the map area (Appendix A). All stratigraphic units are informal and have been divided according to mappable characteristics of the rocks (Figure 4.2; Table 4.1). Volcanic rock names were assigned on the basis of the chemical classification of Priest and others (Chapter 2). The chemical petrology and regional significance of the chemical compositions of the rocks is discussed by Priest and others (Chapter 2) and will not be repeated here. The chemical classification system used to give rock names is summarized by Priest and others (nomenclature section, Chapter 2).

Nomenclature used in this report*	Name	K-Ar dates (m.y.)	Thickness (ft)	Lithology
Volcanic rocks of the late High Cascades	Mazama pumice-fall deposit	Holocene	Variable, max. 10	Unconsolidated, well-winnowed pumice-fall; yellow; with voids between pumice clasts. Appears bedded where undisturbed. Mantles the topography.
	Pleistocene basaltic rocks	Oldest, 1.98 ± 0.25 ; youngest, 0.17 ± 0.48	>1,600	Olivine-bearing basalts and basaltic andesites; black to gray; fresh, undeformed; diktytaxitic to compact. Found in bottoms of glaciated valleys and related to recent drainages. Intracanyon into all older units.
Volcanic rocks of the early High Cascades	Miocene-Pliocene basaltic lavas	5.53 ± 0.41 ; 5.56 ± 0.34 ; 4.32 ± 0.40	1,200	Olivine-bearing basalts and basaltic lavas; compact; gray; fresh. Caps highest ridges.
Volcanic rocks of the late Western Cascades	Andesitic lavas of Moss Mountain	$17.3 \pm 0.8(?)$	2,400	Pyroxene-bearing andesites and basaltic andesites. Lower members are olivine-augite-bearing. Black to gray; very plagioclase phyric.
	Basaltic lavas of Tumblebug Creek	Upper part, 13.1 ± 0.6 ; lower part, 17.0 ± 0.9	>3,000	Olivine-bearing basalts and basaltic andesites; fresh in appearance; compact to diktytaxitic; black to gray.
	Older volcaniclastic sediments and lavas	----		Immature sediments, perhaps hyaloclastic with free hypersthene and aphyric small pastel-colored clasts. Interbedded with fine-grained, altered, vitrophyic, silicic lavas, which may be older, more deformed members of the andesitic lavas of Moss Mountain.

*See Priest and others (Chapter 2) for explanation and regional rock stratigraphic correlations.

Figure 4.2. Stratigraphy of the Cougar Reservoir area.

TABLE 4.1. Estimated reservoir temperatures of Terwilliger Hot Springs from chemical geothermometers of Fournier (1979), Fournier and Rowe (1966), Fournier and Truesdell (1973), and Mariner and others (1980). Data are from Brown and others (1980a).

Date sampled	Lower spring, March 1976	Upper spring, 1973	Upper spring, March 1976
Surface temperature (°C)	38	44	42
Flow rate (liters/min.)	114	200	200
Na:K (°C)	87	74	86
Na:K:Ca, $1/3\beta$ (°C)	104	95	103
Na:K:Ca, $4/3\beta$ (°C)	52	48	51
SiO ₂ , conductive (°C)	99	102	99
SiO ₂ , adiabatic (°C)	100	103	100
SiO ₂ , chalcedony (°C)	68	72	69
SiO ₂ , opal (°C)	-17	-14	-16

Volcanic rocks of the early Western Cascades

Tuffs of Cougar Reservoir (Totc): Thick tuffaceous laharic and mudflow deposits, nonwelded ash-flow tuffs, epiclastic mudstone and sandstone, and minor interbedded rhyodacite to iron-rich andesite (icelandite) flows crop out in the lowest elevations of the South Fork of the McKenzie River. These rocks are here informally called the tuffs of Cougar Reservoir. The lowest part of the sequence, exposed downstream from Cougar Dam, consists of abundant tuffaceous mudstone. Diamond core from U.S. Army Corps of Engineers holes in the area indicate that additional lithic-fragment-rich laharic tuffs underlie the epiclastic mudstone. The majority of the unit is dominated by crystal-poor, pumice-poor, tuffaceous mudflows and probable lahars with numerous mudstone and sandstone interbeds.

Laharic flows and mudflows in the uppermost part of the sequence above Cougar Dam at Rush Creek are locally crystal-rich and contain numerous plagioclase and hypersthene crystals. A dark, hackly, aphyric icelandite flow crops out at the head of Rush Creek near the top of the sequence, and a series of rhyodacite flows occur near the base east of Strubes Forest Camp.

All of the rocks show some alteration to fine-grained birefringent phyllosilicates. Most of these phyllosilicates are probably smectite clays which totally replace glass in most rocks and affect plagioclase and orthopyroxene in many places. Chlorite and calcite were also noted in some samples replacing mafic phases and feldspar, respectively. Alteration imparts a general dull color to the outcrop and frequently causes a greenish tint.

Microscopic examination of the ash-flow tuffs reveals the broken nature of matrix pyroxene and plagioclase crystals and the paucity of crystals in pumice. The fine-grained vitric ash component was partially winnowed out of the matrix during transport. Pumice lapilli are not common in the ash flows and are rare in the tuffaceous mudflows and lahars. Coarse ash is common in the ash-flow tuffs examined. The mudflows contrast with the ash-flow tuffs by having a lithic fragment content equal to, or in some cases exceeding, the vitric component.

The mudflows commonly contain wood fragments, now carbonized, as well as abundant lithic lapilli. Lithic fragments seldom exceed 1 m in size in the mudflows in this area, and most are less than 10 cm. The pyroclastic and epiclastic rocks generally form rounded slopes with frequent cliffs and some "hoodoos." Overall color of the tuffs is a greenish-gray with abundant dark-gray to reddish-purple aphyric lithic fragments. The units are well lithified and show no

tendency to form major landslides.

The tuffs of Cougar Reservoir are too altered to provide material for accurate radiometric dates, but some constraints can be placed on the age of the sequence. The intrusion at Cougar Dam cuts the tuffs and has a K-Ar date of 16.2 m.y. B.P. Sutter (1978) lists a K-Ar date on the Nimrod stock of 15.86 ± 0.18 m.y. B.P. (which recalculates to 16.3 ± 0.2 m.y. B.P. according to Fiebelkorn and others, 1982). This quartz monzonite stock appears to intrude tuffs similar to the tuffs of Cougar Reservoir. Lavas chemically similar to the icelandite lava found near the top of the sequence occur at the top of a similar tuffaceous sequence near Lookout Point Reservoir where they have a K-Ar age of about 22 m.y. B.P. (see Chapter 5). Similar lavas in other parts of the Western Cascade Range have K-Ar ages of between 27 and 19 m.y. B.P. (White, 1980a,c). Priest and others (Chapter 2) consider the early Western Cascade episode to be between 40 and 18 m.y. B.P.

The tuffs of Cougar Reservoir are equivalent to the Little Butte Volcanic Series of Peck and others (1964) and unit Tmp of Wells and Peck (1961). The tuffaceous lower portion of the unit is probably similar in age to the Breitenbush tuff of Thayer (1939) and Breitenbush formation of White (1980a,c) and Hammond and others (1980). The icelandite lava near the top of the section is petrochemically, and possibly temporally, equivalent to the Scorpion Mountain lavas of White (1980a,c) and the lavas of Black Canyon (Woller and Priest, Chapter 5). Like the Scorpion Mountain and Black Canyon lavas, the icelandite lava is iron-rich and occurs in the upper part of the early Western Cascade section.

Volcanic rocks of the late Western Cascades

Introduction: The late Western Cascade sequence is a series of basaltic to dacitic lavas and tuffs which fill a steep topography cut into the underlying tuffs of Cougar Reservoir. The sequence thins against an east-west-trending highland formed of tuffs of Cougar Reservoir in the northwestern part of the map area. The adjacent paleovalley was at least 366 m deep, based on the rise of the lower contact of the late Western Cascade rocks from the Rider Creek area to the Katsuk Butte area (Figure 4.1; Plate 4). About 470 m of late Western Cascade rocks overlie this highland at Katsuk Butte. The highland terminates abruptly at the Cougar fault. A maximum of about 792 m (2,600 ft) of the late Western Cascade sequence is exposed on the east side of the Cougar fault, but no older rocks are exposed. The minimum offset across the fault which could

displace this highland below the lowest exposure of late Western Cascade rock on the east block of the fault is 562 m (1,843 ft). Because the lowest exposed unit on the east block of the fault (the basaltic lavas of the East Fork) is absent from the upthrown west block, it is logical to assume that these lavas may have been present on the west block but have been removed by erosion. If they were present just above the highest point on the west block (Katsuk Butte) prior to erosion, they would have been vertically displaced 1,033 m (3,388 ft) from the lowest exposure on the east block. It is possible that the displacement exceeds this amount, if the East Fork basalt were once present on the west block at an elevation higher than Katsuk Butte.

An alternative hypothesis to the above arguments is that the paleohighland in the northwest part of the area was an isolated high flanked on both the east and south by valleys when the late Western Cascade sequence was deposited. This would require a thicker sequence east of the fault and cause units low in the eastern late Western Cascade section to pinch out to the west. This highland could have been partially formed by movements on the Cougar fault prior to or during deposition of most of the late Western Cascade sequence. Arguments below suggest that the 16.2-m.y. B.P. dacite intrusive of Cougar Dam was roughly contemporaneous with some movement on the Cougar fault. This supports the latter hypothesis.

Additional deep drilling on the east block of the Cougar fault will be necessary to discriminate among these hypotheses. Only then will the complete late Western Cascade stratigraphic history be unraveled.

Dacite intrusive of Cougar Dam (Tmvic): A dark, glassy porphyritic two-pyroxene dacite (63.6 percent SiO₂) forms the east and west abutments of the Cougar Dam. The dacite is a cliff-forming unit which causes a narrows in the South Fork of the McKenzie River at the dam. The unit appears to have a conformable upper contact with the tuffs of Cougar Reservoir on the west abutment but obviously intrudes the tuffs in the upper contact on the east abutment. Numerous dike-like protrusions are injected along the west contact in exposures just north of the dam along Forest Road 19. The lower contact on the west abutment also appears to be conformable with underlying, nearly horizontal tuffaceous mudstones of the tuffs of Cougar Reservoir. No lower contact is exposed on the east abutment where the dacite appears to be a long dike-like mass extending about 2.75 km (1.7 mi) in a north-south- to north-northwest direction. However, abutment exploration by U.S. Army Corps of Engineers' geologists revealed pods of

pyroclastic rock within and below the intrusive at the east abutment (U.S. Army Corps of Engineers, 1964). Northwest-trending shears cut through the east abutment in several places and in some cases are filled with nearly aphyric dikes. Breccia dikes filled with comminuted wall rock and quartz diorite fragments also fill west-northwest-trending fissures in the east abutment. One large north-trending shear at the top of the east abutment has prominent horizontal slickensides.

Lateral contacts between the intrusion and tuffs of Cougar Reservoir on the east abutment are complex. Most contacts are very sharp and steeply dipping, but others show signs of complex interactions between the intrusion and the walls. In one locality near the top of the intrusion, rounded block-size pieces of the dacite are completely surrounded by structureless fine-grained tuff adjacent to an obscure, steeply dipping contact. Thermal metamorphic effects on wall rocks include slight bleaching and very low-grade epithermal alteration with some iron-oxide staining, possibly from minute quantities of weathered sulfides. The intrusion is slightly discolored to a darker, more stoney appearance at the contact. The general appearance of the east abutment contact is indicative of interactions between moist tuffaceous wall rocks and a highly viscous, relatively low-temperature intrusion.

The dacite is hyalopilitic with glomeroporphyritic clusters of 1-mm subhedral orthopyroxene (3 percent), clinopyroxene (4 percent), and plagioclase (18 percent). About 1 percent saponitized 2.2-mm pseudomorphs of an anhedral mafic silicate are also present. The dacite has a hackly jointing pattern which forms closely spaced, highly irregular vertical columns. The columns have near-horizontal discontinuities which give the appearance of flow contacts when viewed from a distance. On closer inspection, however, there is no evidence of a cooling break at these discontinuities.

A plagioclase separate from the dacite yielded a K-Ar date of 16.2 ± 1.8 m.y. B.P. (13 percent radiogenic argon). This corresponds to the early part of late Western Cascade time. The unit is correlative to unit Tmua of Wells and Peck (1961) and the Sardine Formation of Peck and others (1964).

Tuffs of Rush Creek (Tmrt): Light-colored ash-fall, ash-flow, and epiclastic tuffs interfinger with two-pyroxene andesite flows in the lower part of the late Western Cascade sequence at Rush Creek. Most of the ash-flow tuffs are nonwelded, but welded tuffs crop out in three localities. West of the map boundary in the Sugar Creek drainage a densely welded, glomeroporphyritic two-pyroxene

dacite ash-flow tuff crops out at about 3,000-ft elevation (Blue River quadrangle). This tuff can be traced into the map area near the headwaters of Rider Creek. Similar partially welded to nonwelded ash-flow tuffs without the glomeroporphyritic texture are found at about the 3,300-ft elevation in road cuts on the east flank of Harvey Mountain. A densely welded two-pyroxene dacite ash-flow tuff occurs in one outcrop at about 2,400-ft elevation (McKenzie Bridge quadrangle) at the base of the section, below the above-mentioned Harvey Mountain ash-flow tuffs. Although it is possible that one of the Harvey Mountain ash-flow tuffs is the distal facies of the Sugar Creek welded tuff, no certain correlation was established for any of the ash-flow tuff units over significant distances. This may be a function of the high relief which probably characterized the area. All of these welded to partially welded tuffs pinch out to the north at Rush Creek against an old highland formed by the tuffs of Cougar Reservoir. The lower contact of the tuffs of Rush Creek is exposed at the head of Rush Creek where the peak of this old highland is covered by the tuffs. The uppermost tuffs of Cougar Reservoir at this location are a series of gray mudflows. Pieces of the white- to cream-colored Rush Creek tuff are intermixed in the gray mudflow material at the contact. This mixture is probably a mudflow formed from rocks of the underlying sequence during Rush Creek time.

Most of the tuffs of Rush Creek are composed of light-colored hypersthene-bearing dacite pumice lapilli and ash. Welded and partially welded ash-flow tuffs are dark-gray to black with eutaxitic texture. Very low-grade alteration commonly has caused glass in the nonwelded and epiclastic units to alter to clay minerals. Welded ash-flow tuffs have hydrated but otherwise unaltered glass. Broken plagioclase and subordinate orthopyroxene and clinopyroxene make up most of the crystal fraction which forms up to 10 percent of the tuffs, although minor hornblende is present in some of the rocks. The tuffs generally form low-angle slopes and serve as slip planes for major landslides throughout the western half of the map.

A nonwelded ash-flow tuff at the head of Rush Creek (3,200-ft elevation) near the top of the tuffs of Rush Creek yielded a K-Ar date of 13.8 ± 0.8 m.y. B.P. (26 percent radiogenic argon) on a plagioclase separate. A sample stratigraphically above the tuffs of Rush Creek at 4,745-ft elevation yielded a K-Ar date of 11.4 ± 0.5 m.y. B.P. (35 percent radiogenic argon) from a plagioclase separate. A slightly altered flow of two-pyroxene andesite stratigraphically below most of the tuffs of Rush Creek yielded a K-Ar date of 12.4 ± 2.5 m.y. B.P. (7 percent

radiogenic argon). The tuffs are roughly correlative to Wells and Peck's (1961) unit Tmua and tuffaceous units of Peck and others' (1964) Sardine Formation.

Basaltic lavas of the East Fork (Tme): Nearly aphyric basalt to basaltic andesite lavas crop out on both sides of the East Fork of the McKenzie River. These flows dip gently toward the south and are about 90 m (300 ft) thick. They do not crop out anywhere else in the map area. They are in fault contact with the lavas of Walker Creek to the east and are cut off by the Cougar fault on the west. They are overlain by the lavas of Walker Creek to the north and south.

The lavas have phenocrysts of olivine altered to highly birefringent green to orange minerals (serpentine(?), saponite(?), and iddingsite). Orthopyroxene phenocrysts also occur but are commonly rimmed by altered olivine. Clinopyroxene and plagioclase phenocrysts are also common. Phenocrysts are generally quite small (1 mm), seldom exceed 10 percent of the rock, and are set in a felty to pilotaxitic groundmass of plagioclase, clinopyroxene, and orthopyroxene. Overall color of outcrops is black to dark-gray when fresh and red-brown when weathered. The lavas are cliff formers.

One sample collected at about 1,760-ft elevation on the south side of the East Fork yielded a K-Ar date of 8.1 ± 2.3 m.y. B.P. (5 percent radiogenic argon). This date is far too young, since a lava higher in the sequence of Walker Creek has a date of 13.2 ± 0.7 m.y. B.P. The lavas are chemically and mineralogically similar to the rest of the late Western Cascade section so are probably no older than about 16.2 m.y. They are probably no younger than about 13.2 m.y.

Andesites of Walker Creek (Tmw): Megacrystic two-pyroxene andesite lavas and minor debris flows crop out in a 610-m (2,000-ft) section at Walker Creek, where they are capped by the lavas of Tipsoo Butte. Lavas chemically and mineralogically similar to the lavas at Walker Creek crop out intermittently over a vertical distance of 840 m (2,745 ft) on the west side of Cougar Reservoir, where they interfinger with the tuffs of Rush Creek in the lower part of the late Western Cascade section. The writers were not able to demonstrate that individual flow units cropping out on the west side of Cougar Reservoir correlate with specific flows on the east side. An apparent single flow unit on the west side of the reservoir was traced from an elevation of 4,000 ft near Ridge Creek to an elevation of 1,600 ft at Rider Creek. This would indicate that flows of the sequence may have flowed from the west toward the east into a valley similar in relief and position to the current valley of the East Fork. If lavas on the east side of the East Fork flowed from local source areas to the east into this

same topographic low, then there is no reason for individual flow units to correlate across the East Fork. It is still puzzling that very distinctive units like the tuffs of Rush Creek and the basaltic lavas of the East Fork are not found across the South Fork. The Cougar fault zone, which will be discussed in a later section, may have sufficient displacement to juxtapose very different parts of the late Western Cascade section, making outcrop correlation across the fault impossible. If this is the case, then much of the west-side section may lie at depth beneath the east-side section.

The most common rock type in the unit is a two-pyroxene andesite with 2- to 5-mm phenocrysts of plagioclase and subordinate orthopyroxene and clinopyroxene set in a partially divitrified hyalopilitic groundmass. Minor olivine, hornblende, and Fe-Ti oxides and apatite are also commonly present. Phenocrysts and glomerocrysts are up to 1.5 cm in their longest dimension, and such megacrystic rocks are quite common. Nearly aphyric lavas with minor pyroxene phenocrysts are also common locally. In the upper part of the sequence, on both sides of the fault, flows tend to be slightly diktytaxitic. The lavas form spectacular curving colonnades where the flows are thick in steep intracanyon sections. The unit is light reddish gray to dark gray and forms cliffs in solid lava sections. Debris flows and autobrecciated areas form moderate to low slopes.

A sample from the middle part of the Walker Creek section (2,360-ft elevation) yielded a whole rock K-Ar date of 13.2 ± 0.7 m.y. B.P. (28 percent radiogenic argon). Basal Tipsoo Butte lavas above this flow at about 3,840-ft elevation have a K-Ar date of 7.90 ± 0.8 m.y. B.P. On the west side of the Reservoir, the tuffs of Rush Creek, K-Ar dated at 13.8 ± 0.8 m.y. B.P. interfinger with the lower part of the west side two-pyroxene andesite section. The top flow of the west side section at Katsuk Butte (elevation of 4,640 ft) has a K-Ar date on plagioclase of 11.4 ± 0.5 m.y. B.P. (35 percent radiogenic argon).

The top flow of the late Western Cascade section at Lookout Ridge across the McKenzie River from the northern margin of the map area is a hornblende-bearing two-pyroxene dacite with a whole rock K-Ar date of 8.80 ± 0.34 m.y. B.P. (61 percent radiogenic argon). This unit is considered to be the top of the late Western Cascade section and may be about the same age as the undated top flow at Walker Creek. At Lookout Ridge, the basal early High Cascade basalt has a K-Ar date of 8.34 ± 0.36 m.y. B.P. There is thus no evidence in either the Walker Creek or Lookout Ridge area of a significant time break between late Western Cascade andesitic volcanism and early High Cascade basaltic volcanism.

The lavas of Walker Creek are roughly correlative to unit Tmua of Wells and Peck (1961), the Sardine Formation of Peck and others (1964), and the Western Cascade series of Flaherty (1981). Flaherty (1981) distinguished an upper andesite and dacite unit and a lower andesite unit within his Western Cascade series. His dacite unit is probably what was dated in this study at Lookout Ridge.

Andesites of Castle Rock (Tmcr): Light-gray, nearly aphyric two-pyroxene andesite lavas (60 percent SiO₂) cap Castle Rock in the northeastern part of the area. It is possible that these lavas are at their vent area and that they merge into a plug dome at Castle Rock. Field relationships are ambiguous, but wide variations in dip and strike of flow foliation and the limited distribution of the lavas (only at Castle Rock) suggest that this may be a plug dome.

At least two rock types are present, but it is unclear whether they are separate cooling units. Both have similar textures, but one has minor xenocrystic quartz and iddingsitized olivine phenocrysts, whereas the other has both clinopyroxene and orthopyroxene pseudomorphic after minor olivine(?) phenocrysts, but no quartz. The quartz, where present, has reaction coronas of clinopyroxene and minor iddingsitized olivine. Aside from xenocrystic quartz, the lavas are similar. Both rock types have 1- to 3-mm (average 1.2-mm) subhedral plagioclase (2 percent) and orthopyroxene (1 percent), with microphenocrysts of the same minerals plus clinopyroxene (0.5 percent) and either pyroxene or iddingsite pseudomorphs after olivine (0.5 percent). The phenocrysts are set in a pilotaxitic groundmass of plagioclase, orthopyroxene, clinopyroxene with minor Fe-Ti oxides and apatite. Plagioclase is heavily sieved with devitrified glass inclusions in its core in both rock types. The lavas, which are compact and light-gray to medium-gray, form cliffs in the area.

A K-Ar age of 9.31 ± 0.44 m.y. was determined from a whole-rock sample containing xenocrystic quartz. This unit is roughly correlative to the uppermost part of unit Tmua of Wells and Peck (1961), the upper part of the Sardine Formation of Peck and others (1964), and the upper andesite-dacite unit of the Western Cascade series of Flaherty (1981).

Tuffs of Tipsoo Butte (Tmtt): At Tipsoo Butte, three easterly trending paleocanyons incised in the underlying lavas of Walker Creek are filled with from 97 to 122 m (320 to 400 ft) of nonwelded dacitic ash-flow tuff and possibly ash-fall tuff. These tuffs are probably part of the late Western Cascade sequence, although their presence at the top of the Walker Creek section and the relief on their lower contact suggest that they could have been deposited in

early High Cascade time (i.e., after 9.0 m.y. B.P.). Subtle bedding within the sequence, inclusion of some wood fragments, and the large number of lithic fragments relative to pumice are permissive evidence that some of these tuffs may be surge deposits. More pumice-rich layers are free of wood fragments, lack the subtle bedding, and appear to be ash flows. Unfortunately, these observations only apply to the units in the lower part of the sequence; the upper part was inaccessible due to cliffy exposures.

Pumice in two samples cut for thin section is unaltered, but one of these samples contains carbonized wood fragments, and the ash and lithic fragments in it are extensively altered to chlorite and smectite. Pumice in the other sample has minor hornblende phenocrysts, whereas the sample with altered lithic fragments has minor orthopyroxene phenocrysts. Two-pyroxene andesites and hornblende two-pyroxene andesites are the chief lithologies of the lithic fragments. Broken clinopyroxene, orthopyroxene, plagioclase, and hornblende crystals are at least ten times as abundant in the matrix as they are in the pumice. Winnowing during ash-flow or base-surge transport apparently reduced the volume of the vitric component relative to the crystal component in the matrix. The tuffs are cliff formers owing to resistant capping lavas of Tipsoo Butte; the tuffs would probably form low slopes were the capping lavas not present. Overall outcrop color is a cream to tan.

No K-Ar data are available for the tuffs of Tipsoo Butte, but they lie at least 366 m (1,200 ft) above a Walker Creek flow K-Ar dated at 13.2 m.y. B.P. and are capped by basal lavas of Tipsoo Butte K-Ar dated at 7.9 m.y. B.P. These tuffs probably correlate with the uppermost part of Wells and Peck's (1961) Tmua unit, Peck and others' (1964) Sardine Formation, and Flaherty's (1981) upper andesite and dacite unit.

Volcanic rocks of the early High Cascades

Lavas of Tipsoo Butte (Tml): About 457 m (1,500 ft) of dark-gray diktytaxitic basalts and basaltic andesites cap McLennen Mountain, Sawtooth Ridge, and Tipsoo Butte in the eastern half of the area. The lower contact is at nearly the same elevation from ridge to ridge with little obvious relief, except for a slight rise in elevation toward the east. The westward slope of the lower contact suggests that the lavas flowed from vents at higher elevations east of the map area.

The absence of the lavas of Tipsoo Butte in the western half of the area can be explained by three hypotheses. Either (1) thinning or (2) a topographic barrier prevented the lavas from reaching the western part of the area, or (3)

they were eroded from the western ridge tops. The lavas do not seem to thin significantly from east to west, so thinning is not likely. Elevations of ridges in the western part of the area are between 4,000 and 5,000 ft, whereas the lower contact on the lavas of Tipsoo Butte, which slopes toward the west, is at about 3,600 to 4,000 ft. The lavas should thus crop out below 3,600 ft on the west side of the map unless they were stopped by a topographic barrier or uplifted after deposition and eroded off. Because the Cougar fault zone has demonstrated down-to-the-east movement, it is the most likely cause of either a possible barrier or uplift of the western half of the area. Swanson and James (1975) noted pillowed units in lavas correlative to the lavas of Tipsoo Butte north of the map area, suggesting a lake-filled lowland at the western terminus of the flow units there. If the Cougar fault extends to the north, it may have produced a scarp against which the lavas ponded. Lava-dammed lakes may have formed and lava flows entering the lakes could have produced pillowed basalts. No pillow basalts, however, were noted in the map area. The reason for termination of the basalts in the Cougar Reservoir area is not known, but it is probably that it was caused by uplift of the western part of the area (or downdrop of the eastern part) by an amount equal to at least the exposed thickness of the basalts, or about 457 m (1,500 ft). This relief was probably produced by the Cougar fault shortly before and/or during or after early High Cascade time. Pleistocene outwash gravels are not faulted along the trace of the Cougar fault in the East Fork area. The minimum offset necessary to simply erode the basalts from the western part of the area, assuming that they were deposited before uplift, would be the difference in elevation between their lower contact and the elevation of the highest ridges in the western part of the area, or about 427 m (1,400 ft). This last estimate assumes that the topography in the western area had relatively low relief, similar to the relief along the lower contact of the lavas of Tipsoo Butte in the eastern part of the area.

Absence of a current topographic scarp on the west block of the fault and the previously mentioned evidence of ponding of the lavas of Tipsoo Butte suggest that the offset probably occurred shortly before and during eruption of the lavas of Tipsoo Butte. If this is the case, then the total offset may have been as much as, or somewhat more than, the exposed thickness of the lavas of Tipsoo Butte, or greater than 457 m.

The lavas of Tipsoo Butte are chemically and mineralogically distinct from earlier basaltic rocks. They reach lower silica contents (48.3 percent) and

higher iron contents (11.9 percent total iron oxide recalculated volatile-free to FeO) than any of the older basaltic rocks. High P_2O_5 contents of 0.32 to 0.87 percent also characterize the Tipsoo Butte basalts (e.g., compare to the underlying basalts of the East Fork with 0.11 to 0.18 percent P_2O_5). The lavas are also diktytaxitic and commonly contain, in the most mafic samples, brownish ophitic to subophitic clinopyroxene in the groundmass. The groundmass clinopyroxene is a darker color in a sample with a 2.44 percent TiO_2 than in a sample with 1.48 percent TiO_2 , so the color is probably a function of titanium content in the clinopyroxene. Olivine is present in all samples in amounts of 1 percent or less as 0.6- to 1.0-mm anhedral phenocrysts that show no reaction with the former liquid. Plagioclase phenocrysts are subhedral, about 0.3 to 1 mm in size, and generally subordinate to olivine. The absence of a reaction relationship between olivine and liquid, the high TiO_2 and P_2O_5 contents, and the presence of probable titaniferous clinopyroxene are attributes of basalts with alkaline affinities. Basalts with these same characteristics also occur in the late High Cascade section described at Cupola Rock northeast of the area (Flaherty, 1981). The chemical affinity of both the late and early High Cascade basalts to one another and to alkaline basalts is described more completely by Priest and others (Chapter 2).

The lavas of Tipsoo Butte are generally light gray to dark gray and weather to a buff color. They characteristically have widely scattered, large (1- to 3-cm) spherical vesicles in addition to diktytaxitic texture. They tend to form precipitous cliffs and are generally of fresher appearance than all but the uppermost flows of the underlying late Western Cascade sequence.

A K-Ar age at the base of the section at Tipsoo Butte is 7.80 ± 0.77 m.y. (14 percent radiogenic argon). A K-Ar date of 8.34 ± 0.36 m.y. B.P. (39 percent radiogenic argon) was obtained at the base of the section at Lookout Ridge. A K-Ar date of 9.41 ± 0.42 m.y. B.P. (36 percent radiogenic argon) was determined for a flow near the top of Tipsoo Butte. As explained previously (Chapter 2), it is possible that the 9.41 m.y. B.P. date is caused by incomplete degassing of radiogenic argon at the time of eruption. Alternatively, since the 9.41-m.y. B.P. date is characterized by more radiogenic argon than the 7.80-m.y. B.P. date, it may be the more accurate age, making the lower part of the sequence somewhat older than 9.41 m.y. B.P.

The lavas of Tipsoo Butte roughly correlate with Wells and Peck's (1961) unit Tpb within their unit QTba, Peck and others' (1964) unit QTV, and the lower basalt flows of Flaherty's (1981) intermediate series.

Pliocene-Pleistocene mudflow deposits (QTpm)

Partially lithified mudflow deposits occur on the east side of Cougar Reservoir between Walker Creek and the East Fork. One outcrop of these deposits also occurs in a roadcut on the west side of the reservoir 1.6 km (1 mi) north of Terwilliger Hot Springs. The mudflows appear to have flowed from local areas into a river valley essentially identical to the present one. All clasts examined were of lithologies common to the late Western Cascade sequence.

The deposits are friable but more consolidated than overlying Pleistocene gravels. They lack the sorting and rounding of pebble- to cobble-size clasts characteristic of the Pleistocene deposits. They generally contain abundant sub-rounded to subangular pebble- to cobble-size clasts of highly phyric two-pyroxene andesite set in a poorly sorted, argillaceous, partially lithified sand. Overall color is dark gray to dark brownish gray, and the deposits form low slopes.

No radiometric dates are available, but mudflow deposits may be pre-Pleistocene, since they are overlain by Pleistocene gravels at the East Fork which are much less indurated. Because their distribution is clearly controlled by the current topography, they must be younger than the age of the South Fork river valley. Flaherty's (1981) work at McKenzie Bridge suggests that the McKenzie River drainage system was in approximately its present form by at least 2 m.y. B.P. and may have been in existence as early as 3.4 m.y. B.P. (oldest K-Ar date on intracanyon late High Cascade lavas). The deposits correlate with Wells and Peck's (1961) unit QTW.

Glacial and fluvial deposits (Qgf)

Glacial deposits are found in the vicinity of Katsuk Butte. Till, small moraines, and glacial outwash are composed of late Western Cascade lithologies. No mafic lavas of Tipsoo Butte lithology were observed within the deposits, probably because the glacial deposits have provenances west of possible outcrops of the early High Cascade section. The deposits are probably equivalent to Wells and Peck's (1961) glacio-fluvial deposits (Qpgl).

Glacial outwash deposits (Qpg)

Moderately well-sorted gravels, sands, and gravelly sands occur at the mouth of the East Fork where they fill a shallow paleocanyon incised into the Cougar fault zone. They are not cut by the fault. The deposits also occur extensively in terraces at the junction of the South Fork with the main McKenzie River. They are probably outwash gravels from melting of Pleistocene valley glaciers.

The deposits consist of well-rounded cobbles and pebbles of local andesitic lithologies set in a loosely consolidated, moderately well-sorted sand. They form low slopes, except where cut very recently by local drainages. Overall color is gray to brownish-gray.

The deposits are probably Pleistocene in age and correlate with Wells and Peck's (1961) unit Qpgl (glaciofluvial deposits). No radiometric age data are available for the unit.

Unconsolidated Recent colluvium (Qc), alluvium (Qal), and landslide deposits (Qls)

Colluvium, as shown on the geologic map, includes all talus and thin unconsolidated residual soils which mantle bed rock. Alluvium is unconsolidated sand and gravel in overbank deposits and beds of the current streams. Landslide deposits include slump blocks and totally disaggregated landslide debris. All of these deposits are probably Holocene in age, although some of the landslides may well have begun to form during the Pleistocene. Unit Qal corresponds to units Qral and Qal of Wells and Peck (1961); unit Qls corresponds to unit Qls of Wells and Peck (1961); unit Qc was not usually mapped on the small-scale maps of previous workers. The writers used unit Qc on this map as a way of showing areas of bed rock exposure.

STRUCTURAL GEOLOGY

Introduction

The main structure in the area is the Cougar fault zone (Figure 4.1; Plate 4) which cuts through the middle of the map area along a N. 5° W. trend. This very steeply dipping fault offsets the east half of the area downward relative to the west half.

The tuffs of Cougar Reservoir appear to generally dip a few degrees to the south or southwest, although local dips to the east, west, and northeast were also measured. Fine-grained sediments near the Cougar Dam powerhouse are horizontally bedded. The late Western Cascade sequence also probably dips very gently toward the south. The regional tectonic significance of the Cougar fault and other deformation in the area is discussed by Priest and others (Chapter 2) and is not repeated here.

Cougar fault

The Cougar fault is probably a nearly vertical zone with chiefly dip-slip movement. Although one splinter fault in the Cougar Dam intrusion has horizontal

slickensides, all documented stratigraphic offset is dip-slip. A drill hole located about 46 m east of where the Cougar fault zone crops out at the mouth of Walker Creek encountered 152 m of the lavas of Walker Creek, whereas the tuffs of Cougar Reservoir crop out on the west side of the fault. This hole demonstrates that (1) there is at least 152 m of apparent dip-slip offset on the fault, and (2) the minimum easterly dip is 73° . Previously discussed stratigraphic arguments in the section on early High Cascade rocks suggest that the offset on the fault since about 13.2 m.y. ago is probably about or more than 427 m. In the section on late Western Cascade volcanism, various hypotheses led to estimates of displacement on the Cougar fault from 562 m to more than 1,033 m, although the minimum offset which can be constrained by late Western Cascade units is the 152-m offset estimated from the Walker Creek hole.

The age of movements on the Cougar fault is constrained by the following observations:

1. The 16.2-m.y. B.P. Cougar Dam intrusion is immediately adjacent to the Cougar fault and is elongate parallel to the trace of the fault.
2. Breccia dikes and dikes, probably generally related to magmatic activity during the Cougar Dam intrusive event, follow what appear to be north-west-trending splinter faults of the Cougar fault.
3. The fault definitely cuts lavas of Walker Creek dated at 13.2 m.y. B.P.
4. If the Cougar fault or related faults extend northward into the area mapped by Swanson and James (1975), then the scarp may have been responsible for creation of lakes which caused early High Cascade basaltic lavas to be pillowed in that area. These lavas began to flow into the area about 8.34 m.y. B.P., according to a date at Lookout Ridge.
5. A fault zone essentially parallel to the Cougar fault has been mapped to the east in the upper McKenzie River and Horse Creek (Figure 4.1). This fault zone formed between 3.4 and 5.06 m.y. B.P. (Flaherty, 1981).
6. The fault does not cut Pleistocene gravels overlying it at the mouth of the East Fork.

The above observations are consistent with movement on the Cougar fault shortly before 16.2 m.y. B.P. and after 13.2 m.y. B.P. If the Cougar fault or related faults caused ponding of the early High Cascade lavas mapped by Swanson and James (1975), then it may have been active about 8.34 m.y. B.P. If the fault experienced additional displacement when the Horse Creek fault formed, then it may have moved between 3.4 and 5.06 m.y. B.P. It apparently ceased movement

before deposition of Pleistocene outwash gravels in the area, but the exact age of the gravels is not known.

The Cougar fault also appears to affect the pattern of gravity and aeromagnetic anomalies in the area. The west block of the fault has a complete Bouguer gravity value of about -102 mgal, whereas the east block has a value of about -110 mgal (Pitts and Couch, 1978; Pitts, 1979). The decrease in Bouguer gravity occurs approximately along the Cougar fault. Using a reduction density of 2.43 g/cm^3 , Pitts (1979) produced a residual gravity anomaly map which shows a decrease in gravity values of 6 mgal from the west block to the east block. This decrease in residual gravity occurs over an east-west distance of only 3.9 km, producing a very steep north-south trending gradient. The Cougar fault follows the east side of this steep gradient. The residual and Bouguer gravity gradients continue toward the north across Lookout Ridge into the area mapped by Swanson and James (1975), suggesting that the Cougar fault also continues toward the north, lending credence to observation number 4 above.

The aeromagnetic map of Couch and others (1978) also shows a steep change in the pattern of magnetism at the Cougar fault. The west block of the fault has a magnetic high of +250 gammas centered on Harvey Mountain, while the east block of the fault from Walker Creek to Castle Rock is characterized by a broad magnetic low of between -50 and -150 gammas. The transition between these two areas occurs at a steep north-south-trending gradient which terminates at the Cougar fault. A magnetic low along the McKenzie River to the north and an east-west-trending magnetic high at Tipsoo Butte changes the north-south pattern of contours. The north-south pattern, however, appears to re-establish itself north of Lookout Ridge in the area mapped by Swanson and James (1975).

Local tilting and folding

There is no evidence of a major fold in the area. Wells and Peck (1961) plot the axis of the Breitenbush anticline a few kilometers west of the map area, but the general easterly dip of 10° to 20° inferred from their map could not be demonstrated in the map area. Dips measured in the early and late Western Cascade section have many orientations over very small areas, owing to initial slopes during deposition and local deformation related to small faults and probable mass movements.

Dips in fine-grained epiclastic units along the west shore of Cougar Reservoir, however, consistently show tilting of about 7° or less toward the south to southwest. Although there is considerable relief on the late Western Cascade-

early Western Cascade contact, there is little difference in dips across the contact, and the late Western Cascade sequence appears also to slope gently toward the south to southwest. South of the map area, late Western Cascade rocks totally dominate surface outcrops, whereas to the north, the early Western Cascade sequence crops out at higher elevations. As previously explained, this is partly due to a local topographic high which existed in the northern part of the map area when the late Western Cascade lavas began to erupt, but some southerly tilting of the Western Cascade sequence is probably necessary to explain dominance of the late Western Cascade sequence over the region beyond the map area to the south.

There is no indication of any measurable tilting of the early High Cascade sequence. This suggests that a slight angular unconformity may exist between the early High Cascade and late Western Cascade sequence. If the tilting occurred gradually throughout late Western Cascade time, uppermost Western Cascade units, however, may be conformable. The close similarity between the age of an uppermost late Western Cascade lava at Lookout Ridge (8.80 m.y. B.P.) to an overlying early High Cascade lava (8.34 m.y. B.P.) suggests that the latter hypothesis is probably correct. In any case, the total amount of tilting is quite small and not easily measured in this type of volcanic terrane.

The deep (1-km) entrenchment of the McKenzie River drainage system into the rocks west of the Horse Creek fault zone probably occurred between 5.0 and 3.4 m.y. B.P. The Foley Ridge flows, K-Ar dated in this study and Flaherty's (1981) thesis, indicate that essentially all of the current relief in the McKenzie River area was developed before these flows entered the McKenzie River canyon about 3.4 to 2.0 m.y. B.P. The presence of 6- to 5-m.y. B.P. early High Cascade flows on ridgetops as much as 1,237 m (4,060 ft) above the intracanyon Foley Ridge flows indicates that the McKenzie River cut down over a kilometer into the area over a period of about 2 m.y. Flaherty (1981) concludes that all of this erosion occurred between 3 and 5 m.y. B.P., during a period of volcanic inactivity. MacLeod (personal communication, 1982) believes substantial uplift of the Western Cascades rather than only passive subsidence of the High Cascades is necessary to explain this rapid erosion. It may be that both uplift of the Western Cascades and subsidence of the High Cascade axis occurred simultaneously. The similarity of elevation of the base of the Foley Ridge flows and the current McKenzie River indicate that the streams may have been at approximately base level for the past 2.0 to 3.4 m.y. (MacLeod, personal communication, 1982),

except for periodic influxes of glacial outwash sediments during the Pleistocene.

GEOHERMAL RESOURCES

Terwilliger Hot Springs, the only hot springs in the map area, have flow rates of 114 to 200 liters per minute and measured temperatures between 38° C and 44° C (Table 4.1). Calculated reservoir temperatures from chemical geothermometers range between about 48° C and 104° C (Table 4.1). The silica geothermometer, based on the assumption of equilibrium with opal, gives negative reservoir temperatures and so obviously does not apply to the Terwilliger Hot Spring waters. The good agreement among the silica geothermometers, which assume equilibrium with quartz, and the Na:K:Ca (1/3 β) geothermometer suggest that these chemical systems are most applicable to the Terwilliger Hot Spring waters. The range of reservoir temperatures using the latter systems is 95° C to 104° C.

A temperature gradient hole about 1/2 km east of the hot springs intercepted a heavily celadonitized tuffaceous unit at 125 m and, upon penetrating the unit at 140 m, about 378 liters per minute (100 gallons per minute) of 23° C water began to be blown from the hole during airhammer drilling. Water continued to be blown from the hole as the drill penetrated a dark-gray plagioclase-pyroxene-bearing lava flow to a depth of 153.5 m. The average stabilized temperature gradient within the well was 134.7° C/km. The gradient was roughly linear throughout the aquifer; temperatures varied from 23.2° C at 140 m to 24.7° C at 153.5 m, giving a gradient of 112° C/km. The average gradient, corrected for local terrain effects, is 102° C/km (Black and others, Chapter 7).

A hole drilled northeast of the above well, at the mouth of Walker Creek and adjacent to the Cougar fault, had an average gradient of 54.1° C/km in the lower 50 m of the 155-m hole. The terrain-corrected gradient was 52.0° C/km, resulting in a heat-flow value of 83 mW/m² (Black and others, Chapter 7). The terrain-corrected value is similar to terrain-corrected gradients measured in other holes near Cougar Dam which range from about 48.0° C/km to 53° C/km. The heat flow from the Walker Creek hole is thus probably characteristic of the background heat flow in the map area.

This heat-flow value of 83 mW/m² roughly matches the regional heat flow predicted by Blackwell and others (1978). This heat flow is characteristic of the transition zone between the low heat flow (approximately 40 mW/m²) of the Willamette Valley-Coast Range provinces and the high heat flow (greater than

100 mW/m²) of the High Cascades (see Blackwell and others, 1978). The Belknap-Foley Hot Springs area east of the map area (Figure 4.1) has heat-flow characteristic of the High Cascades. Three conclusions may be drawn from the above observations:

1. The hole near Terwilliger Hot Springs has a gradient which is raised by convective upflow of thermal water related to the hot springs.
2. The Walker Creek hole, even though it is next to the largest fault in the area, shows no evidence of temperature disturbance by upwelling thermal waters.
3. Heat flow probably increases from west to east across the map area toward the main part of the High Cascade heat-flow anomaly.

Terwilliger Hot Springs are located on strike with a small N. 35° W. shear zone which dips 79° to the southwest. No shear zone was found at the hot springs themselves, but the thermal water issues from a complex series of joints and fractures. A similar observation applies to Foley Hot Springs to the east, where hot water issues from northwest-trending fractures and small shears. Both Foley and Terwilliger Hot Springs are on upthrown blocks adjacent to major north-south- to northwest-trending fault zones (Figure 4.1), but neither of the springs issues directly from the main fault. It may be that jointed rocks and splinter faults adjacent to the main fault zones offer more permeability than the fault zones themselves. Alternatively, water may rise from depth in certain places along the main faults until it encounters impermeable rock units which force the water into lateral zones of permeability. The water might then reach the surface along local splinter faults or joints. There are insufficient data in the map area to distinguish between these two possibilities, but significant smectite-calcite-zeolite alteration within the Cougar fault zone suggests that some hydrothermal circulation occurred there in the past.

Local terrain-corrected conductive gradients, when projected to a depth of 3 km, predict a temperature of about 165° C. Fluids at this temperature are adequate for Rankine-cycle electrical generators but not for direct-flash generators. Unless drilling can intercept upwelling thermal fluids, it is not likely that the area can be economically exploited for generation of electricity, inasmuch as drilling to 3 km and use of the expensive Rankine-cycle generators may well prove economically not feasible. Drilling of additional temperature-gradient holes along the Cougar fault zone might reveal disturbances of the background heat flow indicative of significant transport of heat from depth by upward-moving

thermal water.

The higher heat flow associated with the Horse Creek fault zone to the east of the map area (Figure 4.1; see Black and others, Chapter 7) makes that area a more attractive exploration target than the Cougar Reservoir area. Curie-point isotherm calculations of Connard (1980) confirm that the depth of the Curie-point isotherm is probably shallow (i.e., 8 to 14 km below sea level) under the High Cascades in the main part of the heat-flow anomaly outlined by Blackwell and others (1978). Connard's model suggests that the Curie-point isotherm may be significantly deeper under the Cougar Reservoir area, although his data were not definitive on this point. Geothermal exploration models relating to the Horse Creek area and other areas in main part of the High Cascade heat-flow anomaly of Blackwell and others (1978) are discussed by Priest and others (Chapter 2).

CONCLUSIONS

The Cougar Reservoir area is cut by a north-south fault which displaces late Western Cascade rocks at least as young as 13.2 m.y. The relative motion on the fault is down to the east by at least 152 m and possibly by more than 1,033 m. The fault may have begun to displace rocks of the area as early as 16.3 m.y. B.P. Geologic and geophysical interpretations suggest that a fault scarp may have existed in the area when early High Cascade lavas began to flow from the east about 8.3 to 7.8 m.y. B.P. The fault does not cut Pleistocene outwash gravels. The Cougar fault may be a late Miocene analogue of the early Pliocene Horse Creek fault mapped by Flaherty (1981) along the margin of the High Cascade province to the east.

The area as a whole has not been significantly folded, but slight tilting toward the south probably occurred during late Western Cascade time (i.e., between 13 and 9 m.y. B.P.). Although deep erosion produced about 366 m or more of relief between the time of deposition of the tuffs of Cougar Reservoir and the time of eruption of late Western Cascade lavas and tuffs, no certain evidence of an angular unconformity was found between these two sequences. Most of the current drainage system probably developed between 5.0 and 3.4 m.y. B.P., during formation of faults in the Horse Creek area. Uplift of the Western Cascades and possible subsidence of the High Cascades occurred between 5.0 and 3.4 m.y. B.P. Deep dissection (1 km) of the area occurred during this interval. When the Western Cascades were uplifted in the early Pliocene, High Cascade

lavas were ponded within the downfaulted High Cascade block. Observations by Hales (1975) and Taylor (1981) at the Green Ridge fault suggest that little or no tilting of the Green Ridge sequence has occurred either before or after subsidence of grabens along the High Cascade axis, yet this area has been deeply dissected by the Metolius River where it flows eastward across Green Ridge. It is, however, possible that part of the low easterly dip of the Green Ridge sequence is from eastward tilting during uplift. The amount of absolute uplift in the Cascades, particularly in the Western Cascades, could probably be estimated from a careful study of erosional surfaces and drainage patterns.

CHAPTER 5. GEOLOGY OF THE LOOKOUT POINT AREA,

LANE COUNTY, OREGON

By Neil M. Woller and George R. Priest,
Oregon Department of Geology and Mineral Industries

ABSTRACT

The Lookout Point area straddles the northwest-trending Eugene-Denio lineament (Lawrence, 1976) in the Western Cascade physiographic province, approximately 7 km northwest of Oakridge, Oregon. Lawrence (1976) postulated that relative motion between the Basin and Range physiographic province, which is characterized by extensional tectonics, and the stable Blue Mountain province to the north has been accommodated by Neogene right-lateral strike-slip faulting on the Eugene-Denio lineament and the parallel Brothers fault zone to the north and Mount McLoughlin zone to the south.

A tholeiitic intracanyon sequence, the lavas of Black Canyon, crosses the Eugene-Denio lineament at approximately right angles. The sequence is dated at 22 m.y. B.P. No substantial lateral movement can be demonstrated on the sequence across the lineament, although vertical displacement may be present. There is evidence that an earlier episode of northwest-trending lateral movement occurred along the lineament.

The stratigraphy in the Lookout Point area records a long history of activity from the late Oligocene to Pleistocene. The age breaks and petrologic changes between regional stratigraphic units correspond very well to findings in other areas of the Oregon Cascades as described in this volume and elsewhere in the literature.

INTRODUCTION

Lookout Point is located 7 km northwest of Oakridge and 58 km southeast of Eugene in Lane County, Oregon. It is a rugged, heavily forested mountain area located within the Western Cascade physiographic province. The northwest-flowing Middle Fork of the Willamette River provides the principle drainage for the area and flows into Lookout Point Reservoir in the northwest part of the map area. Access is by Oregon Highway 58 and an extensive logging-road network.

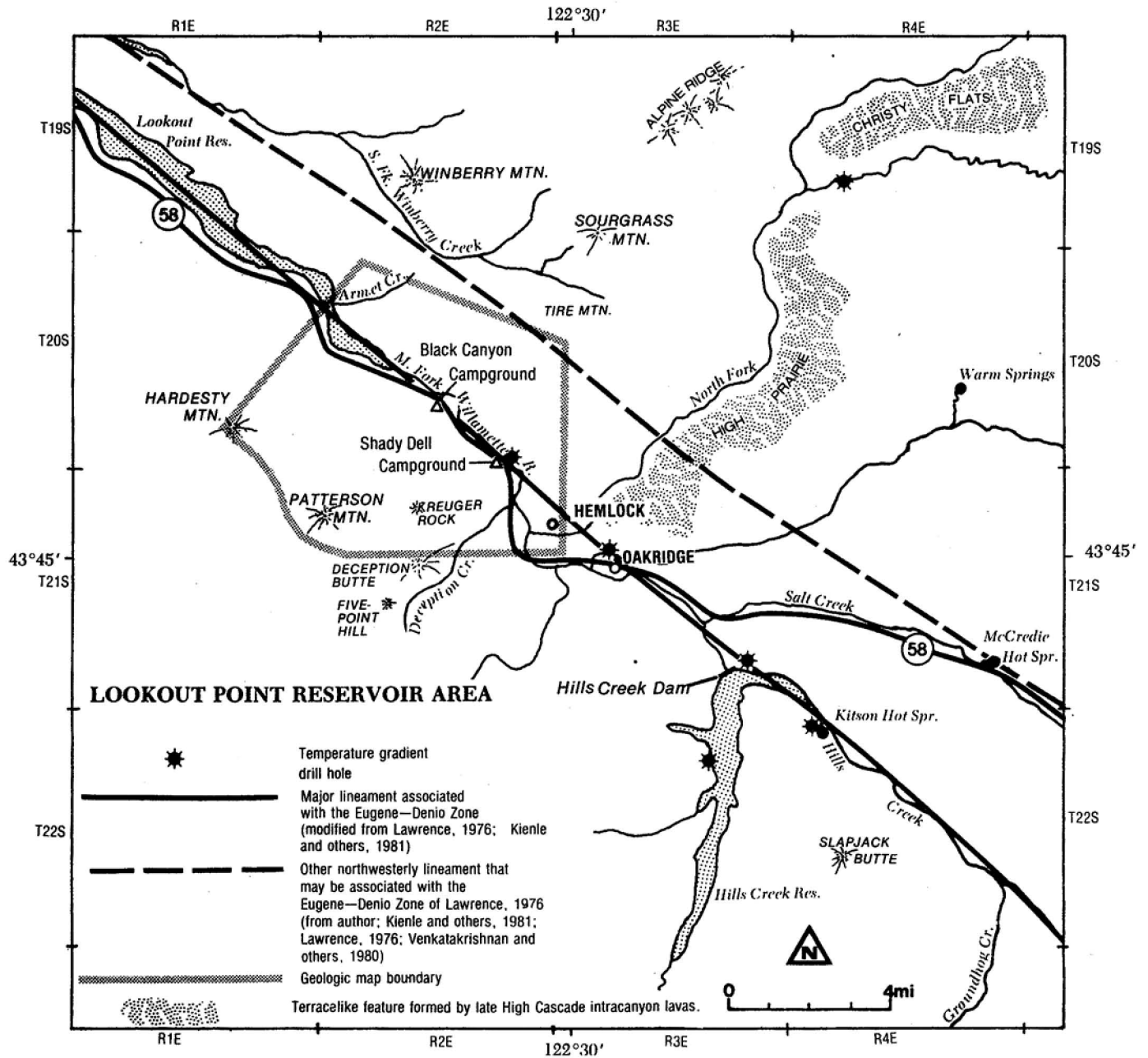


Figure 5.1. Location of the Lookout Point map area, the Eugene-Denio lineament, and other localities mentioned in the text.

Geologic mapping in the area was aimed at identifying right-lateral strike-slip faulting along the Eugene-Denio lineament. Lawrence (1976) postulated that the Eugene-Denio lineament forms one of the boundaries of the Basin and Range province and that right-lateral strike-slip movement along the lineament accommodated relative motion between the Basin and Range province and the stable Blue Mountains province to the north. He cited a 10- to 20-km right-lateral offset of the High Cascade axis across the lineament as evidence for dextral movement on the lineament. The lineament is commonly shown following both the valley of the Middle Fork of the Willamette River northwest of Oakridge and the Hills Creek drainage southeast of Oakridge (Lawrence, 1976; Kienle and others, 1981). Immediately to the north, another expression of the lineament is formed by the Salt Creek-Winberry Creek drainages. Lawrence (1976) notes that the lineament in the Basin and Range area seems to form the boundary between an area of younger faulting to the north and an area of predominantly older faulting to the south. Known periods of activity and relative offset along the lineament within the Western Cascades are discussed in this and the following chapter.

A series of intracanyon tholeiitic lavas cuts across the Eugene-Denio lineament at approximately right angles at Black Canyon near Lookout Point. These flows, informally named the lavas of Black Canyon, are described in this report. Although many small-scale shears and a few faults of moderate displacement are present, the authors could not identify any substantial lateral displacement on the Black Canyon sequence across the lineament.

VOLCANIC STRATIGRAPHY

Introduction

Information nomenclature used by Priest and others (Chapter 2) to discuss and compare petrologic and chemical similarities of temporally equivalent stratigraphic units throughout the Cascades will also be used in this report. Figure 2.2 of that report shows distinctive lithologic and field characteristics that typify, on a regional basis, each of the four age groups. Correlative rock stratigraphic units of Cascade researchers corresponding to each division are also shown (e.g., see Plate 2).

All four divisions are represented in the Lookout Point area. The authors attempted to identify the age breaks between each stratigraphic unit with K-Ar dates supplied by Stanley H. Evans of the University of Utah Research Institute

Nomenclature used in this report*	Name	K-Ar dates (in m.y.)	Thickness (ft)	Lithology
Volcanic rocks of the late High Cascades	Pliocene-Pleistocene(?) basaltic lavas	0.56±0.16	30	Olivine-bearing basalt; diktytaxitic to compact; dark-gray; fresh. Intracanyon into all older units; found related to Quaternary drainages.
Volcanic rocks of the early High Cascades	Upper Miocene lavas	5.81±0.30	240	Olivine-bearing basalt; compact; fresh; gray; caps Patterson Mountain
Volcanic rocks of the late Western Cascades	Miocene andesitic lavas	Upper part, 8.3±5.5 ^a ; lower part, 15.9±7.6 ^a	2,000+	Two-pyroxene andesite with subordinate two-pyroxene dacite, olivine-bearing basaltic andesite and epiclastic interbeds; dark-gray to black; generally altered.
Volcanic rocks of the early Western Cascades	Lavas of Black Canyon	Top, 22.0±1.0; bottom, 21.9±2.9 ^a	890	Tholeiitic basaltic andesite, basalt, and andesite; aphyric to plagioclase-phyric; dark-gray to black; fresh to altered. Interbedded with ash-flow tuffs and epiclastic deposits. Intracanyon into older units.
	Lavas of Hardesty Mountain	----	1,600	Pyroxene andesite and dacite; plagioclase-phyric; extensive alteration of mafic phenocrysts, brown, pink, gray. Clinopyroxene generally present in larger percentages than orthopyroxene; caps Hardesty Mountain.
	Lavas of Lookout Point	----	700 at Lookout Point	Rhyodacitic lavas; dark-gray; sparsely plagioclase phyric; also contains rare megascopic clinopyroxene. Generally altered.
	Oligocene and lower Miocene tuffs and lavas	24.7±2.0 ^a	2,500	Silicic ash-flow tuffs, sediments; laharic(?) lithic-fragment-rich tuffs and lavas; general dacitic to rhyodacitic; altered, with celadonite, chlorite and/or smectite.

* See Priest and others (Chapter 2) for explanation and regional rock-stratigraphic correlations.

^a K-Ar date may be affected by alteration.

Figure 5.2. Stratigraphy of the Lookout Point area.

under a U.S. Department of Energy grant.

Volcanic rocks of the early Western Cascades in the Lookout Point area are Oligocene to lower Miocene tuffs and lavas (undifferentiated). Included within the section are the lavas of Lookout Point, the lavas of Hardesty Mountain, and the lavas of Black Canyon. These units comprise most of the total section in the map area. The bottom of the early Western Cascade section is not exposed.

Younger stratigraphic units are represented by sequentially decreasing volumes. Miocene andesite lavas (late Western Cascades) cap many ridges in the vicinity. Upper Miocene lavas (early High Cascades) are present at the top of Patterson Mountain, and intracanyon Pliocene-Pleistocene basaltic lavas (late High Cascades) invade the map area from the east. A local source for the Pleistocene basaltic lavas is also present.

Geochemical data and related discussions are incorporated into the petrologic discussions and diagrams of Priest and others (Chapter 2) and are not duplicated here in detail.

Volcanic rocks of the early Western Cascades

Oligocene and lower Miocene tuffs and lavas (undifferentiated) (Totl): The oldest rocks in the area are Oligocene to early Miocene tuffs and lavas, commonly called the Little Butte Volcanic Series (Peck and others, 1964; Kays, 1970). They are probably roughly equivalent to the tuffs of Cougar Reservoir (Priest and Woller, Chapter 4).

Tuffs predominate in the unit. In the exposures at river level, the tuffs are green, lithic fragment rich, pumice poor, and generally massive. They contain abundant silicic aphyric clasts of many pastel colors. The matrix is generally green or yellow ash, altered to celadonite, chlorite, or smectite. The texture of these units suggests an origin that is in large part laharc. Large clasts up to half a meter in diameter are locally found in the flows. Pumice is very rarely present, and charred wood occurs in some outcrops. In nearby exposures at Hills Creek Dam, similar deposits carry fragments of lava many meters in diameter. Rare interbeds, seen in excellent roadcut exposures along route 58, are all thin, fine-grained siltstone within identical overlying and underlying laharc(?) lithic-fragment-rich tuff.

In the heat-flow hole drilled at the mouth of Burnt Bridge Creek, 150 m of uninterrupted green, lithic-fragment-rich tuff was penetrated without reaching the bottom of the unit.

Above the lithic-fragment-rich member, true ash-flow and air-fall tuffs

predominate. They are altered, phenocryst poor, and yellow, red, purple, or green in color. Most of the ash-flow tuffs are nonwelded, and all are probably dacitic or rhyodacitic in composition; chemical analyses of the juvenile rocks are affected by alteration. Lithic fragments are generally rare within these ash-flow tuffs, but where found, they commonly are aphanitic rhyodacite of small size. Alteration is very common and includes staining, devitrification of pumice, and the presence of smectite and/or chlorite.

The ash-flow and air-fall tuffs are interbedded with sediments and lavas. The chemical compositions of these lavas range from rhyodacite to basaltic andesite, but silicic lavas predominate. Most lavas are aphyric or slightly plagioclase phyric and are altered with smectite, making it difficult to obtain reliable K-Ar dates. One dark-gray, nearly aphyric basaltic andesite from fairly high in the section was dated at 24.7 ± 2.0 m.y. B.P. The sample contains abundant microphenocrysts of augite (7 percent) and less than 1 percent totally altered hypersthene (to smectite) in an intergranular groundmass. Smectite replaces plagioclase phenocrysts and also occurs as patches within the groundmass. The alteration to smectite may have caused loss of radiogenic argon, resulting in a date that may be too young. The lithic-fragment-rich tuffs below may represent vent-clearing episodes prior to eruption of the ash and lava flows.

Total thickness of the ash and lava flow sequence exceeds 600 m. The dips of the sequence, although highly variable from exposure to exposure, are to the north and northeast.

The silica contents of two analyzed lavas (recalculated to 100 percent volatile-free with total iron as Fe^{+2}) are 56.1 percent and 71.2 percent. The basaltic andesite had 7.2 percent FeO^* , 5.8 percent MgO , and 3.5 percent total alkalis. The rhyodacite had 3.96 percent FeO^* , 0.27 percent MgO , and 5.88 percent total alkalis.

The early Western Cascade rocks tend to form gentle slopes characterized by frequent slumps and slides. Exposures other than in roadcuts and railway cuts are rare, making it difficult to trace individual flows very far. However, three distinctive units within the early Western Cascade section are extensive enough to be mapped separately: the lavas of Lookout Point, the lavas of Hardesty Mountain, and the lavas of Black Canyon.

Lavas of Lookout Point (Tolp): The lavas of Lookout Point are exposed mainly at river level on both sides of the Willamette River. One analyzed lava is a rhyodacite, with a silica content of 71.9 percent. The flows are black

when fresh and pink or gray when altered, with 1 percent plagioclase phenocrysts and sparse pyroxene microphenocrysts in a groundmass which appears glassy in hand sample. Individual flows cannot be distinguished from one another in the field, but thin sections show at least two slightly different lithologic types. The glassy appearance of one flow actually proved to have a pilotaxitic texture. Phenocryst sizes are slightly different in the two sampled flows; although one flow is relatively fresh, the other has extensive calcite and smectite alteration of the plagioclase phenocrysts.

The flows which are more erosionally resistant than the enveloping tuffs tend to form knobs. Lookout Point, a prominent, plug-shaped outcrop on the northeast side of the Willamette River, may be the source of these lavas. The lavas of Lookout Point are not present along the river in some places, probably because they have been removed by river erosion. Exposures of these northeast-dipping lavas along the northwest-trending river banks are evidence that no major faults crosscut the river within the outcrop area of this unit.

Lavas of Hardesty Mountain (Toh): The lavas of Hardesty Mountain are silicic, fine grained, and altered. The color is typically brown, pink, or gray. Plagioclase phenocrysts altered to smectite along twin and cleavage planes are present in nearly every flow sampled. Clinopyroxene is more abundant than orthopyroxene. Other ferromagnesian minerals are also present but are completely unrecognizable due chiefly to alteration to smectite. Groundmass textures include pilotaxitic and intersertal grading into vitrophyric. One chemically analyzed lava proved to be icelandite (Fe-rich andesite). SiO_2 (recalculated, volatile-free) is 60.37 percent; FeO^* , 8.46 percent, and MgO , 1.98 percent (Appendix B).

The lavas of Hardesty Mountain form a resistant cap on Hardesty Mountain. One float sample of lithic-fragment-rich pumice-poor tuff was found associated with the flows and may therefore be interbedded with them, but a tuff unit was not found in outcrop on the single traverse up Hardesty Mountain. The attitude of the flows was not measured, but based on aerial photo analysis they probably dip at a low angle towards the northeast. Over 450 m of lavas are present.

Lavas of Black Canyon (Tml/Tmli): The lavas of Black Canyon are a series of intracanyon tholeiitic lavas that flowed northeast from vents at Kreuger Rock and Deception Butte (immediately south of the map area). Other vents may exist, but they were not located during this study. These flows are stratigraphically and geochemically equivalent to the Scorpion Mountain lavas of White (1980a,c).

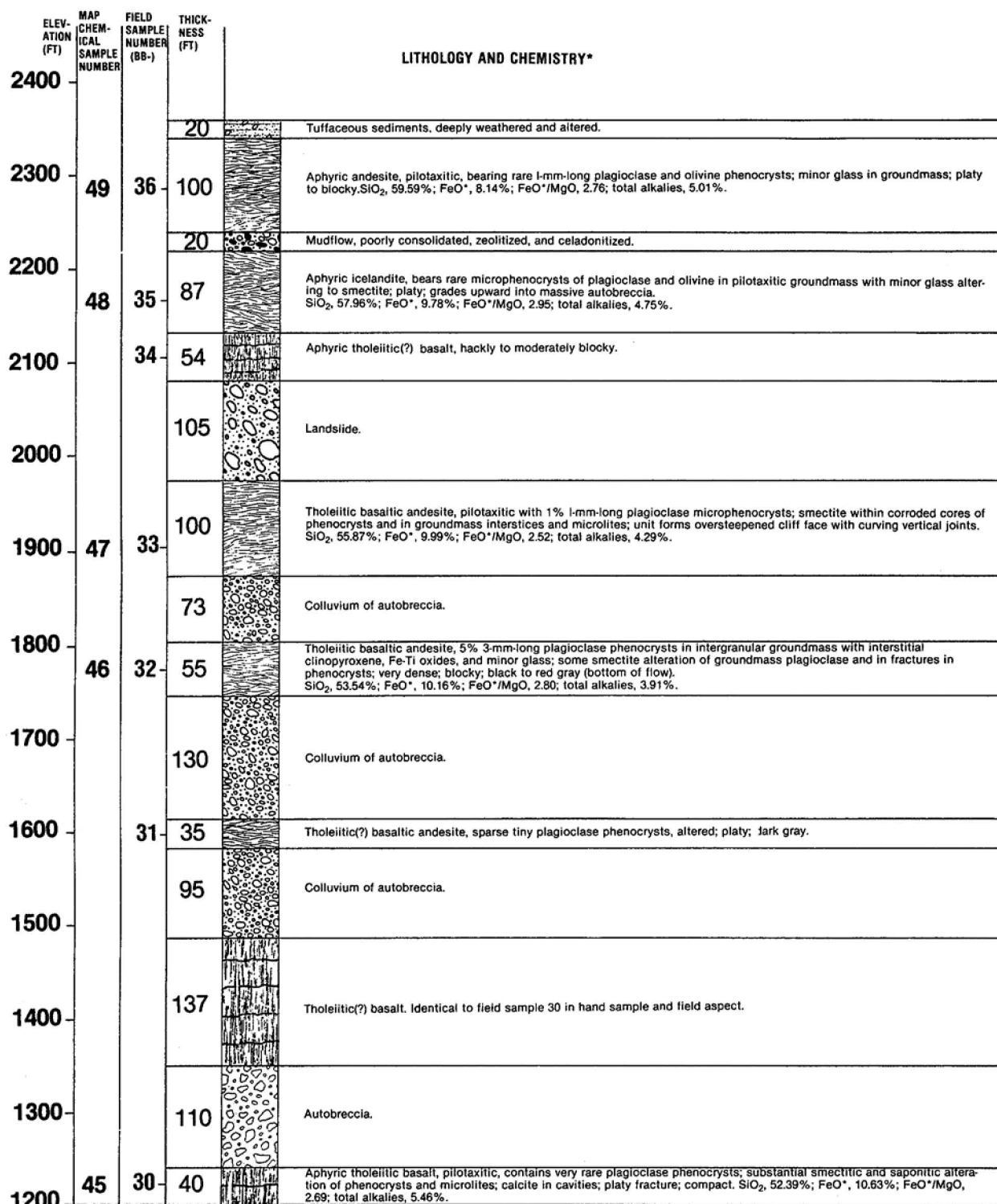
The chemistry of six flows is shown in the appendix as samples 45-50.

Lavas of the Scorpion Mountain chemical type are apparently regionally distributed, as similar aphanitic tholeiites of the same age occur in the Breitenbush, North and Middle Santiam, Calapooya, and North Collawash drainages (White, 1980a). Some researchers have mistaken many of them for basalts of the Columbia River Basalt Group and have used bases of their flows to define the upper contact of the Little Butte Volcanic Series (see White, 1980c). White (1980a,c) describes them as intercalated with, but near the top of, the Oligocene-early Miocene sequence. They are overlain by middle Miocene andesites. A similar pattern is seen in the Black Canyon area. Ash-flow tuffs and epiclastic deposits, very similar in appearance to those of the Oligocene to early Miocene tuffs and lavas which constitute the paleocanyon walls, are interbedded with the Black Canyon lavas on the north side of Patterson Mountain.

In the Lookout Point Reservoir area, the Black Canyon lavas are iron-rich tholeiitic basalt to andesite (icelandite). The rocks are compact, dark gray to black, and generally aphyric. In thin section, most are pilotaxitic with rare plagioclase and very rare augite and olivine microphenocrysts.

On the Deception Creek side of the paleocanyon, the Black Canyon sequence can be followed for miles along a cliff-face exposure resulting from the more resistant lithology. Along the cliff face the dip is low and to the north, but on the north side of Patterson Mountain, dips of 12° - 17° are more common, and at one location a 30° dip to the southeast was measured. On the northeast side of the Willamette River, the dips are gentle (e.g., N. 51° W. 2° N). The predominantly gentle dips contrast with the highly variable attitudes observed in the Oligocene-early Miocene tuffs and lavas comprising the paleocanyon walls and floor. The older tuffs and lavas are affected by omnipresent shears, alteration, and deformation, whereas deformation seems to have had less effect on the Black Canyon lavas. It is clear that major deformation chiefly occurred prior to 22 m.y. B.P., as dates on the lowermost and uppermost flows of the Black Canyon lavas at Black Canyon were 21.9 ± 2.0 m.y. B.P. and 22.0 ± 1.0 m.y. P.B., respectively. The lowermost flow at Black Canyon is extensively altered to smectite, with radiogenic argon at 11 percent, and may therefore have yielded a reset date. The upper dated flow was much fresher, with 35 percent radiogenic argon, and its K-Ar age is probably real. Trace-element chemistry and field relations suggest that the lavas of Black Canyon may be a differentiation series from a single volcanic source and thus may not span much time. Therefore, the authors

Stratigraphic section of the lavas of Black Canyon



*Volatile free, total iron as Fe^{+2} . Complete raw chemistry is listed in appendix.

Figure 5.3. Stratigraphic section of the lavas of Black Canyon.

feet 22 m.y. B.P. does represent a reasonable date for the sequence of flows.

The Black Canyon lavas can best be seen across the Willamette River from the Black Canyon Campground (Figure 5.1). The section here is 350 m thick. Lithologic and geochemical data are presented in Figure 5.3, and complete geochemical analyses are given in the appendix. The lower contact with the underlying Oligocene to early Miocene tuffs and lavas is obscured by colluvium. The upper contact with the Miocene andesites at Black Canyon appears conformable but is unconformable at Patterson Mountain.

Volcanic rocks of the late Western Cascades

Miocene andesitic lavas (Tma/Tmi): The late Western Cascade rocks (Priest and others, Chapter 2) in the Lookout Point area are characterized mainly by andesitic lava flows, with subordinate dacitic and basaltic andesite flows and interbedded epiclastic volcanic rocks and rare olivine basalt flows. They are stratigraphically equivalent to the Sardine Formation of Peck and others (1964) and the Miocene volcanic rocks of Brown and others (1980a,b). They are typically dark-gray, plagioclase-rich, two-pyroxene andesites. Very few of the flows are unaltered. Smectite is the most common alteration mineral, usually replacing mafic phenocrysts and groundmass minerals. Most flows examined in thin section are intergranular with interstitial orthopyroxene and Fe-Ti oxides. Euhedral to subhedral orthopyroxene and clinopyroxene phenocrysts are present in roughly equal proportions. Orthopyroxene is the mafic mineral most often altered to smectite. Olivine and hornblende occur rarely but are invariably highly altered, usually to smectite or other clay minerals.

A dacite flow from low in the section was dated at 15.9 ± 7.6 m.y. B.P., and an andesite flow from high in the section on Patterson Mountain was dated at 8.3 ± 5.5 m.y. B.P. Despite the high statistical error, the older date is consistent with the age of the older part of the late Western Cascade sequence in other areas (e.g., Priest and others, Chapter 2). The Patterson Mountain date corresponds to the latest of late Western Cascade volcanism as dated in other areas (Priest and Woller, Chapter 4). Both rocks have experienced low-grade alteration, generating the presence of smectite in plagioclase phenocrysts. The alteration may have caused loss of potassium or radiogenic argon, which would make these rocks older than the ages reported here.

The Miocene andesitic lavas unconformably overlie the Black Canyon lavas on the northwest side of Patterson Mountain. In other areas, including the cliffs of Black Canyon, the contact appears conformable. Intrusive bodies of these lavas,

dikes, and possibly a plug, occur near river level.

Silica contents of four analyzed samples vary from 58.26 percent to 68.12 percent. FeO*/MgO ratios range from 2.14 to 4.91, increasing with increasing silica.

Volcanic rocks of the early High Cascades

Upper Miocene lavas (Tmu): Early High Cascade-type lavas are present at Patterson Mountain and are here called upper Miocene lavas. They are light-gray, compact, olivine basalts. The olivines are unaltered, and the groundmass texture is subophitic. Two flows were recognized, the lower being very poorly exposed. The unit is equivalent to the lavas of Tipsoo Butte (Priest and Woller, Chapter 4), Outerson formation (Thayer, 1939), and Pliocene volcanic rocks (Brown and others, 1980a,b). A K-Ar date of 5.81 ± 0.30 m.y. B.P. was obtained on the upper flow.

Chemical analysis of the dated flow yielded volatile-free (total iron calculated as Fe^{+2}) values of SiO₂, 50.94 percent; FeO*, 10.00 percent; FeO*/MgO, 121; and total alkalis, 4.60 percent (Appendix B).

The basalts flowed on practically the same northeast-southwest course as the earlier Black Canyon lavas and are intracanyon into the Miocene andesitic rocks. The Patterson Mountain area may have been a prominent highland, with drainage to the northeast throughout the late Tertiary, as evidenced by the Black Canyon vents at Kreuger Rock and Deception Butte and the overall dip of the Oligocene and early Miocene tuffs and lavas and the Hardesty Mountain lavas.

Volcanic rocks of the late High Cascades

Pliocene-Pleistocene(?) basaltic lavas (QTb): Late High Cascade lavas are present at two locations within the Lookout Point area. The terminus of the High Prairie basalts (Brown and others, 1980b) is located immediately north and west of the town of Hemlock. The flow straddles the Willamette River with no apparent offset. It is intracanyon into the Oligocene and lower Miocene tuffs and lavas and is traceable for many miles up the North Fork of the Middle Fork drainage of the Willamette River toward the High Cascades. These flows form the topographic features known locally as High Prairie and Christy Flat and may be traceable to Moolack Mountain near the High Cascade margin. McBirney and others (1974) dated the flow just north of Hemlock at 11.09 ± 0.15 m.y. B.P. However, the date is highly questionable. The flow is related to the Quaternary drainage pattern and is identical mineralogically to the volcanic rocks of the

High Cascades. Late High Cascade flows in nearby areas which are in a similar topographic setting have dates of 2 to 3 m.y. B.P. (e.g., see Flaherty, 1981). The High Prairie flow is a diktytaxitic olivine basalt with a felty groundmass of plagioclase and intergranular olivine, Fe-Ti oxides, and minor oxidized opaque glass. Olivine phenocrysts are moderately iddingsitized.

The other Pleistocene flow forms a fan-shaped lobe into the Willamette River channel at the mouth of Armet Creek. The poorly exposed source is probably located 2 mi up Armet Creek. The flow is geochemically and petrographically identical to the High Cascade lavas. The rock is a fine-grained, almost aphyric, basaltic andesite, bearing olivine and augite microphenocrysts in a pilotaxitic groundmass with scattered interstitial pyroxene and Fe-Ti oxides. The olivine is fresh and anhedral. Some of the microphenocrysts have corroded cores. Volatile-free SiO_2 is 54.25 percent, with a FeO^* of 6.44 percent and a FeO^*/MgO ratio of 1.07. Total alkalies are relatively high, at 5.55 percent. The Armet Creek flow has a K-Ar age of 0.56 ± 0.16 m.y.

The Armet Creek center is unusual in that it occurs so far to the west of the High Cascade province. Other volcanic centers of late High Cascade age, however, have been recognized within the Western Cascade province: Battle Ax Mountain, Snow Peak, and Harter Mountain are examples (Peck and others, 1964). Some of the centers (i.e., Snow Peak) are as far west of the High Cascade margin as the Armet Creek flow. The implication is that partial melting episodes from processes similar to those generating voluminous High Cascade magmas to the east are locally operative in much reduced quantity below the Western Cascades.

STRUCTURE

Lawrence (1976) postulated that right-lateral slip has occurred on the Eugene-Denio lineament. He cited as evidence a right-lateral offset of the High Cascade axis in the vicinity of Willamette Pass. Pitts (1979) and Connard (1980) observed conflicting offsets on residual gravity and aeromagnetic anomalies at the intersection of the High Cascade axis and the Eugene-Denio lineament.

The rocks of the early Western Cascades have been folded, sheared, altered, and obscured by mass movement and vegetation to such an extent that it is difficult to see the structural configuration of the sequence as a whole. Within specific localities, one can measure formational attitudes (e.g., the Deception Creek section dips north to northwest, the Whitehead Bridge Creek sections dip

west), but the location and nature of the transitions between specific localities are not evident.

There is approximately 120 m of visible vertical offset on the Lookout Point lavas across a northwest-trending lineament on the southwest side of the Willamette River, above Shady Dell Campground. Sediments crop out in a switch-back roadcut directly across a northwest-trending ravine from the Lookout Point rhyodacite. Above the sediments, a very heavily altered, decomposed outcrop of what looks like the same rhyodacite is exposed. The apparent relative displacement is thus down to the northeast. The possible fault zone in the ravine is obscured by landslides, colluvium, and vegetation. We were not able to show that the fault zone cuts younger units. The possible fault strikes approximately N. 15° W., and the trace of the lineament implies a steep, nearly vertical dip.

Many low-angle shears occur within early Western Cascade rocks. Numerous shears also have low-angle rakes indicative of strike-slip motion. Most of the low-angle shears with low rake angles are northwest striking. Bedding-plane movement was noted in two exposures.

Two probable vents for the Black Canyon lavas, Deception Butte and Kreuger Rock, lie in a N. 15° W. alignment, roughly parallel to the fault cutting the Lookout Point unit. Other vents to the south and southeast are possible in view of the southern trend of the paleocanyon containing the lavas of Black Canyon southwest of Deception Butte. Five-point Hill, the southernmost locale to which the authors have traced the Black Canyon sequence, may be one of these vent areas. However, it was not mapped in this study.

The north and northeast dips of 2° to 5° of the Black Canyon lavas are in accord with the attitude of the early Western Cascade sequence visible in the Deception Creek area, which is an undeformed section. It is also similar to the attitude of the Hardesty Mountain lavas, which appear to have a distinct northeast dip on photo coverage. The overall dip of the early Western Cascade sequences in the Lookout Point area, exclusive of the Black Canyon lavas, is 10° to 20° to the north.

The Black Canyon lavas have not suffered deformation as extensively as the older units. The flows can be traced for miles, and shearing in the unit is rare compared to the abundant shearing present in the underlying early Western Cascade sequence. The Black Canyon lavas are also rarely altered to the same extent as the older flows. The minimum time span between extrusion of the Black Canyon lavas and older units is 3 m.y., as a minimum age of 24.7 m.y. was obtained

on a slightly altered sample of underlying early Western Cascade rocks, and the Black Canyon lavas are dated at about 22 m.y. B.P. The contrast in degree of shearing between the Black Canyon lavas and older units implies that deformation occurred during the interval. The development of a 350-m-deep paleocanyon into which the lavas of Black Canyon flowed is another possible indication of significant deformation and uplift prior to extrusion of the Black Canyon flows.

The change from the silicic calc-alkaline rocks of the Oligocene and early Miocene tuffs and lavas to the iron-rich, tholeiitic rocks of the Black Canyon sequence and Hardesty Mountain lavas also suggests a significant change in tectonic environments. It may be that the deformation affecting the older calc-alkaline rocks somehow triggered eruption of the Black Canyon and Hardesty Mountain lavas.

The Black Canyon lavas traveled through a paleocanyon on a course which crossed the Eugene-Denio lineament at approximately right angles, ideal for testing for movement along the lineament. The case for vertical movement is somewhat ambiguous and will be discussed first.

The dip of the Black Canyon lavas is toward the northeast. The bottom contact on the southwest side of the Willamette River is at approximately 1,600 ft (488 m), while on the northeast side it is at 1,200 ft (366 m). The drop of the paleovalley across the river is 400 ft (122 m) in 1.5 mi (2.5 km), which may not be anomalous considering the estimated dip of about 3° to 5° on the sequence both on the northeast and northwest. However, the apparent displacement on the lavas of Lookout Point is also 400 ft (122 m). The displacement on the lavas of Black Canyon cannot be accommodated by the projection of the fault that cuts the Lookout Point lavas, because it would appear in the roadcuts of Highway 58 and in the cliffs of the Black Canyon lavas. However, a swing of the trend of the fault or an intersection with an undiscovered structure may hide the trace of the fault. If there is normal fault displacement, it may be a somewhat diffuse zone. Several shears mapped within the older units strike to the northwest and may be a part of a fault-zone system. Thus, we cannot rule out small displacement on normal faults in the Black Canyon lavas.

Visible faults are rare in the Black Canyon lavas. Two faults, probably related, can be seen in secs. 4 and 5 of T. 21 S., R. 2 E. Oblique slickensides of 15° E. were measured on the N. 80° W. 74° N. fault surface in sec. 5. The direction of movement and displacement are not known. While there may be some lateral offset on this (these) fault(s), the course of the main channel of

the paleocanyon does not seem to be appreciably affected. In view of the width of the paleocanyon and relative positions of the canyonfill on either side of the river, it is safe to say there has been no substantial lateral movement in the map area since extrusion of the Black Canyon lavas 22 m.y. ago. No other visible offsets on the Black Canyon sequence have been found in the map area.

A parallel expression of the Eugene-Denio lineament, the Winberry Creek-Salt Creek lineation, should be mapped to cover the entire extent of the lineament in this area. The Winberry Creek-Salt Creek lineation lies just north of the Lookout Point-Swift Creek segments of the Eugene-Denio lineament described in this volume.

DISCUSSION AND CONCLUSIONS

The Lookout Point area has been volcanically active from the late Oligocene to the Neogene. Both early and late Western Cascade and early and late High Cascade volcanic rocks are present.

The Pleistocene basaltic andesite flow at Armet Creek is of the same geochemical and petrologic type as the High Cascade lavas to the east. The Armet Creek center and other late High Cascade centers in the Western Cascades (e.g., the Battle Ax and Snow Peak centers) are evidence that partial melting processes like those occurring below the High Cascade province are taking place below the Western Cascade province as well, albeit at much reduced volume. The sharply reduced volume of the late High Cascade magmatism in the Western Cascades is reflected in the sharp decline in heat flow. Heat flow of 48 mW/m^2 was measured at Burnt Bridge Creek near the Armet Creek vent, whereas heat flow in the High Cascades to the east is greater than 100 mW/m^2 (Black and others, Chapter 7). If the partial melting is linked to tectonic forces, then tectonic forces affecting the High Cascades (e.g., east-west extension discussed by Priest and others, Chapter 2) may be affecting the Western Cascades. One would expect a decrease of occurrences of High Cascade type of volcanism on either side of the predominant axis. The decrease may approximate the shape of a probability bell curve, with one declining side of the curve reflecting the decrease of occurrences westward from the High Cascade axis.

Substantial strike-slip fault displacement on the Eugene-Denio lineament in the Lookout Point Reservoir area has not occurred within the last 22 m.y. However, there is abundant shearing and alteration in older rock units that indicate an earlier episode of structural deformation. Near-horizontal

slickensides on northwest-trending shears from this earlier episode suggest lateral faulting parallel to the Eugene-Denio lineament. Woller (Chapter 6) shows that there is probably no lateral offset of the High Cascade axis across the Eugene-Denio lineament. He also found no evidence of northwest-trending faults in early or late High Cascade units. Brown and others (1980b) were not able to find evidence of lateral faulting in the Eugene-Denio lineament in the Kitson Ridge area in early or late High Cascade rocks. Although numerous dip-slip faults occur along the lineament in the Basin and Range province, no significant lateral offsets have been documented (e.g., Walker, 1977). This may be partially a function of the fact that most of the Basin and Range rocks exposed within the lineament are younger than 22 m.y. old. Some small northwest-trending dip-slip faults do appear to cut the ~22 m.y. B.P. Black Canyon lavas, but there is no evidence that these faults offset late High Cascade rocks. Also, no offset of late High Cascade units was noted by Brown and others (1980b) in the Kitson Ridge-Oakridge area. These dip-slip faults may or may not offset late Western Cascade and early High Cascade rocks. The field relationships are equivocal on this point in the Lookout Point area, although many north-south- to north-northwest-trending normal faults offset early High Cascade units in areas to the southwest (e.g., Brown and others, 1980b). In any case, most major faults and shears in the Lookout Point area have a dominant trend parallel to the Eugene-Denio lineament. The lineament is thus controlled by faulting, although it is still not clear that the Eugene-Denio lineament is a unique zone of weakness and deformation. The Eugene-Denio zone may be just one well-delineated lineament within a broad zone of northwest faulting. Further detailed mapping in adjacent areas will be necessary to determine the importance and uniqueness of the Eugene-Denio zone of Lawrence (1976).

Evidence presented above suggests that a period of north-south- to northwest-trending dip-slip normal faulting is superimposed on a pre-22-m.y. B.P., more westerly trending lateral fault set which controls the Eugene-Denio lineament. In the Lookout Point area, the dip-slip episode followed earlier established zones of weakness parallel to the Eugene-Denio lineament. The dip-slip faults are younger than 22 m.y. and older than lavas of the late High Cascade episode.

CHAPTER 6. GEOLOGY OF THE SWIFT CREEK AREA,
LANE COUNTY, OREGON
By Neil M. Woller,
Oregon Department of Geology and Mineral Industries

ABSTRACT

The Swift Creek area is located west of Diamond Peak, on the east end of the Eugene-Denio lineament (Lawrence, 1976), within the Western Cascades physiographic province. Lawrence postulated right-lateral movement on the lineament to account for extension in the Basin and Range province on the one hand and the relative stability of the Blue Mountains to the north on the other. He cited as evidence for dextral movement 10- to 20-km displacement of the High Cascade axis, based on an offset in the alignment of the High Cascade stratocones.

Peck and others (1964) mapped a thick sequence of middle Miocene mafic volcanic rocks as younger mafic rocks that typify the High Cascade province to the east. A middle Miocene age places constraints on the location in the Swift Creek area of the High Cascade boundary faults mapped by other researchers north and south of the Swift Creek area. These constraints on the location of the boundary faults imply that the High Cascade axis is probably not offset by lateral faulting. Diamond Peak may be located at the intersection of the Eugene-Denio lineament and the High Cascade boundary.

Faulting was found in the Pinto Creek area splintering into north and north-east trends. Oblique slickensides were noted on one of the fault planes, but it was not possible to determine the amount or direction of displacement. This faulting appears to have occurred during the middle Miocene. Another fault may be located along Pinto Creek, trending generally east-west. It does not cut High Cascade-type lavas.

LOCATION AND PHYSIOGRAPHY

Swift Creek is located in southeastern Lane County and is the major drainage gathering runoff from the west side of Diamond Peak (see Figure 6.1). The area lies southeast of Hills Creek Dam and can be reached via Willamette National

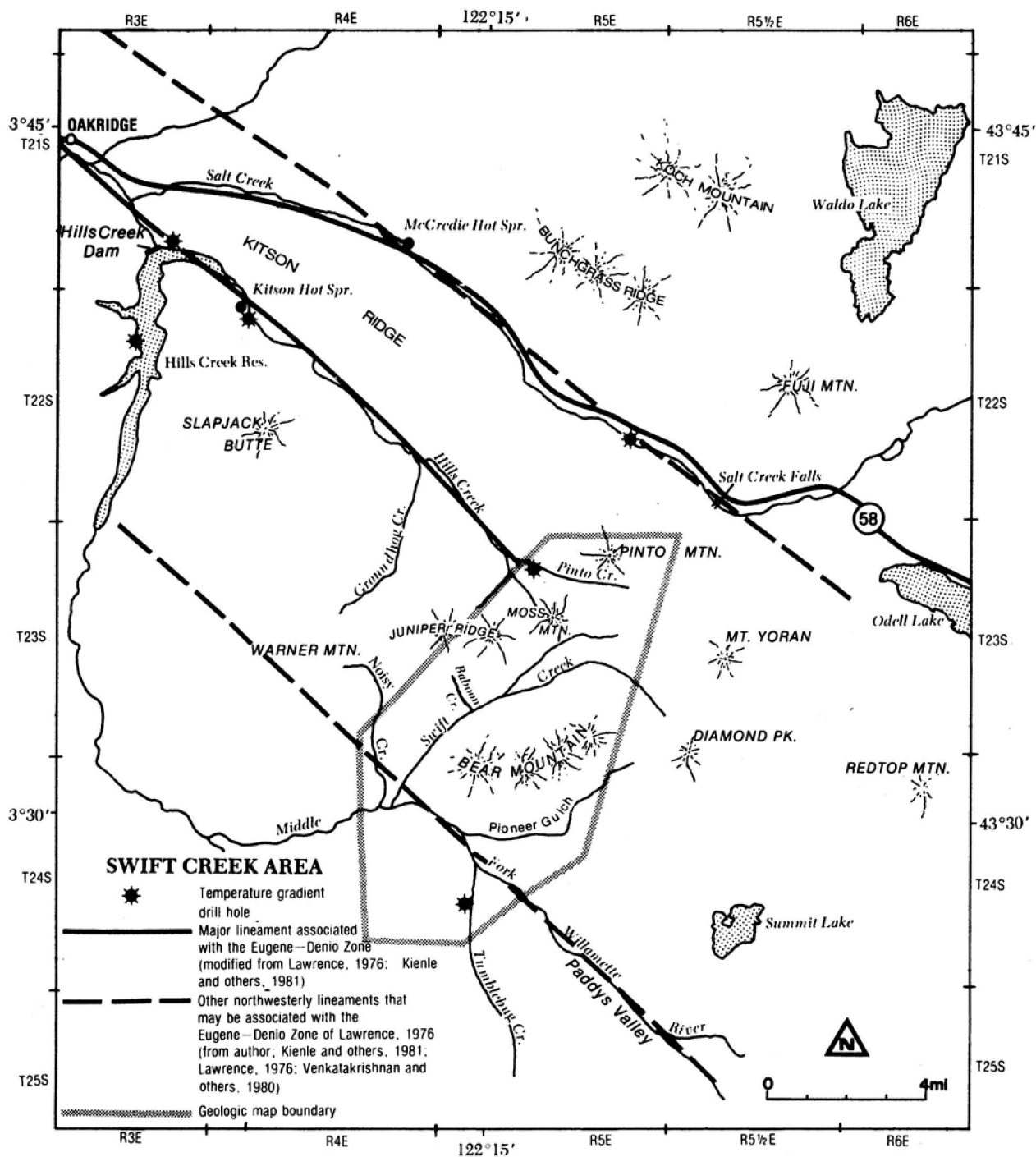


Figure 6.1. Location of the Swift Creek map area, the Eugene-Denio lineament, and other localities mentioned in the text.

Forest road 210 (a trip of 42 km) or forest road 21 (a trip of 67 km).

The map area is characterized by steep, rugged terrain, luxuriant vegetation, numerous creeks and streams, and many glacial features at the higher elevations. The area lies in the Western Cascade geomorphic province and is characterized by youthful topography except for a few areas in-filled with young lava flows from the High Cascade physiographic province to the east.

Swift Creek flows southwest from a low divide that separates it from the Pinto Creek drainage to its confluence with the Middle Fork of the Willamette River. The northwest and northeast lineament fabric of the Cascades, as shown by Venkatakrishnan and others (1980) and Kienle and others (1981), has one of its most prominent intersections at the confluence of Swift Creek and the Willamette River.

EUGENE-DENIO FAULT/FRACTURE ZONE--PREVIOUS WORK

Lawrence (1976) postulated the Eugene-Denio fault/fracture zone as a right-lateral wrench structure and postulated that it, along with the Brothers fault zone farther north, was acting as the northern termination of the Basin and Range physiographic province. He shows it as extending nearly to Eugene along Lookout Point Reservoir and Hills Creek (Lawrence, 1976; Kienle and others, 1981) (see Figure 6.1). Lawrence (1976) cited a 10- to 20-km offset on the axis of the High Cascade province as evidence for dextral movement on the zone. Brown and others (1980b) found no evidence of lateral displacement along the lineament in their reconnaissance mapping of the Known Geothermal Resource Area (KGRA) west of Willamette Pass. Couch (1979) and Connard (1980) reported a right-lateral offset of short-wavelength magnetic anomalies associated with the High Cascades across the lineament, but Couch (1979) and Pitts (1979) show a left-lateral sense on residual gravity anomalies in the same area. Woller and Priest (Chapter 5) showed that at Lookout Point Reservoir no substantial lateral movement occurred in the last 22 m.y., although 400 ft of vertical displacement on a northwest-trending fault may affect early Miocene rocks.

The east end of the Eugene-Denio lineament in the Western Cascades is located near the confluence of Hills Creek and Pinto Creek in the northern part of the map area (Figure 6.1). The lineament loses definition to the east, due to possibly two factors: (1) burial of the topographic expression by younger volcanic rocks, and (2) intersection or interaction with other structures, perhaps reflecting other tectonic forces not on the same trend.

Other lineaments along Salt Creek and Paddys Valley (see Figure 6.1) recognized by Kienle and others (1981) and possibly related to the Eugene-Denio zone of Lawrence (1976) also lose topographic definition to the east where they are buried by young lavas of the High Cascade province.

HIGH CASCADE MARGIN

Taylor (1980) and other researchers propose that the High Cascade province is a graben which is bounded on the west by a series of down-to-the-east, nearly vertical, normal faults.

Mapping by Peck and others (1964) showed High Cascade lava flows extending nearly as far west as Hills Creek Reservoir south of the Eugene-Denio lineament. Mapping and age dating by the author indicate that these lavas are in fact middle Miocene in age and that the High Cascade-Western Cascade boundary lies farther east than previously supposed. The refinement in age of the middle Miocene lavas places the province boundary on an approximate north-south line with mapped locations of the boundary farther to the north (Flaherty, 1981). This study suggests that Diamond Peak must lie on or close to the province boundary. The other major Cenozoic stratocones to the north are centered within the High Cascade province. Thus the position of Diamond Peak does not necessarily imply a dextral structural offset on the axis of the High Cascades along the Eugene-Denio lineament, as postulated by Lawrence (1976).

VOLCANIC STRATIGRAPHY

Introduction

This report uses the informal regional episodes of volcanism nomenclature discussed by Priest and others (Chapter 2, see Figure 2.2) in order to provide a means of comparing this work with that in other areas. Geochemical and petrologic discussions are incorporated into Chapter 2 and will not be repeated here. Chemical data are presented in Appendix B.

The Little Butte Volcanic Series of Peck and others (1964) and Kays (1970) (early Western Cascade sequence of this publication) are exposed a short distance west and north of the map area and are assumed to underlie the area at unknown depth. The section is very thick, probably in excess of 1,500 m, and makes up much of the Western Cascade province. A section approximately 1,500 m thick is very well described by Kays (1970) in an area approximately 30 km southwest of the Swift Creek area. Rocks of the early Western Cascades are silicic ash flows,

Nomenclature used in this report	Unit	K-Ar dates (m.y. B.P.)	Thickness	Lithology
Volcanic rocks of the early High Cascades	Lavas of Tipsoo Butte	Near the top, 9.41 ± 0.42 (R); bottom at Tipsoo Butte, 7.80 ± 0.77 ; bottom at Lookout Ridge, 8.34 ± 0.36	457 m (1,500 ft)	Diktytaxitic olivine-bearing basaltic lavas; light- to medium-gray; fresh.
Volcanic rocks of the late Western Cascades	Tuffs of Tipsoo Butte	----	97-122 m (320-400 ft)	Hornblende-bearing two-pyroxene dacitic nonwelded ash-flow tuff; cream-colored; rhythmically bedded.
	Andesites of Castle Rock	9.31 ± 0.44	----	Pilotaxitic hypersthene andesite; fine-grained; light-gray; may bear xenocrystic quartz; intrusive (plug dome).
	Andesitic intrusives	----	----	Generally plagioclase-porphyritic two-pyroxene andesites.
	Andesites of Walker Creek	Top flow on Lookout Ridge, 11.4 ± 0.5 ; one of the lowest flows on west side, 12.4 ± 2.5 (a)	1,220+ m(?) (4,000 ft)	Plagioclase-rich two-pyroxene andesites; dark-gray to red; interbedded with epiclastic deposits and the tuffs of Rush Creek.
	Basaltic lavas of the East Fork	8.1 ± 2.3 (A)	90 m (300 ft)	Olivine-bearing basaltic lavas; gray to black; very fine-grained; nearly aphyric; interbedded with the andesites of Walker Creek.
	Tuffs of Rush Creek	One of the lowest flows, 13.8 ± 0.8 (a)	274 m (900 ft)	Dacitic welded and nonwelded ash flow; generally bearing hypersthene and plagioclase in the pumice; cream-colored or gray.
	Dacite intrusive of Cougar Dam	16.2 ± 1.8	----	Two-pyroxene dacite; black; glassy with irregular jointing; dike-like on east side of the dam; both dike- and sill-like on west side.
Volcanic rocks of the early Western Cascades	Tuffs of Cougar Reservoir	----	470+ m	Lithic-fragment-rich, pumice-poor tuffs of laharic deposition; also silicic ash flows, lavas, and sediments; generally altered; frequently stained a greenish or reddish color.

R = may be affected by excess radiogenic argon.
A = K-Ar date is affected by slight alteration.
a = K-Ar date may be affected by slight alteration.

Figure 6.2. Stratigraphy of the Swift Creek area.

lavas, and interstratified sediments. The lavas analyzed by the author and reported in other places in this volume are predominantly rhyodacitic to dacitic, though there are many analyzed samples on record from rhyolite to basaltic andesite. The earliest flows in the early Western Cascade sequence are biotite-bearing ash flows that were dated by Smith and others (1980) at 34.9 m.y. B.P.

Volcanic rocks of the late Western Cascades

Within the map area, the rocks of the late Western Cascades include older volcanoclastic sediments and lavas, the basaltic rocks of Tumblebug Creek, and the andesitic lavas of Moss Mountain.

Older volcanoclastic sediments and lavas (Tmo): The oldest units exposed within the map area occur at low elevations on the north side of Pinto Creek. Silicic volcanic lavas, debris flows, and immature sediments crop out in rare roadcut exposures. A questionable attitude of N. 30° W. 35° N. was obtained on epiclastic rocks of the unit.

The lavas of unit Tmo are andesite and dacite with a vitrophyric texture. Plagioclase phenocrysts are surrounded by a dark-brown-red altered matrix. Mafic phenocrysts are usually altered and are sometimes unrecognizable due to smectite. Hypersthene is present in a few flows, usually with corroded cores and/or rims and alteration to smectite. In some of the flows, the groundmass glass contains plagioclase crystallites. Calcite occurs in several flows as cavity and fracture fillings. The silica contents of two analyzed samples are 55.9 percent and 57.8 percent.

Brown, coarse epiclastic rocks with poor sorting and abundant hypersthene crystals are found interbedded with these flows. The clasts in the sediments are aphyric and silicic, up to 1 cm in diameter, and set in a green-brown tight matrix. The colors of these clasts are pastel pinks, tans, and grays, very similar to the lavas and clasts of early Western Cascade rocks elsewhere in the Western Cascades. In thin section these lithic fragments have microphenocrysts of plagioclase and rare hypersthene. Palagonite is present in scattered, small, irregular masses within the matrix.

The alteration of flows of unit Tmo is greater than that of any other mapped unit in the area. The primary jointing in one distinctive, pink, autobrecciated, hypersthene-bearing andesite, containing 50 percent plagioclase phenocrysts 1 mm in diameter, is totally rehealed. The exposure of the unit appears massive yet delicately mottled. In other flows, celadonite lines the vesicles.

These flows were probably erupted early in the late Western Cascade episode.

This episode of volcanism began approximately 18 m.y. B.P. in other areas of the Cascades (see Chapter 2).

Basaltic rocks of Tumblebug Creek (Tmb/Tmbi): The basaltic rocks of Tumblebug Creek are best exposed on the mountainsides west of Tumblebug Creek. They are fresh, gray to black olivine-bearing basalt and basaltic andesite, some with a poorly developed diktytaxitic texture. Wells and Peck (1961) and Peck and others (1964) mistook these lavas for similar but younger lavas of the High Cascades to which they are nearly identical both in hand sample and thin section. The olivine phenocrysts may be fresh or iddingstized, frequently rimmed by clinopyroxene, and usually set in an intergranular groundmass with interstitial orthopyroxene or clinopyroxene and Fe-Ti oxides. In most flows interstitial olivine and clinopyroxene are both present, but in rare flows, olivine is the dominant interstitial groundmass mineral. Augite phenocrysts are often present in smaller percentages than olivine, and in the lower flows rare hypersthene phenocrysts were observed. Volatile-free silica contents vary between 49.40 percent and 56.00 percent and FeO* between 7.35 percent and 8.97 percent for 16 samples (see Appendix B).

A volcanic plug located in the extreme northeast corner of sec. 2, T. 24 S., R. 4 E., was the source of most of the flows. Attitudes on lower Bear Mountain, the lower portions of the Baboon Creek, Noisy Creek, and upper Willamette River drainages have a radial pattern roughly centered on this plug.

There is evidence that the observed dips of the area are initial dips. A radial pattern of dips found around the Tumblebug source indicates the location of the source as well as the flow direction. A similar pattern in the stratigraphically overlying andesitic rocks centered north of Moss Mountain causes the orientation of dips on the south side of that center to dip toward the Tumblebug plug with approximately equal dips to those observed on the north side of the Tumblebug plug, but in the opposite direction. Fine-grained sediments are generally found dipping at very low angles away from their source in both the units. The attitudes obtained on the eutaxitic texture of partially collapsed pumice in minor ash flows in both units likewise indicate little regional tilting.

One of the lowest flows on the slope west of Tumblebug Creek was dated at 14.1 ± 0.8 m.y. B.P. This flow, atypical with respect to the rest of the unit Tmb sequence, is a hypersthene-bearing basaltic andesite with moderate smectitic alteration of the groundmass and relict olivine(?) phenocrysts. Vesicles are lined or filled with smectite. Drill-hole cuttings obtained from the Tumblebug

Creek heat-flow hole revealed 500 ft of almost aphyric basalt below this flow.

The top of the sequence exposed on the slope west of Tumblebug Creek is dated at 15.6 ± 0.6 m.y. B.P. This date is probably of good quality, whereas alteration of the lower flow probably resulted in some loss of radiogenic argon, degrading the quality of that date. This is corroborated by a K-Ar date of 17.0 ± 0.9 m.y. B.P. obtained on the lowest flow exposed on Bear Mountain, stratigraphically low in the section.

A basaltic andesite volcanic center, located at SE $\frac{1}{4}$ NW $\frac{1}{4}$ sec. 25, T. 23 S., R. 4 E. (on Juniper Ridge), began erupting lavas that overlie the flows originating from the Tumblebug Creek source. Basaltic base surge deposits, palagonite tuffs, sediments, and a thin air-fall tuff are found associated with the flows. The lavas are olivine-bearing basaltic andesites with up to 10 percent plagioclase phenocrysts. These lavas appear to be intermediate between the basaltic lavas of Tumblebug Creek and the andesitic lavas of Moss Mountain in that they are less plagioclase- and more olivine-phyric than the Moss Mountain rocks but are more plagioclase-phyric than the Tumblebug lavas. The attitudes of the flows are locally steeply inclined near the source plug, but generally they dip to the north in the upper Baboon Creek area at close to the same attitude as the lavas of the Tumblebug Creek. These lavas originating on Juniper Ridge are grouped with the basaltic lavas of Tumblebug Creek.

A flow from the top of the Baboon Creek sequence was dated at 13.1 ± 0.6 m.y.; at the base of the Baboon Creek section, a basaltic andesite originating from the Tumblebug source was dated at 13.5 ± 1.1 m.y. B.P. The local unconformity is interpreted to be strictly a change in volcanic source area. The two volcanic centers are roughly contemporaneous.

The olivine basalt sequence dips to the northeast approximately 15° in the middle of the map area. It dips below a thick pile of pyroxene andesites to the north.

Andesitic rocks of Moss Mountain (Tma): The andesitic rocks of Moss Mountain are highly plagioclase phyric. Most are porphyritic, dark gray to black, and generally fresh in appearance. The lower flows are porphyritic two-pyroxene andesites; the upper flows are porphyritic olivine-augite basaltic andesites. Plagioclase phenocrysts average 20 percent of the rock, with a range of 10 percent to 45 percent. They onlap the basalts of Tumblebug Creek from a source to the north of Moss Mountain. Silica contents range between 53.84 percent and 57.00 percent for seven samples.

The two-pyroxene andesites are equivalent to the middle to late Miocene andesitic rocks described elsewhere in this volume as the andesites of Walker Creek (Priest and Woller, Chapter 4), Miocene andesitic lavas (Woller and Priest, Chapter 5), the Sardine Formation (Peck and others, 1964), and Miocene volcanic rocks (Brown and others, 1980b). Flows with intergranular texture have interstitial hypersthene and Fe-Ti oxides. Also found are flows with vitrophyric textures, where hypersthene and augite phenocrysts are suspended in brown glass. A few flows with intersertal textures are also present. Hypersthene seems to predominate over augite in the lower part of the section, but the entire sequence of Moss Mountain andesites seems to become more mafic and fresher in appearance as one goes up in the section. Hypersthene varies from euhedral to anhedral and, where altered, suffers from attack by smectite. Where olivine is present, hypersthene is almost always totally altered to smectite.

Olivine-augite basaltic andesites overlie the two-pyroxene andesites. They were not mapped separately because of the gradational and conformable transition between the two types. These basaltic andesites are generally dark gray and very porphyritic. Interstitial hypersthene is commonly found between plagioclase microlites in intergranular textures, but a few flows are vitrophyric. Olivine is frequently fresh, or it may be altered to iddingsite. Some flows have a somewhat sugary appearance, and vesicle margins may be irregular and intruded by plagioclase crystals. However, no true diktytaxitic textures were seen.

The thin-bedded sequence of lavas at Moss Mountain (each flow averaging 3 m thick) is at least six flows thick. Some sediments within the olivine-augite basaltic andesite sequence locally dip toward the south at $29^{\circ} \pm 5^{\circ}$, but the sequence as a whole probably dips about 20° southwards. It is difficult to determine how much of the dip on the sequence is tectonic and how much is from the original depositional slope.

Northwest of Moss Mountain, the sequence dips 10° to 23° to the west. North of Moss Mountain, near Pinto Creek, the volcanic strata are probably affected by tectonic deformation and dip steeply to the northeast. North of Pinto Creek, dips of about 25° to the north are found. A radial pattern of attitudes emerges from a point located somewhere on the north slope of Moss Mountain. Numerous andesitic and basaltic andesite dikes and shears suggest that a volcanic vent area for the olivine-augite basaltic andesites is located on Moss Mountain's north-facing slope. In view of the gradational relationship

of the compositions of the lower part of this sequence with the underlying andesite, it is likely that this was a vent area for some of the andesite as well.

The andesites overlie the older volcanoclastic sediments and lavas (unit Tmo) on the north side of Pinto Creek. The contact is obscured by vegetation and slope wash, but it is probably unconformable. An attitude on the Moss Mountain andesites in this area was N. 65° E. 30° N., while an attitude in the older volcanoclastic sediments was N. 39° W. 35° N. (the latter attitude may be questionable). Here the andesitic sequence is thin due to erosion.

One of the capping flows on Moss Mountain was dated at 17.3 ± 0.8 m.y. B.P. This date does not conform with four younger dates on underlying units already mentioned. If accurate, this date would be among the earliest yet recorded for late Western Cascade volcanism. It is possible that the reversed sense is due to excess radiogenic argon in this sample, resulting from inadequate outgassing during eruption. Although the sample appears fresh, with 90 percent of the plagioclase phenocrysts being fresh, the remaining 10 percent of the plagioclase has very minor minute inclusions of smectite or glass. The sample is liberally studded with fresh euhedral hypersthene and minor olivine phenocrysts. No xenolithic or xenocrystic material was found. The texture is felty intergranular with interstitial orthopyroxene and clinopyroxenes and Fe-Ti oxides. Although there is no textural evidence of significant contamination, it is felt that this date may be too old. Alternatively, the andesite sequence and the Tumblebug sequence may be roughly 17 m.y. old, with the younger ages of the Tumblebug rocks resulting from argon loss.

Volcanic rocks of the early High Cascades

Miocene-Pliocene basaltic lavas (Tpb): The andesites of Moss Mountain are overlain by Miocene-Pliocene basaltic lavas (unit Tpb) of the early High Cascades. The flows are olivine-phyric, light gray, compact to diktytaxitic, and fresh. They cap the highest ridges in the area and are equivalent to the lavas of Tipsoo Butte (Priest and Woller, Chapter 4), Outerson series of Thayer (1939), Outerson formation of White (1980a), Pliocene volcanic rocks of Brown and others (1980a,b) and partially equivalent to the volcanic rocks of the High Cascade Range (Peck and others, 1964). Unlike flows of the same age at Tipsoo Butte, most of these flows are compact rather than diktytaxitic. In thin section, they have felty intergranular textures with interstitial clinopyroxene and Fe-Ti oxides, with or without olivine. Olivine phenocrysts are sometimes iddingsitized. In one sample olivine phenocrysts are heavily rimmed by iddingsite, but groundmass

olivine is unaltered. Clinopyroxene rims olivine in some flows. Two analyzed samples have silica contents of 48.61 percent and 51.68 percent (see Appendix B).

The early High Cascade flows are very similar petrographically and chemically to the middle Miocene Tumblebug basalts. Distinguishing between the two units in the field is often very difficult. A detailed knowledge of attitude, source area, alteration, and structural features, supported by K-Ar dates, is essential. Peck and others (1964) in reconnaissance mapping could not distinguish between the two sequences and grouped them with the late High Cascade lavas as volcanic rocks of the High Cascades.

The contact between the Tumblebug basalts and the Miocene-Pliocene basaltic lavas (unit Tpb) is marked by a topographic break caused by the differing strikes and dips (the Tpb flows have very low dips of 1° to 2°). Shearing is considerably less common in the early High Cascade rocks and nonexistent in the late High Cascade rocks. Freshness is an unreliable indicator of age; many of the Tumblebug flows are as fresh in hand specimen and in thin section as the early High Cascade flows.

The basal early High Cascade basaltic flows were emplaced about 5.5 m.y. ago: two were dated at 5.53 ± 0.41 m.y. B.P. and 5.56 ± 0.34 m.y. B.P., respectively, and a third was dated at 4.32 ± 0.40 m.y. B.P. None of the dated late Western Cascade rocks was more recent than 13.1 m.y. B.P. It is probable that most of the flows filled in topographic lows in the pre-existing terrain. The olivine basalt flow located just west of Hemlock Butte was definitely intracanyon. This flow is also very distinctive for its somewhat high K_2O (1.26 percent) and FeO^* (11.83 percent), low SiO_2 (48.9 percent), and the presence of a distinctive groundmass phyllosilicate. The phyllosilicate is reddish brown in plain light with strong pleochroism to a light orangish-brown and has a "bird's eye" extinction parallel to a single perfect cleavage. The $2V$ is about $2.0^{\circ} \pm 10^{\circ}$. The phyllosilicate may be a vapor-phase biotite or a form of iddingsite after olivine.

On the east side of Swift Creek, the early High Cascade flows seem to have spread out over a broad topographic low. The lower contact there follows contours very closely, and no dip is apparent. It is unlikely deformation has affected initial dips.

Volcanic rocks of the late High Cascades

Pleistocene basaltic rocks (Qb): Late High Cascade volcanism differs from that of the early High Cascades principally by a tendency toward diktytaxitic textures, although nondiktytaxitic textures are also common. All of the

Pleistocene basaltic flows are intracanyon into the other map units in the Swift Creek area. They are usually found in the lowest areas of the present drainage systems. The Pleistocene basalts, when found at higher elevations, are frequently difficult to distinguish from the early High Cascade lavas. The diktytaxitic texture, field relationships, and attitudes allow these flows to be distinguished from the petrographically similar Tumblebug basalts.

Late High Cascade rocks are typically light-gray to black, olivine-phyric basalt and basaltic andesite. The olivine may be fresh or iddingsitized. A clinopyroxene reaction rim is often found on olivine. Felty intergranular textures with interstitial orthopyroxene, clinopyroxene, and/or olivine, as well as Fe-Ti oxides and apatite, are most common. A pilotaxitic flow and an ophitic-diktytaxitic flow were also noted. The flows are neither sheared nor folded. Many of the late High Cascade flows can be traced to the vicinity of Diamond Peak to the east.

Silica percentages in four of five samples analyzed cluster around 53 percent; the fifth is 57.73 percent. Alkali concentrations are moderate (between 3.2 percent and 5.1 percent).

Glacial till and outwash overlie most of the flows, and other flows are glacially scoured or cut. Benchlike areas of glacial till and outwash at lower elevations are generally underlain by late High Cascade flows.

Mazama pumice-fall deposit

The youngest volcanic unit exposed in the Swift Creek area is a thin dacitic air-fall tuff, believed to originate from the 7,500-yr B.P. Mount Mazama eruption. It is not shown on the map because it mantles the landscape and, if shown, would obscure important bedrock relationships. It is unconsolidated, yellow, and appears to be bedded where it is undisturbed. Voids occur between the lapilli- to coarse-ash-sized pumice. No fine ash or block-sized fragments were found.

The chemistry of the pumice is given in Appendix B as field sample P-302 (map sample 89). The water content in the analysis is unreasonably high and casts doubt on the accuracy of the analysis. This may explain the discrepancies between this analysis and other published analyses of Mazama ash. However, the phenocryst assemblage (e.g., the presence of hornblende phenocrysts) and lateral continuity with known Mazama ash deposits support a Mount Mazama source.

STRUCTURE

The andesites of Moss Mountain (upper part of the section) and basalts of

Tumblebug Creek appear very fresh in hand specimen, and their local attitudes reflect primary dips rather than regional deformation. Their fresh aspect in many areas implies they have not been subjected to low-grade regional metamorphism. It does not seem likely these sequences were ever buried to substantial depths.

Lineaments are very prominent on SLAR and ERTS imagery of the area. The northwesterly and northeasterly trends identified by Venkatakrishnan and others (1980) and Kienle and others (1981) are predominant. Northwestern lineaments within the map area are represented by the valley of the Middle Fork of the Willamette River southeast of its confluence with Swift Creek and by the Eugene-Denio zone of Lawrence (1976), Brown and others (1980b), and Kienle and others (1981). Swift Creek forms a cross-cutting northeasterly lineament typical of other northeasterly lineaments in the Cascades. The two trends construct a fabric which appears to support north-south compression with east-west extension (Venkatakrishnan and others, 1980; Kienle and others, 1981).

Faulting along these northwestern and northeastern lineaments is not well substantiated. Peck and others (1964) show normal faulting on the northwesterly trend in the Lookout Point area on the Eugene-Denio zone, also described elsewhere in this volume (Woller and Priest, Chapter 5). Brown and others (1981b) show some normal faulting along the Eugene-Denio lineament and place the Eugene-Denio lineament along Kitson Ridge at the north edge of the map area, while a secondary (?) lineament follows the Hills Creek drainage.

Lawrence (1976) observed that the High Cascade axis, as defined by the position of the major Cascade stratocones, was offset in a right-lateral sense by 10 to 20 km along the Eugene-Denio lineament. Kienle and others (1981) noted the same offset. Misidentification of the middle Miocene basalt and basaltic andesite section as High Cascade basalt by earlier workers (Wells and Peck, 1961; Peck and others, 1964) has apparently led to the misconception that the High Cascade axis lies at Diamond Peak. If Diamond Peak did in fact lie on the axis of the High Cascades, then right-lateral offset across the Eugene-Denio lineament might be a possible explanation. Mapping in the Swift Creek area, however, indicates that Diamond Peak actually lies at the western margin of the High Cascades, at the intersection of the High Cascade margin with the Eugene-Denio lineament. Thus the High Cascade axis is not offset across the Eugene-Denio lineament. It is not known whether rocks older than middle Miocene are laterally offset across the lineament, but it is not likely that younger rocks are.

The geophysics group of Oregon State University noted a left-lateral offset on residual gravity anomalies (Pitts, 1979; Couch, 1979) and a right-lateral offset on aeromagnetic anomalies (Couch, 1979; Connard, 1980a) across the Eugene-Denio lineament in this same area. Older offsets may account for deflections of the geophysical anomalies.

The only major faults mapped within the area are in the vicinity of Pinto Creek. There the most prominent fault zone strikes northeast, cutting lower members of the Moss Mountain andesites. The zone is marked by extreme brecciation, bleaching, silicification, and pyritization. The pyritization and alteration halo is wider than the breccia zone itself. At least two planes of significant displacement, juxtaposing different lavas, were found within the wide, bleached, silica-replaced breccia zone. Both planes were irregular, but attitudes were approximately N. 70° E. 75° S. with a rake of 39° W. and N. 63° W. with a vertical dip.

Faults in the NW¼ sec. 14 and the NW¼ sec. 16 (T. 23 S., R. 5 E.) also juxtapose different andesitic flows and strike toward the same breccia zone, suggesting a complex, splintered pattern. It is believed the zone splinters to the north and northeast, where it is buried by younger middle Miocene flows. One splinter of the zone can be traced north of Pinto Creek in a landslide scar. At the top of the scar, a middle Miocene andesite lies across the fault alteration zone without displacement. The flow is altered, albeit to a lesser degree.

The zone can be traced southwards only a short distance toward a notch immediately west of Hemlock Butte, where it is buried by younger andesitic flows and till. The amount and sense of movement is not clear, but the oblique rake and the extreme brecciation is suggestive of wrenching.

Dips in excess of 50° N. (and possibly as great as 85° N.) in layered units, numerous dikes, and small displacement faults are found just west of the Pinto Creek drill hole, at the eastern end of the Hills Creek (Eugene-Denio) lineament. The older units (older volcanoclastic sediments and lavas), if correctly identified, "sky" out to the south across Pinto Creek; younger units (andesitic lavas of Moss Mountain) crop out on the south side of the creek. These attitudes suggest that an east-west-trending fault with displacement down to the south occurs at Pinto Creek. This possible fault cuts lower members of the Moss Mountain andesites but does not cut High Cascade lavas. Faulting in this area must predate 5.5 m.y. B.P. and may be as old as middle Miocene (17-13 m.y. B.P.).

The great majority of the section exposed on Moss Mountain and Juniper

Ridge is unaffected by deformation or faulting outside of shearing induced by local volcanic activity. Although shears and dikes are common, they frequently have orientations related to local volcanic activity. (These features often strike toward volcanic source areas.) Displacements on shears are small, and oblique slickensides were noted in several places. Several thin ash-flow tuffs were traced for long distances.

DISCUSSION AND CONCLUSIONS

The High Cascade graben (Taylor, 1980) has not been previously located by mapping in the Diamond Peak area. While the area mapped in this report does not cover the probable graben margin, the map extends close enough to it to put important constraints on the possible locations of any western boundary faults that might exist.

Reconnaissance work indicates the presence of late Western Cascade basalt and andesite as far east as the SW $\frac{1}{4}$ sec. 23, T. 24 S., R. 5 E. Late High Cascade lavas from Diamond Peak and surrounding areas overlie the older units east of the late Western Cascade outcrops.

Early High Cascade flows sampled from a ridge (SE $\frac{1}{4}$ sec. 11, T. 23 S., R. 11 E.) that extends eastward to Mount Yoran (at approximately the same longitude as Diamond Peak) were dated at 5.53 m.y. B.P. The High Cascade graben margin, if present, must therefore either underlie Diamond Peak or possibly occur at a possible north-south fault scarp visible on photo coverage between Diamond Peak and Redtop Mountain (located east of Diamond Peak).

Farther north, north-south High Cascade boundary faults can be inferred from aerial photography to lie west of Waldo Lake at the approximate longitude of Fuji Mountain. Still farther north, the boundary faults have been mapped in the Horse Creek drainage (Taylor, 1980; Brown and others, 1980a; Flaherty, 1981). To the south of the Swift Creek area, bounding faults have been mapped along the west side of Diamond Lake (Barnes, 1978) and the west side of the Lake of the Woods (Maynard, 1974). A line connecting these known and mapped segments would show very good linearity on a gross scale. The boundary would have a slight east of north trend, very much as drawn by Allen (1966) (see Figure 2.4 of Priest and others, Chapter 2).

If faults of the Eugene-Denio zone cross the High Cascades, no more than 5 km of right-lateral displacement could be accommodated between the two north-south segments of Diamond Peak-Mount Yoran and Waldo Lake (west side)-Fuji

Mountain. If the boundary were drawn through the visible trace between Diamond Peak and Redtop Mountain, there would be no offset. However, there is no evidence of northwest-trending faults cutting High Cascade rocks. Any offset may be due to pre-existing structural control, crustal weakness, and/or local heat flow controlling the location of emplacement of young lavas. More detailed mapping will be done in the coming field season in the Salt Creek area, a parallel expression of the Eugene-Denio lineament just north of the Swift Creek area.

Northwest-trending faults parallel to the Eugene-Denio and Brothers trends (Lawrence, 1976) cut early High Cascade rocks on the east side of the High Cascade province (Peterson and others, 1976; Kienle and others, 1981), but no researcher has yet documented young northwesterly faults on the west side of the High Cascades or in the central Western Cascades.

GEOHERMAL POTENTIAL

The heat flow for the Pinto Creek drill hole is 101 mW/m^2 (Black and others, Chapter 7). Seven kilometers to the northeast, another heat-flow hole near Salt Creek yields a heat-flow value of 102 mW/m^2 (Blackwell and others, 1978). The Tumblebug drill hole has a heat-flow value of approximately 80 mW/m^2 (Black and others, Chapter 7).

The Swift Creek area lies within the transition zone from low heat flow (approximately 40 mW/m^2) in the Western Cascade and Willamette Valley provinces to higher heat flow (greater than 100 mW/m^2) in the High Cascade province (Black and others, Chapter 7). However, data from the High Cascades are sparse because of technical difficulties involved with drilling young High Cascade lavas and because of the horizontal flow of large volumes of meteoric water which penetrate downward and obscure the postulated regional temperature gradient. The available evidence is that the transition zone is very narrow, normally about 10 km in width, and trends approximately north-south.

Two thermal springs, Kitson and McCredie Hot Springs, lie to the northwest of the Swift Creek area, where some workers have shown the Eugene-Denio lineaments (see Figure 6.1). Many researchers believe the thermal springs of the Western Cascades are fed by deep convective circulation of ground waters originating in the postulated high-heat-flow province of the High Cascades (see Black and others, Chapter 7, for a discussion). The Swift Creek area may have high geothermal energy potential if meteoric water can circulate deeply enough to reach economic temperatures (e.g., temperatures of 200°C).

Faults have been found in the Pinto Creek area. Mineralization of local zones may have decreased or sealed the original permeability that must have existed at one time, as demonstrated by the presence of silica replacement and disseminated pyrite. However, the permeability has not yet been evaluated by drilling in the zone. High heat flow and possible fault-induced permeability make the Pinto Creek area attractive for geothermal exploration.

CHAPTER 7. HEAT FLOW OF THE OREGON CASCADES

By Gerald L. Black,
Oregon Department of Geology and Mineral Industries; and
David D. Blackwell and John L. Steele,
Department of Geological Sciences,
Southern Methodist University, Dallas, Texas

ABSTRACT

Heat-flow data from 170 holes, most of them located in the Willamette Valley, Western Cascade, and High Cascade physiographic provinces, are tabulated. The data indicate that a zone of low heat flow averaging $43 \pm 1 \text{ mW/m}^2$ occupies the Willamette Valley province and most of the Western Cascade province. A zone of higher heat flow averaging $104 \pm 9 \text{ mW/m}^2$ occupies the High Cascade province and extends about 10 km into the Western Cascade province. The transition between the two zones is very narrow, averaging less than 10 km in width throughout most of its length in Oregon. Heat flow in the Willamette Valley and Western Cascade provinces is primarily conductive.

In the High Cascade province, high lateral permeability makes the measurement of meaningful heat-flow values virtually impossible at depths of less than 300 m. A 25-mgal negative gravity anomaly which is superimposed on a regional negative trend occurs at the heat-flow transition zone. Thermal modeling of the heat-flow data and gravity modeling indicate that temperatures as high as 700°C may underlie the High Cascade province and that it is possible that molten rock underlies large portions of the high heat-flow zone. Three conceptual models that may explain the origin of the north-south line of hot springs paralleling the High Cascade-Western Cascade boundary are described. Finally, numerical estimates for the geothermal potential of the Cascade Range of Oregon are made. The estimates are based on the heat-flow data base and thermal modeling.

INTRODUCTION

The Cascade Range in Oregon is separated into two physiographic provinces: the Western Cascades, composed of Oligocene to upper Miocene flows, epiclastic deposits, and pyroclastic rocks; and the High Cascades, composed primarily of Pliocene to Holocene lava flows (Figure 7.1). The High Cascade province lies

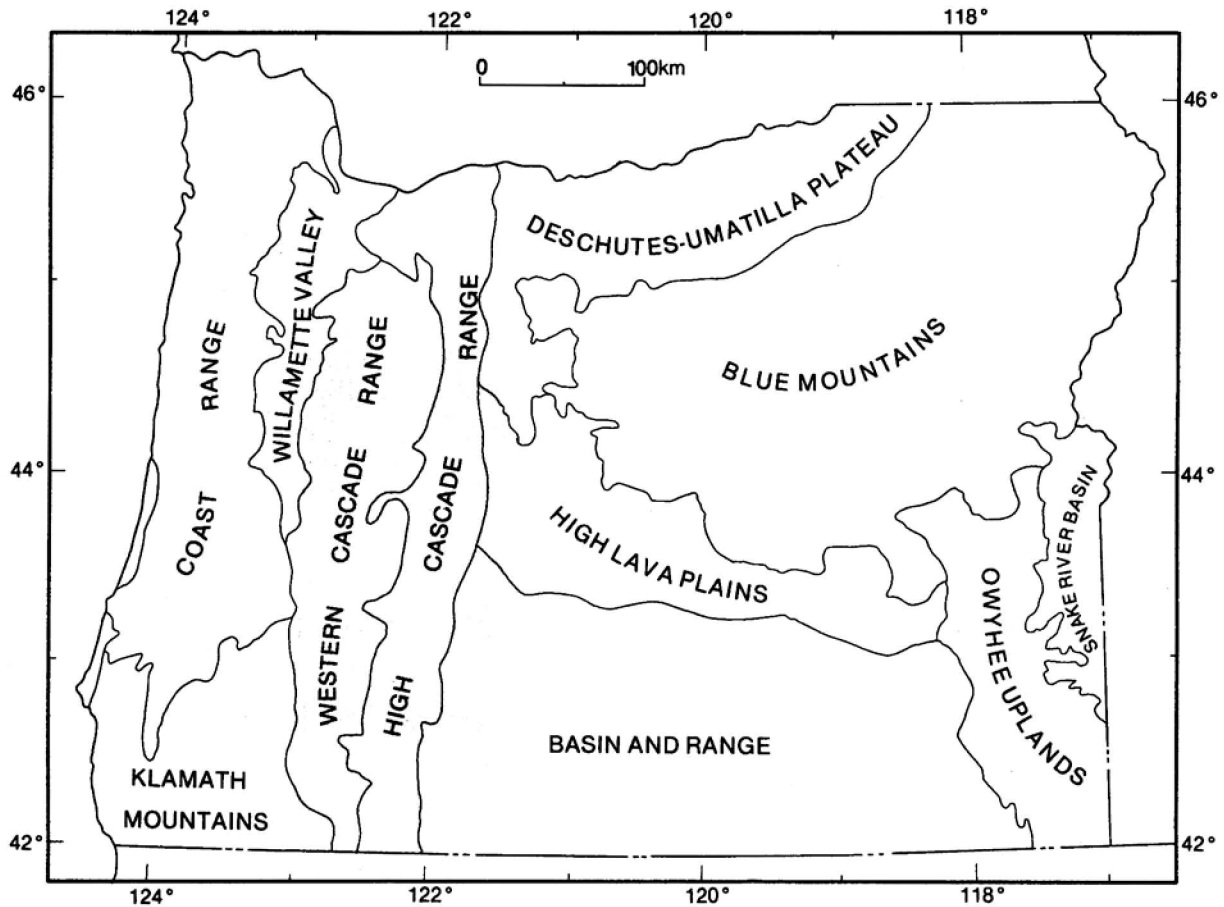


Figure 7.1. Physiographic provinces of Oregon (taken from Dicken, 1950). The rectangle outlines the area discussed in this paper.

east of the Western Cascades and includes the prominent composite volcanic cones which characterize the Cascade Range (e.g., Mount Hood, Mount Jefferson, Three Sisters, and Crater Lake).

In this report only that portion of the Cascade Range south of the Clackamas River (approximately $45^{\circ}05'N$. latitude) will be discussed. The region north of the Clackamas River in the vicinity of the Mount Hood volcano has been discussed in detail by Blackwell and others (1978), Blackwell and Steele (1979), and Steele and others (1981, 1982).

Heat-flow data for 170 holes in the region bounded by longitudes $121^{\circ}30'$ and $123^{\circ}00'$, the California-Oregon border, and latitude $45^{\circ}05'N$. (the rectangle indicated on Figure 7.1) are summarized in Appendix D. Included within the study area are parts of the Basin and Range (BR), High Lava Plain (HL), Deschutes-Umatilla Plateau (DU), High Cascade Range (HC), Western Cascade Range (WC), Willamette Valley (WV), and Klamath Mountain (KM) physiographic provinces (Figure 7.1). Although heat-flow data from the Klamath Falls region are included in Appendix D for completeness, that area will not be discussed in this report.

Listed in Appendix D are the hole location, both by township, range, and section and by latitude and longitude; an abbreviation for the physiographic province in which the hole is found; the hole name and date of logging used for calculation of the temperature gradient; an abbreviation for hole type; collar elevation; hole depth; the depth interval over which the temperature gradient was calculated; the average thermal conductivity; the uncorrected and corrected temperature gradients; corrected heat flow; heat-flow quality; and a brief lithologic summary. Hole locations are given to the nearest quarter-quarter or quarter-quarter-quarter section using a system in which the northeast, northwest, southwest, and southeast quarters are assigned the letters A, B, C, and D, respectively. The hole is first located to the nearest quarter section, then the nearest quarter-quarter section, and finally the nearest quarter-quarter-quarter section (see Appendix C). For example, a hole located in the northeast quarter of the southwest quarter of sec. 2 would be listed in the table as 2Ca. The abbreviations for physiographic province are as given previously except that the abbreviation WH is used for those holes located near the Western Cascade-High Cascade boundary. Hole types include water wells (WW), oil and gas prospects (OW), temperature-gradient holes (TG), damsite-foundation studies (FS), and mineral-exploration holes (ME).

All calculations of thermal conductivity, corrected and uncorrected temperature gradients, and corrected heat flow were performed under the direction of David D. Blackwell at Southern Methodist University. Thermal conductivities were measured on equipment similar to that described by Roy and others (1968). When possible, thermal conductivities were measured on core samples; but inasmuch as cores were only rarely available, conductivities were usually determined from cuttings using the technique of Sass and others (1971).

When cuttings are used to measure thermal conductivity, porosities must be estimated. Typical values vary from 25 to 35 percent for unconsolidated sediments and semiconsolidated sedimentary rocks to 5 to 10 percent for volcanic rocks (Blackwell and others, 1982). Where several cuttings samples were available from a single hole, the results were averaged, and the mean thermal conductivity followed by the standard error in parentheses is listed in Appendix D. Thermal conductivity values from Table 7.1 which are in parentheses are either assumed values based on measurements of typical lithologies in the area or are based on measurements of only one or two cuttings samples from the hole.

For any hole which penetrated basalts of the Columbia River Basalt Group, a thermal conductivity of $1.59 \text{ W/(m}^\circ\text{K)}$ was assumed. Though the scatter is large, this is the mean of many measurements made on these rocks from Oregon and Washington (Blackwell and others, 1982).

The uncorrected temperature gradients result from a least-squares fit to the raw temperature-depth data over the depth interval shown. Standard errors are given in parentheses below the gradient. The corrected temperature gradients have been corrected for the effects of topography using the method of Blackwell and others (1980). Corrected heat flow, in mW/m^2 , is the product of thermal conductivity and the terrain-corrected temperature gradient.

The heat-flow quality is a semiquantitative assessment of the reliability of the heat-flow determination. "A" quality determinations are considered to be ± 5 percent, "B" are ± 10 percent, "C" are ± 25 percent, and "D" values are of uncertain reliability (Blackwell and others, 1982). An "X" indicates that the temperature-depth data are not suitable for heat-flow determinations, usually because of large-scale aquifer effects. Most of the problems in calculating heat flow are due to uncertainties regarding the thermal conductivity (Blackwell and others, 1982), though occasionally problems result from making terrain corrections in areas of unusually complex geometry.

Nearly all of the data in Table 7.1 are either unpublished or have been

Table 7.1 Estimates of the electrical generation potential of the Oregon Cascade Range

Estimate	Reservoir volume (km ³)	Mean reservoir temperature (°C)	Reservoir thermal energy (x10 ¹⁸ Joules)	Electrical energy (MWe for 30 yrs)
1	35,948	190	16,985	401,760
2	33,465	190	15,812	374,000
3	222	190	105	2,485

published only in open-file reports. Sources of published data are Bowen (1975), Hull and others (1976, 1977, 1978), Youngquist (1980), Brown and others (1980a,b), Blackwell and others (1982), and Mase and others (1982).

DATA COLLECTION

The collection of heat-flow data in the Cascade Range of Oregon is an on-going process that began on a large scale in 1976. In that year, an extensive effort was made to locate and log existing holes (mostly domestic water wells) in the Western Cascade and Willamette Valley physiographic provinces (Figure 7.1). The holes were located primarily along the drainages of the Santiam River, McKenzie River, and Middle Fork of the Willamette River. A 16-hole drilling program was also completed in 1976 along the Western Cascade-High Cascade boundary, with most of the holes located near the hot springs (i.e., Austin, Bagby, Breitenbush, Belknap, Foley, and McCredie Hot Springs) that occur in an approximate north-south line along the boundary. Where possible, the holes were drilled to a depth of 152 m (500 ft). In 1977, the emphasis was on the collection of data from existing wells in the High Lava Plain and Deschutes-Umatilla Plateau provinces along the eastern margin of the High Cascades; in 1978, extensive drilling was carried out in the vicinity of Mount Hood. In 1977, some data were also collected from existing wells in the southern Oregon Cascades near Medford and Ashland. In 1979-1980, the emphasis was again on the drilling of temperature-gradient holes. In 1979, six deep holes (up to 600 m) were drilled along the western margin of the High Cascades under the auspices of the Eugene Water and Electric Board (EWEB) to test the geothermal significance of geophysical anomalies (Youngquist, 1980). In 1979-1980, 21 temperature-gradient holes were drilled by the Oregon Department of Geology and Mineral Industries. Most of these holes were again located near the boundary between the High Cascade and Western Cascade physiographic provinces, but three holes were sited on Green Ridge along the east side of the central High Cascades. The objective of the 1979-1980 drilling program was to test, in the northern and central Cascades, the heat-flow model of the Cascade Range that was developed by Blackwell and others (1978) from the data collected in 1976-1977. In 1981, heat-flow data were collected from existing wells in the southern Oregon Cascades in an attempt to increase the data base in that area.

In addition to the above efforts, the U.S. Geological Survey (USGS) recently published a rather extensive data set for the Cascade Range of northern

California. Included in the data set was information on three heat-flow holes drilled in the Klamath Mountain province of southern Oregon (Mase and others, 1982). The data from one of the holes are included in Appendix D.

CASCADE HEAT FLOW

The nature of the regional heat flow in the Cascade Range of Oregon was first discussed by Blackwell and others (1978) and later amplified by Blackwell and others (1982). The single most striking feature of the regional heat flow is a rapid increase from values on the order of 40 mW/m^2 in the Willamette Valley and Western Cascade provinces to values of greater than 100 mW/m^2 in the eastern part of the Western Cascade and the High Cascade provinces (Figure 7.2). The transition from lower to higher heat flow is very abrupt, taking place over a lateral distance of less than 20 km in those portions of the northern and central Cascades for which detailed data are available (Blackwell and others, 1978, 1982).

The transition from average to high heat flow takes place approximately 10 km west of the mean physiographic boundary between the High Cascades and Western Cascades (Blackwell and others, 1982). The geographic boundary is very irregular owing to the fact that the nearly horizontal early High Cascade rocks (lavas between 9 and 4 m.y. B.P., according to Priest and others, Chapter 2) cap ridges formed mostly of Western Cascade rock. Topographic effects thus result in a very complicated boundary. The boundary is also characterized by a nearly north-south line of hot springs which typically occur in Western Cascade rocks or in High Cascade rocks just inside the boundary with the Western Cascades. The origin of the hot springs is of interest with respect to the geothermal potential of the region and is discussed in more detail in a later section.

WESTERN CASCADES-WILLAMETTE VALLEY HEAT FLOW

Heat-flow data from the Western Cascades (west of the transition to higher heat flow) and the adjoining Willamette Valley province are very uniform. The average value for the two provinces is $43 \pm 1 \text{ mW/m}^2$, and the average gradient is $30^\circ \pm 1^\circ \text{ C/km}$ (Blackwell and others, 1982). Typical gradients range from 25° - 35° C/km .

As has been mentioned previously, most of the data from this area were collected from existing water wells located near developments in the drainages

of major streams. Water wells represent a "worst case" situation for the collection of heat-flow data because there is no control over the way in which the well is finished, and intraborehole fluid movements can make the interpretation of temperature-depth curves difficult. However, this lack of control turned out not to be a problem in this region. The heat-flow regime is conductive, and linear temperature-depth relationships are the rule. Pervasive alteration of the Western Cascade volcanic and volcanoclastic rocks to clays and zeolites effectively "seals" the rocks and results in low permeability. Only rarely was there a problem with intraborehole fluid movement, and there was no evidence of regional aquifer effects (Blackwell and others, 1982).

HIGH CASCADE HEAT FLOW

Heat-flow values obtained from shallow drill holes (i.e., less than 300 m) in the High Cascade provinces of Oregon and California (Mase and others, 1982) are typically anomalously low. The effect is regional and apparently results from the high permeability existing at the flow contacts of the young volcanic rocks. The high permeability, coupled with high precipitation in the region, results in the rapid downward percolation and lateral flow of rainfall and snow melt, effectively washing away heat from deeper in the crust. The upper 300 m of the crust is transparent with respect to heat flow, and the effective surface of the earth with respect to heat flow lies at a depth of about 300 m (Blackwell and others, 1982) in this province. This pattern is exemplified by hole T12S/R7E/9Da (Youngquist, 1980) which is isothermal to a depth of 300 m, but which possesses a temperature gradient and heat-flow value below that depth typical of those found in the higher heat-flow portions of the transition zone (see following section).

The above is true only for the youngest rocks in the High Cascades. In the upper Miocene volcanic rocks of the early High Cascades (Priest and others, Chapter 2), alteration has reduced permeability so that in places conductive temperature gradients can be measured in holes 100-150 m deep. A good example is hole T12S/R9E/1Bcd (Appendix D), a 152-m temperature-gradient test drilled in early High Cascade basalt. The temperature-depth curve is linear, indicating conductive heat flow, with an uncorrected gradient of $79.2^{\circ} \pm 1.5^{\circ}$ C/km.

WESTERN CASCADE-HIGH CASCADE BOUNDARY REGION

Those holes in Appendix D which have been assigned a province code of WH are located in or near the boundary between the High Cascades and Western Cascades. As most of the holes were drilled specifically for heat-flow purposes, nearly all of them were collared in the more highly altered rocks of the Western Cascades or early High Cascades, and care was taken to grout the holes in order to prevent intraborehole fluid movement.

Temperature-depth curves from most of the holes in this region are linear, and the heat flow is basically conductive except in the immediate vicinity of some of the hot springs, where geothermal systems are obviously in operation (e.g., holes T6S/R7E/21Cd; T6S/R7E/30Bb; T9S/R7E/20Aa, -20Ac, -2Ad; and T17S/R5E/20Ba). Even in these geothermal areas, holes as close as 1 km to the hot springs frequently showed no anomalous heat flow (e.g., holes near Wall Creek, Terwilliger, and Belknap Hot Springs).

The mean heat flow east of the transition to higher heat flow is 104 ± 9 mW/m², and the mean gradient is $66^\circ \pm 7^\circ$ C/km (Blackwell and others, 1978, 1982). The means were derived from data obtained during the 1976 drilling program, though it should be noted that data from those holes located in obvious geothermal systems were excluded from the calculations. Most of the holes in the 1976 study were located within 1 to 5 km of hot springs (i.e., Austin, Bagby, Breitenbush, Belknap, Foley, and McCredie Hot Springs), so that there was some concern that the data might be prejudiced. We concluded, however, that the very uniform values of terrain-corrected heat flow and temperature gradient indicate that the nearness of the springs has no general effect (Blackwell and others, 1982). The 1979-1980 drilling program was designed to address this potential problem. In general, drill sites were selected that filled in gaps between previous values, were not located near obvious hot springs, were located east of the suspected transition to higher heat flow, and were collared in rock types (i.e., Western Cascade and lower High Cascade rocks) in which heat flow was typically conductive.

The results of the 1979-1980 drilling program (Appendix D; Figure 7.2; Plate 7) confirm, in the central and northern Cascades, the rapid increase in heat-flow values from approximately 40 mW/m² in the Western Cascades to values on the order of 100 mW/m² east of the transition zone. In the south-central Cascades between latitudes $42^\circ 45'$ and $43^\circ 30'$, where there is only one heat-flow point associated with the transition zone, an adequate data base is clearly lacking; in the extreme southern Cascades, there is inadequate information to accurately

constrain the position of the 100-mW/m^2 contour, although the position of the 60-mW/m^2 contour is adequately controlled by a combination of data from domestic water wells and data from the Cascade Range in northern California.

In the southern portion of the Cascades, nearly all of the heat-flow values are based on temperature gradients measured in domestic water wells. For many of these holes, accurate terrain corrections and thermal-conductivity measurements have not yet been completed so that the estimated plotted heat-flow values are subject to large error.

INTERPRETATION OF HEAT-FLOW TRANSITION ZONE

The east-west cross-sections of Figure 7.3 extend from the center of the High Cascade province, through the Western Cascades, and into the Willamette Valley province. Plotted are values for corrected temperature gradient and heat flow. The zero line is the 100-mW/m^2 heat-flow contour (Figure 7.2; Plate 7), which is located about 10 km west of the mean position of the physiographic boundary between the Western and High Cascade provinces (Blackwell and others, 1982).

Also shown (relative to the 100-mW/m^2 contour) are the positions of the hot springs associated with the boundary and the line of young Quaternary volcanoes which make up the youngest part of the High Cascade province. Other versions of Figure 7.3 have appeared in Blackwell and others (1978), Blackwell and Steele (1979), and Blackwell and others (1982). Figure 7.3 has been modified from Blackwell and others (1982) by the addition of heat-flow data obtained during the 1979-1980 DOGAMI drilling program and the 1979 EWEB drilling program (Youngquist, 1980).

For most of the length of the Cascade Range, the data from Figures 7.2 and 7.3 and Plate 7 clearly demonstrate the rapid increase in heat flow from very uniform values on the order of 40 mW/m^2 in the Willamette Valley and Western Cascades to values around 100 mW/m^2 east of the transition zone.

North of the Clackamas River, however, the nature of the transition zone changes. Although the relative position of the transition remains intact, the amplitude of the variation is lower, ranging from about 30 mW/m^2 on the west to 80 mW/m^2 on the east. For this portion of the Cascade Range in Oregon and Washington, heat-flow values in excess of 100 mW/m^2 are found only in "spot", or local, anomalies associated with the young composite volcanoes making up the High Cascade peaks (D.D. Blackwell, personal communication, 1982). The change

in heat-flow pattern at the Clackamas River corresponds to a marked decrease in the volume of basaltic volcanism north of the Clackamas River (Priest, 1982; Priest and others, Chapter 2).

South of the Clackamas River the transition zone is very narrow. It averages about 10 km or less in width in areas where there are adequate data to constrain it, and nowhere is it known to exceed 20 km in width. The uniformity from north to south indicates that crustal conditions beneath the zone are similar throughout the length of the study area (Blackwell and others, 1982).

Heat-flow studies by the USGS have verified the existence of a transition from lower to higher heat flow in the Cascade Range of northern California. There, the position of the 60-mW/m^2 contour has been determined fairly accurately, but the presence of a heat-flow high with a magnitude on the order of 100 mW/m^2 has not been verified, probably due to the masking effects of hydrothermal circulation in the porous young volcanic rocks of the High Cascades (Mase and others, 1982).

A temperature profile is also shown in Figure 7.3. It is based on the heat-flow profile and was obtained by the method of continuation of heat-flow data described by Brott and others (1981). Constant thermal conductivity and steady-state conditions were assumed in the construction of the model (Blackwell and others, 1982). The first assumption is reasonable for the mafic rocks found in the Cascades, whereas the second, though not completely valid, leads to results that do not differ significantly from those obtained using transient models for the depth range shown (Blackwell and others, 1982). The assumptions involved in the construction of Figure 7.3 are discussed in more detail by Blackwell and others (1982).

The temperature profile of Figure 7.3 implies high temperatures at shallow depths east of the 100-mW/m^2 contour (approximately 10 km west of the physiographic boundary). Inasmuch as any one of the isotherms can satisfy the heat-flow anomaly, the temperature does not necessarily have to reach 700°C . The profile does, however, indicate the presence of an intense heat source at relatively shallow levels in the crust (Blackwell and others, 1982).

Further support for the thermal model comes from depth to Curie-point isotherm calculations of Connard (1980) and McLain (1981). Using a Curie-point temperature of 580°C , Connard (1980) calculated a depth to the Curie-point isotherm of 6 to 9 km below sea level beneath much of central Cascades between latitudes $43^\circ00'$ and $44^\circ00'$. McLain (1981), working in the southern Cascades

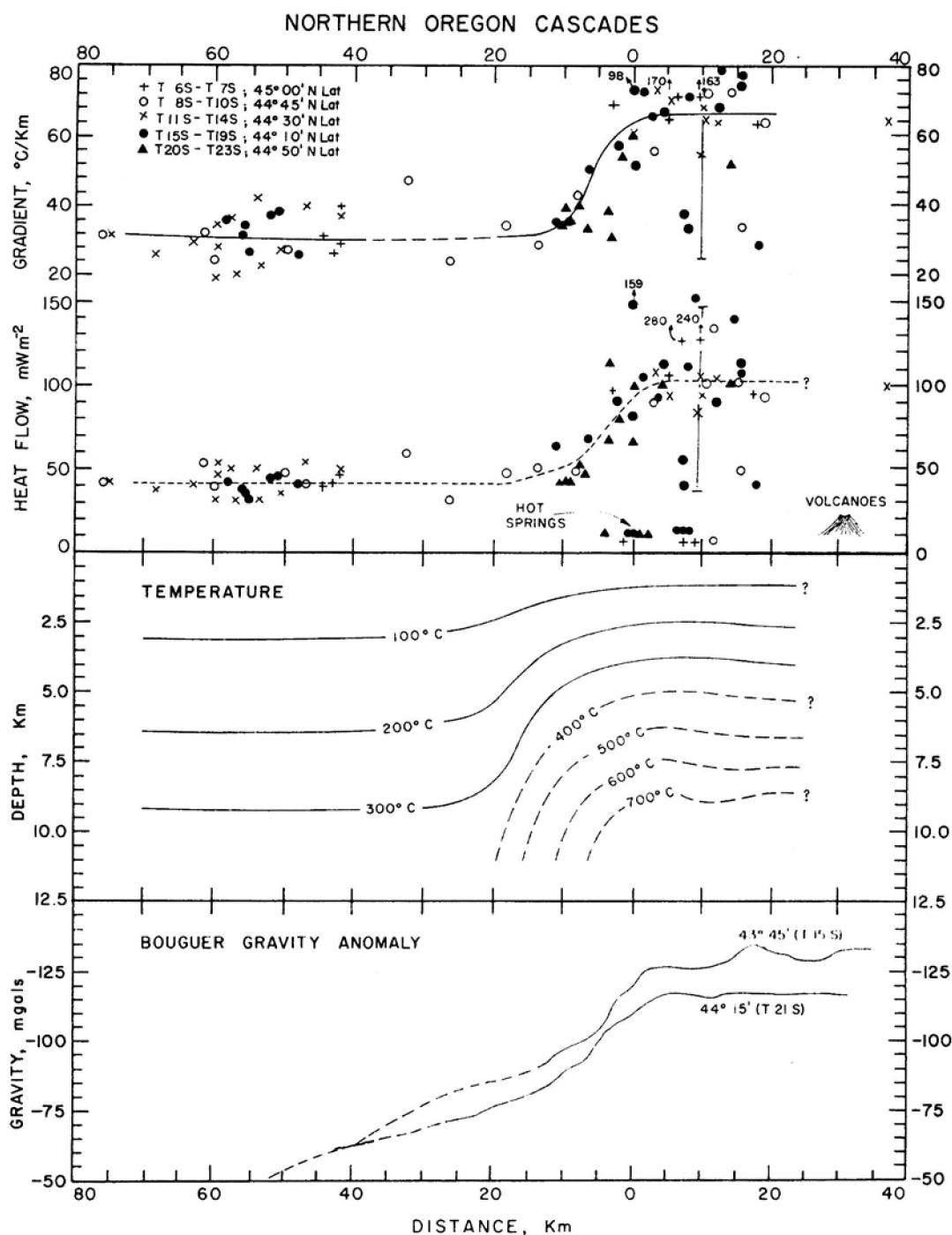


Figure 7.3. Geothermal gradient, heat flow, interpreted crustal temperatures, and regional Bouguer gravity for the western part of the northern Oregon Cascade Range (gravity data are from Couch and Baker, 1977). Heat-flow data between latitudes 43°15'N. and 45°05'N. are projected onto the profile. The zero distance reference is the 100-mW heat-flow contour line (see Plate 7) (modified from Blackwell and others, 1982).

and using the same Curie-point temperature, calculated a depth to the Curie-point isotherm of 4 to 6 km below sea level in the Klamath Falls-Mount McLoughlin area and 5 to 7 km below sea level in the vicinity of Crater Lake. In the intervening areas of the southern Cascades, the depth to the Curie-point isotherm was 6 to 14 km below sea level.

Also shown on Figure 7.3 are two Bouguer gravity profiles which were constructed from the data of Couch and Baker (1977) and Berg and Thiruvathukal (1967). A negative gravity anomaly of 25 mgal is superimposed on background values which decrease eastward toward the crest of the High Cascades.

The 25-mgal anomaly is regional in extent and occurs at the heat-flow transition zone. Blackwell and others (1982) offer four possible explanations for its occurrence: (1) the change in gravity is associated with the same phenomenon which causes the change in heat flow; (2) the gravity gradient corresponds to a western boundary of the proposed High Cascade graben (Allen, 1966) and the presence to the east of low-density volcanic rocks; (3) the anomaly is fortuitously coincidental with the heat-flow boundary, and it reflects a change in the density structure of the crust; and (4) a local negative anomaly is superimposed on the regional trend (Couch, 1979).

Blackwell and others (1982) examined several density models to investigate the above possibilities. They concluded that thermal expansion alone could not account for the gravity anomaly and that the presence of molten material or a change of rock type at depth is required to explain it. Although realizing that large-scale intrusives or normal faulting could generate density differences at levels shallow enough to generate the observed profiles, they preferred a model requiring the presence of molten material at depth because of the close correspondence between the gravity and heat-flow anomalies, and they interpreted the gravity data to indicate the presence of a large zone of partially molten material residing in the upper part of the crust beneath the High Cascades and extending about 10 km west of the High Cascade-Western Cascade boundary.

Although the above hypothesis would explain the coincidence of the gravity and heat-flow anomalies, several geologic questions concerning the model remain to be answered. The molten material must be either mantle-derived magma or partially melted upper crustal material. Most of the volume of late High Cascade volcanism is of basaltic to basaltic andesite composition (Priest and others, Chapter 2), which does not usually form large intrusive bodies. If the molten

material is composed of partially melted early and/or late Western Cascade-type rocks, it should be silicic in composition. Lavas of silicic composition have not reached the surface in the High Cascade province in large quantities. It also seems likely that if molten material underlies the High Cascades at relatively shallow depths, recent volcanic eruptions should be more frequent than they have been in the recent geologic past. The answers to these questions and the ultimate validity of the partial melting model must await the completion of deep drilling in the High Cascade province.

ORIGIN OF HOT SPRINGS

A line of hot springs, which appears to be associated with the heat-flow transition zone, parallels the Western Cascade-High Cascade physiographic boundary. Figure 7.4, taken from Blackwell and others (1982), shows several conceptual models which could explain the existence of the springs. Also included are heat-flow profiles which would result from each of the models. The first (curve 1, Figure 7.4) shows the regional background conductive heat flow. The regional heat flow is assumed to be due to a crustal source underlying the entire High Cascade Range. The other three models (curves 2, 3, and 4) include convective heat transfer. The heat-flow curves for these models show the convective heat flow from the hot springs superimposed on the regional conductive anomaly. In all cases the hot springs result from the deep circulation of meteoric water, assumed to be from east to west, driven primarily by elevation differences between the High Cascades and the stream valleys in which the hot springs issue (Blackwell and others, 1982).

The models differ in the location of the source providing the heat and/or the circulation path of the fluid. In model 2, the water circulates to a depth greater than 2 km and comes up directly beneath the hot springs; in model 3 the water circulates essentially vertically downward beneath the volcano, then rises rapidly to relatively shallow depths and flows laterally along permeable horizons to emerge at the hot springs. In both of these models, the heat source underlies the central portion of the High Cascades. In model 4, the heat source responsible for the hot springs is confined to a narrow band along the physiographic boundary. It could be a shallow heat source offset from the axis of the High Cascades, or alternatively the hot springs could be localized by fractures in intrusives buried beneath the physiographic boundary or by proposed graben-bounding normal faults.

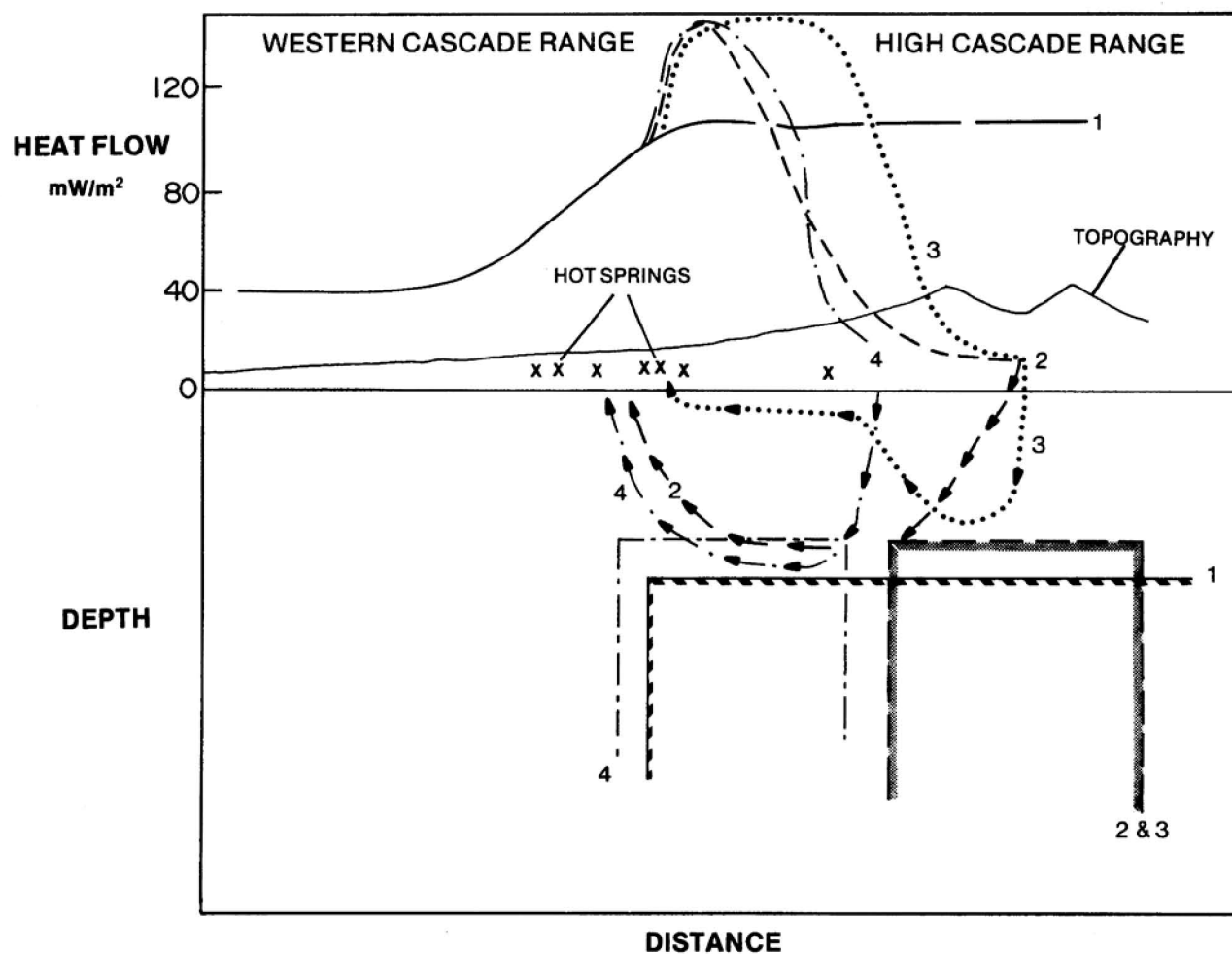


Figure 7.4. Several models of the relationship of hot springs to the heat-flow transition observed at the Western Cascade Range-High Cascade Range boundary. Four curves are shown, with three different variations in fluid circulation. In curve 1, the observed conductive anomaly (see Figure 7.3) is shown. In the other three models, the hot-spring anomalies are interpreted in terms of various controls on water circulation (see text) (from Blackwell and others, 1982).

It is obvious that at least some of the hot springs are controlled by normal faults. In the central Cascades near Belknap Hot Springs, Brown and others (1980a) mapped north-northeast-trending normal faults which clearly control the location of that hot spring and another smaller spring (Bigelow Hot Spring) to the north.

In the model favored by Blackwell and others (1982), the entire region of the Cascades east of the transition zone has a background heat flow on the order of 100 mW/m^2 resulting from a zone of partially molten material lying at a depth of approximately 10 km. Magmatic temperatures at shallower depths probably occur only directly beneath active Quaternary volcanoes. The hot springs and heat-flow values much above or below 100 mW/m^2 are related to ground-water convection. In spite of the difficulties discussed previously in obtaining heat-flow data in the High Cascades, three holes (T18S/R8E/16Dd, T12S/R7E/9Da, and T12S/R9E/1Bcd) tend to support this concept of a regional heat-flow province with a magnitude on the order of 100 mW/m^2 .

GEOHERMAL POTENTIAL OF THE CASCADES

The data set for the Cascade Range of Oregon clearly represents a subduction-zone heat-flow pattern (Blackwell and others, 1982). The linear band of uniform low heat flow, separated by a narrow transition zone from a zone much higher heat flow, is characteristic. The low-heat-flow zone is caused by the subducting slab, which acts as a heat sink until it reaches depths of 100 to 150 km, while the high-heat-flow zone is due to magmatic processes which generate the volcanic arc. A detailed discussion of the plate-tectonic implications inherent in the Oregon data set can be found in Blackwell and others (1982).

Based on the data contained in this report and on the above considerations, it is obvious that the geothermal potential in the Western Cascades west of the transition zone (and other provinces of Oregon farther west) is limited. Typical gradients are only 25° to 35° C/km (Blackwell and others, 1978), so that temperatures above 50° C , the minimum temperature for the direct use of geothermal waters in space-heating applications, will not occur shallower than 1 km. The low gradients do not rule out, of course, the use of lower temperature fluids (down to 10° C) in agricultural, aquacultural, and heat-pump applications. A further hindrance to geothermal exploitation in the Western Cascades is the relative impermeability of the rocks, which may make the utilization of the resource impractical.

The prospects for the exploitation of geothermal energy in the High Cascades

are considerably more promising. It has been shown that the heat-flow transition zone is due to regional crustal effects rather than local upper crustal effects, and temperature modeling (Figure 7.3) has indicated the possibility of a zone of partial melting at a depth of 10 km (Blackwell and others, 1978, 1982). The regional temperature gradient east of the transition zone is 66°C/km (Figure 7.3), so that the circulation of ground water to depths of 5 km could produce temperatures on the order of 300°C .

Inasmuch as volcanic arcs represent major geothermal provinces and are already the sites of power-generating facilities at other places in the world, it seems likely that the Oregon Cascades possess significant potential for the generation of electricity from geothermal fluids. One of the problems with this analogy is the absence of evidence for large high-temperature hydrothermal systems in the High Cascades. The comparative lack of surface manifestations, as has been mentioned previously, is probably due to the masking effect of cold ground-water flow in permeable young volcanic rocks. Another possibility is that there is insufficient heat stored in the shallow parts of the volcanic carapaces of the large composite volcanoes to significantly heat up the ground-water (Blackwell and others, 1982). Whatever the reason, the lack of surface manifestations does not necessarily imply the nonexistence of geothermal resources. In the Western Cascades, where thermal conditions greater than 6 m.y. ago were probably similar to those of the High Cascades of today (Blackwell and others, 1982), there is ample evidence of hydrothermal circulation in the form of exposed plutons and surrounding large areas of altered country rock (Peck and others, 1964). Using oxygen isotope data, Taylor (1971) found evidence for extensive interaction of shallow magma chambers with ground-water systems. This evidence in an extinct volcanic arc so clearly related to the present-day active volcanic arc suggests the presence of similar systems beneath the High Cascades.

Further evidence for the existence of high-temperature geothermal systems beneath the High Cascades comes from deep drill holes at three different localities. In the Meager Creek Geothermal Area, located on the extension of the Cascade Range in British Columbia, Canada, drill hole M7 encountered a bottom-hole temperature of 202.2°C at a depth of 367 m. The temperature gradient at the bottom of the hole was 330°C/km (Fairbank and others, 1981). At Newberry volcano, located in the central portion of the Oregon Cascades, a 930-m hole completed by the USGS in 1981 encountered a bottom-hole temperature of 265°C (Sammel, 1981). Finally, at Mount Lassen, in the Cascade Range of northern

California, drill hole Walker "0" No. 1 encountered a temperature of 176° C at a depth of 610 m. In this last hole, there was a reversal in the temperature-depth curve below 731 m, and the bottom-hole temperature was 124° C at a depth of 1,222 m (Beall, 1981). These three holes clearly demonstrate the presence of temperatures adequate for the generation of electrical energy beneath the High Cascades at major volcanic centers. The demonstration of high temperatures beneath the Cascade chain as a whole must await the completion of a deep (2 to 3 km) drill hole in the High Cascade province between the major volcanic vents.

The data in Table 7.1 represent an attempt to estimate the geothermal electrical-generation potential of the Cascade Range using the methods of Brook and others (1979). In performing the calculations, two assumptions are made concerning the recoverability of electrical energy from geothermal resources. First, a minimum temperature of 150° C is required for the generation of electricity from geothermal fluids; and second, the maximum depth from which geothermal fluids can be recovered is 3 km. The first assumption is conservative, as it ignores generation schemes (e.g., binary cycles) which can generate electricity from fluids at temperatures substantially less than 150° C. It is used to simplify the comparison of estimates between this report and USGS Circular 790 (Brook and others, 1979), which uses the same assumption. The second assumption is more valid, as 3 km represents the maximum depth of production wells drilled in various geothermal areas around the world (Brook and others, 1979).

In order to estimate the electrical-generation potential of the Cascade Range in Oregon, estimates must be obtained for mean reservoir temperature and reservoir volume. Temperature estimates can be derived from the temperature profile of Figure 7.3, the derivation of which was discussed previously. The depth to the 150°-C isotherm is 1.75 km, and the temperature at 3 km is estimated to be 230° C, yielding a mean reservoir temperature of 190° C and a reservoir thickness of 1.25 km.

Estimate 1 (Table 7.1) assumes that the entire area of the Cascade Range bounded by the California-Oregon border, longitude 121°30', the 100-mW/m² contour (Plate 7), and the Clackamas River lineament is underlain by a reservoir 1.25 km thick. Included within this estimate are some areas which are definitely not available for geothermal development (e.g., Crater Lake National Park, Warm Springs Indian Reservation, and the various wilderness areas). In estimate 2 (Table 7.1) these areas have been excluded from the calculations.

Inherent in the calculations of Table 7.1 is the assumption that, due to

nonideal reservoir behavior, only 25 percent of the reservoir thermal energy is recoverable at the wellhead. Limited experience in the vicinity of Mount Hood indicates that this estimate may be high. Drill hole Old Maid Flat 7A (T.D. 6,028 ft) produced a total of less than 4 lpm from the thermal zone in the bottom 915 m of the well (Priest and others, 1982). Though Old Maid Flat 7A bottomed in Western Cascade rocks, which are known from experience to be relatively impermeable, similar conditions may exist at depth beneath the High Cascades due to the alteration of volcanic rocks. To account for this possibility, estimate 3 (Table 7.1) was prepared. In this estimate, permeability was assumed to be present only as fracture permeability in a 100-m (0.1-km)-wide zone associated with north-south lineations. The total length of north-south lineations in the Cascade Range was derived from maps by Venkatakrishnan and others (1980) and Kienle and others (1981). The 100-m width is an arbitrary value based on observations of north-trending faults in the Belknap Hot Springs and Cougar Reservoir (G. Priest, personal communication, 1982) areas of the central Cascades, and north-south lineations were used because they were judged to have the highest probability of remaining open in the state of essentially north-south compression that exists in the Cascades at the present time (Venkatakrishnan and others, 1980).

Estimate 3 was prepared as a sort of worst-case estimate for the theoretical potential of the Cascades. A stratigraphic reservoir (again 1.25 km in thickness) covering an area of only 178 km² would produce the same amount of theoretical potential that the fault model does. By comparison, the total power capacity of The Geysers is rated at 1,610 MW over an area of 60-120 km² (Brook and others, 1979).

The estimates of Table 7.1 are based solely upon the conductive heat-flow anomaly underlying the Cascade Range east of the transition zone. Estimates for known (e.g., Austin and Breitenbush Hot Springs) or undiscovered hydrothermal systems masked by cool ground water are not included, nor are estimates of residual heat remaining in igneous related systems (Smith and Shaw, 1979).

As can be seen in estimate 1 of Table 7.1, there is a tremendous amount of thermal energy contained in the rocks east of the transition zone. The high heat flow, coupled with high background temperature gradients and the evidence for recent volcanism, provides strong inducement for continued exploration in the Cascade Range of Oregon.

REFERENCES CITED

- Allen, J.E., 1966, The Cascade Range volcano-tectonic depression of Oregon, in Lunar Geological Field Conference, Bend, Oregon, August 1965, transactions: Oregon Department of Geology and Mineral Industries in cooperation with Oregon Division of Planning and Development, p. 21-23.
- Anderson, J.L., 1978, The stratigraphy and structure of the Columbia River Basalt in the Clackamas River drainage: Portland, Oreg., Portland State University master's thesis, 136 p.
- Armentrout, J.M., 1981, Correlation and ages of Cenozoic chronostratigraphic units in Oregon and Washington, in Armentrout, J.M., ed., Pacific Northwest Cenozoic biostratigraphy: Boulder, Colo., Geological Society of America Special Paper 184, p. 137-148.
- Armstrong, R.L., Taylor, E.M., Hales, P.O. and Parker, D.J., 1975, K-Ar dates for volcanic rocks, central Cascade Range of Oregon: Isochron/West, no. 13, p. 5-10.
- Atwater, T., 1970, Implications of plate tectonics for the Cenozoic tectonic evolution of western North America: Geological Society of American Bulletin, v. 81, no. 12, p. 3513-3535.
- Atwater, T., and Molnar, P., 1973, Relative motion of the Pacific and North American plates deduced from sea-floor spreading the Atlantic, Indian, and South Pacific Ocean, in Kavach, R.L., and Nur, A., eds., Conference on Tectonic Problems of the San Andreas Fault System, Proceedings: Stanford, Calif., Stanford University Publications, Geological Sciences, v. 13, p. 136-148.
- Avramenko, W., 1981, Volcanism and structure in the vicinity of Echo Mountain, central Oregon Cascade Range: Eugene, Oreg., University of Oregon master's thesis, 156 p.
- Baldwin, E.M., 1981, Geology of Oregon (3rd ed.): Dubuque, Iowa, Kendall/Hunt, 170 p.
- Barnes, C.G., 1978, The geology of the Mount Bailey area, Oregon: Eugene, Oreg., University of Oregon master's thesis, 123 p.
- Beall, J.J., 1981, A hydrologic model based on deep test data from the Walker "O" No. 1 well, Terminal Geyser, California: Geothermal Resources Council Transactions, v. 5, p. 153-156.
- Beeson, M.H., and Moran, M.R., 1979, Stratigraphy and structure of the Columbia River Basalt Group in the Cascade Range, Oregon, in Hull, D.A., investigator, and Riccio, J.F., ed., 1979, Geothermal resource assessment of Mount Hood: Oregon Department of Geology and Mineral Industries Open-File Report 0-79-8, p. 5-77.
- Beeson, M.H., Moran, M.R., Anderson, J.L., and Vogt, B.F., 1982, The relationship of the Columbia River Basalt Group to the geothermal potential of the Mount Hood area, Oregon, in Priest, G.R., and Vogt, B.F., eds., Geology and geothermal resources of the Mount Hood area, Oregon: Oregon Department of Geology and Mineral Industries Special Paper 14, p. 43-46.
- in preparation, Stratigraphy and structure of the Columbia River Basalt Group in the Cascade Range, Oregon.

- Berg, J.W., and Thiruvathukal, J.V., 1967, Complete Bouguer gravity anomaly map of Oregon, in Oregon Department of Geology and Mineral Industries, Gravity maps of Oregon (onshore and offshore): Oregon Department of Geology and Mineral Industries Geological Map Series GMS-4b.
- Black, G.L., 1982, An estimate of the geothermal potential of Newberry volcano, Oregon: Oregon Department of Geology and Mineral Industries, Oregon Geology, v. 44, no. 4, p. 44-46, and no. 5, p. 57.
- Blackwell, D.D., Bowen, R.G., Hull, D.A., Riccio, J.F., and Steele, J.L., 1982, Heat flow, arc volcanism, and subduction in northern Oregon: Journal of Geophysical Research [in press].
- Blackwell, D.D., Hull, D.A., Bowen, R.G., and Steele, J.L., 1978, Heat flow of Oregon: Oregon Department of Geology and Mineral Industries Special Paper 4, 42 p.
- Blackwell, D.D., and Steele, J.L., 1979, Heat flow modeling of the Mount Hood volcano, Oregon, in Hull, D.A., investigator, and Riccio, J.F., ed., Geothermal resource assessment of Mount Hood: Oregon Department of Geology and Mineral Industries Open-File Report O-79-8, p. 190-264.
- Blackwell, D.D., Steele, J.L., and Brott, C.A., 1980, The terrain effect on terrestrial heat flow: Journal of Geophysical Research, v. 85, no. B9, p. 4757-4772.
- Bowen, R.G., 1975, Geothermal gradient data: Oregon Department of Geology and Mineral Industries Open-File Report O-75-3, 114 p.
- Bowen, R.G., Peterson, N.V., and Riccio, J.F., 1978, Low- to intermediate-temperature thermal springs and wells in Oregon: Oregon Department of Geology and Mineral Industries Geological Map Series GMS-10, scale 1:1,000,000.
- Brook, C.A., Mariner, R.H., Mabey, D.R., Swanson, J.R., Guffanti, M., and Muffler, L.J.P., 1979, Hydrothermal convection systems with reservoir temperatures $> 90^{\circ}$ C, in Muffler, L.J.P., ed., Assessment of geothermal resources of the United States—1978: U.S. Geological Survey Circular 790, p. 18-85.
- Brott, C.A., Blackwell, D.D., and Morgan, P., 1981, Continuation of heat flow data: A method to construct isotherms in geothermal areas: Geophysics, v. 46, no. 12, p. 1732-1744.
- Brown, D.E., McLean, G.D., Priest, G.R., Woller, N.M., and Black, G.L., 1980a, Preliminary geology and geothermal resource potential of the Belknap-Foley area, Oregon: Oregon Department of Geology and Mineral Industries Open-File Report O-80-2, 58 p.
- Brown, D.E., McLean, G.D., Woller, N.M., and Black, G.L., 1980b, Preliminary geology and geothermal resource potential of the Willamette Pass area, Oregon: Oregon Department of Geology and Mineral Industries Open-File Report O-80-3, 65 p.
- Bunker, R.C., Farooqui, S.M., and Thoms, R.E., 1982, K-Ar dates for volcanic rocks associated with Neogene sedimentary deposits in north-central and northeastern Oregon: Isochron/West, no. 33, p. 21-22.
- Callaghan, E., 1933, Some features of the volcanic sequence in the Cascade Range in Oregon: American Geophysical Union 14th Annual Meeting, Transactions, p. 243-249.
- Callaghan, E., and Buddington, A.F., 1938, Metalliferous mineral deposits of the Cascade Range in Oregon: U.S. Geological Survey Bulletin 893, 141 p.
- Carmichael, I.S.E., Turner, F.J., and Verhoogen, J., 1974, Igneous petrology: New York, New York, McGraw-Hill, 739 p.

- Chaney, R.W., 1938, Ancient forests of Oregon: A study of earth history in western America: Carnegie Institution of Washington Publication 501, p. 631-648.
- 1956, The ancient forests of Oregon: Eugene, Oreg., Oregon System of Higher Education, Condon Lectures [reprint of 1948 edition], 56 p.
- Chayes, F., 1965, Statistical petrography: Carnegie Institution of Washington Year Book 64, p. 153-165.
- 1966, Alkaline and subalkaline basalts: American Journal of Science, v. 264, no. 2, p. 128-145.
- Christiansen, R.L., and Lipman, P.W., 1972, Cenozoic volcanism and plate-tectonic evolution of the Western United States. II Late Cenozoic: Royal Society of London Philosophical Transactions, Series A, v. 271, no. 123, p. 249-284.
- Clayton, C.M., 1976, Geology of the Breitenbush Hot Springs area, Cascade Range, Oregon: Portland, Oreg., Portland State University master's thesis, 79 p.
- Connard, G.G., 1980, Analysis of aeromagnetic measurements from the central Oregon Cascades: Corvallis, Oreg., Oregon State University master's thesis, 101 p.
- Couch, R.W., 1979, Geophysical investigations of the Cascade Range in central Oregon: U.S. Geological Survey Extramural Geothermal Research Program, Final Report, 95 p.
- Couch, R.W., and Baker, B., 1977, Geophysical investigations of the Cascade Range in central Oregon: U.S. Geological Survey Extramural Geothermal Research Program, Technical Report no. 2, 55 p.
- Couch, R.W., Gemperle, M., and Connard, G.G., 1978, Total field aeromagnetic anomaly map, Cascade Mountain Range, central Oregon: Oregon Department of Geology and Mineral Industries Geological Map Series GMS-9, scale 1:125,000.
- Couch, R.W., Gemperle, M., McLain, W.H., and Connard, G.G., 1981a, Total field aeromagnetic anomaly map, Cascade Mountain Range, southern Oregon: Oregon Department of Geology and Mineral Industries Geological Map Series GMS-17, scale 1:250,000.
- Couch, R.W., and Lowell, R.P., 1971, Earthquakes and seismic energy release in Oregon: Oregon Department of Geology and Mineral Industries, Ore Bin, v. 33, no. 4, p. 61-84.
- Couch, R.W., Pitts, G.S., Braman, D.E., and Gemperle, M., 1981b, Free-air gravity anomaly map and complete Bouguer gravity anomaly map, Cascade Mountain Range, northern Oregon: Oregon Department of Geology and Mineral Industries Geological Map Series GMS-15, scale 1:250,000.
- Couch, R.W., Pitts, G.S., Gemperle, M., Braman, D.E., and Veen, C.A., 1982a, Gravity anomalies in the Cascade Range in Oregon: Structural and thermal implications: Oregon Department of Geology and Mineral Industries Open-File Report O-82-9, 43 p.
- Couch, R.W., Pitts, G.S., Gemperle, M., Veen, C.A., and Braman, D.E., 1982b, Residual gravity maps of northern, central, and southern Cascade Range, Oregon, 122° 30' to 121° 00' E. by 42° 00' to 45° 45' N.: Oregon Department of Geology and Mineral Industries Geological Map Series GMS-26.
- Couch, R.W., Pitts, G.S., Veen, C.A., and Gemperle, M., 1981c, Free-air gravity anomaly and complete Bouguer gravity anomaly map, Cascade Mountain Range, southern Oregon: Oregon Department of Geology and Mineral Industries Geological Map Series GMS-16, scale 1:250,000.
- Crandell, D.R., 1980, Recent eruptive history of Mount Hood, Oregon, and potential hazards from future eruptions: U.S. Geological Survey Bulletin 1492, 81 p.

- Davie, E.I., II, 1980, The geology and petrology of Three Fingered Jack, a High Cascade volcano in central Oregon: Eugene, Oreg., University of Oregon master's thesis, 138 p.
- Davis, G.A., 1981, Late Cenozoic tectonics of the Pacific Northwest with special reference to the Columbia Plateau: Washington Public Power Supply System, Final Safety Analysis Report, Nuclear Project 2, Appendix 2.5#N, revised preliminary draft, 44 p.
- Dicken, S.N., 1950, Oregon geography: Eugene, Oreg., University of Oregon Cooperative Bookstore, 104 p.
- Dickinson, W.R., 1968, Circum-Pacific andesite types: *Journal of Geophysical Research*, v. 73, no. 6, p. 2261-2269.
- Dyhrman, R.F., 1975, Geology of the Bagby Hot Springs area, Clackamas and Marion Counties, Oregon: Corvallis, Oreg., Oregon State University master's thesis, 78 p.
- Elliott, M.A., D'Allura, J.A., and Purdom, W.B., 1981, Geology of the City of Ashland and vicinity, Jackson County, Oregon: Oregon Department of Geology and Mineral Industries unpublished report, 15 p.
- Fairbank, B.D., Openshaw, R.W., Souther, J.G., and Stauder, J.J., 1981, Meager Creek Geothermal Project--an exploration case history: *Geothermal Resources Council Bulletin*, v. 10, no. 6, p. 3-7.
- Fiebelkorn, R.B., Walker, G.W., MacLeod, N.S., McKee, E.H., and Smith, J.G., 1982, Index to K-Ar age determinations for the State of Oregon: U.S. Geological Survey Open-File Report 82-596, 40 p.
- Flaherty, G.M., 1981, The Western Cascade-High Cascade transition in the McKenzie Bridge area, central Oregon Cascade Range: Eugene, Oreg., University of Oregon master's thesis, 178 p.
- Fournier, R.O., 1979, A revised equation for the Na/K geothermometer, in *Expanding the geothermal frontier: Geothermal Resources Council Transactions*, v. 3, p. 221-224.
- Fournier, R.O., and Rowe, J.J., 1966, Estimation of underground temperatures from the silica content of water from hot springs and wet-steam wells: *American Journal of Science*, v. 264, no. 9, p. 685-697.
- Fournier, R.O., and Truesdell, A.H., 1973, An empirical Na-K-Ca geothermometer for natural waters: *Geochimica et Cosmochimica Acta*, v. 37, no. 5, p. 1255-1275.
- Green, T.H., and Ringwood, A.E., 1968, Genesis of the calc-alkaline igneous rock suite: *Contributions to Mineralogy and Petrology*, v. 18, no. 2, p. 105-162.
- Hales, P.O., 1975, Geology of the Green Ridge area, Whitewater River quadrangle, Oregon: Corvallis, Oreg., Oregon State University master's thesis, 90 p.
- Hammond, P.E., 1979, A tectonic model for evolution of the Cascade Range, in Armentrout, J.M., Cole, M.R., and Terbest, H., Jr., eds., *Cenozoic paleogeography of the western United States: Pacific Coast Paleogeography Symposium No. 3*, Anaheim, Calif., Society of Economic Paleontologists and Mineralogists, Pacific Section, p. 219-237.
- 1980, Reconnaissance geologic map and cross-sections of southern Washington Cascade Range, latitude 45° 30'-47° 15' N., longitude 120° 45'-122° 22.5' W.: Portland, Oreg., Portland State University, Department of Earth Sciences, 31 p., 2 sheets, scale 1:125,000.
- Hammond, P.E., Anderson, J.L., and Manning, K.J., 1980, Guide to the geology of the upper Clackamas and North Santiam Rivers area, northern Oregon Cascade Range, in Oles, K.F., Johnson, J.G., Niem, A.R., and Niem, W.A., eds., *Geologic field trips in western Oregon and southwestern Washington: Oregon Department of Geology and Mineral Industries Bulletin 101*, p. 133-167.

- Hammond, P.E., Geyer, K.M., and Anderson, J.L., 1982, Preliminary geologic map and cross-sections of the upper Clackamas and North Santiam Rivers area, northern Oregon Cascade Range: Portland, Oreg., Portland State University Department of Earth Sciences, scale 1:62,500.
- Hart, W.K., 1982, Chemical, geochronologic, and isotopic significance of low-K, high-alumina olivine tholeiite in the northwestern Great Basin, U.S.A.: Cleveland, Ohio, Case Western Reserve University doctoral dissertation, 410 p.
- Hering, C.W., 1981, Geology and petrology of the Yamsay Mountain complex, south-central Oregon: A study of bimodal volcanism: Eugene, Oreg., University of Oregon doctoral dissertation, 194 p.
- Higgins, M.W., 1973, Petrology of Newberry Volcano, central Oregon: Geological Society of America Bulletin, v. 84, no. 2, p. 455-487.
- Hodge, E.T., 1933, Age of Columbia River and lower canyon [abs.]: Geological Society of America Bulletin, v. 44, pt. 1, p. 156-157.
- 1938, Geology of the lower Columbia River: Geological Society of America Bulletin, v. 49, no. 6, p. 831-929.
- Hull, D.A., investigator, and Riccio, J.F., ed., 1979, Geothermal resource assessment of Mount Hood: Oregon Department of Geology and Mineral Industries Open-File Report O-79-8, 273 p.
- Hull, D.A., Blackwell, D.D., and Black, G.L., 1978, Geothermal gradient data: Oregon Department of Geology and Mineral Industries Open-File Report O-78-4, 187 p.
- Hull, D.A., Blackwell, D.D., Bowen, R.G., Peterson, N.V., and Black, G.L., 1977, Geothermal gradient data: Oregon Department of Geology and Mineral Industries Open-File Report O-77-2, 134 p.
- Hull, D.A., Bowen, R.G., Blackwell, D.D., and Peterson, N.V., 1976, Geothermal gradient data, Brothers fault zone, central Oregon: Oregon Department of Geology and Mineral Industries Open-File Report O-76-2, 24 p.
- Irvine, T.N., and Baragar, W.R.A., 1971, A guide to the chemical classification of the common volcanic rocks: Canadian Journal of Earth Sciences, v. 8, no. 5, p. 523-548.
- Jakes, P., and White, A.J.R., 1969, Structure of the Melanesian arcs and correlation with distribution of magma types: Tectonophysics, v. 8, no. 3, p. 223-236.
- 1972, Major and trace element abundances in volcanic rocks of orogenic areas: Geological Society of America Bulletin, v. 83, no. 1, p. 29-39.
- Jan, M.Q., 1967, Geology of the McKenzie River valley between the South Santiam Highway and the McKenzie Pass Highway, Oregon: Eugene, Oreg., University of Oregon master's thesis, 70 p.
- Kays, M.A., 1970, Western Cascades volcanic series, South Umpqua Falls region, Oregon: Oregon Department of Geology and Mineral Industries, Ore Bin, v. 32, no. 5, p. 81-94.
- Kienle, C.F., Nelson, C.A., and Lawrence, R.D., 1981, Faults and lineaments of the southern Cascades, Oregon: Oregon Department of Geology and Mineral Industries Special Paper 13, 23 p.
- Kuno, H., 1966, Lateral variation of basalt magma type across continental margins and island arcs: Bulletin Volcanologique, v. 29, p. 195-222.
- Lawrence, R.D., 1976, Strike-slip faulting terminates the Basin and Range province in Oregon: Geological Society of America Bulletin, v. 87, no. 6, p. 846-850.

- Lux, D.R., 1981, Geochronology, geochemistry, and petrogenesis of basaltic rocks from the Western Cascades, Oregon: Columbus, Ohio, Ohio State University doctoral dissertation, 171 p.
- 1982, K-Ar and ^{40}Ar - ^{39}Ar ages of mid-Tertiary volcanic rocks from the Western Cascade Range, Oregon: *Isochron/West*, no. 33, p. 27-32.
- Macdonald, G.A., and Katsura, T., 1964, Chemical composition of Hawaiian lavas: *Journal of Petrology*, v. 5, pt. 1, p. 82-133.
- MacLeod, N.S., 1978a, Newberry volcano in Oregon [work in progress], in *Geological Survey Research 1978*: U.S. Geological Survey Professional Paper 1100, p. 194.
- 1978b, Newberry volcano, Oregon: Preliminary results of new field investigations: *Geological Society of America Abstracts with Programs*, v. 10, no. 3, p. 115.
- MacLeod, N.S., and Sherrod, D.R., 1979, Latest eruptions at Newberry volcano in Oregon [work in progress], in *Geological Survey Research 1979*: U.S. Geological Survey Professional Paper 1150, p. 182-183.
- MacLeod, N.S., Sherrod, D.R., and Chitwood, L.A., 1982, Geologic map of Newberry volcano, Deschutes, Klamath, and Lake Counties, Oregon: U.S. Geological Survey Open-File Report [in press].
- MacLeod, N.S., Sherrod, D.R., Chitwood, L.A., and McKee, E.H., 1981, Newberry volcano, Oregon, in Johnston, D.A., and Donnelly-Nolan, J., eds., *Guides to some volcanic terranes in Washington, Idaho, Oregon, and northern California*: U.S. Geological Survey Circular 838, p. 85-103.
- MacLeod, N.S., Walker, G.W., and McKee, E.H., 1975, Geothermal significance of eastward increase in age of upper Cenozoic rhyolitic domes in southeastern Oregon, in *Second United Nations Symposium on the Development and Use of Geothermal Resources*, San Francisco, Calif., 1975, *Proceedings*: Washington, D.C., U.S. Government Printing Office, v. 1., p. 465-474.
- Magill, J., and Cox, A., 1980, Tectonic rotation of the Oregon Western Cascades: Oregon Department of Geology and Mineral Industries Special Paper 10, 67 p.
- Mariner, R.H., Swanson, J.R., Orris, G.J., Presser, J.S., and Evans, W.C., 1980, Chemical and isotopic data for water from thermal springs and wells of Oregon: U.S. Geological Survey Open-File Report 80-737, 50 p.
- Mase, C.W., Sass, J.H., Lachenbruch, A.H., and Munroe, R.J., 1982, Preliminary heat-flow investigations of the California Cascades: U.S. Geological Survey Open-File Report 82-150, 240 p.
- Maynard, L.C., 1974, Geology of Mount McLoughlin: Eugene, Oreg., University of Oregon master's thesis, 139 p.
- McBirney, A.R., Sutter, J.F., Naslund, H.R., Sutton, K.G., and White, C.M., 1974, Episodic volcanism in the central Oregon Cascade Range: *Geology*, v. 2, no. 12, p. 585-589.
- McLain, W.H., 1981, Geothermal and structural implications of magnetic anomalies observed over the southern Oregon Cascade Mountains and adjoining Basin and Range Province: Corvallis, Oreg., Oregon State University master's thesis, 151 p.
- Miyashiro, A., 1974, Volcanic rock series in island arcs and active continental margins: *American Journal of Science*, v. 274, no. 4, p. 321-355.
- Nakamura, K., 1977, Volcanoes as possible indicators of tectonic stress orientation--principle and proposal: *Journal of Volcanology and Geothermal Research*, v. 2, p. 1-16.
- Naslund, H.R., 1977, The geology of the Hyatt Reservoir and Surveyor Mountain quadrangles, Oregon: Eugene, Oreg., University of Oregon master's thesis, 127 p.

- Newcomb, R.C., and Hart, D.H., 1958, Preliminary report on the ground-water resources of the Klamath River basin, Oregon: U.S. Geological Survey Open-File Report 58-73, 248 p.
- O'Hara, M.J., 1965, Primary magmas and the origin of basalts: *Scottish Journal of Geology*, v. 1, p. 19-40.
- Peacock, M.A., 1931, Classification of igneous rock series: *Journal of Geology*, v. 39, no. 1, p. 54-67.
- Peck, D.L., Griggs, A.B., Schlicker, H.G., Wells, F.G., and Dole, H.M., 1964, Geology of the central and northern parts of the Western Cascade Range in Oregon: U.S. Geological Survey Professional Paper 449, 56 p.
- Peterson, N.V., and Groh, E.A., 1967, Geothermal potential of the Klamath Falls area, Oregon--a preliminary study: *Oregon Department of Geology and Mineral Industries, Ore Bin*, v. 29, no. 11, p. 209-231.
- Peterson, N.V., Groh, E.A., Taylor, E.M., and Stensland, D.E., 1976, Geology and mineral resources of Deschutes County, Oregon: *Oregon Department of Geology and Mineral Industries Bulletin* 89, 66 p.
- Peterson, N.V., and McIntyre, J.R., 1970, The reconnaissance geology and mineral resources of eastern Klamath County and western Lake County, Oregon: *Oregon Department of Geology and Mineral Industries Bulletin* 66, 70 p.
- Pitts, G.S., 1979, Interpretation of gravity measurements made in the Cascade Mountains and adjoining Basin and Range Province in central Oregon: Corvallis, Oreg., Oregon State University master's thesis, 186 p.
- Pitts, G.S., and Couch, R.W., 1978, Complete Bouguer gravity anomaly map, Cascade Mountain Range, central Oregon: *Oregon Department of Geology and Mineral Industries Geological Map Series* GMS-8, scale 1:125,000.
- Power, S.G., and Field, C.W., 1981, The geology, mineralization, and metallization of mining districts in the Western Cascades of Oregon and southern Washington: *Oregon Department of Geology and Mineral Industries unpublished report*, 83 p.
- Power, S.G., Field, C.W., Armstrong, R.L., and Harakal, J.R., 1981, K-Ar ages of plutonism and mineralization, Western Cascades, Oregon and southern Washington: *Isochron/West*, no. 31, p. 27-29.
- Priest, G.R., 1982, Overview of the geology and geothermal resources of the Mount Hood area, in Priest, G.R. and Vogt, B.F., eds., *Geology and geothermal resources of the Mount Hood area, Oregon*: Oregon Department of Geology and Mineral Industries Special Paper 14, p. 6-15.
- Priest, G.R., Beeson, M.H., Gannett, M.W., and Berri, D., 1982a, Geology, geochemistry and geothermal resources of the Old Maid Flat area, Oregon, in Priest, G.R., and Vogt, B.F., eds., *Geology and geothermal resources of the Mount Hood area, Oregon*: Oregon Department of Geology and Mineral Industries Special Paper 14, p. 16-30.
- Priest, G.R., Black, G.L., Woller, N.M., and King, W.L., 1982b, Geothermal exploration in Oregon, 1981: *Oregon Geology*, v. 44, no. 6, p. 63-68.
- Priest, G.R., Riccio, J.F., Woller, N.M., Gest, D., and Pitts, G.S., 1980, Heat flow along the High Cascade-Western Cascade transition zone, Oregon [abs.]: *Oregon Academy of Science Proceedings*, v. 16, p. 15.
- Priest, G.R., and Vogt, B.F., eds., 1982, *Geology and geothermal resources of the Mount Hood area, Oregon*: Oregon Department of Geology and Mineral Industries Special Paper 14, 98 p.
- Priest, G.R., Woller, N.M., and Evans, S.H., Jr., 1981, Late Cenozoic modification of calc-alkalic volcanism, central Oregon Cascades [abs.]: *American Association for the Advancement of Science, Pacific Division, 62nd Annual Meeting, Eugene, Oreg., 1981, Abstracts*, p. 32.

- Pungrassami, T., 1970, Geology of the western Detroit Reservoir area, Quartzville and Detroit quadrangles, Linn and Marion Counties, Oregon: Corvallis, Oreg., Oregon State University master's thesis, 76 p.
- Ringwood, A.E., 1975, Composition and petrology of the earth's mantle: New York, McGraw-Hill, 618 p.
- Rollins, A., 1976, Geology of the Bachelor Mountain area, Linn and Marion Counties, Oregon: Corvallis, Oreg., Oregon State University master's thesis, 83 p.
- Roy, R.F., Decker, E.R., Blackwell, D.D., and Birch, F., 1968, Heat flow in the United States: *Journal of Geophysical Research*, v. 73, no. 16, p. 5207-5221.
- Sammel, E.A., 1976, Hydrologic reconnaissance of the geothermal area near Klamath Falls, Oregon: U.S. Geological Survey Water-Resources Investigation WRI 76-127, 129 p.
- 1980, Hydrogeologic appraisal of the Klamath Falls geothermal area, Oregon: U.S. Geological Survey Professional Paper 1044-G, 45 p.
- 1981, Results of test drilling at Newberry Volcano, Oregon: *Geothermal Resources Council Bulletin*, v. 10, no. 11, p. 3-8.
- Sass, J.H., Lachenbruch, A.H., and Munroe, R.J., 1971, Thermal conductivity of rocks from measurements on fragments and its application to heat-flow determinations: *Journal of Geophysical Research*, v. 76, no. 14, p. 3391-3401.
- Sass, J.H., and Sammel, E.A., 1976, Heat flow data and their relation to observed geothermal phenomena near Klamath Falls, Oregon: *Journal of Geophysical Research*, v. 81, no. 26, p. 4863-4868.
- Smith, J.G., 1979, Cenozoic volcanism in the Cascade Range, Medford 2° sheet, southern Oregon [abs.]: *Geological Society of America Abstracts with Programs*, v. 11, no. 3, p. 128.
- Smith, J.G., Sawlan, M.S., and Katcher, A. C., 1980, An important lower Oligocene welded-tuff marker bed in the Western Cascade Range of southern Oregon [abs.]: *Geological Society of America Abstracts with Programs*, v. 12, no. 3, p. 153.
- Smith, R.L., and Shaw, H.R., 1979, Igneous-related geothermal systems, in Muffler, L.J.P., ed., *Assessment of geothermal resources of the United States—1978*: U.S. Geological Survey Circular 790, p. 12-17.
- Steele, J.L., Blackwell, D.D., and Robison, J., 1982, Heat flow in the vicinity of the Mount Hood volcano, Oregon, in Priest, G.R., and Vogt, B.F., eds., *Geology and geothermal resources of the Mount Hood area*: Oregon Department of Geology and Mineral Industries Special Paper 14, p. 31-42.
- Stewart, J.H., 1978, Basin-Range structure in western North America: A review, in Smith, R.B., and Eaton, G.P., eds., *Cenozoic tectonics and regional geophysics of the Western Cordillera*: Boulder, Colo., Geological Society of America Memoir 152, p. 1-31.
- Sutter, J.F., 1978, K/Ar ages of Cenozoic volcanic rocks from the Oregon Cascades west of 121° 30': *Isochron/West*, no. 21, p. 15-21.
- Sutton, K.G., 1974, The geology of Mount Jefferson: Eugene, Oreg., University of Oregon master's thesis, 120 p.
- Swanson, F.J., and James, M.E., 1975, Geology and geomorphology of the H.J. Andrews Experimental Forest, Western Cascades, Oregon: Portland, Oreg., U.S. Forest Service, Pacific Northwest Forest and Range Experiment Station, 14 p.
- Taylor, E.M., 1967, Recent volcanism between Three Fingered Jack and North Sister, Oregon Cascade Range: Pullman, Wash., Washington State University doctoral dissertation, 84 p.

- Taylor, E.M., 1968, Roadside geology, Santiam and McKenzie Pass Highways, Oregon, in Dole, H.M., ed., Andesite Conference guidebook: Oregon Department of Geology and Mineral Industries Bulletin 62, p. 3-33.
- 1973a, Geochronology and structure of the central part of the Cascade Range, Oregon: Unpublished report to Oregon Academy of Science, 31st Annual Meeting, Corvallis, Oreg., 1973
- 1973b, Geology of the Deschutes Basin, in Geologic field trips in northern Oregon and southern Washington: Oregon Department of Geology and Mineral Industries Bulletin 77, p. 29-32.
- 1978, Field geology of S.W. Broken Top quadrangle, Oregon: Oregon Department of Geology and Mineral Industries Special Paper 2, 50 p.
- 1980, Volcanic and volcaniclastic rocks on the east flank of the central Cascade Range to the Deschutes River, Oregon, in Oles, K.F., Johnson, J.G., Niem, A.R., and Niem, W.A., eds., Geologic field trips in western Oregon and southwestern Washington: Oregon Department of Geology and Mineral Industries Bulletin 101, p. 1-7.
- 1981, Central High Cascade roadside geology--Bend, Sisters, McKenzie Pass, and Santiam Pass, Oregon, in Johnston, D.A., and Donnelly-Nolan, J., eds., Guides to some volcanic terranes in Washington, Idaho, Oregon, and northern California: U.S. Geological Survey Circular 838, p. 55-58.
- Taylor, H.P., Jr., 1971, Oxygen isotope evidence for large-scale interaction between meteoric ground waters and Tertiary granodiorite intrusions, Western Cascade Range, Oregon: Journal of Geophysical Research, v. 76, no. 32, p. 7855-7874.
- Thayer, T.P., 1936, Structure of the North Santiam River section of the Cascade Mountains in Oregon: Journal of Geology, v. 44, no. 6, p. 701-716.
- 1937, Petrology of later Tertiary and Quaternary rocks of the north-central Cascade Mountains in Oregon, with notes on similar rocks in western Nevada: Geological Society of America Bulletin, v. 48, no. 11, p. 1611-1651.
- 1939, Geology of the Salem Hills and the North Santiam River basin, Oregon: Oregon Department of Geology and Mineral Industries Bulletin 15, 40 p.
- Timm, S., 1979, The structure and stratigraphy of the Columbia River Basalt in the Hood River Valley, Oregon: Portland, Oreg., Portland State University master's thesis, 60 p.
- U.S. Army Corps of Engineers, 1964, Cougar Dam, South Fork McKenzie River foundation report: Portland, Oreg., U.S. Army Corps of Engineers, Portland District.
- Veen, C.A., 1981, Gravity anomalies and their structural implications for the southern Oregon Cascade Mountains and adjoining Basin and Range Province: Corvallis, Oreg., Oregon State University master's thesis, 86 p.
- Venkatakrishnan, R., Bond, J.G., and Kauffman, J.D., 1980, Geological linears of the northern part of the Cascade Range, Oregon: Oregon Department of Geology and Mineral Industries Special Paper 12, 25 p.
- Vogt, B.F., 1979, Columbia River Basalt Group stratigraphy and structure in the Bull Run Watershed, Western Cascades, northern Oregon: Oregon Academy of Science Proceedings, v. 15, p. 51-52.
- 1981, The stratigraphy and structure of the Columbia River Basalt Group in the Bull Run Watershed, Multnomah and Clackamas Counties, Oregon: Portland, Oreg., Portland State University master's thesis, 151 p.
- Walker, G.W., 1977, Geologic map of Oregon east of the 121st meridian: U.S. Geological Survey Miscellaneous Investigations Series Map I-902, scale 1:500,000.

- Waring, G.A., [revised by Blankenship, R.R., and Bentall, R.], 1965, Thermal springs of the United States and other countries of the world--a summary: U.S. Geological Survey Professional Paper 492, p. 38-41.
- Waters, A.C., 1955, Geomorphology of south-central Washington, illustrated by the Yakima East quadrangle: Geological Society of America Bulletin, v. 66, no. 6, p. 663-684.
- Wells, F.G., 1956, Geology of the Medford quadrangle, Oregon-California: U.S. Geological Survey Geologic Quadrangle Map GQ-89, scale 1:96,000.
- Wells, F.G., and Peck, D.L., 1961, Geologic map of Oregon west of the 121st meridian: U.S. Geological Survey Miscellaneous Investigations Series Map I-325, scale 1:500,000.
- White, C.M., 1980a, Geology of the Breitenbush Hot Springs quadrangle, Oregon: Oregon Department of Geology and Mineral Industries Special Paper 9, 26 p.
- 1980b, Geology and geochemistry of Mt. Hood volcano: Oregon Department of Geology and Mineral Industries Special Paper 8, 26 p.
- 1980c, Geology and geochemistry of volcanic rocks in the Detroit area, Western Cascade Range, Oregon: Eugene, Oreg., University of Oregon doctoral dissertation, 178 p.
- White, C.M., and McBirney, A.R., 1978, Some quantitative aspects of orogenic volcanism in the Oregon Cascades, in Smith, R.B., and Eaton, G.P., eds., Cenozoic tectonics and regional geophysics of the western Cordillera: Geological Society of America Memoir 152, p. 369-388.
- Williams, D.L., and Finn, C., 1981, Gravity anomalies in subvolcanic intrusions in the Cascade Range and elsewhere: 51st Annual International Meeting, Society of Exploration Geophysicists, Los Angeles, Calif., 1981, Geothermal Special Session 3, Technical Program Abstracts G3.5.
- Williams, D.L., Hull, D.A., Ackermann, H.D., and Beeson, M.H., 1982, The Mt. Hood region: Volcanic history, structure, and geothermal energy potential: Journal of Geophysical Research, v. 87, no. B4, p. 2767-2781.
- Williams, D.L., and von Herzen, R.P., 1982, On the terrestrial heat flow and physical limnology of Crater Lake, Oregon: Journal of Geophysical Research [in press].
- Williams, H., 1933, Mount Thielsen, a dissected Cascade volcano: Berkeley, Calif., University of California Publications in Geological Sciences, v. 23, no. 6, p. 195-214.
- 1935, Newberry volcano of central Oregon: Geological Society of America Bulletin, v. 46, no. 2, p. 253-304.
- 1942, The geology of Crater Lake National Park, Oregon, with a reconnaissance of the Cascade Range southward to Mount Shasta: Carnegie Institution of Washington Publication 540, 162 p.
- 1944, Volcanoes of the Three Sisters region, Oregon Cascades: Berkeley, Calif., University of California Publications in Geological Sciences, v. 27, no. 3, p. 37-83.
- 1949, Geology of the Macdoel quadrangle [California]: California Division of Mines and Geology Bulletin 151, p. 7-60.
- 1953, The ancient volcanoes of Oregon (2nd ed.): Eugene, Oreg., Oregon State System of Higher Education, Condon Lectures, 68 p.
- 1957, A geologic map of the Bend quadrangle, Oregon, and a reconnaissance geologic map of the central portion of the High Cascade Mountains: Oregon Department of Geology and Mineral Industries in cooperation with the U.S. Geological Survey, scales 1:125,000 and 1:250,000.

- Wise, W.S., 1969, Geology and petrology of the Mt. Hood area: A study of High Cascade volcanism: Geological Society of America Bulletin, v. 80, no. 6, p. 969-1006.
- Yoder, H.S., Jr., 1976, Generation of basaltic magma: Washington, D.C., National Academy of Science, 265 p.
- Yoder, H.S., Jr., and Tilley, C.E., 1962, Origin of basalt magmas: An experimental study of natural and synthetic rock systems: Journal of Petrology, v. 3, pt. 3, p. 342-532.
- Youngquist, W.L., 1980, Geothermal gradient drilling, north-central Cascades of Oregon, 1979: Oregon Department of Geology and Mineral Industries Open-File Report 0-80-12, 47 p.
- Zoback, M.L., and Thompson, G.A., 1978, Basin and Range rifting in northern Nevada: Clues from a mid-Miocene rift and its subsequent offsets: Geology, v. 6, no. 2, p. 111-116.

APPENDIX A.

NEW K-Ar DATA

Table A.1. New K-Ar data, Oregon

Plate no.	Sample no. on plate ^a	Sample no.	Geologic unit	Material dated	% K	% Ar ⁴⁰ atm	Age m.y. $\pm 1\sigma$	Location ^b	Elevation (ft)
3	6	Devil-440	Tmo	Whole rock	0.53	87	5.34 \pm 0.58 ^c	T10S/R7E/11Aad	4000
3	8	DC-4	Tmo	Whole rock	0.66	90	9.5 \pm 1.3	T10S/R7E/2Add	4440
3	16	DC-114	Tmp	Whole rock	1.61	37	6.30 \pm 0.22	T10S/R7E/4Ddd	5220
3	18	DC-14	Tmp	Whole rock	0.49	91	6.0 \pm 0.9	T10S/R7E/10Dac	5180
4	23	Ri-85	Tmrt	Plagioclase	0.349	74	13.8 \pm 0.8	T16S/R4E/36Dcb	3120
4	25	Tmw1	Tmw	Whole rock	0.440	93	12.4 \pm 2.5 ^c	T17S/R5E/8Bbd	2040
4	28	Ri-22	Tmw	Whole rock	1.32	72	13.2 \pm 0.7	T17S/R5E/16Abb	2360
4	34	Cougar	Tmvic	Whole rock	0.237	87	16.2 \pm 1.8	T16S/R5E/32Cca	1880
4	35	Ri-136	Tmcr	Whole rock	0.755	66	9.31 \pm 0.44	T16S/R5E/28Acd	3360
4	37	Ri-62	Tml	Whole rock	0.48	86	7.80 \pm 0.77	T17S/R5E/21Aca	3760
4	39	Ri-64	Tml	Whole rock	1.39	64	9.41 \pm 0.42	T17S/R5E/21Abd	4660
4	--	Ri-112	Tmw	Plagioclase	0.208	65	11.4 \pm 0.5	T17S/R4E/12Bcb	4640
4	--	Foley Ridge	---	Whole rock	0.548	95	2.03 \pm 0.52	T16S/R5E/15Add	1400
4	--	MO-159	---	Whole rock	0.332	92	6.80 \pm 1.18	T16S/R6E/22Bcd	3600
4	--	MO-160	---	Whole rock	0.357	89	7.67 \pm 0.96	T16S/R6E/21Bca	2800
4	--	MO-ENG.-B	---	Whole rock	0.191	86	10.2 \pm 1.0	T17S/R6E/26Bbb	5280
4	--	MO-ENG.-B	---	Whole rock	0.191	81	9.6 \pm 1.5	T17S/R6E/26Bbb	5280
4	--	MB-133	---	Whole rock	0.432	91	2.23 \pm 0.37	T16S/R6E/17Dbc	1920
5	41	BB-16	Totl	Whole rock	0.810	83	24.7 \pm 2.0 ^c	T20S/R2E/26Dad	2520
5	45	BB-30	Tml	Whole rock	0.515	89	21.9 \pm 2.9 ^c	T20S/R2E/22Cda	1320
5	48	Stack/BB35	Tml	Whole rock	0.540	65	22.0 \pm 1.0	T20S/R2E/22Daa	2400
5	52	BB-PAT	Tma	Whole rock	0.100	98	8.3 \pm 5.5 ^c	T21S/R2E/7Cbd	3840
5	53	BB-NSH	Tma	Whole rock	0.241	97	15.9 \pm 7.6 ^c	T20S/R2E/14Dda	2880
5	55	BB-PPAT	Tmu	Whole rock	0.91	70	5.81 \pm 0.30	T21S/R1E/12Aba	3380
5	56	BB-Tpba	QTb	Whole rock	1.18	95	0.56 \pm 0.16	T20S/R2E/18Acb	1080
6	65	T-10	Tmb	Whole rock	1.10	53	15.6 \pm 0.6	T24S/R4E/24Caa	5260
6	67	T-14	Tmb	Whole rock	0.66	72	17.0 \pm 0.9	T24S/R4E/1Dcc	3220
6	72	P-624	Tmb	Whole rock	0.89	82	13.5 \pm 1.1	T23S/R5E/30Cad	4040
6	73	P-626	Tmb	Whole rock	0.87	68	13.1 \pm 0.6 ^a	T23S/R5E/30Ccc	4180
6	74	T-FIZZ	Tmb	Whole rock	0.80	74	14.1 \pm 0.8 ^a	T24S/R5E/18Cbb	3120
6	81	P-509	Tma	Whole rock	0.67	62	17.3 \pm 0.8(?)	T23S/R5E/21Bbb	5880
6	82	P-616	Tpb	Whole rock	1.25	85	4.32 \pm 0.4	T23S/R5E/33Ddd	5360
6	83	P-PHL	Tpb	Whole rock	0.90	76	5.56 \pm 0.34	T23S/R5E/16Dcc	5600
6	84	P-22	Qb	Whole rock	0.71	89	1.98 \pm 0.25	T23S/R5E/9Bbb	3700
6	85	P-Notch	Qb	Whole rock	0.863	96	0.98 \pm 0.34	T23S/R5E/14Bdd	5520
6	86	T-208	Qb	Whole rock	0.62	95	0.77 \pm 0.21	T24S/R5E/16Cdb	3920
6	87	T-210	Qb	Whole rock	0.81	99	0.17 \pm 0.48	T24S/R5E/18Add	2940
6	88	T-211	Qb	Whole rock	0.68	97	0.97 \pm 0.46	T24S/R5E/18Dac	3080
6	--	P-324	Tpb	Whole rock	0.94	81	5.53 \pm 0.41	T23S/R5E/14Aab	5800

a. The map numbers are the sequential sample numbers listed in Appendix B and are plotted on Plates 3 through 6. Unnumbered samples are in areas outside of the areas of the plates, or they lack chemical data (i.e., Ri-112 and P-324).

b. For explanation of Township-Range location system, see Appendix C.

c. Date is probably affected by low-grade rock alteration.

APPENDIX B.

CHEMICAL ANALYSES OF ROCK SAMPLES

Table B.1. Rock chemistry, Outerson Mountain-Devils Creek area, Marion County, Oregon. Sample localities are shown on Plate 3.

Sample no. on Plate 3	1	2	3	4	5	6	7	8	9	10
Geol. unit	Lavas of Outerson Mountain									
Map symbol	Tmo	Tmo	Tmo	Tmo	Tmo	Tmo	Tmo	Tmo	Tmo	Tmo
Sample no.	Devil-60'	Devil-120'	Devil-200'	Devil-260'	Devil-340'	Devil-440'	Devil-480'	DC-4	DC-5	DC-1
Location	T10S/R7E/11Aad	T10S/R7E/11Aad	T10S/R7E/11Aad	T10S/R7E/11Aad	T10S/R7E/11Aad	T10S/R7E/11Aad	T10S/R7E/11Aad	T10S/R7E/2Add	T10S/R7E/2Abc	T9S/R7E/35Cac
SiO ₂	49.60	52.20	51.50	53.00	52.20	53.70	52.80	54.89	54.00	54.40
TiO ₂	1.21	1.20	1.17	1.11	1.23	1.14	1.15	1.14	1.36	1.08
Al ₂ O ₃	19.10	18.54	18.73	17.60	17.70	18.15	18.03	17.92	18.72	18.40
Fe ₂ O ₃	[9.48	[9.26	[8.74	[8.41	[9.18	[8.66	[8.55	[7.82	[8.83	[8.80
FeO										
MnO	0.13	0.14	0.14	0.15	0.13	0.13	0.15	0.11	0.13	0.11
MgO	5.41	5.27	4.82	4.89	5.32	5.12	4.90	5.01	4.63	4.99
CaO	8.11	7.54	8.33	7.99	7.96	8.08	7.83	9.08	8.27	8.82
Na ₂ O	3.34	3.30	3.40	3.30	3.51	3.57	3.59	3.28	3.42	3.65
K ₂ O	0.41	0.65	0.48	0.58	0.78	0.61	0.73	0.92	0.53	1.09
H ₂ O ⁺										
H ₂ O ⁻	[1.57	[1.92	[1.35	[0.82	[0.55	[0.64	[0.74	[0.39	[1.38	[0.99
P ₂ O ₅	0.37	0.36	0.35	0.35	0.34	0.35	0.37	0.21	0.34	0.28
Total	98.73	100.34	99.02	98.20	98.90	100.15	98.84	100.77	101.61	102.61
Total FeO*	9.76	9.41	8.95	8.64	9.33	8.70	8.72	7.79	8.81	8.66
CIPW norms										
Q	0.55	6.28	3.10	5.83	1.40	4.25	3.59	5.38	5.85	2.17
Or	2.42	3.84	2.84	3.43	4.61	3.60	4.31	5.38	3.13	6.44
Ab	28.30	27.90	28.80	27.90	29.70	30.20	30.40	27.80	28.90	30.90
an	35.90	29.00	34.40	31.40	30.40	31.70	30.90	31.50	34.20	30.60
Di(C)	1.79	(1.78)	4.00	5.15	5.85	5.20	4.79	10.10	3.86	9.55
Hy	21.40	21.60	18.10	17.50	18.80	18.20	17.80	14.60	17.40	15.70
Ol	0.00	0.00	0.00	0.00	0.00	0.00	0.00	0.00	0.00	0.00
Mt	3.00	2.93	2.77	2.67	2.90	2.75	2.71	2.48	2.80	2.73
Il	2.30	2.28	2.22	2.11	2.34	2.17	2.18	2.17	2.58	2.05
Trace elements										
(ppm)										
Rb	-----	-----	-----	-----	-----	-----	-----	-----	-----	-----
Ba	340	394	331	385	358	394	412	251	331	429
Sr	652	628	659	637	629	665	657	550	599	908
Co	27	27	30	26	32	72	35	49	35	33
Ni	73	69	67	62	77	63	54	34	43	47
Cr	99	84	92	98	107	79	72	97	66	54
Zn	82	85	76	86	79	77	77	57	74	61
Cu	64	58	59	66	70	58	53	44	44	83
Li	15	12	16	11	8	11	11	9	13	9

*Total iron recalculated to Fe⁺², volatile-free.

**Outside map area.

APPENDIX B.

CHEMICAL ANALYSES OF ROCK SAMPLES

Table B.1. Rock chemistry, Outerson Mountain-Devils Creek area, Marion County, Oregon. Sample localities are shown on Plate 3.--Continued

Sample no. on Plate 3	11	12	13	14	15	16	17	18	(Not on map) Pigeon Prairie
Geol. unit	Tuffs of Outerson Mountain					Upper Miocene-Pliocene lavas			
Map symbol	Tmt	Tmt	Tmt	Tmt	Tmt	Tmp	Tmp	Tmp	----
Sample no.	DC-103	DC-104	DC-105	DC-107	DC-109B	DC-114	DC-111	DC-14	P.P.
Location	T10S/R7E/9Caa	T10S/R7E/9Dbb	T10S/R7E/9Dbb	T10S/R7E/9Dbb	T10S/R7E/9Dbb	T10S/R7E/4Ddd	T10S/R7E/9Acd	T10S/R7E/10Dac	---
SiO ₂	64.18	60.70	61.49	55.29	68.60	56.10	52.80	53.40	48.60
TiO ₂	0.50	1.17	0.73	1.54	0.38	1.14	1.40	1.45	1.23
Al ₂ O ₃	18.12	16.40	15.78	16.35	14.99	17.76	17.38	17.09	17.06
Fe ₂ O ₃	[3.59	[6.47	[4.98	[7.79	[3.17	[8.44	[9.90	[9.47	3.87
FeO									6.21
MnO	0.09	0.11	0.15	0.12	0.06	0.16	0.14	0.14	0.19
MgO	4.84	2.63	1.86	2.91	1.32	3.86	5.31	4.61	7.58
CaO	2.89	4.69	2.98	7.07	2.24	7.52	9.11	8.85	9.55
Na ₂ O	1.07	3.82	3.61	2.12	2.74	3.83	3.36	3.49	3.36
K ₂ O	0.42	1.79	2.67	1.58	4.70	2.57	0.66	0.70	0.43
H ₂ O ⁺	[7.06	[3.50	[4.76	[6.17	[3.96	[0.22	[0.00	[0.55	[----
H ₂ O ⁻									
P ₂ O ₅	0.05	0.25	0.12	0.34	0.06	0.57	0.31	0.26	0.39
Total	102.81	101.53	99.13	101.28	102.22	102.17	100.37	100.01	98.47
Total FeO*	3.75	6.60	5.28	8.19	3.23	8.28	9.86	9.52	9.88
CIPW norms									
Q	41.50	15.80	19.30	15.90	26.60	2.22	2.80	4.33	0.00
Or	2.48	10.60	15.80	9.34	27.80	15.20	3.90	4.14	2.58
Ab	9.05	32.30	30.60	17.90	23.20	32.40	28.40	29.15	28.92
An	14.20	21.90	14.20	30.40	11.00	23.70	30.40	28.90	30.71
Di(C)	(10.3)	(0.15)	(1.75)	2.27	(1.36)	8.64	10.60	11.10	12.08
Hy	15.40	12.00	9.23	12.50	6.30	13.10	17.00	14.40	6.08
Ol	0.00	0.00	0.00	0.00	0.00	0.00	0.00	0.00	12.86
Mt	1.13	2.04	1.58	2.46	1.00	2.67	3.15	3.00	3.48
Il	0.95	2.22	1.39	2.92	0.72	2.17	2.66	2.75	2.38
Trace elements									
(ppm)									
Rb	----	----	----	----	----	----	----	----	5
Ba	242	403	465	287	752	1110	269	242	279
Sr	297	447	322	674	269	1312	578	548	581
Co	38	27	70	126	25	34	48	78	59
Ni	6	11	9	13	11	39	45	22	158
Cr	< 2	10	8	6	10	46	83	63	283
Zn	66	83	84	87	54	81	67	65	88
Cu	13	21	15	31	17	91	53	60	59
Li	29	14	16	7	20	12	7	6	10

*Total iron recalculated to Fe⁺², volatile-free.

**Outside map area.

APPENDIX B.

CHEMICAL ANALYSES OF ROCK SAMPLES

Table B.2. Rock chemistry, Cougar Reservoir area, Lane County, Oregon. Sample localities are shown on Plate 4.

Sample no. on Plate 4	19	20	21	22	23	24	25	26	27
Geol. unit	Tuffs of Cougar Reservoir				Tuffs of Rush Creek		Andesites of Walker Creek		
Map symbol	Totc	Totc	Totc	Totc	Tmrt	Tmrt	Tmw	Tmw	Tmw
Sample no.	Ri-LB	Ri-87	Ri-149	Ri-150	Ri-85	Ri-99a	Tmw1	Ri-40	Ri-43
Location	T16S/R4E/36Ddd	T17S/R4E/1Aad	T16S/R5E/29Bca	T16S/R5E/30Add	T16S/R4E/36Ddb	T17S/R4E/14Dda	T17S/R5E/8Bbd	T17S/R5E/15Cab	T17S/R5E/15Acb
SiO ₂	55.60	58.70	71.46	64.03	61.42	60.66	54.86	57.22	61.08
TiO ₂	0.82	1.47	0.36	0.48	0.44	0.60	0.88	0.89	0.86
Al ₂ O ₃	15.71	15.47	15.15	12.10	12.83	15.01	17.03	17.12	17.04
Fe ₂ O ₃	-----	2.55	2.36	2.71	1.88	2.00	2.12	3.21	2.45
FeO	5.35	4.68	0.40	0.71	0.92	1.56	4.70	3.62	2.80
MnO	1.0	0.13	0.09	0.03	0.04	0.08	0.13	0.12	0.10
MgO	2.52	2.39	0.38	1.30	1.69	1.85	5.29	4.02	2.47
CaO	5.08	6.30	1.66	4.65	3.59	4.38	8.41	7.22	5.59
Na ₂ O	4.42	3.64	4.85	0.43	1.25	2.72	3.00	3.89	3.56
K ₂ O	1.81	1.33	2.31	2.06	1.88	1.91	0.49	1.20	2.06
H ₂ O ⁺	[6.06	1.30	0.95	5.31	5.61	3.43	0.88	0.40	1.18
H ₂ O ⁻		2.12	0.87	5.87	8.70	6.13	1.13	1.05	0.37
P ₂ O ₅		0.49	0.11	0.06	0.07	0.10	0.16	0.17	0.19
Total	91.62	100.57	100.95	99.20	100.33	100.43	99.03	100.13	99.75
Total FeO*	5.84	7.20	2.55	3.56	3.05	3.71	6.82	6.62	5.10
CIPW norms									
Q	Not available	15.60	30.37	45.81	41.66	26.64	9.16	7.99	15.84
Or		8.10	13.85	13.78	12.96	12.43	2.99	7.22	12.43
Ab		31.77	41.63	4.12	12.29	25.33	26.17	33.39	30.76
An		22.59	7.63	25.66	20.20	23.22	32.52	26.10	24.88
Di (C)		5.25	(1.94)	(0.96)	(2.77)	(0.83)	7.62	7.49	1.76
Hy		10.14	2.73	7.23	7.90	8.73	17.04	13.38	10.44
Ol		0.00	0.00	0.00	0.00	0.00	0.00	0.00	0.00
Mt		2.53	0.90	1.26	1.07	1.31	2.40	2.33	1.80
Il		2.87	0.69	1.03	0.97	1.26	1.72	1.71	1.67
Trace elements									
(ppm)	-----	24	47	35	47	41	9	22	27
Rb	-----	24	47	35	47	41	9	22	27
Ba	269	387	497	467	611	530	180	337	578
Sr	343	476	189	913	453	333	628	642	503
Co	17	18	20	3.0	22	33	47	39	31
Ni	13	11	10	7.8	7	12	6	52	21
Cr	16	11	10	12	12	14	132	27	17
Zn	46	85	51	46	49	51	63	78	74
Cu	32	33	18	20	16	17	53	66	26
Li	22	7.5	26	24	13	135	9	13	10

*Total iron recalculated to Fe⁺², volatile-free.

APPENDIX B.

CHEMICAL ANALYSES OF ROCK SAMPLES

Table B.2. Rock chemistry, Cougar Reservoir area, Lane County, Oregon. Sample localities are shown on Plate 4.--Continued

Sample no. on Plate 4	28	29	30	31	32	33	34	35	36
Geol. unit	Andesites of Walker Creek			Basaltic lavas of the East Fork			Dacite intrusive of Cougar Dam	Andesites of Castle Rock	Lavas of Tipsoo Butte
Map symbol	Tmw	Tmw	Tmw	Time	Time	Time	Tmvic	Tmcr	Tml
Sample no.	Ri-22	Ri-60	Ri-146	Ri-28	Ri-34a	EFKA	Cougar Dam	Ri-136	Ri-45
Location	T17S/R5E/16Abb	T17S/R5E/16Ca	T18S/R4E/1Dd	T17S/R5E/4Cba	T17S/R5E/9Daa	T17S/R5E/4Cab	T16S/R5E/32Cca	T16S/R5E/28Acd	T17S/R5E/15Ad
SiO ₂	59.10	59.60	58.77	51.66	51.47	53.41	61.95	58.66	51.32
TiO ₂	0.85	0.84	0.95	1.01	1.06	0.90	1.10	1.06	1.47
Al ₂ O ₃	18.20	18.53	19.97	16.70	16.83	16.83	15.32	16.95	16.26
Fe ₂ O ₃	-----	-----	2.53	3.83	2.61	3.19	1.81	3.06	4.42
FeO	6.69	6.56	3.50	5.03	5.93	4.45	3.94	3.26	6.80
MnO	0.09	0.15	0.12	0.14	0.14	0.13	0.12	0.10	0.18
MgO	3.23	3.14	2.17	7.65	7.37	6.54	2.36	3.14	5.30
CaO	6.49	5.72	6.28	8.92	8.61	8.85	5.10	6.56	7.90
Na ₂ O	3.94	3.80	4.21	3.26	3.34	3.24	4.65	3.85	3.45
K ₂ O	1.77	1.78	1.12	0.61	0.77	0.79	1.08	0.94	1.09
H ₂ O ⁺	[0.40	[0.99	0.69	0.64	1.00	0.74	2.23	0.65	0.57
H ₂ O ⁻			0.85	0.76	0.94	1.33	0.57	0.97	0.47
P ₂ O ₅	0.16	0.16	0.27	0.14	0.18	0.11	0.21	0.19	0.64
Total	100.92	101.27	100.74	100.32	100.24	100.51	100.44	99.39	99.87
Total FeO*	6.66	6.54	5.84	8.59	8.44	7.46	5.72	6.15	10.95
CIPW norms									
Q	9.20	11.20	11.47	0.00	0.00	2.70	16.24	13.21	1.02
Or	10.50	10.50	6.64	3.67	4.61	4.74	6.54	5.68	6.51
Ab	33.30	32.2	35.67	27.97	28.79	27.89	40.32	33.40	29.59
An	26.80	27.7	29.47	29.46	29.16	29.58	18.18	26.84	26.02
Di(C)	3.85	0.21	0.00	11.68	10.63	11.63	5.23	4.31	7.77
Hy	12.3	14.00	11.21	19.70	18.63	18.87	8.85	11.89	20.90
Ol	0.00	0.00	0.00	2.23	2.74	0.00	0.00	0.00	0.00
Mt	2.12	2.07	2.04	3.02	2.97	2.63	2.01	2.17	3.85
Il	1.61	1.60	1.81	1.94	2.05	1.73	2.14	2.06	2.84
Trace elements									
(ppm)									
Rb	-----	-----	-----	8.8	8.5	14	31	16	12
Ba	358	546	505	196	171	380	355	365	696
Sr	643	512	524	418	407	491	313	458	594
Co	35	63	33	42	44	47	24	42	50
Ni	29	13	24	147	140	46	21	33	96
Cr	30	24	14	378	304	331	16	59	125
Zn	52	65	70	77	84	74	74	87	103
Cu	45	46	50	41	172	38	30	80	94
Li	9	15	17	12	9.8	9.9	6.2	13	12

*Total iron recalculated to Fe⁺², volatile-free.

APPENDIX B.

CHEMICAL ANALYSES OF ROCK SAMPLES

Table B.2. Rock chemistry, Cougar Reservoir area, Lane County, Oregon. Sample localities are shown on Plate 4.--Continued

Sample no. on Plate 4	37	38	39	40
Geol. unit	Lavas of Tipsoo Butte			
Map symbol	Tm1	Tm1	Tm1	Tm1
Sample no.	Ri-62	Ri-64	Ri-63	Ri-46
Location	T17S/R5E/21Aca	T17S/R5E/22Cbb	T17S/R5E/21Abd	T17S/R5E/15Ada
SiO ₂	47.35	53.42	47.64	48.20
TiO ₂	2.37	1.26	1.46	1.36
Al ₂ O ₃	16.69	16.93	16.90	17.81
Fe ₂ O ₃	2.98	2.38	1.99	-----
FeO	8.84	6.86	9.21	11.86
MnO	0.20	0.17	0.20	0.18
MgO	6.29	4.29	7.87	7.97
CaO	8.50	7.52	9.72	9.34
Na ₂ O	3.21	3.83	2.42	2.31
K ₂ O	0.61	1.64	0.38	0.38
H ₂ O ⁺	1.00	0.46	0.79	[1.53
H ₂ O ⁻	0.75	0.07	0.53	
P ₂ O ₅	0.68	0.87	0.47	0.32
Total	99.47	100.33	99.58	101.26
Total FeO*	11.84	9.03	11.22	11.89
CIPW norms				
Q	0.00	2.19	0.00	0.00
Or	3.66	9.76	2.30	2.25
Ab	27.76	32.71	20.80	19.26
An	30.06	24.36	34.72	37.10
Di(C)	6.98	6.24	9.10	5.91
Hy	14.69	17.12	19.81	23.5
Ol	6.46	0.00	5.41	3.48
Mt	4.16	3.20	3.94	3.76
Il	4.62	2.41	2.81	2.58
Trace elements				
(ppm)				
Rb	1.5	15	5.9	----
Ba	733	878	317	233
Sr	571	636	398	295
Co	51	38	49	44
Ni	105	46	129	127
Cr	124	63	350	211
Zn	116	101	83	66
Cu	98	81	72	73
Li	12	13	8.3	8

*Total iron recalculated to Fe⁺², volatile-free.

APPENDIX B.

CHEMICAL ANALYSES OF ROCK SAMPLES

Table B.3. Rock chemistry, Lookout Point area, Lane County, Oregon. Sample localities are shown on Plate 5.

Sample no. on Plate 5	41	42	43	44	45	46	47	48	49
Geol. unit	Oligocene-lower Miocene tuffs and lavas		Lavas of Lookout Point	Lavas of Hardesty Mtn.	Lavas of Black Canyon				
Map symbol	-----	-----	-----	-----	-----	-----	-----	-----	-----
Sample no.	BB-16	BB-21	Tolpa	BB-203	BB-30	BB-32	BB-33	Stack (BB-35)	BB-36
Location	T20S/R2E/26Dad	T20S/R2E/35Add	T20S/R2E/35Cbd	T20S/R1E/23Bdb	T20S/R2E/22Cda	T20S/R2E/22Cad	T20S/R2E/22Cad	T20S/R2E/22Daa	T20S/R2E/23Cca
SiO ₂	55.00	70.00	67.86	57.83	50.11	52.22	55.23	56.62	58.42
TiO ₂	0.64	0.97	0.81	1.08	1.53	1.27	1.22	1.95	1.44
Al ₂ O ₃	16.57	14.48	14.05	15.39	16.74	17.72	16.01	14.32	15.52
Fe ₂ O ₃	3.55	3.40	0.31	7.23	7.68	4.43	4.07	4.32	0.16
FeO	3.91	0.85	0.88	1.74	3.35	5.97	6.25	5.79	7.84
MnO	0.16	0.07	0.10	0.12	0.27	0.18	0.18	0.19	0.15
MgO	5.72	0.27	1.23	1.93	3.82	3.56	3.93	3.25	2.89
CaO	9.24	2.61	3.42	5.94	7.30	8.53	7.85	6.77	6.28
Na ₂ O	2.52	4.29	3.98	3.38	4.65	3.30	3.59	4.02	4.07
K ₂ O	0.90	1.49	1.55	1.01	0.58	0.51	0.66	0.62	0.84
H ₂ O ⁺	-----	-----	1.89	1.26	2.02	0.88	0.30	0.76	0.47
H ₂ O ⁻	-----	-----	0.53	2.08	2.51	1.32	0.70	1.34	1.19
P ₂ O ₅	0.20	0.20	0.19	0.32	0.40	0.29	0.27	0.35	0.46
Total	98.41	98.63	100.80	99.87	100.96	100.18	100.26	100.21	99.72
Total Fe*	7.26	3.98	1.23	8.60	10.72	10.21	10.03	9.82	8.14
CIPW norms									
Q	8.51	32.92	31.82	17.23	0.00	5.45	7.67	11.21	13.18
Or	5.41	8.95	9.71	6.25	3.57	3.08	3.94	3.74	5.05
Ab	21.71	36.90	36.68	29.97	41.03	28.56	30.66	34.71	35.05
An	31.81	11.83	16.66	24.98	24.08	32.76	25.86	19.59	21.98
Di(C)	10.99	(1.57)	(0.07)	3.13	9.10	7.14	9.68	10.26	5.53
Hy	17.31	4.09	3.54	12.48	8.75	16.27	15.72	12.42	12.47
Ol	0.00	0.00	0.00	0.00	5.71	0.00	0.00	0.00	0.00
Mt	2.55	1.40	0.43	3.05	3.77	3.59	3.53	3.48	2.86
Il	1.24	1.87	1.63	2.15	3.03	2.47	2.34	3.78	2.78
Trace elements									
(ppm)									
Rb	21	36	59	19	9.1	8.5	11	1.0	13
Ba	250	469	411	243	160	183	213	250	305
Sr	470	226	221	357	360	416	421	407	417
Co	43	23	13.3	24	34	41	40	33	28
Ni	35	3	12	13	19	38	17	15	8.5
Cr	160	11	11	13	26	12	13	11	11
Zn	74	90	90	88	108	97	97	119	102
Cu	40	29	29	30	9.7	133	25	41	9.0
Li	15	24	15	12	39	5.9	13	8.6	24

*Total iron recalculated to Fe⁺², volatile-free.

APPENDIX B.

CHEMICAL ANALYSES OF ROCK SAMPLES

Table B.3. Rock chemistry, Lookout Point area, Lane County, Oregon. Sample localities are shown on Plate 5.--Continued

Sample no. on Plate 5	50	51	52	53	54	55	56
Geol. unit	Lavas of Black Canyon	Miocene andesitic lavas				Miocene-andesitic intrusives	Pliocene- Pleistocene(?) basaltic lavas
Map symbol	Tml	Tma	Tma	Tma	Tmi	Tmu	QTb
Sample no.	BB-227	BB-37	BB-PAT	BB-NSH	BB-SSL	BB-PPAT	BB-Tpba
Location	T20S/R2E/33Bda	T20S/R2E/23Bdc	T21S/R2E/7Cbd	T20S/R2E/14Dda	T20S/R2E/20	T21S/R1E/12Aba	T20S/R2E/18Acba
SiO ₂	57.00	55.99	58.97	67.28	60.64	51.30	54.42
TiO ₂	1.17	1.29	1.07	0.85	1.41	1.34	1.23
Al ₂ O ₃	15.88	16.15	16.85	15.63	15.23	16.23	17.11
Fe ₂ O ₃	5.69	2.72	3.84	3.49	2.78	-----	4.03
FeO	4.06	4.52	3.00	0.75	4.08	10.07	2.83
MnO	0.17	0.14	0.14	0.09	0.15	0.15	0.10
MgO	2.82	3.16	2.61	0.79	2.12	8.32	6.00
CaO	7.12	8.01	6.51	3.36	5.72	8.28	8.60
Na ₂ O	3.84	3.47	3.99	4.68	4.03	3.38	4.18
K ₂ O	0.65	0.63	1.00	1.98	1.12	1.25	1.37
H ₂ O ⁺	-----	1.50	-----	0.80	0.93	[0.00	0.15
H ₂ O ⁻	-----	2.05	-----	0.83	1.45		0.15
P ₂ O ₅	0.32	0.29	0.29	0.21	0.34	0.38	0.45
Total	98.72	99.92	98.27	100.74	100.00	100.70	100.62
Total Fe*	9.35	7.25	6.60	3.94	6.77	10.00	6.46
CIPW norms							
Q	11.34	12.15	13.38	23.34	17.42	0.00	0.00
Or	3.91	3.87	6.03	11.84	6.79	7.39	8.09
Ab	53.03	30.50	34.44	40.06	34.97	28.60	35.34
An	24.57	27.66	25.62	15.47	20.68	25.40	23.86
Di(C)	7.70	9.59	4.46	(0.18)	5.11	11.00	12.75
Hy	13.15	10.44	11.01	5.60	9.10	11.40	12.73
Ol	0.00	0.00	0.00	0.00	0.00	9.63	1.56
Mt	3.29	2.55	2.32	1.39	2.38	3.19	2.27
Il	2.26	2.55	2.07	1.63	2.75	2.54	2.33
Trace elements							
(ppm)							
Rb	14	10	20	47	23	-----	8.4
Ba	213	418	312	266	379	502	650
Sr	476	588	509	280	304	987	451
Co	33	31	25	15	23	50	30
Ni	3	11	11	10	16	161	139
Cr	6.5	15	22	11	14	236	255
Zn	116	97	95	80	97	90	86
Cu	12.8	47	32	7.4	55	67	75
Li	9.4	8.3	12	24	20	9	12

*Total iron recalculated to Fe⁺², volatile-free.

APPENDIX B.

CHEMICAL ANALYSES OF ROCK SAMPLES

Table B.4. Rock chemistry, Swift Creek area, Lane County, Oregon. Sample localities are shown on Plate 6.

Sample no. on Plate 6	57	58	59	60	61	62	63	64	65
Geol. unit	Older volcanoclastic sediments and lavas		Basaltic lavas of Tumblebug Creek						
Map symbol	Tmo	Tmo	Tmb	Tmb	Tmb	Tmb	Tmb	Tmb	Tmb
Sample no.	P-Tmo	P-604	T-1	T-2	T-3	T-4	T-7	T-9	T-10
Location	T23S/R5E/8Baa	T23S/R5E/9Acc	T24S/R4E/13Ada	T24S/R5E/19Baa	T24S/R5E/19Dbc	T24S/R4E/24Ddb	T24S/R5E/19Cba	T24S/R4E/24Dbc	T24S/R4E/24Caa
SiO ₂	55.70	56.50	49.40	54.40	53.20	53.40	52.80	51.60	54.85
TiO ₂	0.95	0.94	1.25	1.36	1.08	1.03	1.03	1.42	1.13
Al ₂ O ₃	18.54	18.61	16.12	16.57	17.40	16.43	17.75	17.14	17.06
Fe ₂ O ₃	[7.83	[7.69	6.02	6.38	3.70	3.18	3.17	4.02	4.31
FeO			3.08	2.65	5.09	5.56	5.58	5.19	3.36
MnO	0.13	0.06	0.17	0.16	0.18	0.16	0.16	0.17	0.15
MgO	4.48	3.74	6.40	5.37	5.21	6.56	5.32	6.13	4.47
CaO	7.63	6.60	7.99	8.62	8.32	8.63	9.00	8.50	8.60
Na ₂ O	3.28	2.76	3.18	3.48	3.53	3.26	3.67	3.50	3.43
K ₂ O	0.89	0.79	1.59	1.05	1.00	0.67	0.73	0.66	1.24
H ₂ O ⁺			-----	-----	-----	-----	-----	-----	-----
H ₂ O ⁻	[0.89	[2.48	-----	-----	-----	-----	-----	-----	-----
P ₂ O ₅	0.30	0.15	0.64	0.55	0.63	0.33	0.39	0.33	0.32
Total	100.62	100.32	95.84	100.59	99.34	99.21	99.60	98.66	98.92
Total FeO*	7.85	7.86	8.92	8.39	8.51	8.51	8.49	8.97	7.35
CIPW norms									
Q	8.21	14.80	0.00	4.12	2.81	3.16	1.11	0.64	5.52
Or	5.20	4.67	9.84	6.20	5.96	4.00	4.34	3.96	7.43
Ab	27.80	23.4	28.19	29.40	30.12	27.84	31.21	30.08	29.42
An	33.30	32.0	26.21	26.45	28.92	28.48	29.96	29.56	27.86
Di(C)	2.38	(1.49)	8.88	10.32	6.99	10.19	10.10	9.00	10.82
Hy	17.40	16.42	14.81	16.41	18.68	20.61	17.43	20.10	13.44
Ol	0.00	0.00	4.89	0.00	0.00	0.00	0.00	0.00	0.00
Mt	2.48	2.44	3.14	2.95	2.99	3.00	2.99	3.15	2.59
Il	1.80	1.82	2.49	2.58	2.07	1.97	1.97	2.74	2.18
Trace elements									
(ppm)									
Rb	-----	-----	25	14	11	6.5	5.0	6.2	21
Ba	293	179	708	438	456	267	409	311	483
Sr	694	602	745	819	854	759	815	569	508
Co	34	17	42	48	65	55	66	53	46
Ni	43	22	97	81	72	150	67	129	68
Cr	44	34	156	154	106	224	106	133	96
Zn	73	61	93	90	98	86	90	84	78
Cu	66	34	66	71	68	72	54	62	77
Li	6	13	13	11	11	8.3	9.5	8.8	9.1

*Total iron recalculated to Fe⁺², volatile-free.

**Outside map area.

APPENDIX B.

CHEMICAL ANALYSES OF ROCK SAMPLES

Table B.4. Rock chemistry, Swift Creek area, Lane County, Oregon. Sample localities are shown on Plate 6.--Continued

Sample no. on Plate 6	66	67	68	69	70	71	72	73	74
Geol. unit	Basaltic lavas of Tumblebug Creek								
Map symbol	Tmb	Tmb	Tmb	Tmb	Tmb	Tmb	Tmb	Tmb	Tmb
Sample no.	T-13	T-14	T-19	T-25	T-205a	P-50	P-624	P-626	T-F1ZZ
Location	T24S/R4E/25Abd	T24S/R4E/10Dcc	T24S/R5E/6Bac	T24S/R4E/2Ccntr.	T24S/R5E/23Cba**	T24S/R5E/28Cdd	T23S/R5E/30Cad	T23S/R5E/30Ccc	T24S/R5E/18Cbb
SiO ₂	53.20	53.60	53.20	51.00	51.20	53.93	53.40	56.00	53.93
TiO ₂	1.01	0.91	0.76	1.31	1.10	1.12	1.11	1.07	1.04
Al ₂ O ₃	17.58	17.54	17.27	18.10	17.26	17.01	17.36	17.61	16.65
Fe ₂ O ₃	4.31	4.49	5.21	4.91	5.69	3.03	3.07	-----	5.74
FeO	3.85	3.77	4.01	4.38	4.06	4.70	4.67	8.24	2.22
MnO	0.16	0.16	0.17	0.18	0.18	0.15	0.15	0.13	0.15
MgO	5.32	5.22	6.04	6.23	5.76	4.79	4.76	4.97	4.36
CaO	8.50	8.53	8.46	8.46	8.50	8.25	8.67	7.91	7.96
Na ₂ O	3.24	3.55	3.65	3.23	3.53	3.27	3.39	3.34	3.46
K ₂ O	0.83	0.83	0.61	0.56	0.87	1.02	1.06	1.12	1.25
H ₂ O ⁺	-----	-----	-----	-----	-----	-----	-----	[(0.21)	-----
H ₂ O ⁻	-----	-----	-----	-----	-----	-----	-----	-----	-----
P ₂ O ₅	0.37	0.38	0.36	0.40	0.44	0.26	0.30	0.30	0.54
Total	98.37	98.98	99.74	98.76	98.59	97.53	97.94	100.90	97.30
Total FeO*	7.89	7.93	8.77	8.95	9.37	7.64	7.61	8.18	7.64
CIPW norms									
Q	4.34	3.23	1.37	1.01	0.00	5.89	4.02	6.82	5.78
Or	5.00	4.97	3.63	3.36	5.23	6.19	6.40	6.68	7.62
Ab	27.94	30.43	31.06	27.75	30.40	28.41	29.33	28.30	30.21
An	31.57	29.86	29.10	33.75	29.19	29.49	29.67	29.70	27.05
Di(C)	7.29	8.56	8.77	5.06	8.83	8.80	10.03	6.38	8.23
Hy	18.27	17.53	20.70	22.46	18.75	15.75	15.01	16.90	15.09
Ol	0.00	0.00	0.00	0.00	1.13.	0.00	0.00	0.00	0.00
Mt	2.78	2.79	3.08	3.15	3.29	2.69	2.68	2.61	2.69
Il	1.96	1.75	1.45	2.53	2.13	2.18	2.16	2.03	2.04
Trace elements									
(ppm)									
Rb	10	10	6.2	2.0	10	16	15		21
Ba	598	400	339	477	546	399	417	375	559
Sr	538	560	598	538	626	514	561	563	556
Co	58	42	52	62	55	42	45	32	33
Ni	89	75	134	142	119	54	66	49	60
Cr	118	101	190	270	93	45	80	81	86
Zn	86	87	89	92	92	88	84	74	95
Cu	73	75	58	53	120	61	63	63	59
Li	9.1	9.9	9.8	9.2	10	6.5	7.8	9	7.8

*Total iron recalculated to Fe⁺², volatile-free.

**Outside map area.

APPENDIX B.

CHEMICAL ANALYSES OF ROCK SAMPLES

Table B.4. Rock chemistry, Swift Creek area, Lane County, Oregon. Sample localities are shown on Plate 6.--Continued

Sample no. on Plate 6	75	76	77	78	79	80	81	82 Miocene- Pliocene basal- tic lavas	83 Pleistocene basaltic rocks
Geol. unit	Andesitic lavas of Moss Mountain								
Map symbol	Tma	Tma	Tma	Tma	Tma	Tma	Tma	Tpb	Tpb
Sample no.	P-21	P-28	P-32	P-33	P-39	P-40	P-509	P-616	P-PHL
Location	T23S/R5E/9Bbd	T23S/R5E/20Bdc	T23S/R5E/19AcB	T23S/R5E/19Aca	T23S/R5E/19Bda	T23S/R5E/20Bdd	T23S/R5E/21Bdd	T23S/R5E/33Ddd	T23S/R5E/16Dcc
SiO ₂	53.50	55.70	55.78	55.60	52.60	56.15	56.29	51.20	48.70
TiO ₂	0.73	0.92	0.95	0.90	0.92	0.62	0.84	0.76	1.88
Al ₂ O ₃	19.29	18.58	18.31	18.01	19.96	18.37	18.27	17.53	15.78
Fe ₂ O ₃	3.93	4.04	2.13	3.62	3.57	4.04	3.36	5.12	
FeO	3.26	2.85	4.98	3.53	3.66	3.05	3.62	4.32	11.79
MnO	0.17	0.12	0.12	0.13	0.13	0.12	0.10	0.17	0.17
MgO	3.80	4.17	4.60	4.36	3.77	4.20	4.32	7.30	7.50
CaO	8.78	7.55	8.28	7.91	9.08	7.62	7.91	8.78	9.41
Na ₂ O	3.67	3.42	3.55	3.54	3.77	3.58	3.53	3.43	3.14
K ₂ O	0.60	0.71	0.70	0.74	0.45	0.72	0.73	0.70	1.26
H ₂ O ⁺	-----	-----	-----	-----	-----	-----	-----	-----	-----
H ₂ O ⁻	-----	-----	-----	-----	-----	-----	-----	-----	-----
P ₂ O ₅	0.17	0.15	0.14	0.15	0.14	0.15	0.14	0.27	0.55
Total	97.90	98.21	99.54	98.49	98.05	98.62	100.45	99.58	99.63
Total FeO*	6.97	6.64	6.95	6.92	7.03	6.81	6.72	9.01	11.77
CIPW norms									
Q	4.29	8.95	6.79	7.59	2.76	8.20	8.27	0.00	0.00
Or	3.63	4.28	4.16	4.45	2.72	4.33	4.36	4.17	7.45
Ab	31.80	29.54	30.19	30.48	32.60	30.79	30.19	29.23	26.60
An	35.21	33.94	32.12	31.61	37.00	32.45	32.19	30.59	25.20
Di(C)	6.77	2.69	6.72	5.98	6.64	4.07	5.34	9.35	14.90
Hy	14.04	16.13	15.44	15.38	13.70	16.21	15.34	14.78	3.04
Ol	0.00	0.00	0.00	0.00	0.00	0.00	0.00	6.64	13.06
Mt	2.45	2.33	2.44	2.43	2.48	2.40	2.37	3.17	3.74
Il	1.42	1.78	1.81	1.74	1.79	1.20	1.61	1.45	3.57
Trace elements									
(ppm)									
Rb	6.5	6.5	6.5	8.0	3.0	8.0	7.9	5.0	
Ba	179	180	203	181	217	180	150	429	570
Sr	744	744	784	763	885	767	822	659	852
Co	43	44	48	51	144	50	34	48	42
Ni	46	46	59	52	52	48	40	182	96
Cr	197	44	54	57	58	42	42	292	194
Zn	71	71	84	81	74	72	71	86	96
Cu	98	32	53	62	98	61	23	65	64
Li	7.1	7.1	6.3	7.1	8.4	5.8	7.4	10	9

*Total iron recalculated to Fe⁺², volatile-free.

**Outside map area.

APPENDIX B.

CHEMICAL ANALYSES OF ROCK SAMPLES

Table B.4. Rock chemistry, Swift Creek area, Lane County, Oregon. Sample localities are shown on Plate 6.--Continued

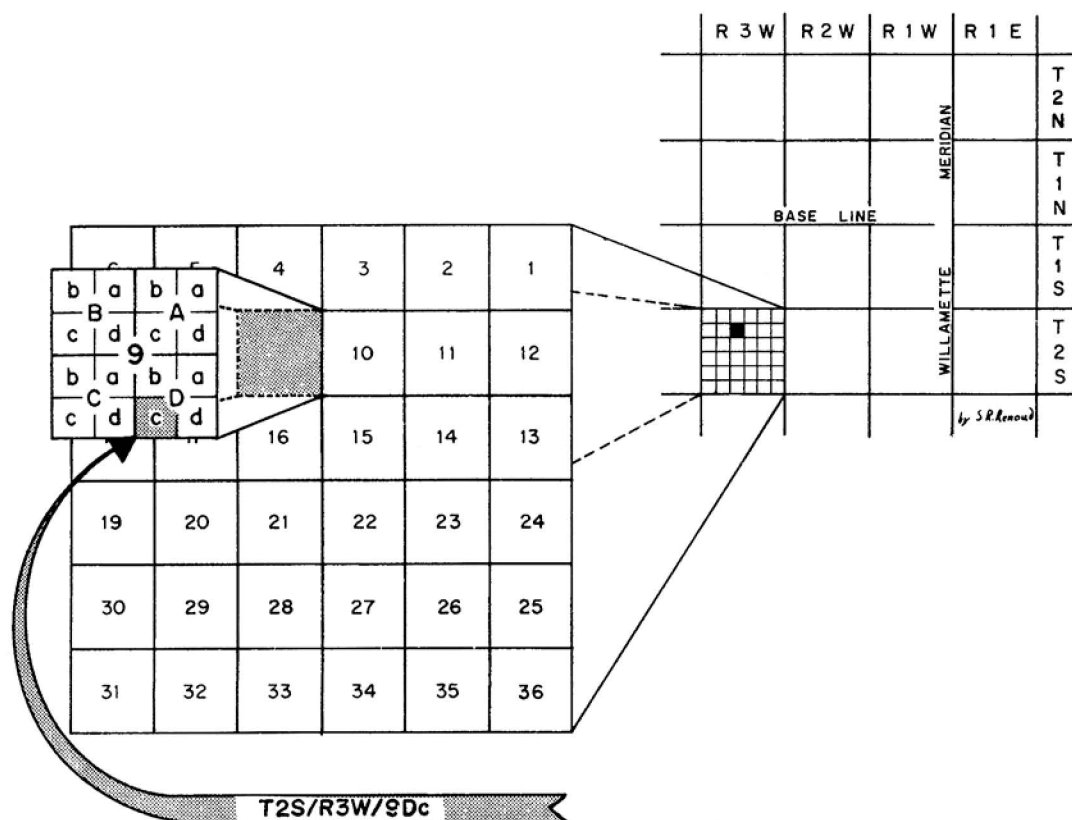
Sample no. on Plate 6	84	85	86	87	88	89
Geol. unit	Pleistocene basaltic rocks					Holocene(?)
Map symbol		Qb	Qb	Qb	Qb	air-fall pumice
Sample no.	P-22	P-Notch	T-208	T-210	T-211	Not shown
Location	T23S/R5E/9Bbb	T23S/R5E/14Bdd	T24S/R5E/16Cdb	T24S/R5E/18Add	T24S/R5E/18Dac	P-302 T23S/R5E/15Cntr.
SiO ₂	53.30	57.04	52.20	52.80	50.32	33.74
TiO ₂	0.81	0.83	1.29	1.03	1.27	0.92
Al ₂ O ₃	17.62	18.39	16.82	17.50	17.01	8.25
Fe ₂ O ₃	4.13	2.90	5.33	4.74	6.81	0.92
FeO	3.74	4.00	4.07	3.69	2.19	0.90
MnO	0.14	0.14	0.18	0.17	0.14	0.03
MgO	6.41	2.99	6.89	6.56	5.57	0.52
CaO	8.53	7.35	8.90	8.10	9.02	1.66
Na ₂ O	3.74	4.02	3.57	3.82	2.85	2.30
K ₂ O	0.82	1.07	0.70	0.71	0.39	1.05
H ₂ O ⁺	-----	-----	-----	-----	-----	6.51
H ₂ O ⁻	-----	-----	-----	-----	-----	42.96
P ₂ O ₅	0.32	0.37	0.33	0.39	0.33	0.06
Total	99.54	99.10	100.28	99.51	100.70	99.82
Total FeO*	7.53	6.69	8.89	8.04	8.74	3.45
CIPW norms						
Q	0.21	8.37	0.00	0.00	4.08	23.61
Or	4.88	6.39	4.14	4.23	2.41	12.34
Ab	31.87	34.37	30.22	32.58	25.27	38.67
An	29.07	29.28	27.81	28.73	34.03	15.59
Di (C)	9.37	4.23	11.52	7.46	8.64	(0.91)
Hy	19.71	12.55	17.98	21.21	19.16	3.90
Ol	0.00	0.00	1.99	0.10	0.00	0.00
Mt	2.65	2.35	3.13	2.83	3.07	1.21
Il	1.55	1.59	2.45	1.97	2.53	3.47
Trace elements						
(ppm)						
Rb	10	15	6.9	11	9.7	22
Ba	412	444	302	382	230	380
Sr	898	683	738	673	696	166
Co	59	30	51	44	36	0
Ni	158	68	134	156	76	7.8
Cr	197	51	219	253	145	11
Zn	79	80	92	92	114	22
Cu	98	66	57	52	56	10
Li	10	11	10	12	13	15

*Total iron recalculated to Fe⁺², volatile-free.

**Outside map area.

APPENDIX C.

EXPLANATION OF THE TOWNSHIP-RANGE LOCATION SYSTEM



Locations listed in this report are designated according to official systems for the rectangular subdivision of public lands. The numbers indicate the location by township, range, section, and position within the section. In the symbol T2S/R3W/9Dc, the "T2S" indicates the township south of the base line and "R3W" the range west of the Willamette Meridian. The "9" indicates the section, "D" the quarter section, and "c" the 40-acre plot within that quarter.

APPENDIX D.

TEMPERATURE AND HEAT-FLOW DATA

Table D.1. Temperature and heat-flow data for the Oregon Cascades

Location	Prov. ^a	N. lat. deg.-min.	W. long. deg.-min.	Hole name (date)	Hole type ^b	Collar elev. (m)	Total depth (m)	Depth interval (m)	Average thermal conductivity	Uncorr. grad. ^c °C/km (1σ)	Corr. grad. ^c (°C/km)	Corr. heat flow ^c mW/m ²	Quality ^d	Lithologic summary
T6S/R1E/13Da	WC	45-2.8	122-37.2	TWW (10/6/76)	WW	326	140	35-95 95-140	1.59 (1.17)	26.2 (0.1) 34.7 (0.7)	28.6 37.7	45 44	A A	Basalt and siltstone
T6S/R1E/35Cb	WC	45-0.3	122-39.4	MC-WW (10/6/76)	WW	285	195	95-195	(1.17)	30.9 (0.2)	34.3	40	C	Siltstone
T6S/R2E/18Ba	WC	45-3.3	122-36.7	QWW (10/6/76)	WW	259	90	55-90	----	29.1 (0.5)	29.0	--	B	Oligocene marine sediments
T6S/R6E/23Ca1	WC	45-1.8	122-2.7	DH-5000 (11/4/75)	FS	487	22.5	15-22.5	----	70 (4.3)	----	--	D	Oligocene and Miocene volcanics
T6S/R6E/34Cd	WH	44-60.0	122-3.8	RDHCRCR (9/30/76)	TG	487	150	10-150	1.64 (0.04)	81.8 (0.5)	65.0	106	A	Diorite sill, basalt
T6S/R7E/4Dc	HC	45-4.3	121-57.6	RDHCRKH (7/25/77)	TG	686	40	0-38	----	----	----	--	X	Porphyritic andesite
T6S/R7E/21Cd	WH	45-1.8	121-57.7	AUST HSE (6/29/77)	TG	603	40	10-40	1.47 (0.07)	231.6 (8.7)	162.8	239	B	Basalt, tuff and andesite
T6S/R7E/30Bb	WH	45-1.3	122-0.5	RDHCRAHS (9/30/76)	TG	512	132.5	95-130	1.65 (0.08)	240.7 (2.0)	169.5	279	B	Basalt, tuff and rhyolite
T7S/R1E/11Aca	WC	44-58.8	122-38.8	OW-W1 (7/ /62)	OW	214	2379	0-2379	(1.59)	26.0	26.0	41	C	Eugene and Spencer Fms.
T7S/R7E/4Dd	HC	44-59.0	121-57.0	EWEB-TS (5/28/80)	TG	1273	193.5	165-190	1.62 (0.04)	----	----	--	X	Basalt (Q)
T7S/R8E/5Dd	HC	44-59.0	121-50.8	EWEB-PC (5/28/80)	TG	975	187	70-185	1.58 (0.04)	----	----	--	X	Basalt (Q)
T7S/R8E/10Ad	HC	44-58.5	121-48.4	EWEB-CC (5/30/80)	TG	1140	137	110-137	1.45 (0.10)	----	----	--	X	Basalt (Q)
T7S/R5E/22Aa	WC	44-57.1	122-10.4	CR-BHS (9/30/76)	TG	655	152	20-90	1.46 (0.05)	84.3	66.8	97	B	Basalt, 10-85 m
T8S/R1W/32Bb	WC	44-50.3	122-50.4	SWW (9/27/76)	WW	115	80	30-80	(1.59)	34.4 (0.4)	34.4	54	C	Basalt
T8S/R2W/24Bc	WC	44-51.7	122-53.0	CWW (8/10/76)	WW	127	61	22.5-60	(1.59)	24.7 (0.2)	24.7	39	C	Col. Riv. Basalt
T8S/R1E/8Db	WC	44-53.3	122-42.5	H-1-WW (10/8/76)	WW	303	218	95-215	1.72	27.6 (0.1)	27.6	47	B	Basalt
T8S/R1E/9Bd	WC	44-53.47	122-41.63	WOLFF (4/30/80)	WW	338	100	30-100	----	34.9 (4.7)	----	--	C	Basalt
T8S/R1E/17Da	WC	44-52.3	122-42.3	SM-WW (10/6/76)	WW	315	112	10-110	(1.59)	28.5	27.0	43	C	Basalt
T8S/R5E/31Cc	WC	44-49.9	122-14.8	CDR CRK (10/26/77)	ME	705	345	35-345	1.80 (0.33)	32.3 (0.5)	28.6	51	A	Volcanics
T8S/R8E/6Dd	HC	44-54.3	121-52.9	EWEB-SB (4/29/80)	TG	860	460	150-460	1.49 (0.13)	71.5 (1.1)	63.3	94	B	Basalt and andesite
T8S/R8E/31C	HC	44-50.0	121-52.9	CUB-CRK (9/28/79)	TG	1072	98	70-98	1.47 (0.08)	37.8 (1.4)	34.0	50	C	Basalt and andesite
T9S/R2E/21Da	WC	44-46.2	122-33.6	G1-WW (10/7/76)	WW	213	49	22.5-47.5	1.26	53.2 (2.4)	47.5	59	B	Tuffs and clays
T9S/R3E/11Ba	WC	44-48.5	122-24.5	EV2-WW (10/14/76)	WW	317	85	47.5-85	1.34	27.3 (0.8)	24.0	32	B	Clay

APPENDIX D.

TEMPERATURE AND HEAT-FLOW DATA

Table D.1. Temperature and heat-flow data for the Oregon Cascades --Continued

Location	Prov. ^a	N. lat. deg.-min.	W. long. deg.-min.	Hole name (date)	Hole type	Collar elev. (m)	Total depth (m)	Depth interval (m)	Average thermal conductivity	Uncorr. grad.C °C/km (1σ)	Corr. grad.C (°C/km)	Corr. heat flowC mW/m ²	Quality ^d	Lithologic summary
T9S/R3E/11Cb	WC	44-48.1	122-24.8	EV1-WW (10/7/76)	WW	333	67	25-60	1.34	26.5 (0.1)	23.6	31	B	Clay and sandstone
T9S/R3E/28Cb	WC	44-45.4	122-27.1	GR-WW (10/14/76)	WW	268	55	25-52.5	----	30.0	28.0	--	C	-----
T9S/R6E/23Bb	WH	44-47.0	122-2.4	RDH-BHSW (9/30/76)	TG	550	150	30-105	1.61 (0.11)	67.6 (0.4)	55.7	89	B	Crystal lithic tuff
T9S/R7E/20Aa	WH	44-46.9	121-58.3	BEAMER 3 (4/29/80)	WW	677	309.5	5-35	1.27 (0.13)	1300	1100	1393	B	Tuff, clay, and basalt
								0-309.5	1.55 (0.13)	277.2	261.0	404	B	
T9S/R7E/20Ac	WH	44-46.9	121-58.6	BEAMER 1 (2/6/78)	WW	682	150	0-150	(1.46)	600.0	521.7	763	D	Tuff, clay, and basalt
T9S/R7E/20Ad	WH	44-46.8	121-58.3	BEAMER 2 (4/29/80)	WW	680	74	6-74	1.27 (0.13)	407.3 (40.3)	339.4	430	B	Tuff, clay, and basalt
T9S/R7E/21Ad	WH	44-46.7	121-57.1	RDH-BHSE (9/30/76)	TG	725	152	90-150	1.65 (1.17)	92.9 (1.4)	82.6	135	B	Tuff, clays and basalt
T10S/R5E/30cc	WH	44-43.7	122-10.8	FS-DRSWW (6/26/78)	WW	518	180.5	10-170	(1.17)	52.0	43.2	50	C	Volcanics
T10S/R7E/11Aa	HC	44-43.4	121-54.4	RDH-DVCK (11/5/79)	TG	1194	155	70-150	1.40 (0.04)	83.5 (1.6)	72.6	101	B	Basalt
T11S/R1W/14Dd	WC	44-36.5	122-45.9	BL-WW (10/4/76)	WW	182	160	30-125	1.17 (1.59)	41.3 (0.3)	42.3	49	B	Claystone
T11S/R1W/32Bbb	WV	44-36.6	122-50.6	OW-LCD (12/11/58)	OW	108	1350	0-1345	(1.59)	18.9	18.9	30	C	Tuff, basalt, silt- stone
T11S/R1E/7Da	WC	44-37.5	122-43.3	RL-WW (10/13/76)	WW	158	58	40-57.5	1.34 (1.4)	28.1 (4.1)	26.7	35	C	Claystone
T11S/R6E/22Db	WH	44-36.01	122-3.39	BUCK MTN (7/31/80)	TG	1333	152	30-50	----	90.8 (4.1)	----	--	X	0-110 m andesite
T11S/R7E/10Dc	HC	44-37.6	121-56.1	RDH-MTCK (7/31/80)	TG	762	109	30-109	1.64 (0.13)	68.4 (3.7)	64.0	105	D	Basalt, andesite, and mudflows
T11S/R10E/5Acb	DU	44-38.78	121-33.47	CASTLERX (7/23/80)	TG	1194	153	25-153	----	18.2 (1.1)	----	--	X	Lavas with auto- breccia
T12S/R1W/4Dc	WC	44-33.1	122-48.6	B-9 (10/29/74)	WW	135	65	30-65	1.34 (0.13)	37.1 (1.0)	36.4	50	A	Volcanic conglomerate
T12S/R1W/30Ca	WC	44-29.7	122-51.3	MC PHRSON (4/10/79)	WW	219	125	180-125	(1.59)	34.2 (0.4)	34.2	54	B	Basalt
T12S/R1W/30Db	WC	44-29.7	122-51.1	LEBN GLF (4/10/79)	WW	170	70	40-70	(1.59)	28.3 (1.0)	28.3	45	C	Basalt
T12S/R7E/9Da	HC	44-32.7	121-57.8	EWEB-TM (5/29/80)	TG	1195	600	300-600	1.36 (0.08)	71.4 (1.3)	69.4	94	B	Volcanics
T12S/R9E/1Bcd	DU	44-33.70	121-36.42	GREENRDG (7/23/80)	TG	999	152	70-105	(1.60)	79.2 (1.5)	(63.4)(101)		B	Tuff, conglomerate, basalt
T13S/R2W/3Aa	WV	44-28.3	122-54.4	TVR-WW (8/25/76)	WW	317	95	40-95	1.34 (0.5)	29.0 (0.5)	29.4	39	B	Sandstone and basalt

APPENDIX D.

TEMPERATURE AND HEAT-FLOW DATA

Table D.1. Temperature and heat-flow data for the Oregon Cascades --Continued

Location	Prov. ^a	N. lat. deg.-min.	W. long. deg.-min.	Hole name (date)	Hole type ^b	Collar elev. (m)	Total depth (m)	Depth interval (m)	Average thermal conductivity	Uncorr. grad. ^c °C/km (σ)	Corr. grad. ^c (°C/km)	Corr. heat flow ^c mW/m ²	Quality ^d	Lithologic summary
T13S/R2W/18Cb	WV	44-26.2	122-59.1	WB-WW (8/25/76)	WW	378	198	95-190	(1.59)	15.5 (0.1)	25.8	37	C	Basalt
T13S/R1W/8Db	WC	44-27.1	122-49.9	RJ-WW (10/12/76)	WW	329	95	15-95	(1.59)	19.0 (0.3)	20.0	31	B	Basalt
T13S/R1W/10Ca	WC	44-27.1	122-47.7	BJ-WW (8/11/76)	WW	149	62.5	27.5-62.5	1.34	23.3 (0.6)	22.7	30	C	Claystone and sediments
T13S/R1E/20Ba	WC	44-25.9	122-43.0	MR-WW (8/11/76)	WW	402	130	90-130	(1.34)	33.6 (1.8)	39.9	53	C	Basalt and sandstone
T13S/R1E/35Ab	WC	44-24.1	122-38.9	MWW (8/11/76)	WW	310	152	90-150	(1.34)	31.5 (0.3)	37.4	50	C	Consolidated sedi- ments, basalt, sand- stone
T13S/R7E/9Abb	WC	44-27.7	121-58.97	DETRO-FM (7/23/80)	WW	1128	79	----	----	----	----	--	X	Olivine basalt
T13S/R7E/32Dc	HC	44-23.3	121-59.7	EWEB-CL (10/30/79)	TG	955	557	50-205	1.44	112.0 (2.2)	102.8	148	B	Andesite and volcanics
								0-555	1.40	25.6 (11.4)	23.9	33	C	
T13S/R10E/5Ab	DU	44-28.75	121-33.41	FLY CRK (7/24/80)	TG	1194	120	----	----	----	----	--	X	Basaltic andesite
T14S/R6E/32Dc	WH	44-18.2	122-7.3	WOLF MDW (8/1/80)	TG	999	155	42.5-155	1.46 (0.13)	87.2 1.6	72.7	110	B	Altered basalt and breccia
T14S/R3W/24Dc	WV	44-20.0	122-59.6	NWW (10/1/76)	WW	207	47.5	10-47.5	(1.59)	24.7 (0.4)	25.0	39	D	Claystone
T15S/R6E/11Dc	WH	44-16.1	122-3.3	RDHCRTBR (7/26/77)	TG	716	64	0-52	----	----	----	--	X	Basalt and cinders
T15S/R7E/28Aa	WH	44-14.8	121-58.4	RDH-CRSM (7/26/77)	TG	1143	55	----	----	----	----	--	X	Basalt and cinders
T15S/R10E/5Bb	HC	44-18.3	121-34.4	CENTWEST (4/5/80)	WW	978	106	10-30	----	104.8 (14.5)	----	--	C	----
T16S/R2E/26Bc1	WC	44-9.0	122-32.5	OH-2Z (11/26/75)	FS	310	30	20-30	----	25.0 (0.6)	----	--	X	----
T16S/R4E/14Db	WC	44-10.1	122-17.5	BH-3Z (11/26/75)	FS	457	45	12.5-45	1.80 (0.33)	37.8 (0.4)	35.0	63	D	Volcanics
T16S/R5E/30Ab	WH	44-9.2	122-14.9	DDH-15 (6/26/78)	FS	367	85	15-85	1.33	54.0	51.0	68	D	Tuff and basalt
T16S/R5E/30Ab	WH	44-9.1	122-15.0	ST DAM 1 (8/8/79)	FS	368	80	45-70	----	55.9 (2.8)	53.0	--	C	Alluvium
T16S/R5E/30Aa	WH	44-9.3	122-14.6	ST DAM 2 (8/8/79)	FS	389	87	25-61	1.32	56.3 (1.2)	53.0	70	C	Tuff
T16S/R6E/2Ca	WH	44-12.1	122-3.0	RDH-CRFP (8/5/76)	TG	701	150	100-150	1.74 (0.03)	84.1 (1.4)	88.3	153	C	Andesite
T16S/R6E/27Bb	WH	44-9.1	122-4.7	RDH-CRHC (9/29/76)	TG	573	152	30-150	1.57 (0.05)	96.2 (0.9)	70.9	111	B	Basalts and tuffs
T17S/R1W/26Da	WC	44-3.7	122-47.1	CWW (9/29/76)	WW	327	145	20-145	(1.59)	26.2 (0.2)	25.6	40	B	Basalt and cinders

APPENDIX D.

TEMPERATURE AND HEAT-FLOW DATA

Table D.1. Temperature and heat-flow data for the Oregon Cascades --Continued

Location	Prov. ^a	N. lat. deg.-min.	W. long. deg.-min.	Hole name (date)	Hole type ^b	Collar elev. (m)	Total depth (m)	Depth interval (m)	Average thermal conductivity	Uncorr. grad. ^c °C/km (1σ)	Corr. grad. ^c (°C/km)	Corr. heat flow ^c mW/m ²	Quality ^d	Lithologic summary
T17S/R1W/32Cc	WC	44-2.5	122-50.5	DWW (10/1/76)	WW	292	133	50-130	(1.17)	35.4 (0.9)	37.7	44	B	Pyroclastics or sediments
T17S/R2W/36Ca	WC	44-2.8	122-52.7	79S-WW (9/29/76)	WW	213	106	40-105	(1.17)	29.5 (0.3)	26.7	31	C	Claystone
T17S/R5E/8Ac	WH	44-6.4	122-14.0	WLKR-CR (7/24/80)	TG	585	155	105-155	(1.59)	54.1 (0.7)	52.0	83	B	Pyroxene andesite
T17S/R5E/20Ba	WH	44-4.9	122-13.8	R1DR-CRK (7/31/80)	TG	536	154	60-154	2.64 (0.04)	128.5 (3.6)	97.5	159	B	Andesite
T17S/R6E/25Ad	HC	44-3.9	122-1.4	RDH-MQCK (8/1/80)	TG	1005	152	115-152	1.55	62.8 (1.4)	73.8	114	C	Basaltic andesite
T18S/R2W/4Ad	WC	44-2.2	122-55.8	HB-WW (9/2/76)	WW	175	125	45-125	(1.17)	38.0 (0.5)	36.1	42	B	Claystone, sandstone
T18S/R1W/32Cc	WC	43-57.3	122-50.4	PR-WW (8/26/76)	WW	192	215	70-215	(1.17)	39.4 (0.3)	38.4	45	B	Claystone
T18S/R5E/11Bd	WH	44-1.1	122-9.8	RDH-RBCK (7/31/80)	TG	780	152	55-78	1.55	34.4 (1.0)	36.6	56	C	Basaltic andesite
T19S/R2W/2Ac	WV	43-56.9	122-53.8	JA-WW (8/19/76)	WW	231	120	25-120	(1.26)	35.5 (0.3)	34.6	43	C	Sandstone, shale
T19S/R2W/10Ad	WV	43-55.9	122-54.6	ER-WW (9/30/76)	WW	218	108	42.5-105	(1.17)	34.6 (0.5)	31.5	36	B	----
T19S/R4E/29Cc	WC	43-53.0	122-22.15	CHRS-CRK (7/31/80)	TG	579	154	70-154	1.75 (0.09)	64.0 (1.1)	52.3	92	B	Silicified dacite plug
T19S/R5E/27B	WH	43-53.1	122-12.61	BRCK-CRK (7/31/80)	TG	987	154	135-154	1.75 (0.09)	65.8 (0.4)	65.6	115	B	Olivine basalt flow
T19S/R6E/8Ba	HC	43-57.0	122-1.8	RDHELKCK (7/9/80)	TG	877	135	40-135	1.22 (0.04)	43.2 (1.0)	33.3	41	B	Sand and gravel
T19S/R6E/25Dc	HC	43-53.0	122-4.11	N. FORK (7/31/80)	TG	951	154	30-154	1.35 (0.05)	78.4 (5.1)	67.5	91	B	Olivine basalt
T20S/R2E/35Ac	WC	43-47.5	122-32.0	BTBR-CRK (7/2/80)	TG	160	155	20-155	(1.41)	42.6 (2.3)	34.1	48	B	Lithic-rich laharic tuff
T20S/R3E/26Cd	WC	43-47.9	122-25.2	AE-WW (8/19/76)	WW	707	124	10-80	(1.59)	25.8 (0.5)	25.6	40	B	Basalt and cinders
T20S/R3E/26Da	WC	43-48.0	122-25.0	CS-WW (9/28/76)	WW	719	142	45-70	(1.59)	25.3 (1.8)	25.1	39	B	Basalt and cinders
								70-140	(1.17)	39.0 (0.5)	38.8	45	B	
T20S/R4E/27Dd	WC	43-47.9	122-18.8	WALL-CRK (7/11/80)	TG	582	137	30-135	1.13 (0.13)	72.6 (0.9)	60.5	69	B	Tuff
T21S/R3E/10Ad	WC	43-45.6	122-25.9	FC-WW (9/28/76)	WW	548	100	25-100	(1.17)	36.5 (0.5)	35.6	41	B	Quaternary basalt
T21S/R3E/17Da	WC	43-44.8	122-28.3	OAKR-CW6 (11/8/80)	TG	345	345	70-240	(1.82)	47.7 (2.9)	40.5	74	B	Sandstone
								240-340	(1.84)	42.3	36.0	66	B	
T21S/R3E/26Caa	WC	43-43.05	122-25.17	HILLSCDRM (11/8/80)	TG	427	160	30-160	(3.71)	36.9	31.3	116	B	Silicified volcanics

APPENDIX D.

TEMPERATURE AND HEAT-FLOW DATA

Table D.1. Temperature and heat-flow data for the Oregon Cascades --Continued

Location	Prov. ^a	N. lat. deg.-min.	W. long. deg.-min.	Hole name (date)	Hole type ^b	Collar elev. (m)	Total depth (m)	Depth interval (m)	Average thermal conductivity	Uncorr. grad. ^c °C/km (1σ)	Corr. grad. ^c (°C/km)	Corr. heat flow ^c mW/m ²	Quality ^d	Lithologic summary
T21S/R4E/28Ad	WH	43-43.1	122-20.0	CR-MCHSE (9/29/76)	TG	533	154	10-150	1.67	82.3 (0.4)	60.0	99	B	Intrusives, lithic tuff
T21S/R5E/16Ac	WH	43-44.9	122-13.0	BLCK-CRK (8/1/80)	TG	829	104	45-104	----	6.2 (0.6)	----	--	X	Basalt
T21S/R11E/25Bb	HL	43-43.9	121-21.7	BFZ-MB (8/4/76)	TG	1515	35	27.5-35	1.51	65.3 (4.3)	65.3	100	C	Obsidian and cinders, rhyolite
T22S/R3E/10Dd	WC	43-40.3	122-27.0	PCCPG-WW (6/28/78)	WW	490	106	20-90	1.33	39.0 (0.6)	40.0	53	B	Claystone, sandstone
T22S/R5E/26Bc	WH	43-38.2	122-11.3	RDH-MHSW (9/29/76)	TG	975	155	30-150	1.97 (0.06)	54.0 (0.4)	51.8	102	B	Amgydaloidal basalt, andesite
T23S/R5E/8Da	WH	43-35.5	122-14.0	PNTD-CRK (8/1/80)	TG	1219	154	40-154	1.52 (0.04)	83.3 (3.3)	66.1	101	B	Andesite and tuff
T23S/R9E/36Bb	HC	43-32.6	121-36.1	SH-WW (10/1/75)	WW	1320	130	----	----	----	----	--	X	Basalt (QTb)
T24S/R5E/18Ca	WH	43-29.4	122-15.9	TBUG-CRK (8/1/80)	TG	951	155	35-154	----	54.2 (8.6)	----	--	C	Basalt and altered basalt
T24S/R7E/7Db	HC	43-30.3	121-55.8	WP-WW (10/5/76)	WW	1463	45	----	----	----	----	--	X	Quaternary basalt
T26S/R2W/23Aa	WC	43-17.8	122-53.5	SUSCRCPG (7/24/81)	WW	289	52	----	----	----	----	--	-	Alluvium and basalt(?)
T26S/R3E/25Aa	WH	43-17.0	122-24.0	PPL-TCS (7/23/81)	WW	780	25	7.5-25	----	41.7	----	--	C	----
T28S/R8E/5Aa	BR	43-10.8	121-47.0	SHD-1 (8/25/73)	WW	1430	75	----	----	----	----	--	X	----
T29S/R6E/9Bc	HC	43-5.6	122-5.4	CLKPRK (8/2/81)	WW	1844	305	----	----	----	----	--	X	Pyroclastics
T31S/R2W/11Bc	WC	42-54.2	122-56.0	JWILSON (7/21/81)	WW	466	67.5	----	----	----	----	--	-	Silicic lithic tuffs
T31S/R3E/3Da	WH	42-54.2	122-26.5	USFS-NUC (7/23/81)	WW	1024	52.5	----	----	----	----	--	X	Silicic pyroclastics, basalt
T32S/R2W/4Ca	WC	42-49.0	122-56.4	CLR-7 (12/29/72)	WW	937	215	105-215	2.93 (0.17)	20.5 (0.4)	20.9	61	A	Chlorite schist
T32S/R3E/29Ba	HC	42-45.8	122-29.3	USFSPRS (7/23/81)	WW	805	46	----	----	----	----	--	X	High Cascade clas- tics
T33S/R2E/11Ac	WC	42-43.0	122-32.7	WILDWOOD (8/7/77)	WW	705	60	----	----	----	----	--	X	----
T33S/R2E/17Add	WC	42-42.1	122-35.9	LCRKDAM2 (7/22/81)	FS	597	92.5	----	----	----	----	--	-	Basalt
T33S/R2E/17Adc	WC	42-42.2	122-36.0	LCRKDAM1 (7/22/81)	FS	683	131	----	----	----	----	--	-	Basalt
T33S/R2E/19Dd	WC	42-40.9	122-37.3	DMND-CRK (8/18/77)	WW	592	45	----	----	----	----	--	X	----
T34S/R1W/4Dd	WC	42-38.3	122-49.2	MARTINSN (7/31/81)	WW	491	212	----	----	----	----	--	-	Basalt and andesite

APPENDIX D.

TEMPERATURE AND HEAT-FLOW DATA

Table D.1. Temperature and heat-flow data for the Oregon Cascades --Continued

Location	Prov. ^a	N. lat. deg.-min.	W. long. deg.-min.	Hole name (date)	Hole type ^b	Collar elev. (m)	Total depth (m)	Depth interval (m)	Average thermal conductivity	Uncorr. grad. ^c °C/km (1σ)	Corr. grad. ^c (°C/km)	Corr. heat flow ^c mW/m ²	Quality ^d	Lithologic summary
T34S/R1E/34Aa	WC	42-34.5	122-40.7	JVARGO (7/30/81)	WW	548	40	7.5-35	----	49.7	----	--	C	Volcanics
T34S/R1E/34Bb	WC	42-34.7	122-41.6	MATHER (7/31/81)	WW	555	52.5	10-52.5	----	33.2	----	--	C	Basalt flows(?)
T35S/R2W/28Cc	WC	42-29.5	122-57.1	SAMS VAL (8/9/77)	WW	389	165	30-165	(1.88)	16.7 (0.5)	17.0	33	B	Claystone
T35S/R2W/30Da	WC	42-29.8	122-58.5	SAMS VLF (8/9/77)	WW	395	85	10-85	(1.88)	19.2 (1.7)	19.0	33	B	Claystone
T35S/R1E/13Ad	WC	42-31.8	122-38.3	RAMBO (8/15/77)	WW	853	40	25-40	(1.59)	29.6 (1.4)	31.0	49	C	Basalt (Miocene)
T36S/R2W/31Dc	WC	42-23.4	122-58.7	WLWCK-2 (8/10/77)	WW	443	150	95-150	(1.88)	12.9 (0.1)	12.0	40	B	Mudstone
T36S/R2W/31Dd	WC	42-23.3	122-58.8	WLWCK-1 (8/10/77)	WW	437	40	----	----	----	----	--	X	----
T36S/R1E/18Cc	WC	42-26.1	122-45.3	OWENS (8/10/77)	WW	437	45	10-45	----	35.3 (1.3)	35.3	--	B	Volcanic flows
T37S/R2W/34Dc	WC	42-18.2	122-55.3	JCKSNVIL (8/10/77)	WW	449	40	20-40	----	19.6 (1.4)	18.0	--	C	Mudstone
T37S/R1W/27Cb	WC	42-19.4	122-48.7	PHOEN-BL (8/9/77)	WW	529	220	75-220	(1.88)	25.0	24.0	46	B	Mudstone
T37S/R2E/4Ad	WC	42-23.0	122-34.8	MORTEN (8/27/81)	WW	561	96.5	30-96.5	----	34.6	----	--	-	Basalt
T37S/R7E/15Ba	BR	42-21.4	121-59.0	WEYEH (75)	--	---	---	-----	----	----	----	42	D	----
T38S/R2E/25Bb	WC	42-14.6	122-32.4	MILLER (8/26/81)	WW	1164	29	10-29	----	50.0	----	--	C	Volcanic sediments and basalts
T38S/R2E/27Ca	WC	42-14.2	122-34.2	HARRGTON (8/81)	WW	963	46	20-46	----	68.8	----	--	C	Andesite(?)
T38S/R2E/35Ac	WC	42-13.4	122-32.4	JM MILLR (8/4/81)	WW	1231	45	15-45	----	14.3	----	--	C	Basalt
T38S/R3E/12Ad	WH	42-17.0	122-24.5	LILYGLEN (8/4/81)	WW	1400	38.5	-----	----	----	----	--	-	Sediments and basalt
T38S/R9E/20Ac	BR	42-15.1	121-46.9	PH-WW (8/21/74)	WW	1329	465	0-465	> 0.75	160.0	160.0	121	C	----
T38S/R9E/28Ac	BR	42-14.3	121-46.0	MOLATORE (6/16/79)	WW	1359	170	105-170	----	71.9	----	--	C	----
T38S/R9E/28Dc	BR	42-14.0	121-46.8	BH-WW (7/17/74)	WW	1292	78	0-78	> 0.75	950.0	950.0	715	C	----
T38S/R9E/29Aa	BR	42-14.4	121-46.6	PF-WW (7/18/74)	WW	1277	60	0-59	> 0.75	130.0	130.0	98	C	----
T38S/R9E/32Da	BR	42-13.2	121-46.6	MODOC LMR (9/22/81)	WW	1247	631	380-625	----	186	----	--	B	----
T38S/R9E/33Ab	BR	42-13.6	121-45.7	AG-WW (7/17/74)	WW	1262	109	0-109	> 0.75	716.0	716.0	537	C	----
T39S/R1E/2Bc	WC	42-12.7	122-40.6	COOK (8/4/81)	WW	622	180	20-177	----	27.5	----	--	A	Siltstone and sand- stone

APPENDIX D.

TEMPERATURE AND HEAT-FLOW DATA

Table D.1. Temperature and heat-flow data for the Oregon Cascades --Continued

Location	Prov. ^a	N. lat. deg.-min.	W. long. deg.-min.	Hole name (date)	Hole type ^b	Collar elev. (m)	Total depth (m)	Depth interval (m)	Average thermal conductivity	Uncorr. grad. ^c °C/km (1σ)	Corr. grad. ^c (°C/km)	Corr. heat flow ^c mW/m ²	Quality ^d	Lithologic summary
T39S/R1E/4Bb	WC	42-12.7	122-42.8	ASLDGRHSE (10/14/81)	WW	536	136	18-136	----	76.5	----	--	C	-----
T39S/R1E/13Da	WC	42-31.6	122-38.5	RAMBO (8/1/81)	WW	884	69	40-68	----	21.1	----	--	C	-----
T39S/R1E/15Cdb	WC	42-10.4	122-41.3	STURDEVNT (8/3/81)	WW	731	257	----	----	18.0	----	--	-	-----
T39S/R1E/32Ac	WC	42-08.1	122-43.5	WC 1	TG	1025	310	283-310	3.05 (0.06)	16.27 (0.08)	----	42	A	Granodiorite
T39S/R2E/7Cc	WC	42-11.3	122-38.2	LITHIASP (8/8/77)	WW	583	130	95-130	(2.09)	16.6 (0.3)	15.0	31	B	Claystone
T39S/R8E/31Ac	BR	42-8.0	122-55.2	RP-WW (3/8/74)	WW	1262	52	15-52	> 0.75	55.0	55.0	> 42	C	-----
T39S/R9E/30d	BR	42-12.0	121-44.3	CW-WW (1/25/74)	WW	1251	150	25-150	> 0.75	170.0	170.0	>130	C	-----
T39S/R9E/8Ad	BR	42-11.7	121-46.5	KLADZ-WW (8/26/74)	WW	1247	85	4-84	> 0.75	160.5	160.5	>121	C	-----
T39S/R9E/12Bc	BR	42-11.5	121-42.8	GH-WW (8/22/79)	WW	1259	150	80-150	> 0.75	138.0	138.0	>105	C	-----
T39S/R9E/7Da	BR	42-11.5	121-48.0	FRHVNSCH (8/18/77)	WW	1282	50	15-50	> 0.75	245.7 (34.6)	223.0	>167	C	Pliocene-Pleistocene volcanics
T39S/R9E/2Cd	BR	42-12.1	121-43.6	WP-WW (8/22/74)	WW	1262	290	30-290	> 0.75	165.0	165.0	>125	C	-----
T39S/R9E/9Cb	BR	42-11.4	121-46.3	KLAOI-WW (8/26/74)	WW	1257	69	15-69	> 0.75	110.0	110.0	> 84	C	-----
T39S/R9E/30Ad	BR	42-9.3	121-41.9	ED-WW (1/25/74)	WW	1251	70	40-70	> 0.75	90.0	90.0	> 67	C	-----
T39S/R9E/35Cb	BR	42-8.0	121-44.1	JB-WW (6/12/74)	WW	1247	50	10-50	> 0.75	86.0	86.0	> 63	C	-----
T39S/R10E/6Cd	BR	42-12.1	121-41.5	OWC-WW (8/18/74)	WW	1304	223	0-223	1.05	104.0	104.0	105	C	-----
T39S/R10E/14Cc	BR	42-10.4	121-37.1	MB-WW (6/18/74)	WW	1268	115	0-115	> 0.75	400.0	400.0	>301	C	-----
T39S/R10E/18Bc	BR	42-10.7	121-41.7	HW-1-WW (6/18/74)	WW	1268	80	30-80	> 0.75	48.0	48.0	> 33	C	-----
T39S/R10E/19Ac	BR	42-9.9	121-40.9	KT-1-WW (5/29/74)	WW	1256	120	100-120	> 0.75	28.5	28.5	> 21	C	-----
T39S/R10E/21Bb	BR	42-10.2	121-39.2	CT-WW (6/5/74)	WW	1253	48	10-48	> 0.75	47.0	47.0	> 33	C	-----
T39S/R10E/30Ad	BR	42-9.0	121-40.7	BA-WW (5/20/74)	WW	1248	73	20-73	> 0.75	80.0	80.0	> 59	C	-----
T39S/R10E/30Ad	BR	42-8.9	121-40.7	EJ-WW (5/20/74)	WW	1248	54	20-54	> 0.75	82.0	82.0	> 63	C	-----
T40S/R2W/21Bb	KM	42-5.0	122-57.0	USGS	TG(?)	1245	---	----	2.72	----	12.3	63	A	-----
T40S/R1E/36Ab	WC	42-3.3	122-38.7	COLESTIN (8/11/77)	WW	1094	140	10-140	(1.88)	31.2 (0.7)	28.0	52	B	Colestin Fm., volcanic conglomer- ates

APPENDIX D.

TEMPERATURE AND HEAT-FLOW DATA

Table D.1. Temperature and heat-flow data for the Oregon Cascades --Continued

Location	Prov. ^a	N. lat. deg.-min.	W. long. deg.-min.	Hole name (date)	Hole type ^b	Collar elev. (m)	Total depth (m)	Depth interval (m)	Average thermal conductivity	Uncorr. grad. ^c °C/km (1σ)	Corr. grad. ^c (°C/km)	Corr. heat flow ^c mW/m ²	Quality ^d	Lithologic summary
T40S/R2E/6Bb	WC	42-5.6	122-32.3	FORD (8/25/81)	WW	963	137	20-137	----	24.6	----	--	C	Fine sediments
T40S/R2E/12Acc	WC	42-6.3	122-31.8	HARRELL (8/26/81)	WW	817	47	10-47	----	47.0	----	--	C	Basalts
T40S/R3E/5Ddd	WC	42-6.8	122-29.0	MURRAY (8/27/81)	WW	1359	73	45-73	----	26.4	----	--	C	Basalt
T40S/R8E/3Cd2	BR	42-6.8	121-51.9	VW-WW (5/21/74)	WW	1245	72	20-72	> 0.75	146.0	146.0	>109	C	-----
T40S/R8E/17Ba	BR	42-5.7	121-54.2	EG-17-WW (3/18/74)	WW	1254	55	15-55	> 0.75	17.0	17.0	> 13	D	-----
T40S/R9E/6Ab	BR	42-7.5	121-48.1	RD-WW (6/20/74)	WW	1248	150	0-150	> 0.75	----	50.0	> 4	D	-----
T40S/R9E/19Dc	BR	42-4.2	121-48.3	TF-1-WW (6/4/74)	WW	1243	50	28-50	> 0.75	45.0	45.0	> 33	C	-----
T40S/R9E/28Ad	BR	42-3.8	121-45.5	LA-WW (6/14/74)	WW	1256	30	20-30	> 0.75	74.0	74.0	> 54	C	-----
T40S/R10E/17Cc	BR	42-5.1	121-40.5	JG-WW (2/8/74)	WW	1245	58	18-49	----	----	82.0	--	D	-----
T40S/R10E/18Cb	BR	42-5.3	121-41.8	CM-WW (6/13/74)	WW	1245	140	12-140	> 0.75	77.0	77.0	> 59	C	-----
T40S/R10E/26Bc2	BR	42-3.8	121-36.9	BHL-WW (6/26/74)	WW	1262	89	60-89	> 0.75	58.0	58.0	> 42	C	-----
T40S/R10E/25Cc	BR	42-3.3	121-35.8	LC-WW (6/27/74)	WW	1280	38	20-38	> 0.75	120.0	120.0	92	C	-----
T41S/R8E/13Ac	BR	42-0.3	121-49.3	LISKEY-WW	WW	1244	179	51-179	0.75 (0.01)	16.8 (0.9)	16.8 (0.9)	13	A	-----
T41S/R9E/3Db	BR	42-1.8	121-44.8	OC-1-WW (8/21/74)	WW	1244	176	53-176	0.75 (0.01)	78.6 (0.3)	78.6 (0.3)	60	A	-----
T41S/R10E/1Cd2	BR	42-1.5	121-35.5	BC-WW (5/11/74)	WW	1240	87	25-87	> 0.75	74.0	74.0	> 54	C	-----
T41S/R10E/7Db	BR	42-1.0	121-41.1	OC-3-WW (1/24/74)	WW	1253	150	0-150	> 0.75	130.0	130.0	> 96	C	-----
T41S/R10E/15Ab	BR	42-0.4	121-37.7	RK-WW (6/13/74)	WW	1248	73	45-73	> 0.75	110.0	110.0	> 84	C	-----

FOOTNOTES FOR TABLE D.1.

^aPhysiographic province: BR = Basin and Range; HL = High Lava Plains; DU = Deschutes-Umatilla Plateau; HC = High Cascades; WC = Western Cascades; WV = Willamette Valley; KM = Klamath Mountains; WH = Western-High Cascade boundary.

^bHole type: WW = water wells; OW = oil and gas prospects; TG = temperature-gradient holes; FS = damsite foundation studies; ME = mineral exploration holes.

^cCalculations performed under direction of David D. Blackwell, Southern Methodist University, Dallas, Texas.

^dHeat-flow quality: Assessment of reliability of heat-flow determination. A[±]=5 percent; B[±]=10 percent; C[±]=25 percent; D = uncertain reliability; X = temperature-depth data not suitable for heat-flow determinations.